THE ROLE OF PHOTORECEPTOR ABC TRANSPORTER ABCA4 IN RETINAL AND LIPID TRANSPORT AND STARGARDT MACULAR DEGENERATION

by

Faraz Quazi

A THESIS SUBMITTED IN PARTIAL FULFILLMENT OF

THE REQUIREMENTS FOR THE DEGREE OF

DOCTOR OF PHILOSOPHY

in

THE FACULTY OF GRADUATE AND POSTDOCTORAL STUDIES

(Biochemistry and Molecular Biology)

THE UNIVERSITY OF BRITISH COLUMBIA

(Vancouver)

December 2013

Abstract

ABCA4 is a member of the superfamily of ATP-binding cassette (ABC) transporters implicated in the clearance of retinoids from photoreceptor outer segments and associated with Stargardt macular degeneration. Stargardt patients display lipofuscin deposits and photoreceptor degeneration that invariably lead to the loss of central vision. In biochemical and knockout mice studies, ABCA4 has been implicated in the transport of *N*-retinylidene-PE, the Schiff base conjugate formed from all-*trans* retinal and phosphatidylethanolamine (PE). The principal challenge in assessing direction and transport has been impeded by the unstable hydrophobic nature of the proposed substrate. As part of this study, a novel biochemical transport assay was developed and used to show that ABCA4 actively flips *N*-retinylidene-PE from the lumen to the cytosolic side of membranes. This is the first mammalian ABC transporter shown to function as an importer.

11-*cis* retinal delivered in excess to photoreceptors is a defining cause of lipofuscin/A2E formation. Purified ABCA4 transports 11-*cis* retinylidene-PE. By HPLC analysis, 11-*cis* retinal also showed isomerization to all-*trans* retinal with PE present in discs. Thus, ABCA4 insures the complete removal of *N*-retinylidene-PE conjugates from the disc-lumen, thereby preventing accumulation of lipofuscin precursors including A2PE. Stargardt mutants which showed reduced functionality were rescued by allosteric enhancement of ATPase with dronedarone, an anti-arrhythmic drug, acting in concert with an increase in *N*-retinylidene-PE transport. Additionally, protein misfolding was selectively restored by 4-phenylbutyrate, a chemical chaperone.

Genetic mutations in several ABCA subfamily transporters cause severe-inherited lipid disorders. The structure-function relationships underlying substrate specificity remain unclear. ABCA1 linked to Tangier disease has been implicated in the export of cholesterol and phospholipids to the apolipoproteinA-I acceptor by cell-based assays. In this study, biochemical analysis indicated that purified and reconstituted ABCA1 actively flipped phosphatidylcholine, phosphatidylserine, and sphingomyelin from the cytoplasmic to the lumenal side of membranes, while ABCA7 preferred phosphatidylserine. In contrast, ABCA4 transported PE in the reverse direction. Tangier and Stargardt mutants showed reduced lipid transport activities.

This thesis demonstrates the importance of ABCA4 as a unique ABC importer, reports the first reconstitution of phospholipid flippase activity for ABCA transporters, and identifies several compounds as potential therapeutic drugs for Stargardt disease.

Preface

A version of chapter 2 has been published. [Quazi, F.], Lenevich. S., Molday, R.S., 2012. *The ABC Transporter ABCA4 Linked to Stargardt Disease Functions as an N-retinylidene-phosphatidylethanolamine and Phosphatidylethanolamine Importer*. Nat Comm. 3:925. Stepan Lenevich synthesized the *N*-retinyl PE analog. Mice retina were dissected by Laurie Molday and Hidayat Djajadi. I performed the experiments and wrote the original manuscript. The final manuscript was edited by Molday, R.S.

A version of chapter 4 has been accepted. [Quazi, F.], Molday R.S. 2013. *Differential Phospholipid Substrates and Directional Transport by ATP Binding Cassette Proteins ABCA1, ABCA7, and ABCA4 and Disease-causing Mutants.* J. Biol. Chem. *In press*. I performed the experimental work and wrote the original manuscript. The final manuscript version was edited by Molday, R.S.

Table of Contents

List of Tables

List of Figures

Acknowledgements

As someone inspired by classical music, I'd like to take a moment and picture the retina from a musical perspective. In nature, drawing parallels among different aspects occurs quite often and more than one would like to believe. So, in this resemblance, to me the visual cycle in the eye is like a grand cascade as achieved by Tchaikovsky in his 'piano concerto 1'. You might ask what a typical format of a concerto is after all: The orchestra begins, the soloist enters, both forces build to an exciting cadenza, and then the orchestra finishes with a bravura. Tchaikovsky accomplishes all of this in his introduction: the piano (*light*) accompanies a grand theme played by the orchestra (*rhodopsin*), then the piano plays the theme itself (*various opsin isoforms*) and breaks into a cadenza (*release and reduction of retinal*), and finally the orchestra concludes the drama again stating the theme. Essentially, Tchaikovsky has accomplished everything the first movement of a concerto is supposed to do in about 3 minutes. Such is the remarkable feat and beauty of the visual cycle as well.

I like Bob's approach of cuing up people with different scientific backgrounds and interests. It enforces that assumptions are never absolute and that there is always a better way to approach the problem than the path that was taken. This is essential for making progress. In the course of our discussions and revisions, we brainstormed about devising new approaches to understanding mechanisms and the cellular basis of visual disorders and possible treatment regiments. Talking science can be fun. Thank you, Bob!

My committee members Dr. Orson Mortiz and Dr. Lawrence McIntosh were also invaluable in guiding and helping me progress in the past few years. I also appreciate the support of the many members of the Molday lab from the last few years. The pedigree of this work in the lab was started out by Michelle Illing, and succeeded by studies from Jinhi

Ahn, Stephanie Bungert, and Seelochan Beharry. In particular, I would like to thank Ming Zhong who continued this project as part of his Doctorate thesis, Laurie Molday for uncompromising support, experimental guidance and jovial conversations, Hidayat Djajadi for help in dissections, Theresa Hii for help in maintaning hybridoma cell lines, Frank Dyka and Ming Zhong for the countless hours teaching me biochemical techniques, Jonathan Coleman for clear and navigational insights, and Jiao Wang for immense "bubbly factor". I would also like to thank Stepan Lenevich, Seifollah Azadi, Emmanuelle Reboul, Christiana Cheng, Martin Bush, Julie Wong, Mahadev Chalat, Karen Chang, Fabian Garces, and Aleeza Tam.

I would like to acknowledge the University of British Columbia and NSERC for financial support. Finally, I would like to thank my family for their support.

Abbreviations

ABC	ATP Binding Cassette
ATR	All-*Trans* Retinal
ABCA1	ABC Transporter A1
ABCA7	ABC Transporter A7
AMD	Age-Related Macular Degeneration
AMP-PNP	Adenosine 5′-(β,γ-imido)triphosphate
ATP	Adenosine Triphosphate
ApoA-I	ApolipoproteinA-I
BCA	Bicinchoninic Acid
BSA	Bovine Serum Albumin
CFTR	Cystic Fibrosis Transmembrane Regulator
CHAPS	3-[(3-Cholamidopropyl)dimethylammonio]-1-Propanesulfonic acid
CHOL	Cholesterol
DTT	Dithiothreitol
DOPC	Dioleoylphosphatidylcholine
DOPE	Dioleoylphosphatidylethanolamine
DOPG	Dioleoylphosphatidylglycerol
DOPS	Dioleoylphosphatidylserine
ECD	Extracellular Domain
ER	Endoplasmic Reticulum
Fl-PL	Fluorescent-labeled Phospholipid
GPCR	G Protein-Coupled Receptor

GRK	G Protein-Receptor Kinase
HEPES	4-(2-Hydroxyethyl)-1-Piperazineethanesulfonic Acid
HPLC	High Pressure Liquid Chromatography
NBD	Nucleotide Binding Domain
N-ret-PE	*N*-retinylidene PE
OS	Outer Segment
PBA	4-Phenyl Butyrate
PBS	Phosphate-Buffered Saline
PC	Phosphatidylcholine
PDE	Phosphodiesterase
PGP	P-Glycoprotein
PE	Phosphatidylethanolamine
PG	Phosphatidylglycerol
PS	Phosphatidylserine
ROS	Rod Outer Segment
RP	Retinitis Pigmentosa
RPE	Retinal Pigment Epithelium
SD	Stargardt Disease
SM	Sphingomyelin
TBS	Tris Buffer Saline
TLC	Thin Layer Chromatography
TMD	Transmembrane Domain

Chapter 1: Introduction

1.1 Casting Light

In our 24/7 society, from early start at work or school to long tasks, cooking, travelling, or just mere relaxing relies on the dominant influence of light interfacing with our privileged sense: visual perception. Just as the ear has hearing and balance, the eye has two functions. First, rods and cones enable sight; and second, intrinsically photosensitive ganglion cells relegate information to the central nervous system and enable 'sightless' visual responses. As such, many body tissues are regulated by a circadian clock that contributes to metabolic activity, immune-cell proliferation, memory, sleep, and numerous critical functions. Today, many people are born with impaired vision, and others experience loss of vision later in life. Diseases of the retina are common causes of untreatable blindness and in many cases a genetic component to the etiology has been identified, making the development of retinal-based treatments a logical long-term goal.

1.1.1 Anatomy of the Eye

The vertebrate eye is an opaque sac with a transparent aperture facing incident light. It is divided into anterior and posterior segments. The anterior segment of the eye is filled with aqueous humour and includes the cornea, iris, ciliary body, and lens (Fig. 1.1). The cornea is the transparent part of the eye and covers the iris, pupil, and anterior segment. Light enters the eye through the pupil and the iris controls the aperture size of the pupil and the amount of light. The refractive index of the air and the cornea are different, so the cornea does nearly 70% of the light focus. The ciliary body muscles adjust the lens shape and the lens provides fine resolution in refracting light onto the retina by changing curvature and the focal distance of the eye (Rodieck, 1998).

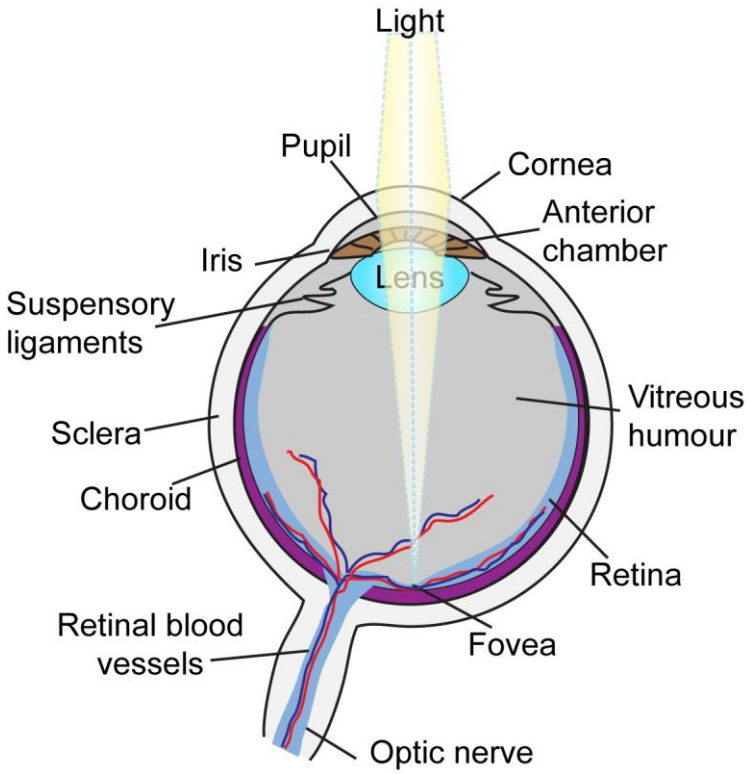

Figure 1.1 Anatomy of the Vertebrate Eye

Three layers form the posterior chamber of the eye. The sclera, outer layer, provides shape and prevents damage to the contents of the eye. The choroid layer contains vasculature and provides nourishment to the retina. In the innermost layer, the retina harbors photoreceptors together with other neuronal cells involved in light phototransduction. Light photons pass through the anterior chamber including the cornea, aqueous humour, and lens and the vitreous humour before reaching the retina. Modified from (http://en.wikipedia.org/wiki/File:Schematic_diagram_of_the_human_eye_en.svg)

The posterior segment of the eye consists of the sclera, vitreous humor, choroid, retina, and optic nerve (McIlwain, 1996; Rodieck, 1998). The sclera protects the eye and forms the opaque, tough, fibrous outer surface composed of collagen and elastin. The vitreous humor maintains the shape of the posterior segment by occupying the space between the lens and the retina. Between the scleral and retinal layer, the choroid provides O_2 and nutrients to photoreceptors *via* a networked vasculature. The light-sensitive neural tissue, known as the retina, lines the inner layer of the eye where the optics portray a visual image. Light striking neuronal cells start a cascade of chemical and electrical signaling for visual

processing and eventually triggers nerve impulses. These are sent to higher visual centers in the brain through fibers of the optic nerve.

In humans, eye movements are precisely coordinated to maintain fixation of visual targets. Precise ocular alignment is critical for binocular fusion. Mice are commonly used as a model for studies of the mammalian visual system. They have laterally facing eyes and a panoramic field of view extending in front, above, and behind the head. Together with low acuity, mice vision is specialized along different lines to that of humans.

1.1.2 The Retina

The retina contains three layers of neuronal cells and two layers of synapses: photoreceptor cells (cones and rods), intermediate neurons (bipolar, horizontal, and amacrine cells), and ganglion cells (Fig 1.2) (Forrester, 2002; Mcllwain, 1996; Rodieck, 1998). The cell bodies of both photoreceptor cells form the outer nuclear layer whereas the cell bodies of bipolar and horizontal cells are in the inner nuclear layer together with amacrine cells. Two layers of synapses are also distinguished in the retina. The synapses of the photoreceptors establish contact with horizontal and bipolar cells form the outer plexiform layer. Synapses among the bipolar, amacrine, and horizontal cells constitute the inner plexiform layer. Both dendrites and axon terminals of horizontal cells make synapses with cells in the outer nuclear layer. The bipolar cells, however, make synapses with dendrites of ganglion cells within the inner plexiform layer.

During the visual process, light signal is detected by photoreceptor cells at the back of retina. Several hyperpolarization and neurotransmitter release processes allow the bipolar cells to link the signals in the outer and inner plexiform layers. The visual signals are then relayed by the cells in the inner nuclear layer to the ganglion cells. The nerve fibers of

ganglion cells converge into the optic nerve where signals are further transmitted to the visual cortex for visual processing.

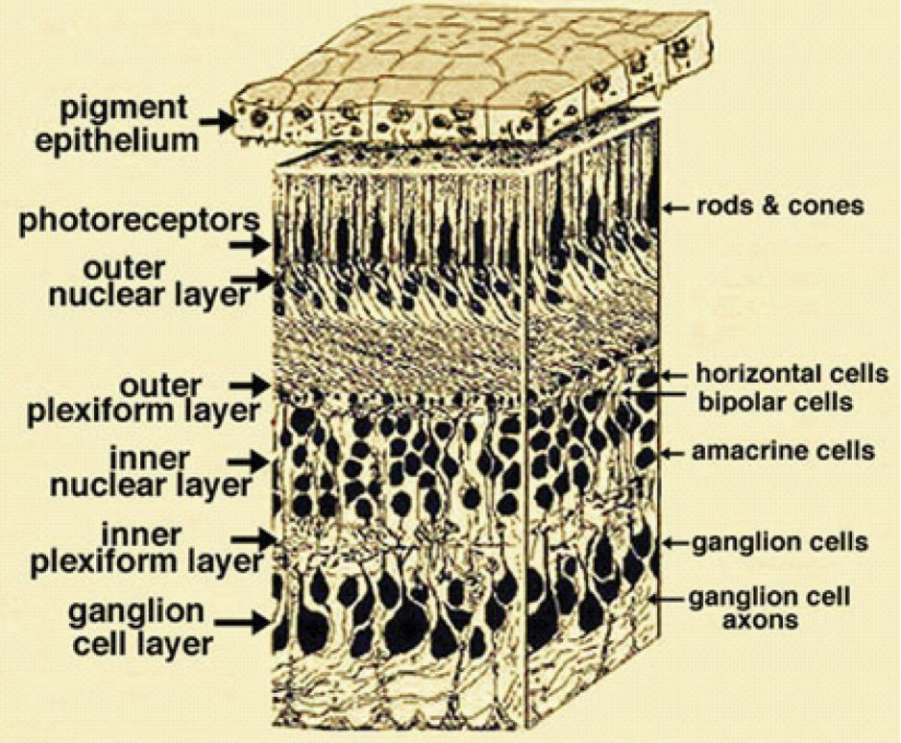

Figure 1.2 Organization of the Vertebrate Retina

The retina consists of three layers of neuronal cells: the photoreceptor cell layer contains rods and cones; the intermediate layer contains bipolar, horizontal, and amacrine cells; and the outer ganglion cell layer. Light passes through the ganglion and intermediate layers before reaching the photoreceptor cell layer. Visual signal is transmitted and processed by the intermediate cells and converge along the axons of the ganglion cells of the optic nerve. Adapted with permission from (http://webvision.med.utah.edu/wp-content/uploads/2011/01/3dlabel.jpeg)

1.1.3 Photoreceptors and Retinal Chromophore

Rod and cone photoreceptors are one of the most polarized cells in terms of structure and function (Fig 1.3) (Rodieck, 1998). Rod photoreceptor cells are sensitive and since they respond to a single photon, they function in dim light. Structurally, rods are distinguished by five segments – the outer segment (OS), cilium, the inner segment (IS), the cell body and the synaptic terminal.

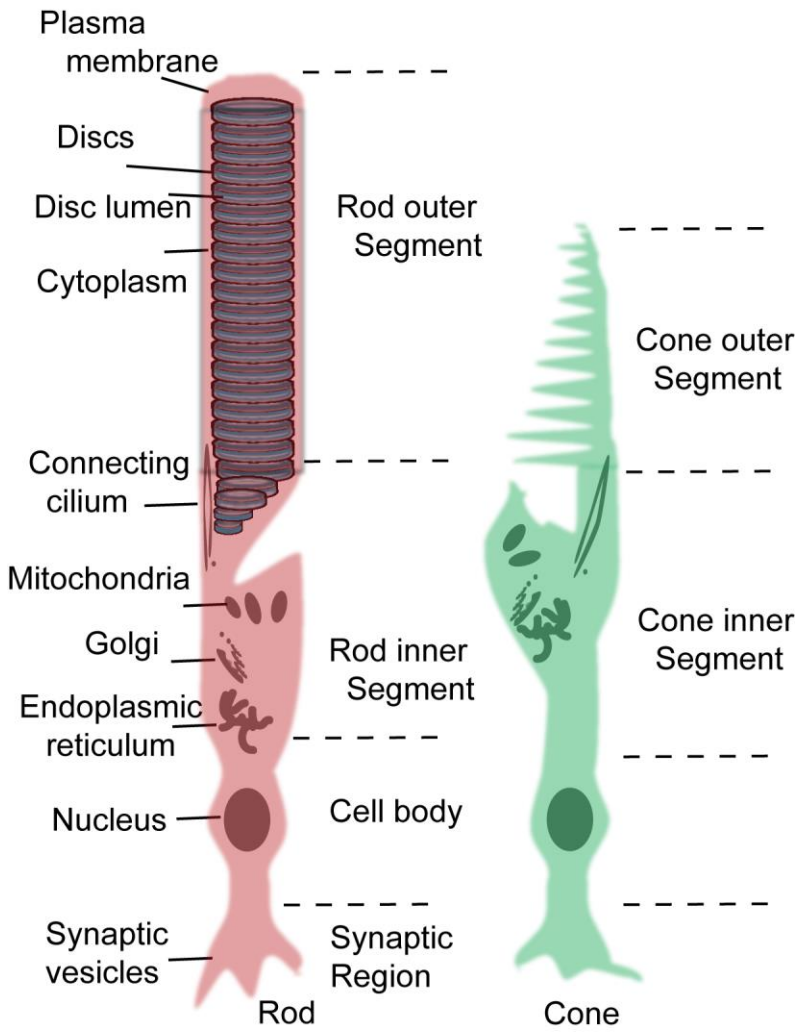

Figure 1.3 The Rod and Cone Photoreceptor Cells

Two morphologically distinct photoreceptor cells are present in the vertebrate retina: rods and cones. Both cell types are highly polarized and can be divided into four areas: the outer segment, the inner segment, the cell body, and the synaptic terminus. The outer segment in rods contains closely arranged membranous discs enclosed by a separate plasma membrane while the outer segment of cones is continuous with the discs. (Adapted from Molday, 2007)

The rod OS contains over a 1000 stacked, disc-shaped membranes perpendicularly aligned to the OS and densely packed with visual pigment rhodopsin. The IS is more typical of the cell body region of a neuron, with the exception that it contains densely packed mitochondria to meet the large energy needs of the photoreceptor (Loewen et al., 2004; Sung

and Tai, 2000). The cell body contains the nucleus. Large numbers of synaptic vesicles are found in synapses tethered to a synaptic ribbon in close proximity to the presynaptic membrane. In contrast, cones are morphologically short . Cones are responsible for color vision. They are not as sensitive as rods but have higher resolution, faster kinetics and respond to many different intensities of light. It has fewer OS discs that are continuous with the PM forming a highly convoluted surface membrane.

In primates, the central part of the retina bears a concentrated region of cones known as the macula. Unlike the periphery regions of the retina, the centre of the macula, known as the fovea centralis, is devoid of rods and consists of densely packed cones (McIlwain, 1996; Sakai et al., 2007). Each fovea cone is connected to only one bipolar and one ganglion cell and the cell bodies of the secondary retinal neurons have been shifted to the side, enabling light paths to enter photoreceptors with minimal distortion. These structural and compositional features make this region responsible for the highest visual acuity in humans. Outside the central retina is the peripheral retina, where rod photoreceptor cells are much more abundant. This region is responsible for peripheral vision and motion detection, as well as vision in dim light.

Light-absorbing protein-chromophore complexes play critical roles in vision. The function of this system depends on the modulation of spectroscopic properties through protein-chromophore interactions. Humans have 130 million photoreceptors and 5 million cone cells (Osterberg, 1935). In photoreceptor cells, rods absorb light maximally at 500 nm and cones have three separate visual pigments – blue, green, red – that absorb light maximally at ~420, ~530, and ~560 nm, respectively (Nathans et al., 1986). The color imparted to the visual pigment is the chromophore, 11-*cis* retinal, and is bound *via* an

iminium, protonated Schiff base, through the side chain of a lysine residue (Palczewski, 2006). A model retinal chromophore in methanol absorbs maximally at 380 nm, but its absorption is mostly red shifted in visual pigments. Nonetheless, in each visual pigment the retinal chromophore remains the same. The energy difference between 380 nm and the absorption of the pigment is affected by factors such as electrostatic stabilization either directly or through a water-mediated network by a counter anion, the presence of charged or polar amino acids in the chromophore binding pocket, as well as protein-induced twist of the polyene system (Merbs and Nathans, 1992). 11-*cis* retinal also serves as a chaperone to cone opsin – though this is not critical for rhodopsin – that assists in the trafficking of newly synthesized opsins to the OS (Rohrer et al., 2005). Several carrier proteins in the photoreceptors and the retinal pigment epithelium also bind retinal but are not conjugated like opsin (Deane et al., 2004; Liu et al., 2005; Saari and Crabb, 2005).

1.1.4 Retinal Pigment Epithelium

The retinal pigment epithelium (RPE) is a continuous layer of pigmented epithelial cells attached to the underlying choroid and overlying the photoreceptors (Forrester, 2002). The basolateral side is bound by the Bruch's membrane separating the choroid from the RPE. Long microvilli extend into the photoreceptor layer on the apical surface of RPE. Furthermore, on the apical side, excess light passing through the retina and photoreceptors are absorbed by RPE melanosomes, dense pigment granules of melanin. The RPE is important for photoreceptor cell function, survival, and maintenance by transport and storage of metabolites. The RPE layer routinely phagocytoses aged OS discs of photoreceptors. As part of the OS renewal process, discs are ingested and taken up into phagosomes and degraded by lysosomes. This process occurs daily with the onset of light and new discs are

added to the base of OS near the cilium. It takes nearly 10 days for a complete renewal of OS disc membranes (Young, 1971).

1.1.5 Phototransduction Cascade

Rod phototransduction constitutes a classical G-protein coupled receptor pathway that initiates a change in the cell membrane potential in the outer segments of the photoreceptors (Molday, 1998; Palczewski, 1994; Pugh and Lamb, 1993). Absorption of photon by rhodopsin causes its retinal chromophore to isomerize from the 11-*cis* to the all-*trans* configuration. Rhodopsin becomes enzymatically active (metarhodopsin II) and catalyzes the activation of the transducin, a signal amplifying GTP binding protein. Active transducin, the heterotrimeric G protein, in turn dissociates and stimulates the effector phosphodiesterase (PDE). PDE hydrolyzes the diffusible messenger cGMP to 5'-GMP, lowering its internal concentration. When the cGMP level drops, cGMP dissociates from its binding sites, and the light-sensitive cGMP-gated channels close. Closure of the channels reduces the influx of Na^+ and Ca^{2+} cations in the photoreceptor OS triggering the hyperpolarization (intracellular voltage becomes more negative). This phenomenon is in contrast to depolarization observed in other sensory cells. Finally, closure of voltage-gated calcium channels reduces the Ca^{2+} concentration at the synapse bringing about a concomitant reduction in neurotransmitter release.

The phototransduction machinery returns to the dark state by Ca^{2+}-dependent and inherent mechanisms of the visual cascade (Nakatani and Yau, 1988). The shutoff of the cascade system includes the following steps: (a) GTPase activating protein (GAP) interacts with the α-subunit of transducin. This hydrolyzes its bound GTP preventing phosphodiesterase from hydrolyzing cGMP (de Vree et al., 1998); (b) The Na^+/Ca^{2+}-K^+

exchanger effluxes Ca^{2+} from the OS reducing intracellular Ca^{2+} levels (Kim et al., 1998); (c) low Ca^{2+} levels promotes dissociation of rhodopsin kinase from rhodopsin and phosphorylation of rhodopsin. Binding of arrestin to phosphorylated rhodopsin inactivates rhodopsin and turns off the transduction cascade (Mendez et al., 2000); (d) Guanylate cyclase activating protein (GCAP) activates guanylate cyclase 1 (GC1) and the synthesis of cGMP from GTP (Gorczyca et al., 1995). The increase of cGMP levels results in the reopening of cGMP gated channels allowing Na^{+} and Ca^{2+} to enter into and return the photoreceptor to its depolarized state.

1.1.6 Visual Cycle

Once all-*trans* retinal dissociates from the bleached visual pigment, it is rendered insensitive to light. In a process known as the visual cycle, restoring light-sensitivity occurs by reisomerization of all-*trans* retinal to 11-*cis* retinal, which recombines with opsin to form a new pigment molecule (Fig 1.4). This involves the transport of retinoid intermediates derived from a series of enzyme catalyzed reactions that occurs in both the photoreceptors and RPE cells (Lamb and Pugh, 2004; Saari, 2000). Upon isomerization and release of chromophore from rhodopsin to all-*trans* retinal, all-*trans* retinal is reduced to all-*trans* retinol in the cytoplasmic side of disk membranes by all-*trans* retinol dehydrogenase (Ishiguro et al., 1991). All-*trans* retinol diffuses from the photoreceptor cell to the interphotoreceptor matrix where it can bind to the interphotoreceptor retinoid binding protein and translocate to the RPE. Simple diffusion may also play a role in the transfer of all-*trans* retinol to RPE cells. Once in the RPE cells, it is esterified to all-*trans* retinyl ester by lecithin-retinol acyltransferase. Hydrolysis and isomerization to 11-*cis* retinol is mediated by an isomerohydrolase, RPE65 (Jin et al., 2005; Moiseyev et al., 2006). 11-*cis* retinol is

oxidized to 11-*cis* retinal by 11-*cis* retinal dehydrogenase, Rdh5, and this retinoid is transported back to the rod photoreceptor where it recombines with opsin in disc membranes to regenerate rhodopsin (McBee et al., 2001).

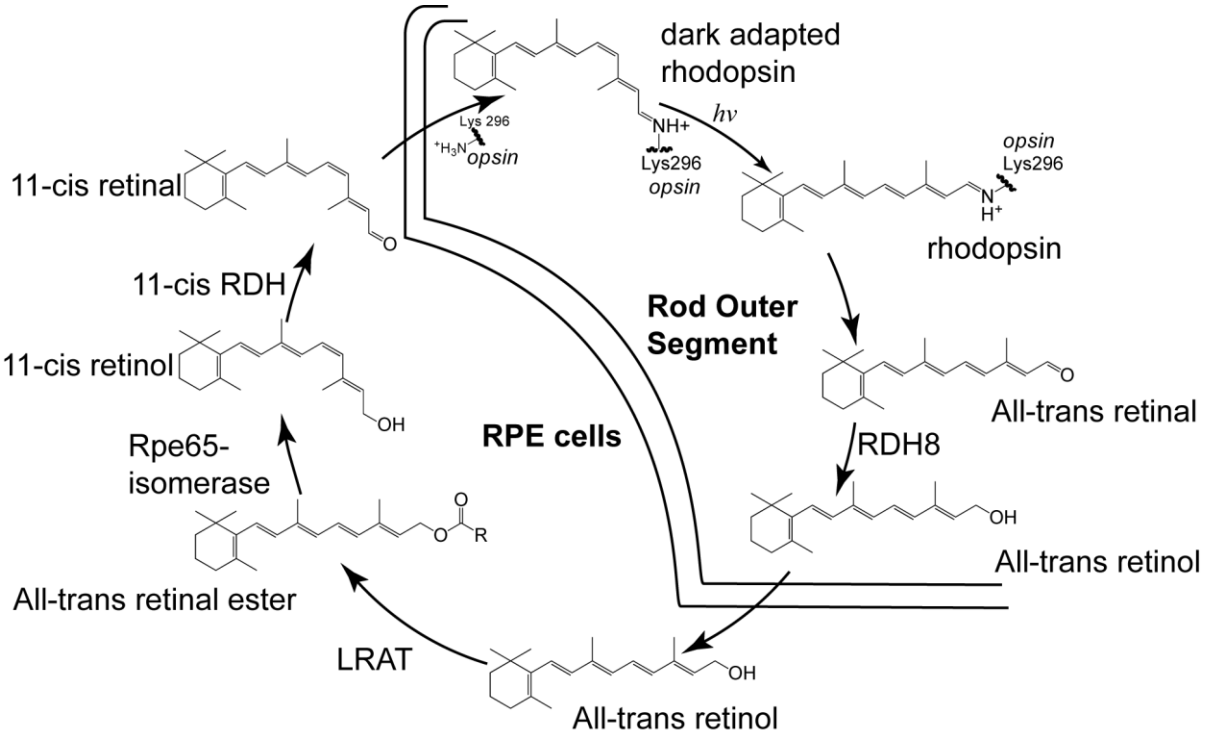

Figure 1.4 The Visual Cycle

Light isomerizes 11-*cis* retinal to all-*trans* retinal in rhodopsin. All-*trans* retinal dissociates from opsin and is reduced to all-*trans* retinol by retinol dehydrogenase (RDH8). All-*trans* retinol is esterified by lecithin retinol acyl transferase (LRAT), isomerized to 11-*cis* retinol by Rpe65-isomerase, and oxidized to 11-*cis* retinal by 11 *cis* retinol dehydrogenases. 11-*cis* retinal is transported back to the outer segment where it can recombine with opsin to produce rhodopsin.

1.2 Retinoid Fluxes and Lipofuscin

Throughout the eye, bulk flow of retinoids between photoreceptors and the RPE play a vital role in the visual cycle. Photoreceptors that run in parallel with RPE microvilli have small tissue distances allowing diffusion and bulk flow a seemingly efficient process (Fig 1.5). Specifically, all-*trans* retinal flux is reduced in the OS cytosol by Rdh8 (Maeda et al., 2007), the major retinol dehydrogenase responsible for retinal reduction. In the IS, Rdh12

contributes to its reduction, although several redundant retinol dehydrogenases also exist in photoreceptors and other layers of the retina (Maeda et al., 2009a; Maeda et al., 2006). The interphotoreceptor matrix (IPM), the region between the RPE and the retina, facilitates all-*trans* retinol flux by diffusion or by interphotoreceptor retinoid binding protein (IRBP) (Hollyfield, 1999; Jin et al., 2009). As all-*trans* retinol exchanges with the RPE, vectorial fluxes drive 11-*cis* retinal from the RPE to the OS plasma membrane either by diffusion, by IRBP, or by cellular retinaldehyde binding protein (CRALBP) (Pepperberg et al., 1993; Saari et al., 2009). In photoreceptors, diffusion has been suggested to govern 11-*cis* retinal flux in the cytosolic gap from the plasma membrane to the disc membrane and opsin is regenerated (Frederiksen et al., 2012).

Regardless of the route, retinal ultimately reaches the respective compartment, where it is metabolized. However, free all-*trans* retinal is toxic. The reactive aldehyde reacts with the amine headgroup of phospholipid phosphatidylethanolamine (PE) to form an equilibrium mixture with a Schiff base conjugate, *N*-retinylidene PE, similar to the opsin Schiff base linkage. Under some conditions, *N*-retinylidene PE instead of hydrolyzing back to retinal and PE reacts with another all-*trans* retinal. This nonenzymatic reaction generates bisretinoid mixtures that include phosphatidylpyridinium bisretinoid, A2PE, phosphatidyl-dihydropyridine bisretinoid, A2-DHP-PE, all-*trans* retinal dimer and the related PE conjugate, all-*trans* retinal dimer PE (Ben-Shabat et al., 2002; Fishkin et al., 2005; Liu et al., 2000). Photoreceptors are continually being replaced as part of RPE phagocytic renewal process and the bisretinoids are, hence, deposited in the RPE (Young, 1971). A2PE undergoes hydrolysis within RPE lysosomes to generate Di-retinoidpyridinium-ethanolamine, A2E, a major component of lipofuscin. A2E and related bisretinoids

accumulate with age because the RPE enzymes do not have specificity to degrade it further (Ben-Shabat et al., 2002). RPE cell death usually occurs with excess toxic accumulation of lipofuscin and underlies several macular disorders (Travis et al., 2007). Lipofuscin pigments vary in structure and are characterized by their yellow fluorescent color (Fig 1.6).

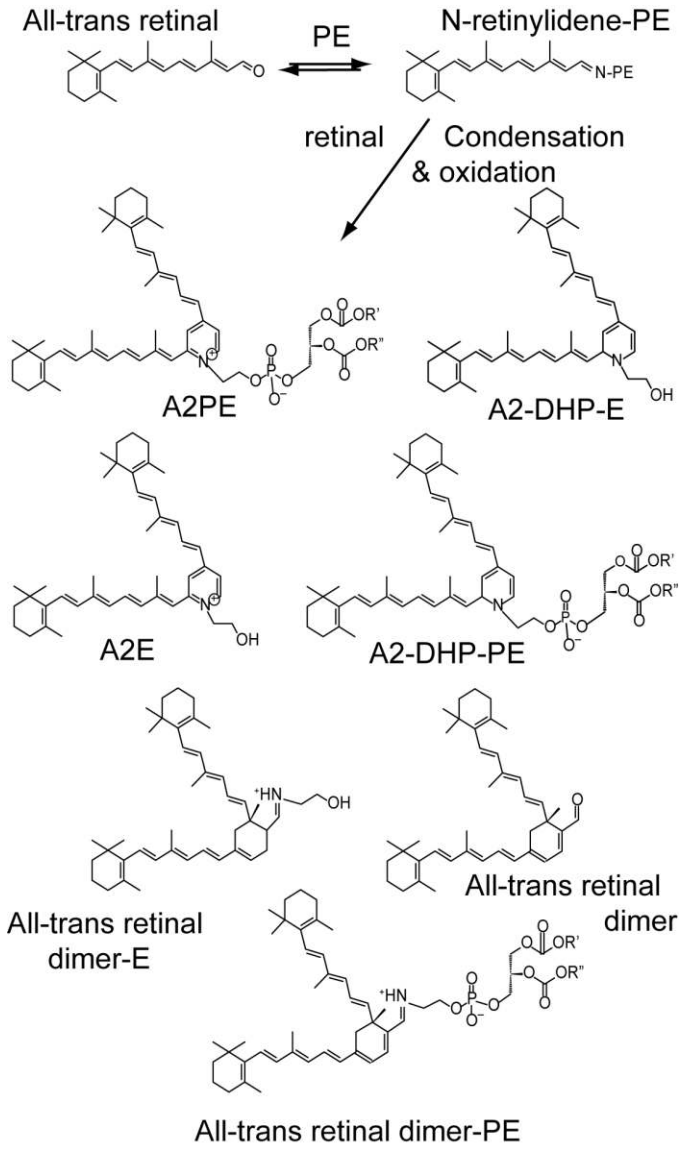

Figure 1.5 Structures of Bisretinoids Found in Lipofuscin Mixture

Reactions of all-*trans* retinal and phosphatidylethanoloamine leading to the formation of bisretinoid compounds. Phosphate cleavage of A2PE, A2-DHP-PE, and all-*trans* retinal dimer-PE generates A2E, A2-DHP-PE, and all-*trans* retinal-E.

Studies of mice also support the formation of lipofuscin. Rdh8 and Rdh12 knockout mice, which impair retinal reduction, exhibit several-fold increases in A2E (Chrispell et al., 2009; Maeda et al., 2008). Abnormal all-*trans* retinol and 11-*cis* retinal fluxes between the retina and RPE were noted in $IRBP^{-/-}$ mice along with increased amounts of A2E (Jin et al., 2009). $CRALBP^{-/-}$ mice delayed 11-*cis* retinal fluxes by 10-fold as indicated by production of the retinal isomer and impeded rhodopsin regeneration (Saari et al., 2001).

1.3 Retinal Disorders

Retinal dystrophies are a heterogeneous group of disorders in which an inherited gene defect leads to impaired visual function (Michaelides et al., 2003). To date, mutations in nearly 240 different genes are implicated in retinal disorders (https://sph.uth.edu/retnet/). Common retinal diseases include age-related macular degeneration (AMD), retinitis pigmentosa (RP), Leber's congenital amaurosis (LCA), and cone-rod dystrophy (CRD). AMD and RP are the most common forms of inherited blindness. AMD refers to the vision loss in the macula due to the degenerative effects of aging. It is the leading cause of severe vision loss in the developed world affecting individuals over 60 years of age. (Berdeaux et al., 2005; Friedman et al., 2004). A proper understanding of AMD has been hindered by its late onset, complex genetics and environmental factors. In the USA, AMD currently affects at least 1.75 million people and is expected to rise due to a rapidly aging population (Friedman et al., 2004). RP occurs in 1 in 4000 causing impaired night vision and peripheral vision, due to rod dysfunction, but can progress to complete blindness (Haim, 2002). This results from the primary loss in rod photoreceptors followed by secondary loss in cone photoreceptors. In contrast, Cone-Rod Dystrophy (CRD) is characterized by primary cone involvement, or, sometimes, by concomitant loss of both cones and rods. Decreased visual

acuity followed by progressive loss in peripheral vision and night blindness are associated with CRD (Hamel, 2007).

A range of genes are responsible for retinal disorders, many of which are translated to key proteins involved in phototransduction, photoreceptor cell structure, and the visual cycle (Michaelides et al., 2003). As rhodopsin comprises 75% of the OS protein, rods are susceptible to changes in its expression (Rossmiller et al., 2012; Sung and Chuang, 2010). Overexpression of rhodopsin in transgenic mice causes disk enlargement while the knockout is devoid of OS (Aller et al., 2009; Humphries et al., 1997). In RP, at least 100 mutations are associated with the rhodopsin gene (Roof et al., 1994). It has been suggested that functional and stable rhodopsin tolerates few amino acid changes (Rossmiller et al., 2012). Normal rhodopsin folding but inefficient trafficking to the OS causes constitutive activation or an increased transducing activation rate leading to photoreceptor cell death (Hollingsworth and Gross, 2012; Mendes et al., 2005). Improper folding and retention of opsin in the ER originates from another class of mutations that does not permit 11-*cis* retinal chromophore reconstitution (Kang and Ryoo, 2009). Another major form of autosomal dominant RP is due to mutations in peripherin-2 ,which forms an oligomeric complex with Rom1 important for the maintenance of OS structure (Kajiwara et al., 1994; Loewen et al., 2004).

Mutations in RDH5 genes cause *Fundus albipunctatus,* a form of night blindness (Jang et al., 2001) and RDH12 is responsible for a subset class of LCA (Janecke et al., 2004) All-*trans* retinyl ester accumulation arises from defects in RPE65 linked to recessive RP and LCA (Fig 1.5). In *Rpe65*$^{-/-}$ mice, lipofuscin autofluorescence is undetected consistent with the absence of 11-*cis* retinal and lipofuscin (Fig 1.5). Patients with LCA owing to mutations in the RPE65 gene show undetectable autofluorescence (Lorenz et al., 2004). In AMD, several

complement factor polymorphisms are attributed to heritable risk (Gold et al., 2006; Hageman et al., 2005). Increased autofluorescence of lipofuscin is also commonly seen in patients with AMD (Bindewald et al., 2005; Einbock et al., 2005).

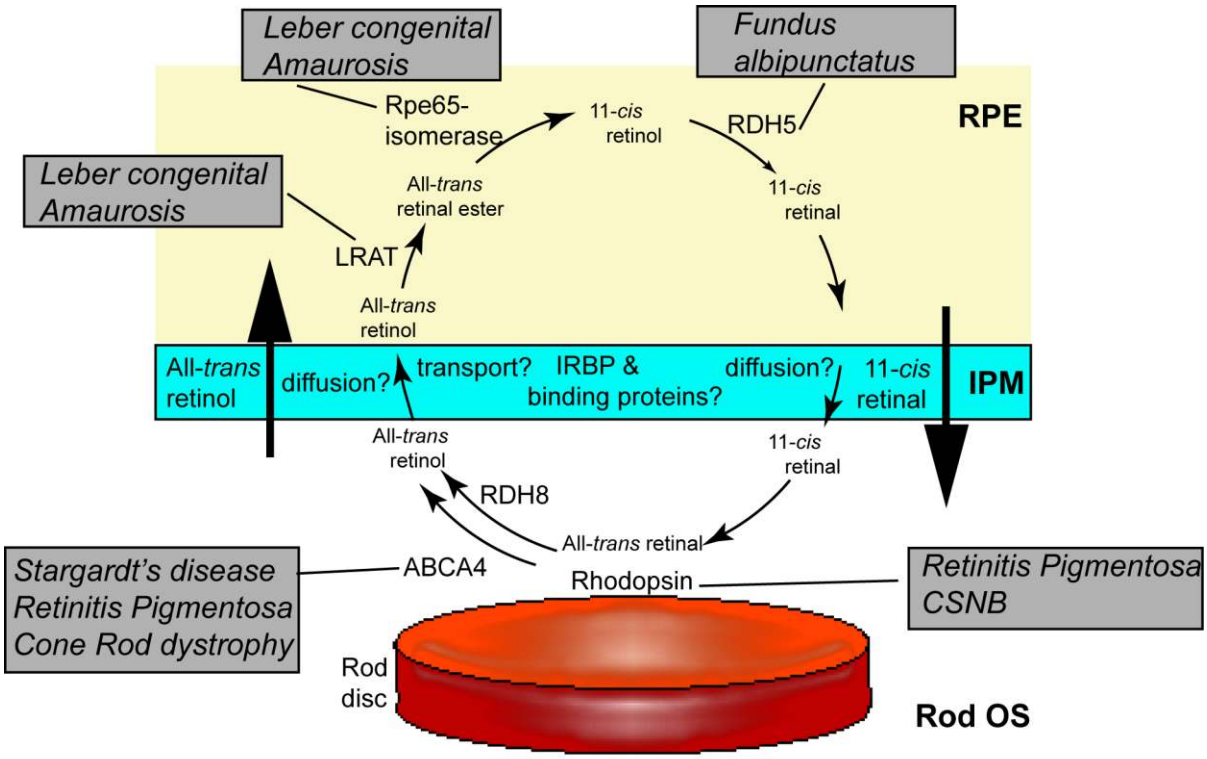

Figure 1.6 General Scheme of Retinoid Fluxes, Transport, and Disorders

All-*trans*-retinol is taken up by the RPE from the photoreceptor and the bloodstream, and converted to retinyl ester by LRAT. Rhodopsin receives its supply of 11-*cis*-retinal from the RPE, and the isomerized chromophore, all-*trans*-retinal, is recycled along the pathway shown. Fluxes of all-*trans* retinol, 11-*cis* retinal, and related retinoids are governed by diffusion, IRBP binding and perhaps other transport binding proteins. Defects in genes encoding essential components of the visual cycle may lead to severe retinal dystrophies. Adapted from (Baehr et al., 2003).

1.3.1 Stargardt Disease

Autosomal recessive Stargardt disease (SD) is an inherited macular disorder with an estimated prevalence of 1:10,000 (Allikmets et al., 1997; Gelisken and De Laey, 1985). It is characterized by a loss in central vision in the first or second decade of life, accumulation of

lipofuscin deposits in RPE cells, progressive atrophy of rod and cone photoreceptors and underlying RPE cells in the macula region of the retina, and a delay in dark adaptation (Cremers et al., 1998; Fishman et al., 1991; Weleber, 1994). Histologically, SD is associated with lipofuscin deposition in the RPE layer beneath the macula. In advanced SD, its buildup causes atrophy of the macula and the underlying RPE (Allikmets, 2000; Stone et al., 1999).

Disease mutations arising from the gene encoding for a retinal specific ATP binding cassette transporter (ABC), ABCA4, cause SD (Allikmets et al., 1997; Illing et al., 1997). Unlike other macular disorders, SD is one of the most prevalent genetic diseases arising from a single gene in humans, with over 800 mutations known to cause photoreceptor and macular degeneration (Allikmets, 2000; Maugeri et al., 1999; Rozet et al., 1999; Stone et al., 1999; Webster et al., 2001). In addition to SD, mutations in ABCA4 have been linked to related retinal degenerative diseases including autosomal recessive CRD and RP (Cremers et al., 1998; Martinez-Mir et al., 1998; Maugeri et al., 2000). Genetic analysis has also suggested an association of heterozygous ABCA4 alleles with AMD (Allikmets et al., 1997; Rivera et al., 2000; Schmidt et al., 2003).

1.4 The ABC Transporter Superfamily

ATP binding cassette (ABC) transporters are found in all living organisms from bacteria to mammals (Davis, 2011) (Higgins, 1992). They typically use ATP binding and hydrolysis to actively translocate a wide variety of compounds across cell membranes including amino acids, peptides, ions, metabolites, vitamins, fatty acid derivatives, steroids, organic anions, phospholipids, drugs and other compounds. Prokaryotic ABC transporters can function either as exporters or importers. Eukaryotic ABC transporters have been initially thought to only function as exporters, but several studies have now shown that some

plant ABC transporters function as importers translocating substrates from the exocytoplasmic (extracellular/lumen) to the cytoplasmic side of biological membranes (Shitan et al., 2003; Smriti et al., 2002).

ABC transporters consist of four principal domains: two transmembrane domains (TMDs) containing multiple membrane-spanning segments that provide a pathway for the translocation of a substrate across the membrane and two cytoplasmic ATP-binding cassettes or nucleotide binding domains (NBDs) that provide the energy for substrate transport (Fig 1.7A). Eukaryotic ABC transporters are typically synthesized as full transporters in which all four domains reside on a single polypeptide chain with a modular organization of TMD-NBD-TMD-NBD or half transporters in two polypeptides each containing a TMD and NBD assemble as homo- or hetero-dimers. Some transporters contain additional domains attached to the TMD or NBD which regulate the activity of these ABC transporters. In prokaryotes, the TMDs and NBDs can reside on individual polypeptide chains or fused together in various arrangements (Higgins, 1992).

Eukaryotic ABC transporters typically contain 6 membrane spanning segments per core TMD. NBDs approximately 200 amino acids in length have a number of conserved structural features including Walker A and Walker B motifs found in many ATPases and the ABC signature motif (LSSGQ), D, H and Q loops characteristic of ABC proteins. Structural and biochemical studies indicate that the two NBDs dimerize in a head-to-tail manner with the two ATP molecules present at the dimer interface (Chen et al., 2003; Fetsch and Davidson, 2002; Jones and George, 2004; Zaitseva et al., 2005).

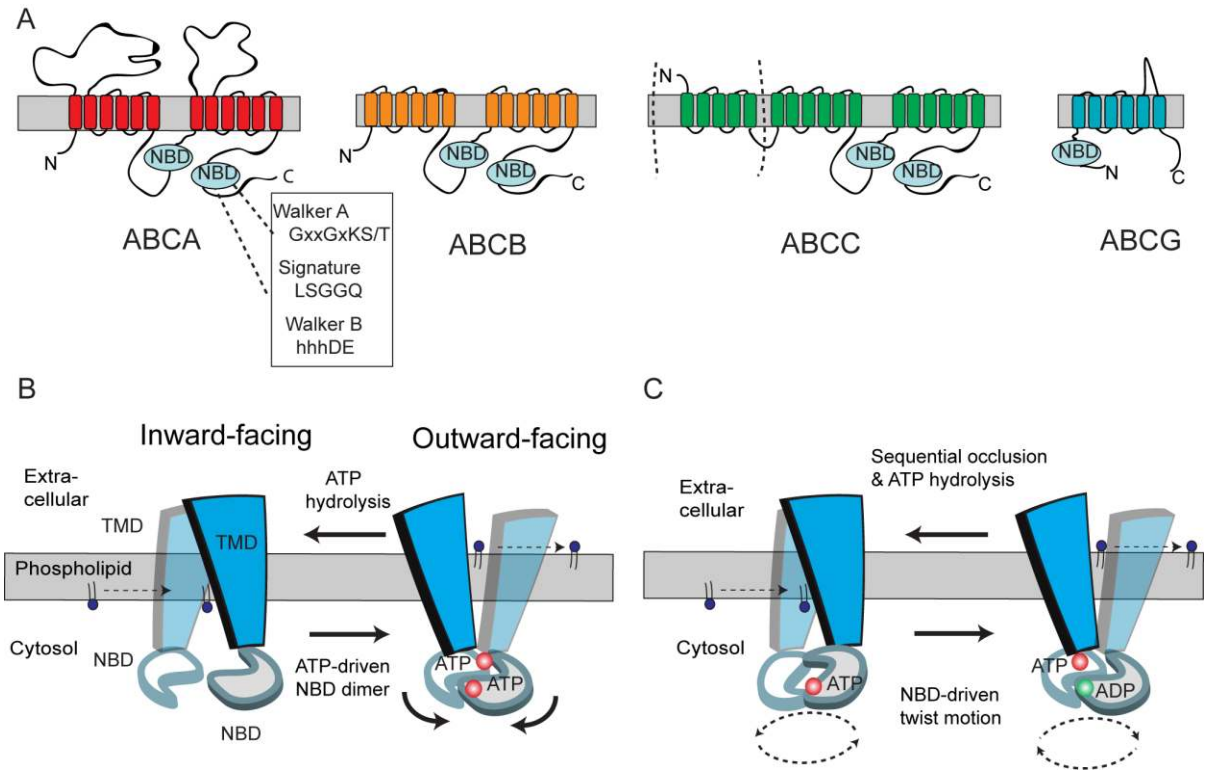

Figure 1.7 2D Topology of Lipid ABC Transporters and Models of Mechanism

A. The two transmembrane domains (TMDs) and nucleotide binding domains (NBDs) arrange to form full transporter in ABCB members and ABCA members with additional exocytosolic domains. Some ABCC members are full transporters with an additional N-terminal TMD while ABCG members are half transporters B. 'Switch Model': In the inward-facing conformation, the NBDs are separated and nucleotide-free. Phospholipid substrate entry into the substrate binding site occurs from the cytosolic leaflet of the membrane bilayer. ATP-dependent dimerization of NBDs progresses to pull the TMDs from an inward- to outward-facing conformation. Phospholipid is translocated to the extracellular side of the membrane and ATP hydrolysis resets the transporter. C. 'Constant-contact Model': The two NBDs are associated in the sandwich dimer and direct TMD conformational changes. Twisting motion of NBDs with ATP hydrolysis alternates with one site hydrolyzing nucleotide that facilitates the binding and hydrolysis in the other site.

The human genome is known to contain at least 48 genes that encode ABC proteins (Dean and Allikmets, 1995). These transporters have been organized into seven subfamilies (ABCA-ABCG) based on their amino acid sequence and structural organization (Fig 1.7A). Two subfamilies ABCE and ABCF, which contain NBDs, but no TMDs, do not function as transporters, but instead are involved in the regulation of protein biosynthesis. Several members of various ABC subfamilies are known to transport specific membrane

phospholipids across cell membranes from the cytoplasmic to the extracytosolic side serving as floppases or export phospholipids to an acceptor molecule serving as effluxers (Woehlecke et al., 2003).

1.4.1 Role of ABC Proteins in Phospholipid Transport

Assembly and maintenance of the various cellular membranes requires translocation of lipids from one leaflet of the bilayer to the opposing leaflet. The plasma membrane, endosomes, and lysosomes depend completely on lipid transport and synthesis from other organelles, in particular from the ER. The lipid composition of separate leaflets of the membrane bilayer show a clear asymmetric arrangement, with the majority of the aminophospholipids, phosphatidylserine (PS) and PE, typically present in the inner, cytoplasmic leaflet, and phosphatidylcholine (PC), sphingomyelin and glycolipids predominantly if not exclusively localized in the outer, exoplasmic leaflet. The plasma membranes, Golgi, and endosomal membranes display high lipid asymmetry, unlike the membranes of the ER, resulting in a non-random distribution of lipids across the bilayer. This bilayer asymmetry is less governed by the size, charge, and polarity of the headgroup, but more so by ATP-dependent and protein mediated translocators. This type of distribution influences important physiological functions such as cell viability, membrane fusion, cell-cell recognition, and protein function and regulation.

Maintenance of the asymmetric distribution of lipids is accomplished by integral membrane transporters that specifically flip (out-to-in translocation), flop (in-to-out translocation), or scramble lipids across the bilayer. Lipid flippases and floppases are ATP-dependent membrane proteins that maintain transbilayer distribution of phospholipids of the bilayer. P4-type ATPases have been identified as phospholipid flippases, whereas ABC

transporters have been generally shown to act as lipid floppases (Coleman et al., 2013; van Meer et al., 2008). In contrast, asymmetric lipid distribution can be undone by the Ca^{2+}-dependent, bidirectional activities of scramblases that tend to act with a low head-group specificity (van Meer et al., 2008). Studies have shown that ATP8A2, a P-type ATPase, in OS disc membranes maintains lipid asymmetry by translocating PS and to a certain extent PE to the cytosolic side of disc membranes (Coleman et al., 2009; Coleman and Molday, 2011). Recently, opsin derived from rod OS discs demonstrated phospholipid scramblase activity in disc membranes (Menon et al., 2011). The function of ABC transporters in generating lipid asymmetry in the photoreceptor OS membranes remains unknown.

P-glycoprotein (ABCB1) responsible for multiple drug resistance in tumour cells was found to transport various phospholipid analogues including PC and PE, as well as the sphingolipid glucosylceramide from the cytoplasmic to the plasma membrane leaflet (Fig 1.8) (Mizutani et al., 2008). Expressed mainly in the liver ABCB4 is primarily a floppase for PC (van Helvoort et al., 1996). Mutations in ABCB4 have been associated with progressive familial intrahepatic cholestasis (PFIC), a disorder involving liver inflammation and fibrosis (de Vree et al., 1998). Cholestasis is thought to result from the toxicity of bile in which detergent bile salts are not effectively neutralized by phospholipids, leading to bile canaliculi and biliary epithelium injuries. PC, PS, and SM also act as substrates for other xenobiotic transporters ABCG2 and ABCC1 (Fig 1.8) (Raggers et al., 1999). Altogether, these studies support a key role of ABC proteins in regulating membrane composition, asymmetry, and stability *via* translocation of key membrane phospholipids across cellular membranes. A list of ABC transporters associated with lipid transport, various cellular processes and any genetic diseases is shown in Table 1.1.

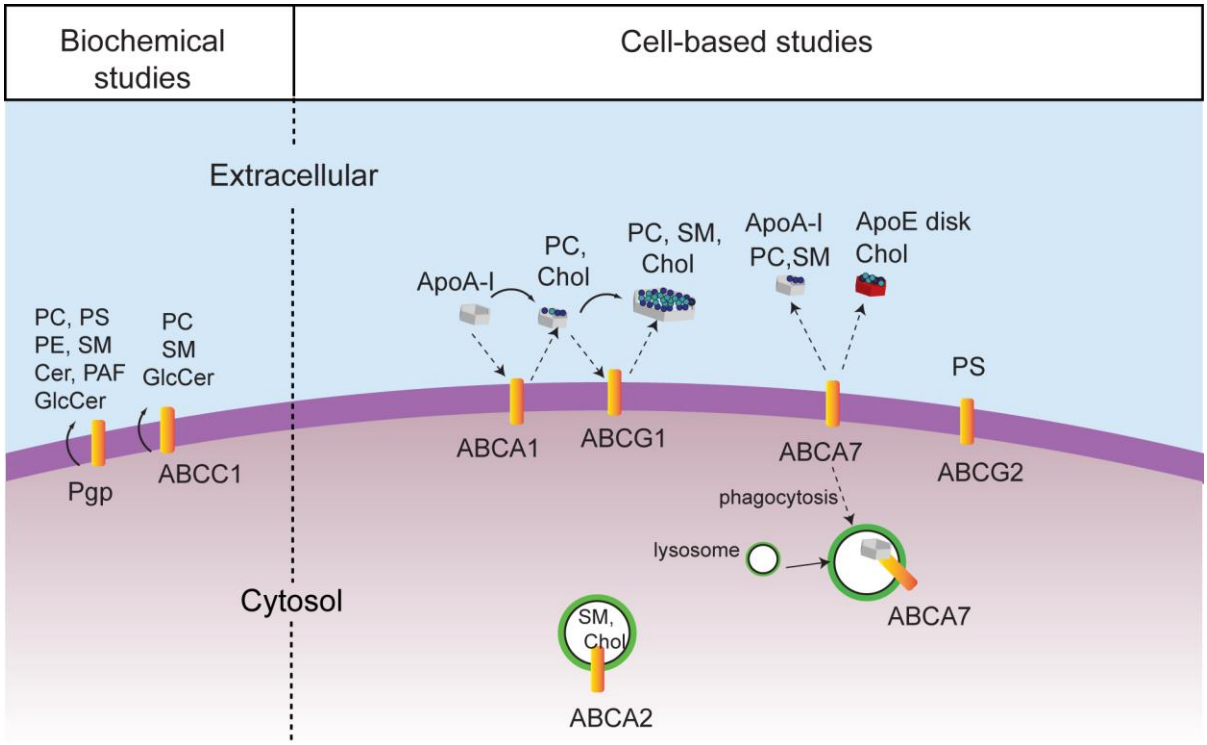

Figure 1.8 ABC Transporters, Known Substrates, Acceptors, and Transport Direction

Overview of ABC transporters involved in lipid efflux. Vectorial transport depicted by black arrows at the plasma membrane. Vectorial transport in many ABC transporters and by intracellular ABC transporters has not been firmly established except for Pgp and ABCC1. ABCA1 effluxes lipids to ApoA-I. Lipids such as PC, SM, and glycolipids are found in the extracellular or lumenal leaflet while phospholipids PE and PS are preferentially located on the cytosolic leaflet. Abbreviations used: ApoA-I/E, apolipoprotein; HDL High Density Lipoprotein; Chol, cholesterol; PC, phosphatidycholine, PE, phosphatidylethanolamine; PS, phosphatidylserine; Cer, ceramide; GlcCer, glucosylceramide; SM, sphingomyelin.

1.4.2 General Mechanisms

Crystal structures of several ABC exporters (Sav1866, murine P-glycoprotein (Pgp), MsbA, TM287/TM288) together with biochemical studies have provided insight into the transport mechanism of ABC proteins (Aller et al., 2009; Dawson and Locher, 2006; Dawson and Locher, 2007; Hohl et al., 2012; Ward et al., 2007). The ‘alternating-access model’ proposed for ABC transporter drug export function can be adapted for lipid translocation (Dawson and Locher, 2006; Jardetzky, 1966). In the absence of nucleotide, the NBDs impose separation in the TMDs. and create a large central cavity towards the cytoplasmic side of the

membrane that represents an 'open-inward' conformation. The transport cycle is initiated when a phospholipid(s) enters the substrate binding site from the inner leaflet that is assumed to represent a high affinity binding interaction. Binding of ATP induces a conformational change in the NBDs and significant rearrangement of the TMDs resulting in a central cavity facing the extracellular/lumen side of the membrane. This is termed as the 'outward-closed' conformation for the ABC transporter, and is similar to that observed for Sav1866 (Dawson and Locher, 2006). The polarity of the TMD substrate-binding site then becomes reversed with a concomitant reduction in substrate affinity, and release of the lipid substrate to the outer leaflet. The conformational change in the TMDs may be driven either by ATP binding, in which case hydrolysis of ATP subsequently resets the ABC transporter to the inward-facing conformation or by the energy released on ATP hydrolysis. Alternatively, the transporter may only bind to the polar head group of the phospholipid similar to ion or pore channel mechanisms (Zou and McHaourab, 2009).

The events that occur at the NBDs are also incompletely understood but two models are generalized to link substrate binding and the catalytic cycle: the switch model and the constant-contact model. The 'Switch-model' proposes that sequential ATP hydrolysis is required to destabilize the NBDs and the adjacent Walker A motifs and signature motifs in the sandwich dimer move apart before the transport cycle can begin again (Fig 1.7B)(Higgins and Linton, 2004). ATP binding switches from the dissociated NBD dimer to the closed dimer, reduces the substrate binding affinity, and facilitates substrate translocation *via* corresponding conformational changes in the TMDs. Evidence from electron paramagnetic resonance (EPR) analysis of the NBDs of MsbA, a lipid transporter, shows large conformational changes (10-20 Å) following ATP hydrolysis suggestive of NBD

dissociation, and is consistent with the crystal structure conformations of MsbA (Borbat et al., 2007; Ward et al., 2007).

In contrast, the 'Constant-contact model' proposes that the NBD dimer is stabilized regardless of nucleotide or substrate content and that each NBD twists about enabling the exchange of nucleotide hydrolysis products (Fig 1.7C) (Senior et al., 1995; Senior and Bhagat, 1998). This effect occludes ATP in one site while the other site opens to release ADP and P_i. The transition from the inward to the outward facing conformation of the TMDs requires a twisting motion of the NBDs and a rearrangement of the consensus site, which allows binding of the second ATP. The bound lipid substrate may then be released to the outer leaflet of the membrane bilayer. A cross-linking study in which the two-halves of the TMDs in Pgp were clamped in the closed conformation displayed high affinity and transport activity of drugs (Loo et al., 2003), although the open-inward conformation of the Pgp structure showed a 30 Å NBD separation bound to some substrates (Aller et al., 2009). A recent crystal structure of the putative drug TM287/TM288 transporter from *T. maritima* presents an inward-facing conformation with contacting NBDs (Hohl et al., 2012), which is uniquely different to the ABC exporter structures of inward-facing conformations with dissociated NBDs (Aller et al., 2009; Ward et al., 2007).

To date, only one ABC exporter, Pgp, has been resolved with a bound substrate (Aller et al., 2009). The TMDs bear hydrophobic, aromatic and polar amino acids where multiple ligands can bind through different interactions with distinct sets of amino acids and provide multiple substrate binding sites, as found in Sav1866 (Dawson and Locher, 2006). The proposed models account for both lipid and drug efflux. In this case, translocation of lipids may be similar to that of drug substrates but partitions into the outer leaflet of the membrane

bilayer, instead of being expelled into the aqueous environment. Alternatively, the transporter may promote dissociation of the lipid from the donor membrane, thereby facilitating its efflux from the cell. Such a case would require the incidental movement of lipids to a region of partial hydrophobicity on the exocytolic face of the protein. This places the substrate in an environment which energetically favors its binding and removal by an acceptor molecule like a bile salt or a docking protein such as apolipoproteinA-I (ApoA-I) (van Meer et al., 2006). This mechanism may govern the functionality in several ABCA and ABCG proteins.

1.4.3 ABCA Transporters

The A subfamily of ABC transporters consist of 12 members. All are full-length transporters organized in two tandem halves, each with a hydrophobic TMD followed by a cytoplasmic NBD. In addition, these transporters contain two large extracellular domains (ECDs) between the first and second membrane-spanning segment of each TMD (Bungert et al., 2001). Although the substrates of most ABCA members remain to be identified, disease-associated phenotypes, analysis of knockout mice, and cell based studies suggest that most ABCA proteins play a role in phospholipid translocation and cellular homeostasis. Mutations in ABCA1 are known to cause Tangier disease and familial high density lipoprotein deficiency associated with defective cholesterol and phospholipid efflux from cells and a deficiency in the formation of high density lipoprotein (HDL) (Bodzioch et al., 1999; Oram, 2002; Rust et al., 1998; Singaraja et al., 2006; van Dam et al., 2002). Defects in ABCA3 are associated with neonatal surfactant deficiency and pediatric interstitial lung disease resulting from abnormal surfactant secretion into the alveoli of the lungs and the formation of abnormal lamellar bodies (Ban et al., 2007; Shulenin et al., 2004). As mentioned earlier, disease mutations in ABCA4 cause autosomal recessive SD and related

retinal degenerative diseases (Allikmets et al., 1997). Mutations in ABCA12 are associated with harlequin ichthyosis, a disease arising from defective lipid transport in the skin (Akiyama et al., 2005; Lefevre et al., 2003).

1.4.3.1 ABCA1

ABCA1 is the prototypical member of the ABCA subfamily and is recognized as the principal protein involved in cholesterol efflux from peripheral tissues in a process known as the reverse cholesterol transport (RCT) (Attie, 2007; Oram, 2002). It mediates the efflux of cellular phospholipid and cholesterol to lipid poor apolipoprotein acceptors as a key step in the production of high-density lipoprotein (HDL). The loss of ABCA1 function leads to Tangier disease, a disorder associated with severe HDL deficiency and increased risk of atherosclerosis. To date, more than 100 mutations in the gene encoding ABCA1 have been linked to Tangier disease in which patients have absent or low circulating HDL (Singaraja et al., 2006). An inverse relationship between plasma HDL levels and the risk of coronary artery disease has been reported (van Dam et al., 2002).

Abca1$^{-/-}$ mice and chickens with dysfunctional ABCA1 also exhibit HDL deficiencies further highlighting the role of ABCA1 in the RCT pathway (Attie et al., 2002; Hamon et al., 2000; Mulligan et al., 2003). Tissue specific deletion of ABCA1 in liver and intestines of mice resulted in an 80% and 30% reduction in plasma HDL, respectively (Brunham et al., 2006; Timmins et al., 2005), while ablation of ABCA1 in macrophages did not alter HDL levels (Zuo et al., 2008).

In cultured cells, ABCA1 mediates the secretion of PC and cholesterol when lipid-free ApoA-I, an extracellular lipid acceptor in the plasma, is added to the medium (Fig 1.8) (Tanaka et al., 2003; Yokoyama, 2000). Cell based studies of 15 disease-associated

mutations in ABCA1 showed decreased phospholipid, predominantly PC, and cholesterol efflux (Fitzgerald et al., 2002; Singaraja et al., 2006). Direct interaction between ApoA-I and ABCA1 has been reported in numerous studies using cross-linking, immunoprecipitation, radiolabelling, and biotinylation techniques (Chroni et al., 2004; Denis et al., 2004; Fitzgerald et al., 2004). Recently, Nagao *et al.* reported that initial binding of ApoA-I is mediated through electrostatic interactions with the ECDs of ABCA1 (Nagao et al., 2011).

Although it is well established that ABCA1 mediates the efflux of cholesterol and phospholipids from cells, the actual substrates transported by ABCA1 are unclear (Table 1.1). Several models of ABCA1-mediated cholesterol efflux have been proposed, including a two-step model in which ABCA1 first mediates PC efflux to ApoA-I, and this ApoA-I PC complex accepts cholesterol in an ABCA1 independent manner (Fig) (Fielding et al., 2000). A concurrent process model in which PC and cholesterol efflux by ABCA1 to ApoA-I are coupled to each other has also been proposed (Nagao et al., 2009). A third model has been proposed in which ABCA1 generates a specific ApoA-I binding site through PS translocation to the outer leaflet of the plasma membrane with subsequent translocation of PC and cholesterol to ApoA-I (Hamon et al., 2000). Resolution of these transport models will be aided by biochemical characterization of lipids transported directly or indirectly to ApoA-I.

1.4.3.2 ABCA7

ABCA7 is a 220 kDa transporter sharing a ~54% sequence homology to ABCA1 (Kaminski et al., 2000). The highest levels of expression are found in the brain, lung, myelo-lymphatic tissues, kidneys, macrophages, and platelets (Kim et al., 2006). Given the homology of ABCA7 to ABCA1, it was predicted that ABCA7 may stimulate cellular phospholipid and cholesterol efflux to ApoA-I or Apo-E. Initial studies confirmed ABCA7

expression promoting efflux of PC and SM, but not cholesterol to ApoA-I (Fig 1.8) (Wang et al., 2003). ABCA7 generates mostly small cholesterol-poor HDL particles, unlike ABCA1, which forms predominantly big-cholesterol loaded HDL particles. A residual phospholipid efflux role for ABCA7 was suggested but *Abca1*$^{-/-}$ macrophages display no detectable ApoA-I stimulated phospholipid efflux activities, inconsistent with this notion (Linsel-Nitschke et al., 2005). Recent studies point to a pivotal role of ABCA7 in phagocytosis and engulfment of apoptotic cells (Fig 1.8)(Iwamoto et al., 2006; Jehle et al., 2006; Tanaka et al., 2010). A biochemical functional analysis is needed to clarify the lipid substrates transported by ABCA7 and understand its associated cellular events

1.4.3.3 ABCA4

ABCA4 shares ~50% sequence identity to ABCA1 and ABCA7 but has a restricted distribution in the OS disc membranes of photoreceptor cells (Fig 1.9) (Ahn et al., 2000; Illing et al., 1997). Recently, a 18 Å structure generated by single-particle analysis of native ABCA4 showed monomeric membrane proteins with an 'ice-cream cone' like shape with an elongated 'handle' representing the tightly interacting ECDs (Tsybovsky et al., 2013). Both ECD1 and ECD2 contain multiple N-glycosylation sites and possess disulfide intramolecular bonds necessary for the location and conformation of these domains in the disc lumen (Bungert et al., 2001). The steric factor of the globular shaped ECDs may account for the localization of ABCA4 in the rim regions of OS disc membranes surrounded by a curved lipid bilayer.

Photoreceptor specific expression of ABCA4 led to the initial suggestion that ABCA4 may transport a substrate critical for photoreceptor function or survival. Substrates of ABC transporters stimulate ATPase activities of reconstituted transporters and has been

extensively studied in Pgp and other drug transporting ABC transporters (Ambudkar et al., 2006; Seres et al., 2008; Shapiro and Ling, 1994; Urbatsch et al., 1994). Purified ABCA4 reconstituted into proteoliposomes had a basal ATPase activity that was stimulated by all-*trans*, 13-*cis*, and 11-*cis* retinal and was dependent on PE (Ahn et al., 2000; Sun et al., 1999). Solid-phase binding studies further demonstrated that *N*-retinylidene PE is a high-affinity substrate of ABCA4 and is quantitatively released by ATP addition (Beharry et al., 2004). These studies revealed that ABCA4 may play a role in retinal or *N*-retinylidene PE.

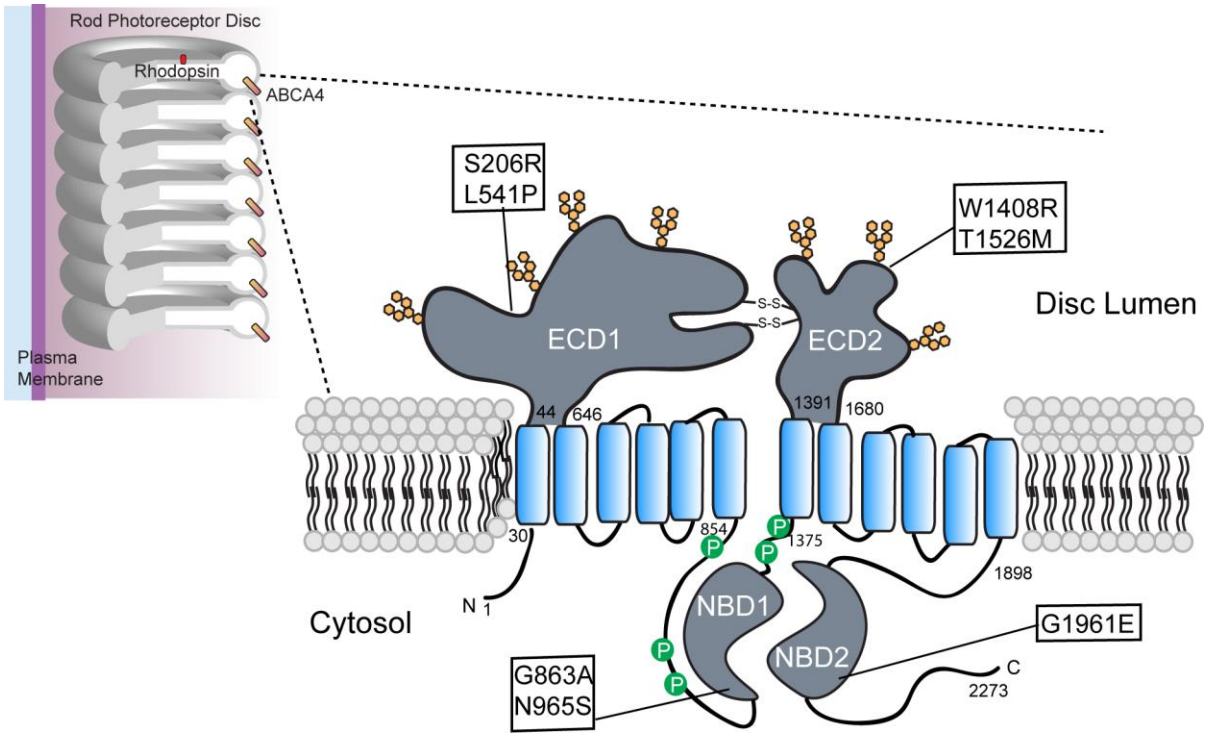

Figure 1.9 General Topology of ABCA4 with Disease Mutations

Cross-section of rod photoreceptor representing rod discs and the rim region localization of ABCA4. The general topological model for ABCA4 showing the exocytoplasmic domains (ECD), transmembrane domains, and nucleotide binding domains (NBD) in both the N- and C-tandem halves of the transporter. N-linked glycosylated chains are shown with hexagons, disulfide bonds are shown in ECD1 and ECD2. The phosphorylation sites are shown in the cytosolic NBD1 (Tsybovsky et al., 2011). Two intramolecular disulfide bonds are inferred from ABCA1 biochemical studies (Hozoji et al., 2009). Location of several characterized Stargardt disease variants in the soluble domains of ABCA4.

1.4.3.3.1 ABCA4 Knockout Mice

In addition, Travis and colleagues examined the role of ABCA4 by generating and characterizing *Abca4*$^{-/-}$ mice (Mata et al., 2000; Weng et al., 1999). The mice retinas showed well-preserved outer segments devoid of disorganization often associated with photoreceptor degeneration. Ultrastructural studies of mice exposed to cyclic light conditions revealed the presence of lipofuscin in the RPE cell layer and increased levels of A2E species was observed by HPLC chromatographic analysis. Furthermore, compared to WT, light-dependent elevated levels of all-*trans* retinal, PE, and *N*-retinylidene PE were observed. A similar accumulation of A2E and related bisretinoids in the RPE have been found in tissue samples of SD individuals (Delori et al., 1995; Mata et al., 2000). More recently, Boyer *et al.* confirmed the finding that *Abca4*$^{-/-}$ mice show a large increase in A2E and lipofuscin, in large part by 11-*cis* retinal, compared to WT mice, but in this study the increase in A2E in *Abca4*$^{-/-}$ mice was light-independent (Boyer et al., 2012). Free 11-*cis* retinal, for instance, may form *N*-retinylidene PE with disc PE and generate A2E precursors. In addition, studies in *Abca4*$^{-/-}$ mice show excessive RPE lipofuscin accumulation and photoreceptor cell death (Bui et al., 2006). Specifically, albino *Abca4*$^{-/-}$ mice display progressive photoreceptor cell loss from 8 months to 12 months old mice (Radu et al., 2008).

1.4.3.3.2 ABCA4 and the Visual Cycle

Do the biochemical and genetic findings explain the role of ABCA4 in the visual cycle? On the cytoplasmic surface of disc membranes, all-*trans* retinal is reduced to all-*trans* retinol by RDH8 and is subsequently converted to 11-*cis* retinal in RPE cells as discussed earlier. When all-*trans* retinal partitions in the bilayer of discs after photoexcitation and dissociation from opsin, a fraction also reacts with PE and maintains equilibrium with the

Schiff base conjugate, *N*-retinylidene PE. However, *N*-retinylidene PE formed on the lumen side cannot undergo dissociation from equilibrium and, hence, reduction. ABCA4 is proposed to bind and translocate or flip *N*-retinylidene PE from the lumen to the cytoplasmic side of the disc membrane utilizing ATP hydrolysis. Once *N*-retinylidene PE reaches the cytoplasmic side of the disc membrane it dissociates into PE and all-*trans* retinal with the latter available for subsequent reduction. ABCA4 mediated retinal transport to the cytoplasmic side of the disc membrane may be very small but ABCA4 insures that all-*trans* retinal produced from the photobleaching of rhodopsin is made accessible for reduction thereby preventing accumulation of retinoids in the disc membrane. Given the rapid binding of 11-*cis* retinal to opsin, it is unclear how ABCA4 regulates flipping of 11-*cis* retinylidene PE in a similar manner. Measuring *N*-retinylidene-PE across the disc membrane will help clarify the role of ABCA4 in all-*trans* and 11-*cis* retinal transport across disc membranes. In addition, with the sequence similarity and topology of ABCA1 and ABCA7, the proposed direction of transport of ABCA4 from the lumen to the cytoplasm is opposite for mammalian ABC transporters involved in lipid and drug export and a functional assay is needed to understand the directionality of transport.

1.4.3.3.3 ABCA4 and Implication in Stargardt Disease

The loss of photoreceptors and death of RPE that occurs in patients in SD are traditionally considered to result from accumulation of A2E and lipofuscin. Correct molecular diagnosis and genotype-phenotype correlations are important for understanding the broad spectrum of ABCA4 mutations. Possible roles of ABCA4 involving residual/lost activity, impaired expression, and protein misfolding are generally viewed as multiple pathways contributing to lipofuscin formation.

In a large-scale recombinant mutation analysis by Sun *et al*. (2000), examination of mutations according to topology highlighted distinctive differences in the retinal-stimulated ATP hydrolysis (Sun et al., 2000). Abolished ATP binding among variants expressed with similar protein yield compared to wild-type occurred with some mutations within either of the two NBDs (T971N, L1971R, G1977S, and E2096K) (Fig 1.9). Low activity was observed for S206R and L541P in the ECD1 domain, but the defects in ATPase were mild for W1408R and T1526M in ECD2. While several NBD1 mutants (N965S, T971N, A1038V) had low basal ATPase activities with residual retinal stimulation, NBD2 mutants (G1961E, L1971R, G1977S) displayed either retinal inhibition or slightly enhanced basal and retinal stimulated activities. These studies suggest the coupling nature of the NBDs to effect conformational changes to the TMDs, as described for Pgp. Furthermore, Sun *et al*. noticed that, in HEK293T expression studies, ABCA4 mutants particularly in the TMDs have reduced protein amounts and defective azido-ATP labeling, indicative of a less-folded protein (Sun et al. 2000). G818E in TMD1 had disrupted yield and reduced ATP binding. In addition, two in-frame deletions and G851D and G1886E introducing charged amino acids into TMDs also showed reduced amounts of protein. Using *Xenopus Laevis*, Wiszniewski *et al.* transgenically introduced ABCA4 mutants and newly synthesized ABCA4 showed protein retention in the ER and inner segments (Wiszniewski et al. 2005). Quality control is imposed when the folding process fails and ABCA4 doesn't traffic to outer segments leading to cellular stress. A strong disease link exists in cystic fibrosis, which results in loss of Cl^- channel activity and the most common mutant, CFTR-ΔF508, barely escapes the ER (Riordan, 2008). Several small molecules termed 'chemical chaperones' identified through high-throughput screens are effective in stabilizing polypeptide folding and rescuing the

trafficking defect exhibited by CFTR-ΔF508 in cells (Pedemonte et al., 2005; Van Goor et al., 2006). Determination of appropriate chemical chaperones may be useful for treating misfolded ABCA4 proteins.

In humans, mutations in NBD1 and NBD2 that result in only a single functional copy adversely affects the retina tissue that have distinct spots of lipofuscin accumulation and RPE and atrophy. G863A in NBD1 is a common allele in Northern Europe and genotype-phenotype correlations suggest that it is a substantially impaired allele (Maugeri et al., 1999). Another NBD1 mutant, N965S is a mild allele and that leads to severe SD when paired with a more severe allele (Rosenberg et al., 2007). Functional defects include mild atrophy of RPE, slowed dark adaptation and have a medium to severe impact on phenotype (Fig 1.10). In NBD2, G1961E had reduced visual acuity with patients of advanced disease progression demonstrating extensive atrophy of the RPE and the choroid (Fig 1.10) (Fishman et al., 1999; Genead et al., 2009; Lewis et al., 1999). Deriving biochemical data on ABCA4 disease mutations through a functional assay is essential to understand the SD disease mechanisms.

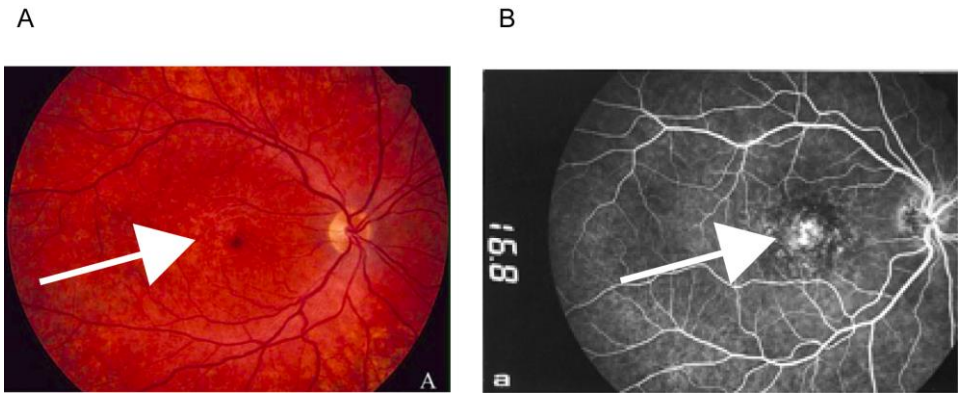

Figure 1.10 Stargardt Disease Patient Eyes with Affected Macula

A. Photograph of the interior retina of the eye of a patient homozygous for ABCA4-N965S in a 17 yr old patient. Punctate atrophy in the macula and peripheral regions are observed. (Rosenberg et al., 2007) B. Injection of fluorescent dye into the systemic circulation and photograph of emitted fluorescence from a patient with ABCA4-G1961E mutation on a single allele. RPE atrophy observed largely in the macula (Simonelli et al., 2000)

Accumulation of lipofuscin precedes macular degeneration and visual loss in SD patients (Cideciyan et al., 2004). A2E has an injurious effect on RPE function and survival. At sufficient concentration, it exerts detergent properties and acts as an inhibitor of RPE degradative processes (Sparrow et al., 2006; Sparrow et al., 1999). Several bisretinoids including A2E are also differentially photoreactive and cause DNA base lesions, proteasome stress, and protein modifications resulting in RPE cell death (Sparrow et al., 2003; Sparrow et al., 2010). In SD, lipofuscin may (1) accumulate in RPE cells; (2) functionally impairs and degenerates RPE owing from A2E cytotoxicity; (3) and results in secondary cell death of photoreceptors leading to blindness (Travis et al., 2007). One avenue to counter A2E accumulation is to reduce the presence of A2E precursors, in particular *N*-retinylidene PE. In ATPase studies, amiodarone, an antiarrhythmic drug, enhanced retinal stimulated activities of ABCA4 and may provide support for a role in alleviating residual activity among SD mutants (Sun et al., 1999).

By contrast, excess all-*trans* retinal also elicits light-induced retinal degeneration in mice due to loss of ABCA4 in combination with Rdh8 and Rdh12. The *Rdh8*$^{-/-}$*Abca4*$^{-/-}$ retinas displayed progressive severe degeneration. The *Rdh8*$^{-/-}$*Rdh12*$^{-/-}$ retinas showed slow, mild rod/cone dystrophy (Atshaves et al., 2007; Maeda et al., 2008; Maeda et al., 2007). Critically, A2E accumulation was highest in *Rdh8*$^{-/-}$*Rdh12*$^{-/-}$*Abca4*$^{-/-}$ and *Rdh8*$^{-/-}$*Abca4*$^{-/-}$mice and was at least 3- and 2-fold higher than *Abca4*$^{-/-}$ knockout mice (Maeda et al., 2009b). However, both mice combinations did not elicit retinal degeneration under dark conditions. In addition, all-*trans* retinal dimer is a significant generator of singlet oxygen compared to A2E (Kim et al., 2007). All-*trans* retinal may accumulate in the disc lumen and within other compartments

and the distribution may also lead to variation of the onset and progression of SD. ABCA4 frees the intracellular retinal buildup and facilitates the proper functioning of the visual cycle.

1.5 Thesis Investigation

To complement the genetic and biochemical studies, this thesis examines the biochemistry of ABCA4 to assess the direction and transport of the proposed substrate. Furthermore, given its structural similarity in the ABCA subfamily, the phospholipids/other lipids transported by several ABCA transporters are investigated. Little is known about the defects of SD mutations prompting the analysis of drug interaction and protein folding rescue of ABCA4.

Chapter 2 introduces the development of retinal exchange using artificial liposomes. Added synthesized radiolabeled retinal partitions into two different liposomes: empty acceptor liposomes and donor proteoliposomes reconstituted with purified ABCA4. ABCA4 mediates the ATP-dependent transport of *N*-retinylidene PE from the lumen to the cytosolic side of proteoliposomes. The retinal released from the Schiff base conjugate then further partitions to the empty liposomes in a time-dependent manner. When *N*-retinyl PE and *N*-retinylidene PE are present, *N*-retinyl PE binds and competitively inhibits the ABCA4 transfer reaction. Membrane vesicles derived from bovine and mice rod outer segments further established the direction of transfer and transport properties of retinal. A fluorescent lipid assay was used to define lipid specificity and properties of this membrane protein. This study provided the first direct biochemical evidence that ABCA4 is involved in retinal clearance from outer segment disc membranes and that a mammalian ABC transporter can serve as an active substrate importer.

Chapter 3 probes the relevance of 11-*cis* retinal handling by ABCA4 and by photoreceptor membranes. In ATPase analysis, 11-*cis* retinal stimulates ABCA4 much more efficiently with a 3-fold increase in activation compared to 2-fold activation with all-*trans* retinal. ABCA4 also flips 11-*cis* retinylidene PE from the lumen to the cytosolic side of proteoliposomes. A pivotal question is how 11-*cis* retinal fluxes are tightly controlled in photoreceptors. Significant levels of 11-*cis* retinal isomerization occur due to the presence of phospholipid PE in rod outer segments, although all-*trans* retinal also shows partial isomerization to 13-*cis* retinal. The rate of all-*trans* and 11-*cis* retinal isomerization with naturally or synthetic lipid mixtures was characterized by normal-phase HPLC analysis. Formation and levels of A2PE/A2E was investigated by reverse-phase HPLC analysis. On the basis of these studies, a retinal-flux balance model is proposed.

In chapter 4, we identify and characterize the phospholipid substrates transported by homologous members of the ABCA subfamily: ABCA1, ABCA7, and ABCA4. The fluorescent flippase assay shows how ABCA1 and ABCA7 transport phospholipids, PC and PS, in the export direction unlike ABCA4 transporting PE in the opposite direction. Disease mutations of Tangier disease (ABCA1) and Stargardt disease (ABCA4) in various domains including the TMDs, NBDs, and ECDs were constructed and the effect of these mutants on expression, lipid flipping, ATP hydrolysis, and cellular localization were investigated.

In chapter 5, we report that dronedarone allosterically activates ABCA4 producing synergistic activity ATPase activity and enhanced *N*-retinylidene PE transport capabilities. A series of mutants generated from near or in NBDs revealed how structurally unrelated compounds achieve specific enhanced transport in the mutated protein, which in some mutants show transport rescue to WT levels. In addition, disease causing mutants often result

in low protein levels after. Of the three chemical and pharmacological chaperones tested, 4-phenylbutyrate was the most effective at restoring NBD1 mutants to near wild-type levels. These findings reveal an unexpected aspect of the pharmacology of dronedarone and 4-phenylbutyrate and might translate into their improved medical use.

Table 1.1 Mammalian ABC Transporters, Related Lipid Substrates, and Associated Genetic Disorders

Gene	Major sites of expression	Substrates	Modulators	Acceptors	Associated genetic disorders
ABCA1	Ubiquitous	PC, PS, Chol, SM	Cer (stimulates), LacCer (inhibits)	ApoA-I, A-II, E,	Tangier disease
ABCA2	Brain	Chol, PE, PS		LDL	
ABCA3	Lung, brain, heart, pancreas	PC, PG, PE		Surfactant	Neonatal surfactant lung deficiency, chronic interstitial lung disease
ABCA4 (ABCR)	Rod photoreceptors	*N*-ret-PE, PE	All-*trans* retinal 11 *cis*-retinal	(Cytosolic)	Stargardt disease, cone-rod dystrophy, retinitis pigmentosa, age-related macular degeneration
ABCA7	Myelolymphatic system, brain, kidney, skin	PC, SM, Chol, (PS?)		ApoA-I/Apo-A-II, ApoE disc	(Sjogren's syndrome?)
ABCA12	Skin keratinocytes	Cer, GlcCer			Harlequin ichthyosis, lamellar ichthyosis type 2
ABCB1 (Pgp)	Brain, liver, kidneys, GI, placenta	PC, PS, PE, Chol, SM, GlcCer, PAF	short chain PC (8:0), DHA PC (22:0) (inhibits)		
ABCB4	Liver, canalicular membrane, placenta	PC, PE, SM		Bile salts	Progressive familial intrahepatic cholestasis type 3
ABCB11	canalicular membrane	Bile salt			Progressive familial intrahepatic cholestasis type 2
ABCC1	Ubiquitous	PC, PS, SM, GlcCer	GSH (stimulates)		

Gene	Major sites of expression	Substrates	Modulators	Acceptors	Associated genetic disorders
ABCG1	Ubiquitous	Chol, PS, PC, SM,	Thyroxin (inhibits) Benzamil (inhibits) SM (stimulates)	HDL, LDL, PC vesicle, BSA, cyclodextrin	
ABCG2	Placenta, breast, liver, GI	PC, PS	Chol (stimulates)		
ABCG4	Macrophage, brain, eye, spleen, liver	Chol			
ABCG5/ G8	Liver, GI	Plant sterols, Chol		HDL, Bile salts	β-Sitosterolemia

Apo, apolipoprotein; Cer, ceramide; Chol, cholesterol; DHA, docosahexaeonic acid; LacCer, Lactosylceramide; LDL, low density lipoprotein; GlcCer, glucosylceramide; GSH, glutathione, GI, gastrointestinal tract; ; HDL, high-density lipoprotein; PAF, platelet activating factor

Chapter 2: The ABC Transporter ABCA4 Linked to Stargardt Disease Functions as an *N*-retinylidene-phosphatidylethanolamine and Phosphatidylethanolamine Importer*

2.1 Introduction

ABCA4 is a member of the superfamily of eukaryotic ABC transporters involved in the export/translocation of chemically diverse substrates from the cytoplasm to the extracellular side of cellular membranes (Allikmets et al., 1997; Dean and Allikmets, 1995). Heritable mutations in the ABCA4-encoding gene result in Stargardt disease, an autosomal recessive disease associated with the loss in central vision, a delay in dark adaptation, macular accumulation of fluorescent deposits, and progressive atrophy of photoreceptor and RPE cells (Fishman et al., 1991; Weleber, 1994).

Following photoexcitation of photoreceptor cells, all-*trans* retinal rapidly diffuses across lipid bilayers and between disc organelles and the plasma membrane (Noy and Xu, 1990; Rando and Bangerter, 1982). In the presence of disc phospholipid PE, the most abundant form of free all-*trans* retinal exists as an equilibrium mixture with a Schiff base conjugate, *N*-retinylidene PE. ABCA4, which specifically binds to *N*-retinylidene PE, is expressed at the rim regions of photoreceptor disc organelles where it is implicated in the removal of *N*-retinylidene PE from disc membranes (Allikmets et al., 1997; Beharry et al., 2004; Illing et al., 1997). Previous characterizations have shown that ABCA4 ATPase activity is stimulated at least 2-fold by all-*trans* retinal in a phospholipid PE-dependent

* This chapter is available as a published article.
Quazi. F, Lenevich, S., Molday, RS. (2012). The ABC Transporter ABCA4 Linked to Stargardt Disease Functions as an *N*-retinylidene-phosphatidylethanolamine and Phosphatidylethanolamine Importer. Nat Comm. 3:925

manner (Ahn et al., 2000; Sun et al., 1999). Moreover, *Abca4*$^{-/-}$ mice display a light-dependent accumulation of all-*trans* retinal, PE, and *N*-retinylidene PE in the retina, and accumulation of lipofuscin and A2E in RPE cells (Mata et al., 2000; Weng et al., 1999). Hypothesis for ABCA4 retinoid transporter includes the active clearance of all-*trans* retinal and related retinoids from the lumen to the cytosolic side disc membranes. However, the precise role of ABCA4 and the nature of transport direction during this process remain uncertain.

Here we demonstrate the development of a biochemical transport assay assessing retinal transfer activity between two artificial liposome populations. Purified ABCA4 reconstituted into donor proteoliposomes actively transports *N*-retinylidene PE from the inner to the outer leaflet of vesicles. The dissociating substrate in the outer leaflet results in a net transfer of all-*trans* retinal to empty acceptor liposomes. Notably, disc membrane vesicles derived from bovine and mice outer segments, but not *Abca4*$^{-/-}$mice, showed robust *N*-retinylidene PE transport activities. Additionally, purified ABCA4 was also able to flip fluorescent-labeled PE in the same direction from the lumen to cytoplasmic side of proteoliposomes. Importantly, Stargardt disease mutant proteins exhibited reduced transport activities. These findings demonstrate the first evidence of a mammalian ABC transporter serving as an active importer uniquely localized in photoreceptor cells. The transport assay forms a starting point for characterizing disease mutations in a biochemical quantitative-manner and will be relevant for understanding mechanisms of Stargardt disease.

2.2 Experimental Procedures

2.2.1 Materials

Porcine brain polar lipid (BPL), 1,2 dioleoyl-*sn*-glycero-3-phosphoethanolamine (DOPE), 1,2 dioleoyl-*sn*-glycero-3-phosphocholine (DOPC), fluorescent-labeled [7-nitro-2-1,3-benzoxadiazol-4-yl)] phospholipids, C6 *NBD*-PS (Fl-PS), C6-*NBD*-labeled-PC (Fl-PC), C6-*NBD*-labeled-PE (Fl-PE), C-12-*NBD*-labeled-PE 1,2-dioleoyl-*sn*-glycero-3-phosphoethanolamine-N-(7-nitro-2-1,3-benzoxadiazol-4-yl) (*N*-Fl-PE), 1,2-dioleoyl-*sn*-glycero-3-phosphoethanolamine-N-(lissamine rhodamine B sulfonyl) (*N*-Rh PE) were purchased from Avanti Polar Lipids (Alabaster, AL). ATP, ADP, and AMP-PNP were purchased from Sigma, dithionite was from Fisher, CHAPS was from Anatrace (Maumee, OH), radiolabeled sodium borohydride (NaB^3H_4) was obtained from American Radiolabeled Chemicals, [α^{32}P] ATP was from Perkin Elmer. Organic solvents (chloroform, hexane, methanol) were HPLC grade and water was distilled and deionized. All-*trans* retinal was radiolabeled and isolated as described Garwin and Saari and stored under N_2 gas (Garwin and Saari, 2000). Stock solutions of ATP, ADP, and AMP-PNP were adjusted to pH 7.5 with NaOH and filter sterilized. Buffers were degassed, filter sterilized, and light protected prior to usage. Assays and reactions performed with retinoids were light protected. The extinction coefficients for all-*trans* retinal, all-*trans* retinol, *N*-retinyl PE, and all-*trans* retinal oxime were 42.9, 52.8, 37.8, and 59.3 $mM^{-1}cm^{-1}$ (Bindewald et al., 2005; Plack and Pritchard, 1969). The Rim3F4 and Rho1D4 monoclonal antibodies have been described previously (Illing et al., 1997; MacKenzie et al., 1984).

2.2.2 Isolation of Retina and Outer Segment Membranes

Retina and ROS membranes from frozen bovine retinas were prepared as previously described (Chan et al., 2008; Molday and Molday, 1987; Papermaster and Dreyer, 1974).

2.2.3 Generation of ABCA4 Mutant Constructs

Human ABCA4 with a C-terminal 1D4 tag subcloned into a pCEP4 vector (Invitrogen) at its *Not*I/*AsiS*I sites was used as a template for site-directed mutagenesis. Mutations were introduced by overlap-extension PCR using Pfu DNA polymerase and the following mutagenic primers (with introduced mutations shown in bold): G863Af, gagcccct**agcc**gaggaaacg; G863Ar, cgtttcctc**ggc**taggggctc, N965Sf, gcattcctgggccac**agc**ggagctgggaaaacc; N965Sr, ggttttcccagctcc**gct**gtggcccaggaatgc. G863A was constructed with ABCA4-fwd (aatattgcggccgccaccatgggcttcgtgagac) and ABCA4-*Fse*I-rev (gccacagggctcaaaaatct) primers and subcloned into the *Not*I and *Fse*I sites of the ABCA4 construct. N965S was constructed with ABCA4 *Fse*I-Fwd (agatttttgagccctgtggc) and ABCA4-*Sbf*I-rev (ccctggtgctgcacctgc) primers and subcloned into the *Fse*I and *Sbf*I sites. K969M, K1978M, K969M/K1978M previously cloned into ABCA4-pcDNA3 (Ahn et al., 2000) were cut out *via Fse*I and *Sbf*I restriction sites and replaced as inserts into the ABCA4-1D4-pCEP4 vector. The presence of these mutations was confirmed by DNA sequencing.

2.2.4 Expression and Purification of ABCA4-1D4 from HEK293T Cells

Wild-type (WT) and mutant ABCA4 containing a 9 amino acid 1D4 tag (T-E-T-S-Q-V-A-P-A) in pCEP were expressed in HEK293T cells as previously described (Zhong et al., 2009). For purification, a cell suspension from two 10-cm dishes was added slowly to 1.0 ml Buffer B (50 mM HEPES, pH 7.6, 0.5 mg/ml BPL, 100 mM NaCl, 1 mM DTT) containing 18 mM CHAPS and protease inhibitor and stirred for 60 min at 4 °C. The supernatant after a

10 min centrifugation at 100,000 ×g (TLA110.4 rotor in a Beckman Optima TL centrifuge) was mixed with 100 µl of Rho1D4-Sepharose 2B for 1 h at 4 °C. The matrix was washed six times in Buffer B containing 10 mM CHAPS and the ABCA4 protein was eluted twice at 12 °C over 30 min in the same buffer with 0.2 mg/ml Rim 1D4 peptide.

2.2.5 Purification of ABCA4

The Rim3F4 monoclonal antibody conjugated to Sepharose 2B was used to isolate ABCA4 from 3-[(3-cholamidopropyl)dimethylammonio]-2-hydroxy-1-propanesulfonate (CHAPS)-solubilized bovine ROS membranes and the Rho1D4 monoclonal antibody conjugated to Sepharose 2B was used to purify WT and mutant ABCA4 containing a C-terminal 9 amino acid 1D4 tag (T-E-T-S-Q-V-A-P-A) from CHAPS-solubilized, transfected HEK293T as described previously (Ahn et al., 2000) (Zhong et al., 2009). In each case, the purified ABCA4 was directly used for reconstitution into proteoliposomes.

2.2.6 Preparation of Donor Proteoliposomes and Acceptor Liposomes

For proteoliposomes, dioleoylphosphatidylcholine (DOPC), dioleoylphosphatidylethanolamine (DOPE), and porcine brain polar lipid (BPL) obtained from Avanti Polar Lipids were mixed at a weight ratio of 6:2:2 and dried under N_2. BPL was used in our studies since earlier studies suggested that this phospholipid mixture having variable fatty acyl groups was required to stabilize functional ATPase activity of ABCA4 (Sun et al., 1999). The donor lipids were resuspended at a concentration of 5 mg/ml in buffer containing 20 mM (4-(2-hydroxyethyl)-1-piperazineethanesulfonic acid (HEPES) buffer, pH 8.0, 150 mM NaCl, 2 mM $MgCl_2$, and 18 mM CHAPS with bath sonication. The donor lipids and the ABCA4 protein (in CHAPS detergent with dithiothreitol (DTT) were mixed to yield a final protein-to-lipid ratio of 1:100 (wt/wt) with a reduction in CHAPS concentration

to 6 mM. After incubation at 4 °C for 1 h, the detergent was removed by dialysis at 4 °C over a 24 h period with a minimum of 3 changes of buffer containing 10 mm HEPES, pH 8.0, 150 mM NaCl, 2 mM $MgCl_2$, and 1 mM DTT. For acceptor liposomes, DOPC and DOPE at a weight ratio of 7:3 were resuspended in 20 mM HEPES pH 8.0, 150 mM NaCl, 2 mM $MgCl_2$, and 18 mM CHAPS with 300 mM sucrose, incubated at room temperature for 4 h, and dialyzed as above against 10 mM HEPES, pH 8.0, 300 mM sucrose, 2 mM $MgCl_2$, and 1 mM DTT. Vesicle sizes were measured on a Nicomp Submicron Particle Sizer Model 370. Proteoliposomes displayed a narrow Gaussian distribution with vesicles having a mean diameter of 74 ± 18.8 nm; liposomes containing 10% sucrose showed a wider distribution in the range of 50-450 nm and a mean diameter of 203.2 ± 115.8 nm.

2.2.7 Measurement of ATP-Dependent [^{3}H]-All-*Trans* Retinal (ATR) Transfer

[^{3}H] all-*trans* retinal ([^{3}H]-ATR) or [^{3}H] all-*trans* retinol (1.68 kBq, 3.36 GBq/mmol) was dried under N_2 for 5 min. and subsequently incubated with donor proteoliposomes for 2 h at 4 °C. Reconstituted proteoliposomes (~40 µl) containing approximately 1 µg of protein were added to 200 µl of buffer B (20 mM HEPES, pH 8.0, 150 mM NaCl, 3 mM $MgCl_2$, and 1 mM DTT). Prior to the reaction, a total of 200 µg, ~20 µl, of acceptor liposomes were added to the reaction mixture reducing the external sucrose concentration to 30 mM. The tubes were wrapped in tin-foil and reaction was typically carried out for a 60 min at 37 °C in the presence of 1 mM ATP or AMP-PNP. The reaction mixture was then added to the top of a centrifuge tube containing 2.5 ml separation buffer (20 mM HEPES, pH 8.0, 75 mM NaCl, 150 mM sucrose) and centrifuged using a Beckman TLA110.4 rotor at 100,000g for 20 min. The difference in the densities of the two vesicles was sufficient for separation by centrifugation. The supernatant was transferred to a scintillation vial and the pellet was

resuspended in 200 μl of buffer B and transferred to a second scintillation vial. The radioactivity of the fractions was determined by liquid scintillation counting. ABCA4 proteoliposomes with acceptor vesicles in the absence of nucleotide was used as a control to subtract the background counts primarily arising from the spontaneous [^{3}H]-retinoid partitioning between the proteoliposomes and liposomes from nucleotide treated reactions. For substrate competition assays, all-*trans* retinal was used at 10 μM together with increasing concentrations of unlabeled all-*trans* retinol and *N*-retinyl PE.

2.2.8 Preparation of Rod Outer Segment (ROS) Disc Vesicles

Bovine ROS (25 mg) purified from previously frozen retina were used to prepare disc vesicles by the Ficoll centrifugation procedure (Smith et al., 1975). The sealed disc vesicles collected at the Ficoll-water interface were washed with 20 mM Tris, pH 7.6 and stored in 20 mM Tris, pH 7.6, and containing 600 mM sucrose.

Mouse retina dissected from three month old wild type and *abca4* knockout (*abca4*$^{-/-}$) mice (Kim et al., 2004) and resuspended in 10 mM Tris, pH 7.6, 20% sucrose. For each experiment, 5 retinas from WT and *abca4*$^{-/-}$ resuspended in 0.25 ml buffer were vortexed for 30-60s. The samples were then centrifuged at 200g for 40 s, and the supernatant containing ROS was gently removed. This was repeated six times. The supernatant was loaded on 50% sucrose in 20 mM Tris, pH 7.6, and centrifuged in a TLA55 rotor at 40,000 g for 45 min at 4 °C. ROS was collected on top of the 50% sucrose buffer layer, washed 3 times in buffer (10 mm HEPES pH 8.0, 100 mm NaCl, 1 mm $MgCl_2$) and layered on 20 mM Tris, pH 7.6, 30% sucrose for a second round of purification. The ROS was subjected to osmotic lysis treatments in 10 mM Tris, pH 7.6, 1 mM EDTA for 1 h and in 2 mM Tris, pH 7.6 for 5 h. The ROS disc vesicles were washed three times by centrifugation at 40,000 g in a TLA110

rotor and treated with neutralized 3 mM hydroxylamine for 10 min. The disc vesicles were subsequently washed three times to remove excess hydroxylamine and retinyloxime and resuspended in buffer C (10 mM HEPES pH 8.0, 100 mM NaCl, 300 mM sucrose, 1 mM $MgCl_2$) for the retinal transfer assays.

2.2.9 Retinoid Transfer Assay in Bovine/Mouse Outer Segment Disc Vesicles

For retinoid transfer studies from ROS disc vesicles, acceptor liposomes consisting of DOPC/DOPE (7:3) were prepared by sonication in buffer B. Bovine vesicles were bleached and the endogenous retinal was derivatized with 5 mM of freshly neutralized hydroxylamine for 30 min at 25 °C. The bovine vesicles were then washed thrice with buffer C at 50,000 g and resuspended in the same buffer. [^{3}H]-all-*trans* retinal (1.68 kBq, 3.36 GBq/mmol) was dried under N_2 for 5 min and incubated together with unlabeled all-*trans* retinal (2.5 - 30 μM) with 30 μg of bovine ROS disc vesicles for 1 h at 30 °C with 200 μg acceptor vesicles, 1 mM ouabain, 5 mM ATP or AMP-PNP or buffer (control). A higher concentration of nucleotide was used in these studies to compensate for the ouabain-insensitive endogenous ATPase activity of ROS disc membranes. Reactions were then layered on top of a 2.5 ml of separation buffer containing 10 mM HEPES, pH 8.0, 600 mM sucrose and centrifuged at 100,000 g for 20 min. After the separation, the supernatant was removed and the pelleted ROS disc vesicles were resuspended in buffer C and radioactivity determined with liquid scintillation counting. In this case, the ROS disc vesicles were present in the pellet while the acceptor vesicles remained in the supernatant atop the sucrose gradient. Control reactions with acceptor vesicles and ROS vesicles (bovine/mice) and no nucleotide addition were used as control to subtract radioactivity from retinal partitioning between vesicle populations. At least three independent experiments were performed for each transfer reaction.

2.2.10 Fl-Labeled Phospholipid Flipping Assay

Samples were prepared by adding 40 µl proteoliposomes with 0.6% Fl-labeled lipid (w/w) to 50 µl of buffer containing 20 mM HEPES, pH 7.0, 100 mM NaCl, 5 mM $MgCl_2$, 1 mM DTT. To initiate transport, ATP (1 mM) or AMP-PNP (1 mM) was added to the proteoliposomes for 1 h at 37 °C. The fluorescence was recorded with a Varian spectrofluorometer using excitation and emission wavelengths of 468 nm and 540 nm, respectively. After a baseline was established, 4 mM of sodium dithionite solution in 1 M Tris-HCl (pH 10.0) was added to quench the fluorescence of Fl-labeled lipids in the outer leaflet of the proteoliposomes. When a baseline was re-established, the proteoliposomes were permeabilized by adding 1% Triton X-100 (TX-100). The net percent NBD-labeled lipid translocated in the proteoliposomes was calculated from the difference that was accessible to dithionite (outer leaflet), or protected from dithionite (inner leaflet), using the following equations.

$$\% \text{ accessible (outer leaflet)} = [(F_T - F_D)/(F_T - F_0)] \times 100$$

$$\% \text{ protected (inner leaflet)} = [(F_D - F_0)/(F_T - F_0)] \times 100$$

where F_T is the total fluorescence of the sample before addition of dithionite, F_D is the fluorescence of the sample following quenching with dithionite, and F_0 is any residual fluorescence of the sample following permeabilization with TX-100.

2.2.11 Analysis of Retinoid Binding

Solid phase binding assay using [^{3}H]-labeled all-*trans* retinal was carried out as described previously (Zhong et al., 2009). All incubations were carried out at 4 °C. Briefly, HEK293T cells transfected with 1D4-tagged ABCA4 were harvested from one dish, centrifuged at 2800×g for 3 min, and resuspended in 0.5 ml solubilization buffer. The

supernatant fraction obtained after centrifugation (100,000 g for 10 min) was incubated with 30 µl Rho1D4-Sepharose 2B immunoaffinity matrix pre-equilibrated in column buffer. After 1h, the matrix containing the bound 1D4-tagged protein was washed several times with 0.4 ml column buffer by low speed centrifugation and mixed with 0.25 ml of 10 µm [^{3}H]-labeled all-*trans* retinal (specific activity of 500 dpm/pmol, 2.5 x 10^6 dpm total) in column buffer for 30 min. The matrix was washed several times with 0.4 ml column buffer to remove unbound [^{3}H]-labeled all-*trans* retinal and then incubated in the presence or absence of 0.5 mM ATP, for 15 min. The matrix was washed 2 more times with 0.4 ml column buffer before being transferred to Ultrafree-MC (0.45 µm filter) spin column (Millipore). The samples containing the immobilized 1D4 tagged ABCA4 protein was extracted from the matrix with 0.5 ml of ice-cold ethanol for 15 min at room temperature and eluted by centrifugation. Radiolabeled all-*trans* retinal in the ethanol extractions was determined by liquid scintillation counting.

2.2.12 Preparation and Purification of *N*-retinyl PE

Synthesis of *N*-retinyl PE was carried out under dim light in glassware wrapped in aluminum foil to minimize photoisomerization of retinoids. Freshly prepared solutions of all-*trans*-retinal (29 mg, 0.1 mmol) in 1 ml of methanol and 1,2-dioleoyl-sn-glycero-3-phosphatidylethanolamine (100 mg, 0.135 mmol) in 2 ml of chloroform were mixed and incubated at room temperature for 1 hour. The color of the reaction mixture changed from yellow to deep red due to formation of corresponding Schiff base. $NaBCH_3CN$ (31 mg, 0.5 mmol) was added and the reaction mixture was stirred for 12 hours. The color of the reaction mixture gradually changed from deep red to light yellow. Five ml of $CHCl_3$ was added to the reaction mixture and $NaBH_3CN$ was neutralized by addition of 5 µL of water. Organic layer (bottom layer) was collected, concentrated under reduced pressure and the product was

purified by flash chromatography ($CHCl_3$: MeOH = 8:1) yielding *N*-retinyl PE with a 40 % yield. The desired product was contaminated with cis isomers of retinyl-PE (~10% impurities total based on normal phase HPLC with diode array detection at 330 nm). The analytically pure sample was purified by normal phase HPLC purification (gradient elution starting with 100% "A"= 100% $CHCl_3$+0.2% Et_3N (v/v), linear change over the course of 40 minutes to 100% "B" = 100% MeOH +0.2% Et_3N (v/v), followed by 100% B (10 minutes), linear gradient to 100% A (2 minutes) and equilibration of the column with 100% A (15 minutes). ^1H NMR (300 MHz, $CDCl_3$): 10.105 (broad singlet, 2H, $(R_2N\underline{H}_2)^+$); 6.668 (t, j = 11.7 Hz, 1H, a); 6.1-6.4 (m, 4H, a); 5.652 (broad s, 1H, a); 5.348 (s, 4H, a); 5.234 (s, 1H, a); 4.270 (dd, j=67.5 Hz, j=11.7 Hz, 4H, b); 4.106 (d j=42.6 Hz, 2H, b); 4.035 (broad m, 2H, b); 3.785 (broad s, 2H, c); 3.097 (broad s, 2H, d); 2.294 (two overlapping triplets, j=8.0 Hz, 4H, e); 2.2-2.4 (m, 5 H); 1.91-2.05 (m, 18 H); 1.900 (s, 3H); 1.722 (s, 3H); 1.52-1.65 (m, 5H); 1.4-1.5 (m, 3H); 1.2-1.4 (broad s, 56H); 1.038 (s, 9H); 0.8-0.9 (m, 10H). ^{31}P: 0.703 (s). Mass Spec: Sample was dissolved in 80:20:0.2=CH_3CN:H_2O:formic acid and infused directly on Agilent LC/MSD 3D Ion Trap instrument. MH^+ calculated =1012.77; observed 1012.7; MS/MS on 1012.7 peak yields 408.3; 603.7; 625.7; 723.7; 766.8; 951.9; 978.8; 992.9.

2.2.13 ATPase Assay

ATP assays were carried out using [α-32P]ATP (PerkinElmer Life Sciences) and thin layer chromatography as previously described (Ahn et al., 2000). ATPase assays were carried out in a 10-µl total reaction volume consisting of 8 µl (20–40 ng) of reconstituted protein and 1 µl of 10x retinoid or buffer. The reaction was initiated by the addition of 1 µl of a 10x ATP solution (0.2 µCi) to achieve a final concentration of 200 µM. After 30 min at 37 °C, 4 µl of 10% SDS was added. One µl of the reaction mixture was spotted onto a

polyethyleneiminecellulose plate (Sigma) and chromatographed in 0.5 M LiCl, 1 M formic acid. The plate was exposed to a storage phosphor screen for 8 h and scanned in a Typhoon Variable Mode Imager (GE Healthcare). Spots corresponding to ATP and ADP were quantified using ImageQuant TL software (Amersham Biosciences). The ratio of the amount of ADP produced to the initial amount of ATP present in the reaction mixture was calculated. Each sample was assayed in triplicate. Buffer blanks were included to determine nonenzymatic ATP hydrolysis, which was subtracted from the total ATP hydrolyzed.

2.2.14 SDS-PAGE and Western Blots

Proteins harvested from H293T cells or bovine/mice ROS were separated by SDS gel electrophoresis on 8% polyacrylamide gels and either stained with Coomassie Blue or transferred to Immobilon FL membranes (Millipore, Bedford, MA) in buffer containing 25 mM Tris, 192 mM glycine, 10% methanol, pH 8.3. Membranes were blocked with 1% milk in PBS for 30 min, incubated with culture supernatant diluted in PBS for 40 min, washed stringently with PBST (PBS containing 0.05% Tween 20), incubated for 40 min with secondary antibody (goat anti-mouse conjugated with IR dye 680 (LI-COR, Lincoln, NE) diluted 1:20,000 in PBST containing 0.5% milk), and washed with PBST prior to data collection on a LI-COR Odyssey infrared imaging system.

2.3 Results

2.3.1 ATP-Dependent Transfer of Retinal between Lipid Vesicles

To characterize the transport function of ABCA4, we have developed a biochemical assay that measures ATP-dependent transfer of radiolabeled retinoids from ABCA4-containing donor proteoliposomes to acceptor liposomes. The basis for this assay is illustrated in Fig 2.1. All-*trans* retinal (ATR) rapidly equilibrates between the two vesicle populations (Rando and Bangerter, 1982) and reversibly reacts with PE to form *N*-retinylidene PE, a portion of which is trapped in the inner leaflet of the vesicles. Using ATP as an energy source, ABCA4 transports *N*-retinylidene PE from the inner to the outer leaflet of the proteoliposomes. The increase in *N*-retinylidene PE on the outer leaflet coupled with its dissociation into ATR and PE results in a net solution transfer of ATR to the acceptor liposomes where it reacts with PE to form *N*-retinylidene PE.

The increase in retinoid in the acceptor liposomes can be quantified after separation from the proteoliposomes. The separation of the dense acceptor vesicles from donor proteoliposomes by centrifugation is highly efficient as analyzed using fluorescently labeled lipids (Appendix A.8) and occurs without vesicle fusion as confirmed by fluorescent lipid quenching measurements (Appendix A.9).

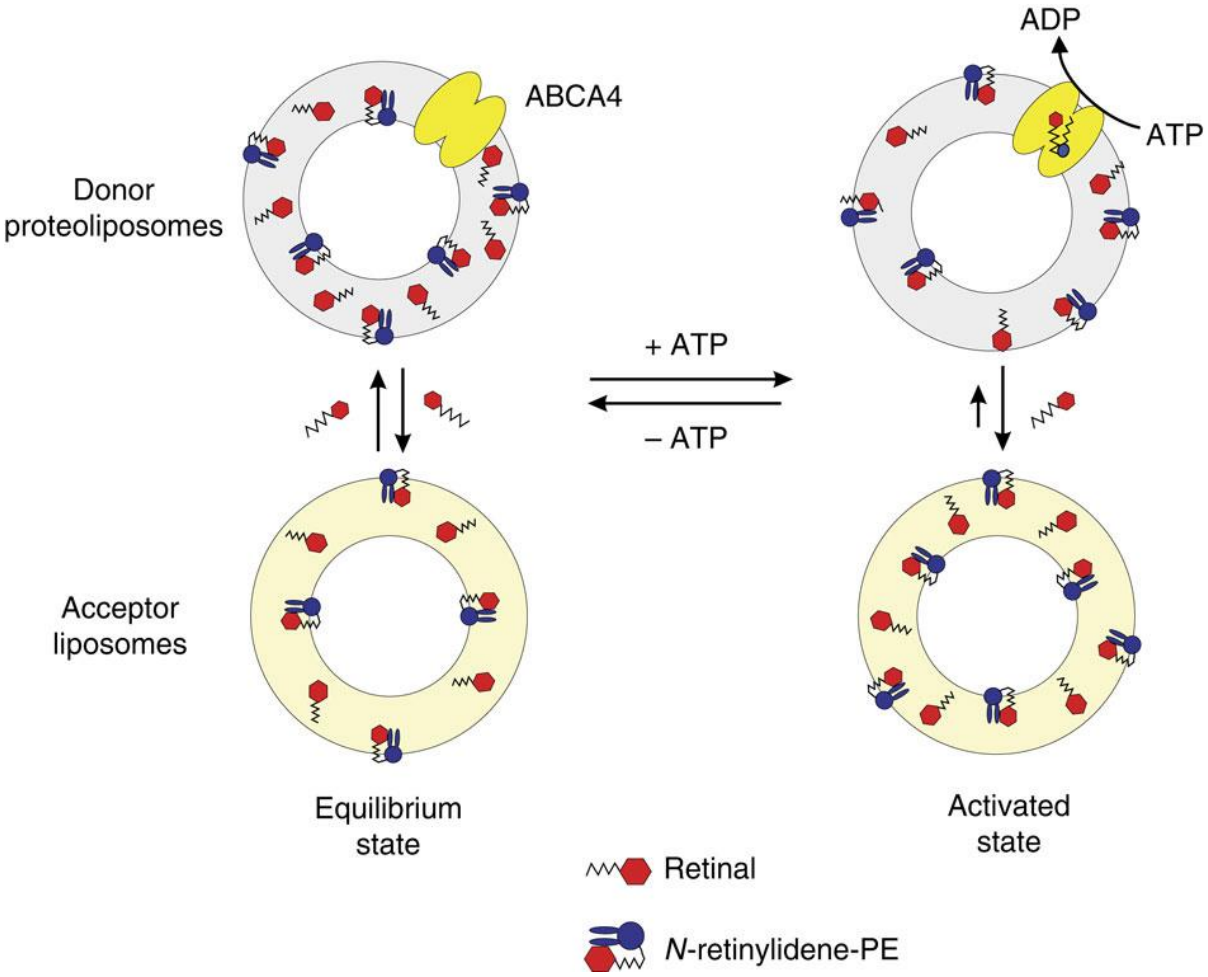

Figure 2.1 Rationale for ABCA4 Retinoid Transport between Donor & Acceptor vesicles

In the absence of ATP (equilibrium state), retinal rapidly equilibrates between the donor proteoliposomes (or disc membranes) containing ABCA4 and acceptor liposomes. The distribution of retinal in each population is dependent on the phospholipid composition. Retinal freely diffuses in the lipid bilayer and reacts with PE to form an equilibrium mixture with *N*-retinylidene PE which is distributed on both sides of the lipid bilayer. Addition of ATP to the NBDs of ABCA4 results in the active transport or flipping of *N*-retinylidene PE from the lumen side of the bilayer to the outside (equivalent to the cytoplasmic) of the bilayer resulting in an accumulation of *N*-retinylidene PE on the outer leaflet. This increase coupled with its dissociation to PE and retinal results in a higher concentration of retinal on the outer leaflet and a net transfer of retinal to the acceptor liposomes. This can be measured by determining the accumulation of radiolabeled retinoid in the liposome after separation from donor proteoliposomes by centrifugation. The density of the liposomes is increased by encapsulated sucrose thereby facilitating separation by centrifugation.

Fig 2.2A-C shows the results of experiments using donor proteoliposomes reconstituted with ABCA4 purified from photoreceptor rod outer segments (ROS). [^{3}H]-ATR rapidly partitioned between the donor proteoliposomes and acceptor liposomes with

approximately 28% of the retinoid being present in the liposomes (Fig 2.2A). Addition of 2 mM ATP resulted in a linear increase in transfer of [^{3}H]-ATR from the donor to acceptor vesicles for 60 minutes. The rate of transfer was dependent on the ATR concentration and showed sigmoidal kinetics with a $K_{0.5}$ of 4.9 ± 0.2 μM, a V_{max} of 35.5 ± 0.7 pmol/min/μg of protein, and a Hill coefficient of 2.3 ± 0.3 at 37^{o}C (Fig 2.2B). ATP-dependent transfer of [^{3}H]-ATR increased with increasing amounts of ABCA4 and was specific for ATR since ATP-dependent transfer was not observed for [^{3}H]-all-*trans* retinol (Appendix A.1). Removal of MgATP by EDTA chelation of Mg^{2+} led to a reduction in accumulated ATR in the acceptor liposomes (Appendix A.2).

The effect of nucleotides and ATPase inhibitors on the rate of [^{3}H]-ATR transfer was investigated. When ATP was replaced with its non-hydrolyzable derivative, AMP-PNP, no significant [^{3}H]-ATR transfer was observed above background implicating ATP hydrolysis in the transfer reaction (Fig 2.2A,C). GTP could partially substitute for ATP, whereas ADP and GDP showed substantially reduced activity. The sulfhydryl reagent N-ethylmaleimide (NEM) previously shown to inhibit the ATPase activity of ABCA4 (Ahn et al., 2000), also inhibited [^{3}H]-ATR transfer to acceptor vesicles. Orthovanadate, a phosphate analog and a weak inhibitor of ABCA4 ATPase activity (Sun et al., 1999), partially inhibited the [^{3}H]-ATR transfer at a concentration of 1 mM, whereas 0.2 mM beryllium fluoride, another phosphate analog, strongly inhibited [^{3}H]-ATR transfer. The effect of various divalent metal ions on the ATR transfer reaction was studied (Appendix A.3). Transfer activity was observed with either Mg^{2+} or Mn^{2+}, but not Zn^{2+} or Ca^{2+}.

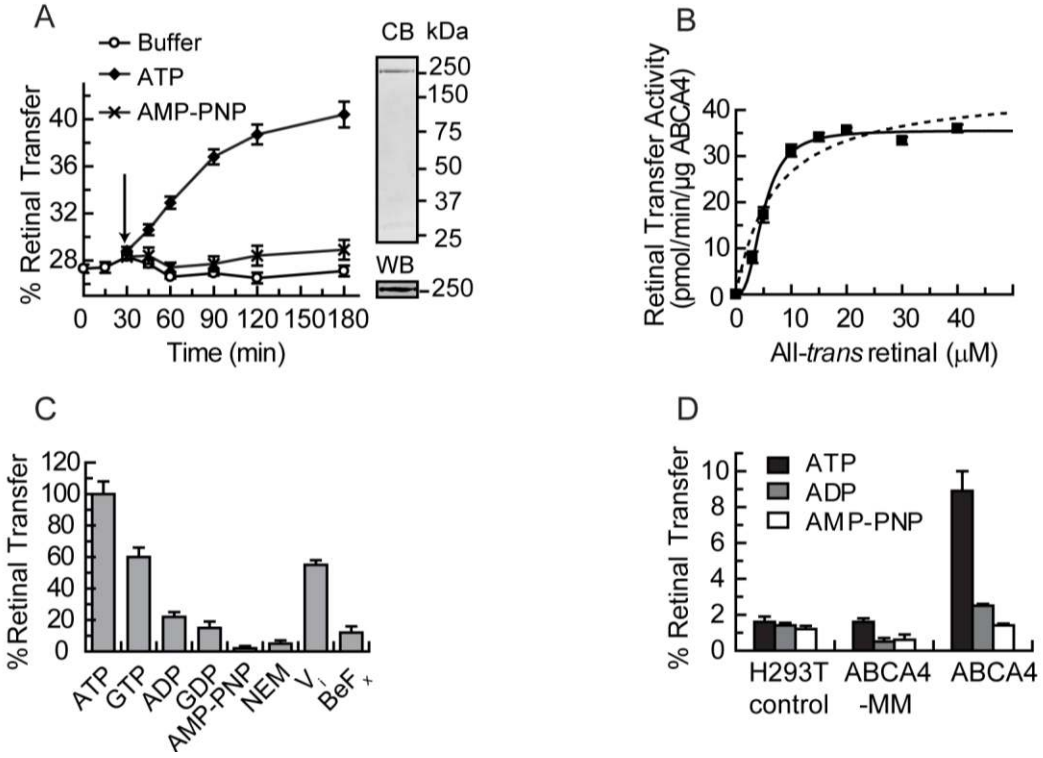

Figure 2.2 All-*Trans* Retinal Transfer from ABCA4 Proteoliposomes to Liposomes

Donor proteoliposomes consisted of PC, PE, and BPL at a weight ratio of 6:2:2 reconstituted with ABCA4 purified from either bovine ROS membranes (**A-C**) or ABCA4 purified from transfected HEK293 cell extracts (**D**). Acceptor liposomes consisted of DOPC and DOPE at a weight ratio of 7:3. **A.** Time course for the transfer of [^{3}H] all-*trans* retinal ([^{3}H] ATR) from donor proteoliposomes to acceptor liposome vesicles. [^{3}H] ATR rapidly distributed between donor proteoliposomes and acceptor liposomes with ~28% of the ATR partitioning into the acceptor liposomes at 37^{o}C. After 30 min., 2 mM ATP or AMP-PNP or control buffer was added (arrow) and radioactivity in the acceptor liposomes was measured at various times. Coomassie blue (CB) stained gel and western blot (WB) shows the purity of the ABCA4 used for reconstitution. **B.** ATP-dependent rate of [^{3}H] ATR transfer as a function of ATR concentration. Solid line shows best-fit sigmoidal curve for $K_{0.5}$ of 4.9 ± 0.2 µM and a V_{max} of 35.5±0.7 pmol/min/µg protein yielding a Hill coefficient of 2.3 ± 0.3. Dotted line shows a best-fit Michaelis-Menten curve for comparison. **C.** The effect of nucleotides (1 mM) and inhibitors (10 mM *N*-ethylmaleimide (NEM), 1 mM orthovanadate (V_i) or 0.2 mM beryllium fluoride (BeF_x) on [^{3}H] ATR transfer from proteoliposomes to liposomes. **D.** Effect of ATP, ADP, and AMP-PNP on [^{3}H] ATR transfer from donor proteoliposomes reconstituted with WT ABCA4 or the ATPase impaired K969M/K1978M double mutant (ABCA4-MM) purified from transfected HEK293 cells. ATR concentration was 10 µM. For all experiments, data are plotted as a mean ± s.e.m for n = 3.

Although ABCA4 isolated from ROS by immunoaffinity chromatography has been shown to be highly pure (Ahn et al., 2000; Sun et al., 1999; Zhong et al., 2009), it is possible that a residual protein contaminant may be responsible for the ATP-dependent [^{3}H]-ATR

transfer. This was examined using donor proteoliposomes reconstituted with wild-type (WT) ABCA4 or the ATPase deficient K969M/K1978M double mutant (ABCA4-MM) (Fig 2.2D). ATP-dependent [^{3}H]-ATR transfer was observed for WT ABCA4, but not ABCA4-MM. These studies provide strong evidence that ATP-dependent ATR transfer from donor to acceptor vesicles is mediated by ABCA4 and displays many characteristic properties previously observed for retinal stimulated ATPase activity of ABCA4 (Ahn et al., 2000; Sun et al., 1999).

2.3.2 Nonprotonated *N*-retinylidene PE is the Substrate for ABCA4

To further identify the substrate for ABCA4, we examined the effect of all-*trans* retinol as an analog of ATR and *N*-retinyl PE as a stabilized reduced derivative of *N*-retinylidene PE on the [^{3}H]-ATR transfer reaction. All-*trans* retinol had no effect on the [^{3}H]-ATR transfer, whereas *N*-retinyl PE strongly inhibited the transfer with an IC_{50} of 9 μM (Fig 2.3A)(Appendix A.1). Since *N*-retinylidene PE is in equilibrium with ATR and PE, the ATP-dependent [^{3}H]-ATR transfer reaction should depend on PE. ATR transfer does not occur when ABCA4 is reconstituted into phosphatidylcholine (PC) vesicles lacking PE (Fig 2.3B). Furthermore, transfer is strongly dependent on the PE concentration (Fig 2.3C).

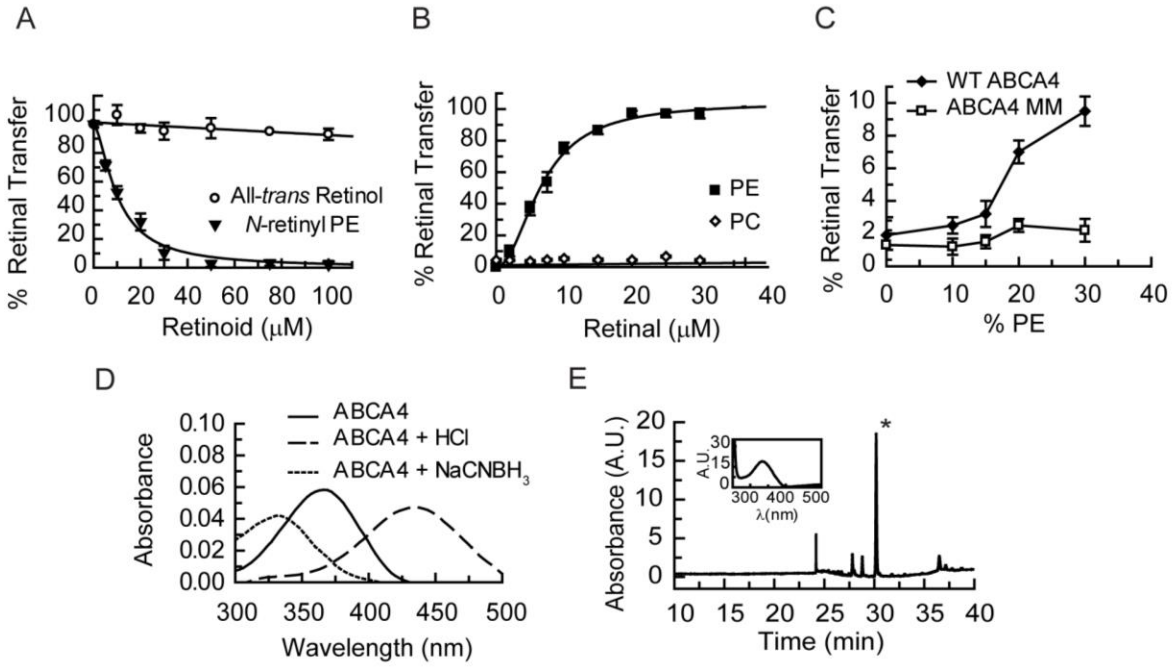

Figure 2.3 Effect of Retinoids and PE on ATP-Dependent Transfer of All-*Trans* Retinal
A. Inhibition of ATP-dependent [^{3}H] ATR transfer (10 μM) from ABCA4-containing donor proteoliposomes to acceptor liposomes with increasing concentrations of all-*trans* retinol or *N*-retinyl PE. Donor proteoliposomes were reconstituted with ABCA4 purified from bovine ROS membranes. Data plotted as a mean ± s.d. for $n = 3$. **B.** ATP-dependent transfer of [^{3}H] ATR from ABCA4 containing proteoliposomes composed of only DOPC (PC) or DOPC containing 30% DOPE (PE). Sigmoidal curve for PE was generated for $K_{0.5} = 6.7$ μM ± 0.3 with a Hill coefficient of 2.1 ± 0.2. Data plotted as a mean ± s.d. for $n = 3$. **C.** Effect of increasing DOPE on the ATP-dependent transfer of [^{3}H] ATR from DOPC/DOPE proteoliposomes reconstituted with either WT ABCA4 or ABCA4-MM mutant. Data plotted as mean ± s.e.m. for $n = 6$ for 2 independent experiments. **D.** Absorption spectra of purified ABCA4 with bound retinoid substrate. Spectrum at neutral pH (solid line) shows a maximum of 360 nm characteristic of nonprotonated *N*-retinylidene PE. Treatment with HCl resulted in an absorption maximum of 440 nm characteristic of protonated *N*-retinylidene PE. Treatment with $NaCNBH_3$ resulted in a shift to 330 nm characteristic of *N*-retinyl PE. **E.** HPLC chromatograph of $NaCNBH_3$ reduced retinoid substrate in ABCA4. Retention time and spectrum (inset) of the predominant peak (*) are characteristic of *N*-retinyl-PE.

The Schiff base of *N*-retinylidene PE in PC/PE vesicles undergoes protonation with an apparent pK_a of 6.9 (Appendix A.4). To investigate whether the protonated or nonprotonated form of *N*-retinylidene PE binds to ABCA4, ATR and PE were added to ABCA4 immobilized on a Rim3F4-Sepharose immunoaffinity matrix. After removing excess ATR and PE, ABCA4 with its bound substrate was released from the matrix with the

3F4 competing peptide for analysis by absorption spectroscopy. As shown in Fig 2.3D, the bound retinoid substrate had an absorption maximum at 360 nm, characteristic of nonprotonated *N*-retinylidene PE. Treatment with HCl or $NaCNBH_3$ resulted in a shift in the absorption maximum to 440nm or 330nm, respectively, characteristic of protonated *N*-retinylidine PE and *N*-retinyl PE. Solvent extraction of $NaCNBH_3$ treated ABCA4 followed by HPLC chromatography confirmed that the reduced Schiff base compound was *N*-retinyl PE (Fig 2.3E). The transport activity of ABCA4 was also dependent on pH reaching a maximum at pH 8.0 (Appendix A.5). Collectively, these studies indicate that the nonprotonated form of *N*-retinylidene PE is the retinoid substrate transported by ABCA4.

2.3.3 ABCA4-Mediated Transport of ATR from ROS Discs

To determine if ABCA4 mediated ATR transfer can occur from a more physiological system, we replaced the reconstituted proteoliposomes with closed ROS disc membrane vesicles (Fig 2.4A) which retain their orientation with the cytoplasmic surface exposed to the buffer (Clark and Molday, 1979; Illing et al., 1997; Smith et al., 1975). In this assay, disc vesicles comprised the dense fraction and acceptor liposomes prepared in the absence of sucrose made up the light fraction. [^{3}H]-ATR rapidly partitioned between the disc and acceptor vesicles (Fig 2.4B). Addition of ATP, but not AMP-PNP, resulted in a linear transfer of [^{3}H]-ATR to the acceptor vesicles. The rate of [^{3}H]-ATR transfer was dependent of ATR concentration yielding a sigmoidal curve with a $K_{0.5}$ of 6.8 ± 0.3 μM, a V_{max} of 4.9 ± 0.1 nmol/min/mg protein, and a Hill coefficient of 1.8 ± 0.1 (Fig 2.4C). Importantly, the direction of transport was consistent with the movement of *N*-retinylidene PE from the inner lumen leaflet to the outer cytoplasmic leaflet of the disc vesicles.

To confirm that that the ATP-dependent transfer of ATR is mediated by ABCA4, we compared the ATR transfer reaction from disc membrane vesicles of WT mice with those of *abca4* knockout mice. With the exception of ABCA4, the disc protein compositions were similar (Fig 2.4D). ATP-dependent transfer of [^{3}H]-ATR was observed from WT disc membranes but not *Abca4* knockout membranes (Fig 2.4E).

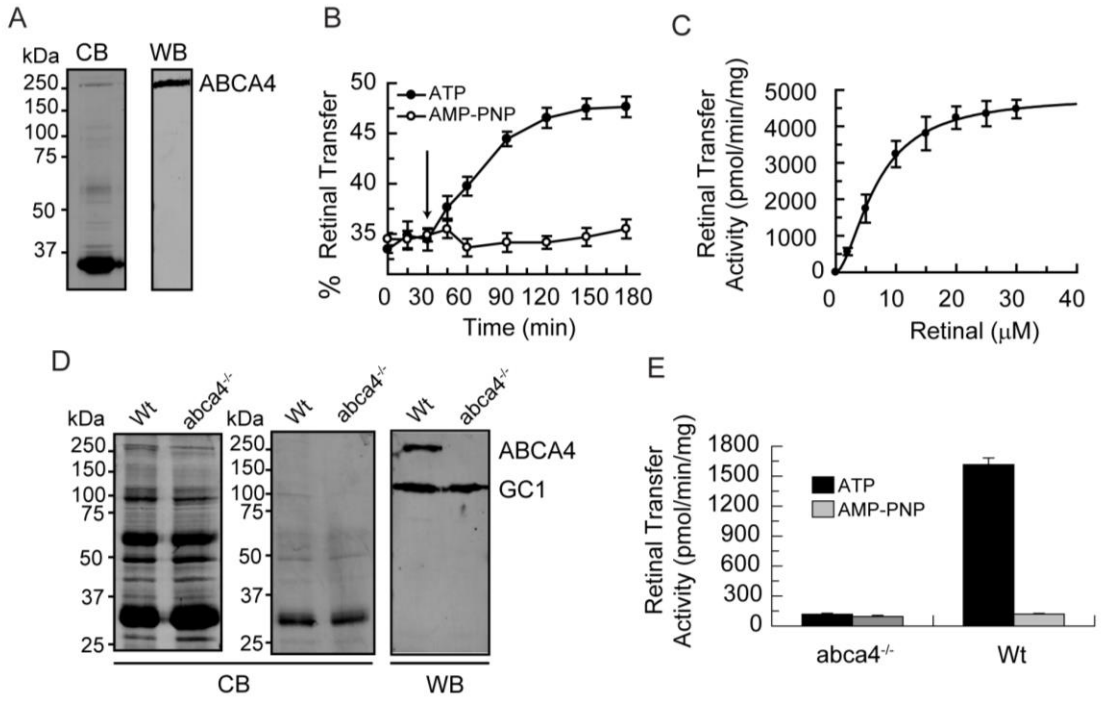

Figure 2.4 ATP-Dependent Transfer of All-*Trans* Retinal from ROS Discs

A. Coomassie blue stained SDS gel (CB) and Western blot (WB) of bovine ROS disc vesicles used in the ATR transfer reactions. **B.** Time course for the transfer of [^{3}H] ATR from donor disc vesicles to acceptor vesicles. At 30 min, 5 mM ATP or AMP-PNP (arrow) was added to start the transfer reaction. A higher ATP concentration was required to compensate for the presence of nonspecific ATPase in the disc membranes. Data plotted as a mean ± s.d. for $n = 3$. **C.** ATP-dependent rate of [^{3}H] ATR transfer (retinal transfer activity) from disc vesicles to acceptor liposomes as a function of ATR concentration. The best fit sigmoidal curve was generated for a $K_{0.5}$ of 6.8 ± 0.3 μM and a V_{max} of 4.9 ± 0.1 nmol/min/mg protein, and yielded a Hill coefficient of 1.8 ± 0.1. Data plotted as a mean ± s.d. for $n = 3$. **D.** Coomassie blue (CB) stained gels of ROS (left panel) and hypotonically lysed and washed discs (middle panel) from wild-type (Wt) and *abca4* knockout (abca4$^{-/-}$) mice. Western blot (right panel) labeled for ABCA4 and guanylate cyclase 1 (GC1). ROS and disc membranes from WT and *abca4*$^{-/-}$ mice display similar protein profiles except for the absence of ABCA4 in the *abca4*$^{-/-}$ preparations as revealed by western blotting. **E.** ATP-dependent [^{3}H] ATR transfer from disc membranes of WT and *abca4*$^{-/-}$ mice to acceptor vesicles. Data plotted as a mean ± s.e.m. for $n = 9$.

2.3.4 ABCA4 Functions as a PE Importer

ABCA4 reconstituted into PE-containing lipid vesicles exhibits basal ATPase activity in the absence of retinal (Ahn et al., 2000; Sun et al., 1999). We reasoned that this activity may be associated with the transport of a phospholipid across the lipid bilayer, a function which has been reported for other ABC transporters notably ABCB1 (P-glycoprotein) (Romsicki and Sharom, 2001). To test this, we used the well-established fluorescence spectroscopic technique to measure the active transport of fluorescent 7-nitro-2-1,3-benzoxadiazol-4-yl-labeled (Fl-labeled) phospholipids across the lipid bilayer (Borst et al., 2000; Coleman et al., 2009; McIntyre and Sleight, 1991; Romsicki and Sharom, 2001). In this assay ATP or its nonhydrolyzable analogue AMP-PNP was added to ABCA4 proteoliposomes containing Fl-labeled-PE, Fl-labeled-PC or Fl-labeled-PS. After 1 hour the impermeable reducing agent dithionite was added to selectively bleach Fl-labeled lipids on the outer leaflet. Complete bleaching of the Fl-labeled lipids was achieved by the addition of Triton X-100 (Appendix A.6). The amount of Fl-labeled lipid transported to the outer leaflet was determined from the difference in fluorescence after dithionite addition between samples treated with ATP and AMP-PNP and expressed as a percentage of Fl-labeled lipid transported.

When ABCA4 was reconstituted into PC vesicles containing Fl-labeled phospholipids, ATP-dependent transport was observed for Fl-labeled-PE, but not Fl-labeled-PS or Fl-labeled-PC (Fig 2.5A). The direction of transport was from the lumen to the cytoplasmic leaflet of the vesicles similar to the direction of *N*-retinylidene PE transport. Fl-labeled-PE transport increased with increasing Fl-labeled-PE incorporated into the proteoliposomes (Fig 2.5b) and was suppressed by the addition of 30% unlabeled PE (Fig

2.5A). Transport activity was not observed for the ATPase defective mutant, ABCA4-MM. As in the case of *N*-retinylidene PE transport, GTP could partially substitute for ATP and beryllium fluoride and NEM acted as strong inhibitors (Fig 2.5C).

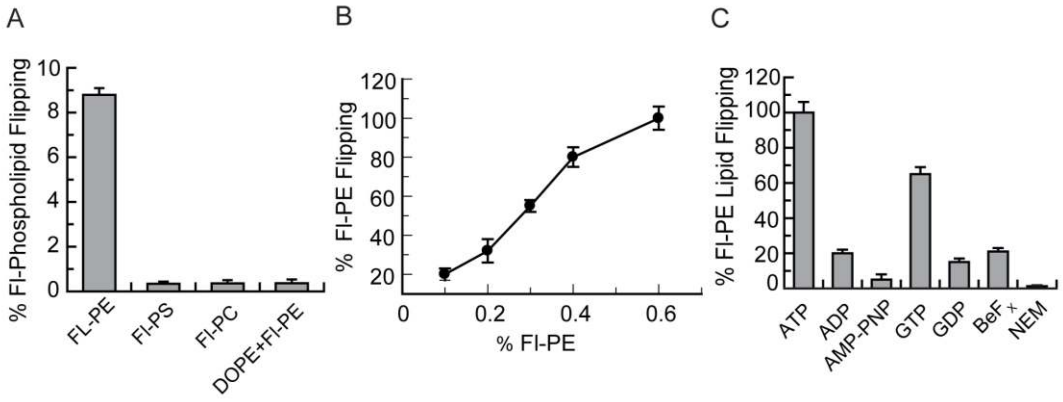

Figure 2.5 Phosphatidylethanolamine (PE) Flippase Activity of ABCA4

A. ABCA4 was reconstituted into DOPC vesicles containing 0.6% Fl-labeled-PE (Fl-PE), Fl-labeled-PS (Fl-PS), Fl-labeled-PC (Fl-PC) or 0.6% Fl-labeled-PE plus 30% unlabeled DOPE (DOPE/Fl-PE). Data plotted as a mean ± s.e.m., $n = 9$ for 3 independent experiments. **B.** Dependence of Fl-labeled-PE flipping or transport across the bilayer as a function of % Fl-labeled-PE. Data plotted as a mean ± s.d. for $n = 3$. **C.** The effect of nucleotides (1 mM), beryllium fluoride (BeF_x 0.2 mM) and NEM (10 mM) on the Fl-labeled-PE flippase activity. Data plotted as a mean ± s.d. for $n = 3$.

2.3.5 Stargardt Mutations Cause a Decrease in Transport Activity

To gain further insight into the molecular mechanisms underlying ABCA4 mediated transport activity and Stargardt disease, we examined the functional properties of ABCA4 containing G863A and N965S mutations associated with Stargardt disease and Walker A mutations, K969M in NBD1, K1978M in NBD2, and the double mutant K969M/1978M. The K1978M mutant expressed at the same level as WT ABCA4 while the G863A, N965S, K969M and K969M/K1978M mutants expressed within 50% that of WT ABCA4. All mutants could be readily purified by immunoaffinity chromatography (Fig 2.6A).

All mutants reconstituted into proteoliposomes showed a severe loss in *N*-retinylidene PE transfer activity with the three Walker A mutants showing essentially undetectable activity and the G863A and N965S Stargardt mutants displaying ~18% and 37% of WT activity (Fig 2.6B). Retinal stimulated ATPase activities of these mutants were also analyzed (Fig 2.6C,D) with Stargardt mutants showing very modest retinal stimulation and Walker A mutants showing some inhibition of ATPase activity with increasing retinal concentration. Next we studied the effect of the mutations on *N*-retinylidene PE binding to immobilized ABCA4 and its release by ATP (Fig 2.6E). All mutants bound *N*-retinylidene PE at similar levels to WT ABCA4. Addition of ATP resulted in release of the substrate from the G863A, N965S, and K1978M mutants, but impaired release from the K969M mutant and no significant release from the K969M/K1978M double mutant. Finally, we determined the effect of these mutations on Fl-labeled-PE flippase activity. All mutants showed significantly reduced PE flippase activity in general agreement with their loss in basal ATPase activity (Fig 2.6F).

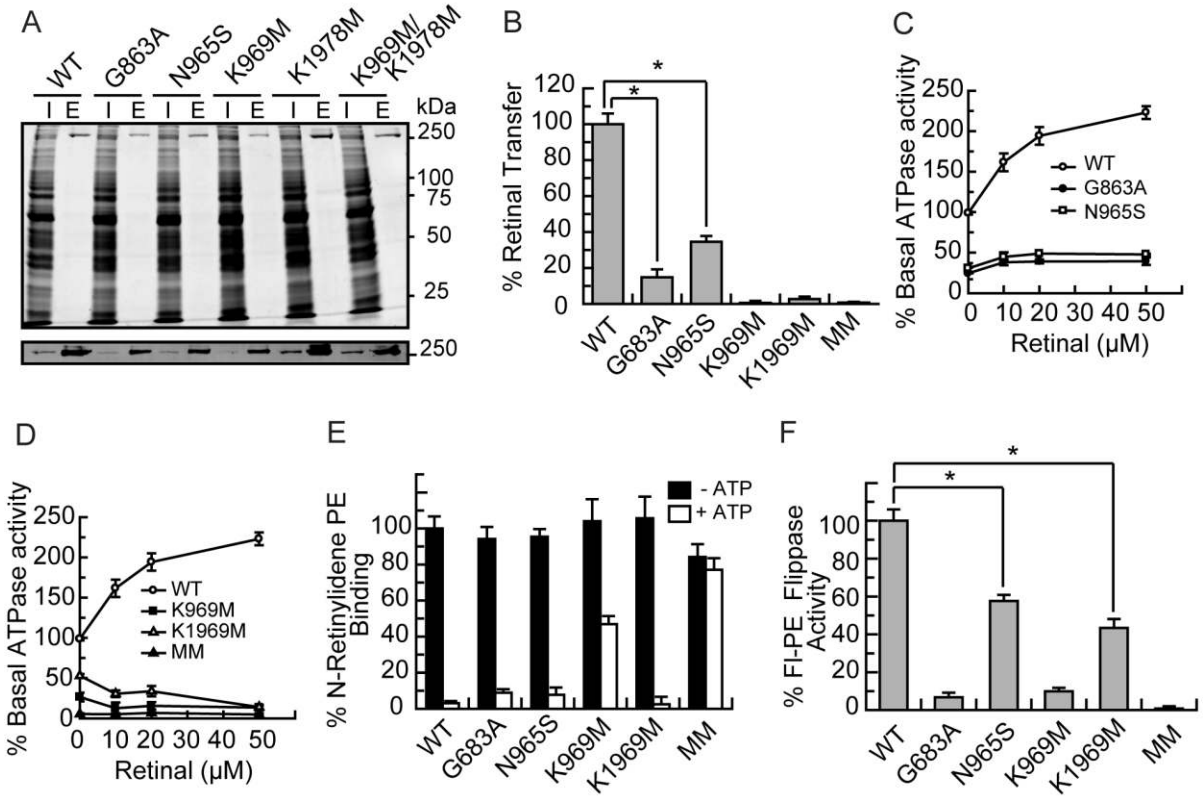

Figure 2.6 Effect of Walker A and SD Mutations on All-*Trans* Retinal Transfer Activity

A Wild-type and mutant ABCA4 containing a 1D4 epitope were expressed in HEK293T cells and purified on a Rho-1D4 immunoaffinity matrix. Commassie blue stained gel (upper) and western blot (lower) for the various ABCA4 mutants. Lanes labeled I (input) are the HEK293T detergent solubilized extract applied to the immunoaffinity matrix. Lanes labeled E (eluted) are fractions released from the immunoaffinity matrix with the 1D4 peptide. **B.** ATP-dependent [^{3}H] ATR transfer activity for the various mutants relative to wild-type ABCA4. Data plotted as a mean ± s.e.m. for $n = 9$ from 3 independent experiments. Statistically significant differences ($p < 0.05$) are denoted with * and ** for datasets, as determined by ANOVA. **C.** ATPase activity of the Stargardt mutants as a function of ATR concentration and expressed as a % of WT activity in the absence of retinal. Data plotted as a mean ± s.e.m. for $n = 6$ from 2 independent experiments. **D.** ATPase activity of the Walker A mutants as a function of ATR concentration. Data plotted as a mean ± s.e.m. for $n = 6$ from 2 independent experiments. **E.** Binding of *N*-retinylidene PE to immobilized WT and mutant ABCA4 and release by 0.5 mM ATP. Binding normalized to WT ABCA4. Data plotted as a mean ± s.e.m. for $n = 9$ from 3 independent experiments. **F.** ATP-dependent flippase activity of Fl-labeled-PE by mutant ABCA4. Data plotted as a mean ± s.e.m. for n=9 from 3 independent experiments. Statistically significant differences ($p < 0.05$) are denoted with '*', as determined by ANOVA.

2.4 Discussion

In this study, we provide direct biochemical evidence for the full eukaryotic ABC transporter ABCA4 functioning as an 'importer' translocating its substrates *N*-retinylidene PE and PE from the lumen to the cytoplasmic side of photoreceptor disc membranes. This is supported in 3 different experimental systems. First, the addition of ATP, but not AMP-PNP, to the outside of donor vesicles reconstituted with purified ABCA4 promotes the time-dependent transfer of retinal (ATR) to acceptor liposomes. Since ATP is negatively charged, it can only interact with the NBDs of ABCA4 exposed on the outside of the vesicle, an orientation equivalent to the cytoplasmic side of biological membranes, and drive transfer of retinal to acceptor liposomes, a direction expected for an importer. The reaction is specific for functional ABCA4 since ATP-dependent retinal transfer activity is not observed for ATPase-defective ABCA4 mutants (Sung and Tai, 2000). Furthermore, NEM and beryllium fluoride both of which inhibit the ATPase activity of ABCA4 (Ahn et al., 2000) also abolish ABCA4 mediated retinal transfer activity. Second, ATP-dependent retinal transfer is observed from bovine and WT mouse photoreceptor disc membranes, but not *Abca4* knockout disc membranes. Third, ABCA4 reconstituted into lipid vesicles can actively flip PE from the inner to the outer surface of vesicles, a direction which is consistent with an 'import' direction of PE transport.

All mammalian and mostly all well-characterized eukaryotic ABC transporters have been shown to act as 'exporters' extruding or flipping their substrates from the cytoplasmic to the extracellular or lumen side of biological membranes (Borst et al., 2000; Kobayashi et al., 2006; Oancea et al., ; Romsicki and Sharom, 2001; Vaughan and Oram, 2006; Velamakanni et al., 2008). Exceptions are found in the plant kingdom where several ABC

transporters have been reported to function as importers (Shitan et al., 2003). Direct substrate transport has not been measured for other members of the ABCA subfamily, but cell-based studies have suggested that these transporters function as lipid exporters (Attie, 2007; Linsel-Nitschke et al., 2005; Vaughan and Oram, 2006). In particular ABCA1 which is 50% identical in sequence to ABCA4 is known to facilitate the export of cholesterol and phospholipids from cells to ApoA-I although this remains to be confirmed at a biochemical level. Indeed, if all other ABCA transporters are found to function as lipid exporters, it will be of interest to determine the molecular basis which defines ABCA4 as a unique importer in this subfamily.

Although the assay developed in this study measures the transfer of retinal from donor to acceptor vesicles, the true substrate for ABCA4 is *N*-retinylidene PE. Retinal is a hydrophobic compound which readily diffuses across the lipid bilayer and hence does not need a specific transporter. However, retinal readily reacts with PE which comprises about 40% of the phospholipid in disc membranes to form *N*-retinylidene PE, a compound which cannot diffuse across membranes. We have confirmed earlier studies that ABCA4 tightly binds *N*-retinylidene PE in the absence of ATP (Beharry et al., 2004), and further show here that it binds the nonprotonated form of *N*-retinylidene-PE on the basis of spectral measurements and HPLC analysis. Furthermore, *N*-retinyl PE, the stabilized covalent analog of *N*-retinylidene PE, competes with *N*-retinylidene PE for binding to ABCA4 (Beharry et al., 2004), and inhibits its transport activity. Collectively, our studies suggest that the addition of retinal to a mixture of PE-containing donor and acceptor vesicles results in its rapid partitioning between these vesicle populations with retinal and PE in dynamic equilibrium with *N*-retinylidene PE. ABCA4 catalyzes the active transport of *N*-retinylidene PE from the

inside to the outside of donor proteoliposomes or disc vesicles as a rate limiting step. The increase in *N*-retinylidene PE on the outer leaflet of the donor proteoliposomes coupled with its dissociation into retinal and PE leads to the observed ATP-dependent transfer of retinal to acceptor liposomes.

A number of high resolution structures of prokaryotic and eukaryotic ABC transporters, both importers and exporters, have been determined by X-ray crystallization, some bound with ATP or their transport substrate (Aller et al., 2009; Dawson and Locher, 2006; Hollenstein et al., 2007; Zolnerciks et al., 2007). These studies have led to the proposal that both types of transporters use broadly similar alternating access transport mechanisms(Dawson and Locher, 2007; Jones et al., 2009). In the absence of ATP, exporters bind their substrate at a high affinity binding site accessible to the cytoplasmic side of the membrane. The binding of ATP results in the dimerization of the NBDs, a process that is coupled to a conformational change in the transmembrane domains and conversion to low affinity outwardly oriented binding site and dissociation of the substrate from the transporter on the exocytoplasmic side of the membrane. ATP hydrolysis together with the release of ADP and P_i results in another conformational change which resets the protein to its initial state. Prokaryotic importers, on the other hand, typically bind their substrate on the exocytoplasmic side of the membrane in the presence of ATP, often facilitated through interaction with a substrate binding protein. Hydrolysis of ATP leads to the conversion to a low affinity inward oriented binding site and release of the substrate on the cytoplasmic side of the membrane. Our studies suggest a model in which ABCA4 in the absence of ATP and a substrate binding protein has a high affinity outward (lumen) facing site for the binding of *N*-retinylidene PE or PE (Beharry et al., 2004) . The binding of ATP induces a protein

conformational change which switches the high affinity site to a low affinity inward (cytoplasmic) facing site enabling *N*-retinylidene PE or PE to be released on the cytoplasmic leaflet of the disc membrane. In this model ATP hydrolysis would restore the initial conformation of ABCA4 to initiate another cycle of transport.

This model is supported by our studies on the effect on Stargardt mutations on the properties of ABCA4. The binding of *N*-retinylidene PE and its release by ATP is not affected by the G863A and N965S mutations (Fig 2.6E), but the basal and retinal stimulated ATPase activity and ATP-dependent retinal transfer activity are significantly reduced. Similarly, mutations in the Walker A motif also abolish retinal stimulated ATPase activity and ATP-dependent retinal transfer activity without affecting *N*-retinylidene PE binding and with the exception of the double mutant not drastically affecting substrate release by ATP. Previous *in vitro* biochemical studies have relied on the purification and reconstitution of ABCA4 into liposomes for analysis of its basal and retinal stimulated ATPase activities. Such activities could not be accurately measured in disc membrane preparations due to the high nonspecific ATPase activity in these preparations (Coleman et al., 2009). However, as shown in this study active retinoid transport activity of ABCA4 can be measured in disc membranes resulting in a V_{max} of 4.9 nmoles/min/mg protein. Since ABCA4 represents about 5% of the disc membrane protein by weight (Sun and Nathans, 1997), this suggests the specific activity of ABCA4 is about 98 nmoles/min/mg, a value comparable to the value of ~53 nmoles/min/mg for ABCA4 derived from kinetic measurements of proteoliposomes having 75% of the ABCA4 oriented with its NBDs accessible to ATP (Appendix A.7). The turnover numbers for the reduction of all-*trans* retinal to all-*trans* retinol by the retinol dehydrogenase Rdh8 have been reported to range from 0.3 min^{-1} (*in vitro*), 0.06 min^{-1} (*in*

situ), and 0.0003 min^{-1} (*in vitro*) (Chen et al., 2009; Heck et al., 2003; Ishiguro et al., 1991). The estimated turnover number (24.5 min^{-1}) for ABCA4 in disc membranes is several orders of magnitude higher. Given that ABCA4 and Rdh8 occur at 1:120 and 1:140 of rhodopsin levels (Rattner et al., 2000; Sun and Nathans, 1997), this suggests that *N*-retinylidene PE transfer is at least two orders of magnitude faster than the reduction reaction. On this basis ABCA4 appears to assure that all of the all-*trans* retinal is made accessible on the cytoplasmic side of disc membranes where it can be either reduced to retinol by Rdh8 or diffuse from the disc and undergo reduction by retinol dehydrogenase isoforms localized in different photoreceptor subcellular compartments (Fig 2.7). Interestingly, the dependence of *N*-retinylidiene PE transport activity on retinal concentration results in a sigmoidal curve (Fig 2.2B and Fig 2.3B) suggesting that retinal can act as an allosteric activator of retinoid transport. This is consistent with earlier studies showing that ABCA4 contains a binding site for retinal which is distinct from the *N*-retinylidene PE binding site (Beharry et al., 2004; Biswas-Fiss et al.).

In addition to flipping *N*-retinylidene PE, ABCA4 can also flip PE across membranes in the same 'import' direction (Fig 2.7), an activity which is related to the basal ATPase activity of ABCA4 (Ahn et al., 2000; Sun et al., 1999). The distribution of phospholipids across the disc membrane is not clearly resolved. Several earlier studies have reported an asymmetrical distribution of PS and PE with 67%-87% of the PE and 77%-88% of PS on the cytoplasmic leaflet (Miljanich et al., 1979; Wu and Hubbell, 1993). Other studies suggest a more symmetrical distribution of PE and a modest asymmetry for PS possibly arising from ATP-independent flippase activity of opsin (Hessel et al., 2001; Menon et al.). In the former case, ABCA4 may contribute to the generation and maintenance of PE asymmetry whereas in

the latter case, this activity may be overwhelmed by the flippase activity of opsin. More studies are needed to resolve phospholipid asymmetry in photoreceptor membranes and the involvement of ABCA4 in this process.

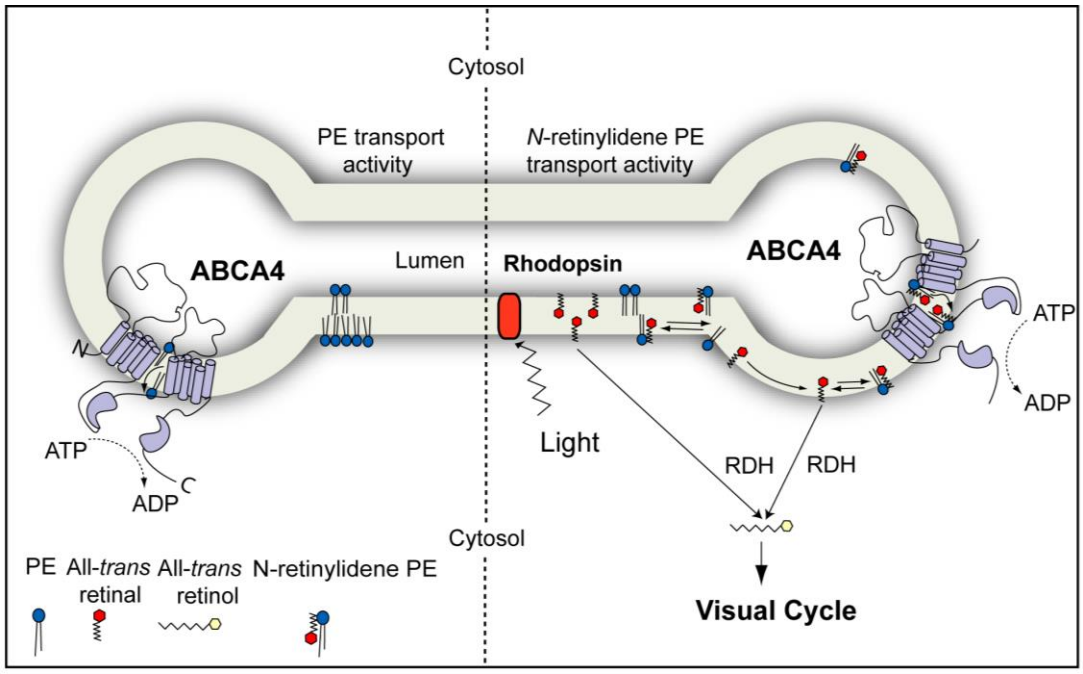

Figure 2.7 Scheme of ABCA4 in Transport of *N*-retinylidene PE and PE in Rod Disc
Left: ABCA4 functioning in the transport of PE from the lumen to the cytoplasmic leaflet of the disc membrane. Right: ABCA4 functioning in the transport of *N*-retinylidene PE from the lumen to the cytoplasmic side of the disc membrane following the photobleaching of rhodopsin. *N*-retinylidene PE dissociates into all-*trans* retinal and PE on the cytoplasmic side of the disc membrane with all-*trans* retinal subsequently being reduced to retinol by the retinol dehydrogenase (RDH) before entering the visual cycle for regeneration of 11-*cis* retinal.

Chapter 3: ABCA4 Mediates the Removal of 11-*Cis* Retinal from Rod Outer Segment Disc Membranes*

3.1 Introduction

RPE cells mediate the production of 11-*cis* retinal for photoreceptor cells and disc organelles. Studies of opsin pigment regeneration showed that the cytosolic gap between the plasma membrane and the disc organelles governs the rate of 11-*cis* retinal diffusion and flux properties (Frederiksen et al., 2012). Retinol dehydrogenases, in particular retinol dehydrogenase 8 (Rdh8), expressed in the cytosol of photoreceptor outer segments requires the NADPH dependent activity to reduce all-*trans* retinal to all-*trans* retinol. Rdh8 reduces a wide range of retinal isomers to corresponding retinols but uniquely lacks reduction specificity for 11-*cis* retinal (Palczewski et al., 1994). Recent evidence shows that *Abca4*$^{-/-}$ mice displays light-independent accumulation of RPE lipofuscin and A2E and that continuous supply of 11-*cis* retinal has been proposed to contribute to the process (Boyer et al., 2012). Early biochemical characterization of ABCA4 showed enhanced ATPase stimulation with various retinal isomers including all-*trans*, 13-*cis*, and 11-*cis* isoforms (Sun et al., 1999). Ligand-interaction studies with ABCA4 domains heterologously expressed and purified from *E.coli* demonstrated high-affinity binding of 11-*cis* retinal and all-*trans* retinal to NBD1 and ECD2, respectively (Biswas-Fiss et al., 2012; Biswas-Fiss et al., 2010). ABCA4 transports *N*-retinylidene PE to the cytosolic side of disc membranes (Quazi et al., 2012). However, the precise roles of 11-*cis* retinal handing and transport by ABCA4 and by disc membranes remain vague.

* This chapter is under manuscript preparation.
Quazi. F, Molday, RS. (2013). 11-*cis* retinal isomerization in rod disc phospholipids and transport of 11-cis retinylidene PE by ABCA4.

In this study, we investigated the transport properties of ABCA4 in the presence of retinal isomers, phospholipids, and allosteric drugs as an important step in understanding mechanisms of the ABC transporter. Using the transfer assay in conjunction with ATPase kinetics, co-immunoprecipitation, and HPLC analyses, we show here that ABCA4 ATPase is preferentially stimulated by 11-*cis* retinal compared to all-*trans* retinal. The transport function of ABCA4 with the *cis*-isomer shows energy dependent clearance in both proteoliposomes and rod disc membranes from the lumen to the cytoplasmic side. In addition, we also demonstrate that 11-*cis* retinal undergoes non-protein mediated isomerization to all-*trans* retinal and 13-*cis* retinal and is governed mainly by the phospholipid PE, which is largely present in photoreceptor disc membranes. Our results demonstrate that 11-*cis* retinylidene PE is another preferred substrate of ABCA4 actively transported out of lumen of disc membranes. Regeneration of opsin and part isomerization of the isomer to all-*trans* retinal with its subsequent reduction during bleached and dark conditions of photoreceptor cells may regulate 11-*cis* retinal fluxes in the visual cycle.

3.2 Methods

3.2.1 Materials

Digitonin, (Fluka); all-*trans*-retinal, amiodarone, phospholipase D were from Sigma. 11-*cis* retinal was obtained from Dr. Rosalie Crouch through NIH and tritiated to generate a radiolabeled analog as described in Chapter 2.2.1. Anti-HA (F-7) antibody was purchased from Santa Cruz Biotechnology. The remaining materials are as described in Chapter 2.2.1.

3.2.2 DNA Constructs

In addition to using a 1D4 tag construct, human ABCA4 (Chapter 2.2.4) with a C-terminal Human influenza hemagglutin HA tag (YPYDVPDYAstop) was also subcloned into Pcep4 using the *Not*I and *Nhe*I restriction sites.

3.2.3 Purification and Functional Analysis of ABCA4

Expression, Western blotting, retinal transfer activities with reconstituted proteoliposomes of ABCA4 were performed as described (Chapter 2).

3.2.4 ATPase Activity

ATPase assays were carried as stated in Chapter 2. Appropriate dilutions and/or mixtures of test compounds were prepared in hexane and were added to 0.1% of the volume of the ATPase reaction; control reactions received the same volume of hexane alone. For experiments to differentiate the effects of retinal isomers, the ATPase assay was manipulated under dim red light and incubated in the dark. All other ATPase assays are performed in room light. Drugs were added to samples and controls as hexane solutions and preincubated for 5 min before ATP addition.

3.2.5 Extraction of Phospholipids from ROS Membranes

Rod OS phospholipids were extracted from rod OS membranes as previously described (Ahn et al., 2000; Folch et al., 1957; Miljanich et al., 1979). Briefly, 25 mg rod OS were washed thrice in 10 mM potassium phosphate, pH 7.0, and resuspended in 0.8 ml of buffer . Derivatization of retinal to the corresponding oxime was achieved by adding 0.8 ml of 1 M NH_2OH (neutralized using $NaHCO_3$) and 4.2 ml of methanol to the membranes and incubated on ice for 10 min. Organic phase extraction was performed thrice with 7.5 ml of chloroform (with 50 mg/ml butylated hydroxytoluene) and 4 ml of water. The organic phase

was pooled, washed with 5.6 ml of 0.3 M NaCl and 4.2 ml of MeOH, followed by N_2 evaporation. The lipids were resuspended in 0.2 ml of $CHCl_3$/MeOH (1:1). This was applied to a thin-layer chromatography plate (0.5-mm Silicagel) under N_2 and developed in a tank exposed to N_2, using a solvent phase of hexane/ether (1:1). The retinal oxime migrated near the solvent front, whereas the phospholipids remained at the origin. The phospholipids were scraped and eluted from Silicagel using $CHCl_3$/MeOH (1:1).

3.2.6 Dark Isomerization of 11-*Cis* Retinal in Membrane/Phospholipid Suspensions

DOPC, DOPC/DOPE, or rod outer segment lipids suspensions were prepared from dry films, obtained by evaporating the organic solvent with nitrogen. Sixty mM PBS buffer was added to a concentration of 1.25 mM lipids. One hundred μM of retinal (all-*trans* or 11-*cis*) was added as a concentrated solution in ethanol, at 37 ºC in darkness. After incubation, 10 mM hydroxylamine was added and the retinoids were extracted twice with hexane followed by normal phase HPLC. A2PE was analysed by CHCl3/MeOH (2:1) extraction and reverse phase HPLC analysis. Similarly, for A2E derivatization and reverse phase analysis, 0.3 unit/μl of phospholipase D and 15mM $CaCl_2$were added to the reaction mixture, incubated at 37 ºC for 2h and extracted with $CHCl_3$/MeOH (2:1) containing 0.1% trifluoroacetic acid (TFA). The final sample was redissolved in $CHCl_3$/MeOH (1:1).

3.2.7 Normal-Phase HPLC Analysis of Retinoid Oximes

Chromatography was performed using a normal phase column (Agilent ZORBAX Rx-SIL; 4.6 ×250 mm, 5 μ m) and elution with a gradient of hexane (A) and hexane/ethyl acetate (9:1) (B): 0-3 min, 100% A, 1.0 ml/min; 3-55 min, 0-100% B, 1.0 ml/min; 55-60 min, 100% A, 1.0 ml/min. Absorbance peaks were identified by comparison with external standards (11-*cis* retinal and all-*trans* retinal, and molar quantities per reaction were

calculated by comparison to standard concentrations determined spectrophotometrically using published extinction coefficients, and normalized to total sample volumes.

3.2.8 Reverse-Phase HPLC Analysis of A2E and A2PE

For quantification of A2E and A2PE, a C4 column (Phenomenox 4 x 250 mm, 5 µm) was used with the following gradients of acetonitrile in water (containing 0.1% trifluoroacetic acid): 75% (5min; flow rate, 1ml/min), 75-100% (5 min; flow rate 1 ml/min, and 100% (15 min; flow rate, 1 ml/min), and monitored at 430 nm.

3.2.9 Native PAGE Analysis of ABCA4 from ROS Membranes

ROS membranes (5 mg) were washed and resuspended in 200 µl of low salt buffer (50 mM NaCl, 1 mM EDTA, 2 mM 6-aminohexanoic acid, 50 mM Imidazole/HCl, pH 7.0) and solubilized with 8 µl of CHAPS (10%), 4 µl of dodecylmaltoside (10%), or 4 µl of TX-100. Similarly, after 30 min, samples were centrifuged (100,000 x g) for 5 min. Twenty µl of sample was added to 1 µl of 5% Coomassie Blue G-250 solution. Similarly, ABCA4 derived from HEK293T transient transfections was purified and processed accordingly. The samples were loaded onto an 8% acrylamide gradient gel and ran at 4 ºC overnight. After electrophoresis, the gel was destained and transferred onto PVDF for immunoblotting.

3.3 Results

3.3.1 ABCA4 ATPase is Stimulated by 11-*Cis* Retinal

We first explored whether 11-*cis* retinal transport is functionally mediated by ABCA4. For ATPase analysis, 1D4-tagged expressed ABCA4 was purified from HEK293T cells and reconstituted into brain polar lipid proteoliposomes. The initial ATPase rates determined within 15 min at increasing ATP concentrations displayed simple Michaelis-Menten kinetics (Fig. 3.1A). The apparent K_m values for ATP were similar (K_m = 0.23 ± 0.02

mM with either 40 µM 11-*cis* retinal or 40 µM all-*trans* retinal). However, when compared to the basal ATPase activity, 11-*cis* retinal resulted in a 3-fold increase in V_{max} compared to a ~2-fold activation for all-*trans* retinal. Half-maximal activation occured at ~10 µM for both retinal isomers (Fig 3.1A and 3.1B). These findings suggest that retinal stimulation of ABCA4 ATPase is preferentially enhanced by 11-*cis* retinal.

In addition to substrate binding, high affinity allosteric binding (K_d ~70 nM) of 11-*cis* retinal to NBD1 and all-*trans* retinal to ECD2 domains suggest that the isomers may modulate or regulate ABCA4 activity in different ways (Biswas-Fiss et al., 2012; Biswas-Fiss et al., 2010). Therefore, we assessed a combination of the isomers for potential modulation of ABCA4 ATPase. In DOPC/DOPE or DOPC reconstituted proteoliposomes, 11-*cis* retinal was doped against a fixed concentration of all-*trans* retinal (40 µM) (Fig 3.1C). We observed a modest increase in retinal stimulation ranging from a 2-fold ATPase stimulation without 11-*cis* retinal that increased to 3.5-fold in the presence of 40 µM or 60 µM 11-*cis* retinal. Although competition of the isomers may lead to enhanced activation, the findings suggest both isomers do not produce an additive effect *per se* in ABCA4 ATPase and the stimulation increase may be reflective of the cumulative retinal concentration in assay conditions.

In a previous study two compounds, amiodarone and digitonin, behaved as allosteric activators of ABCA4 ATPase which when combined with all-*trans* retinal, resulted in a multiplicative effect of ranging from 4- to 10-fold in retinal ATPase stimulation (Sun et al., 1999). To assess the allosteric activation with the retinal isomers, we examined whether doping 20 µM of these compounds affected the ATPase stimulation. In these experiments, it was observed that amiodarone significantly stimulated both 11-*cis* and all-*trans* retinal

dependent ATPase activities by 6- and 4-fold without significantly affecting the basal activity in ABCA4-PC proteoliposomes (Fig 3.1D). In addition, the retinal stimulation was approximately 8- and 5-fold higher in the presence of digitonin for the *cis* and *trans* isomers. In contrast, retinal synergistic stimulation was unaffected with CHAPS (20 μM) suggesting the specific interaction of digitonin with ABCA4. These data therefore indicates that 11-*cis* retinal, compared to all-*trans* retinal, induces an enhanced multiplicative synergistic activation with drugs on ABCA4 ATPase and suggest that 11-*cis* retinal is a preferred substrate of ABCA4.

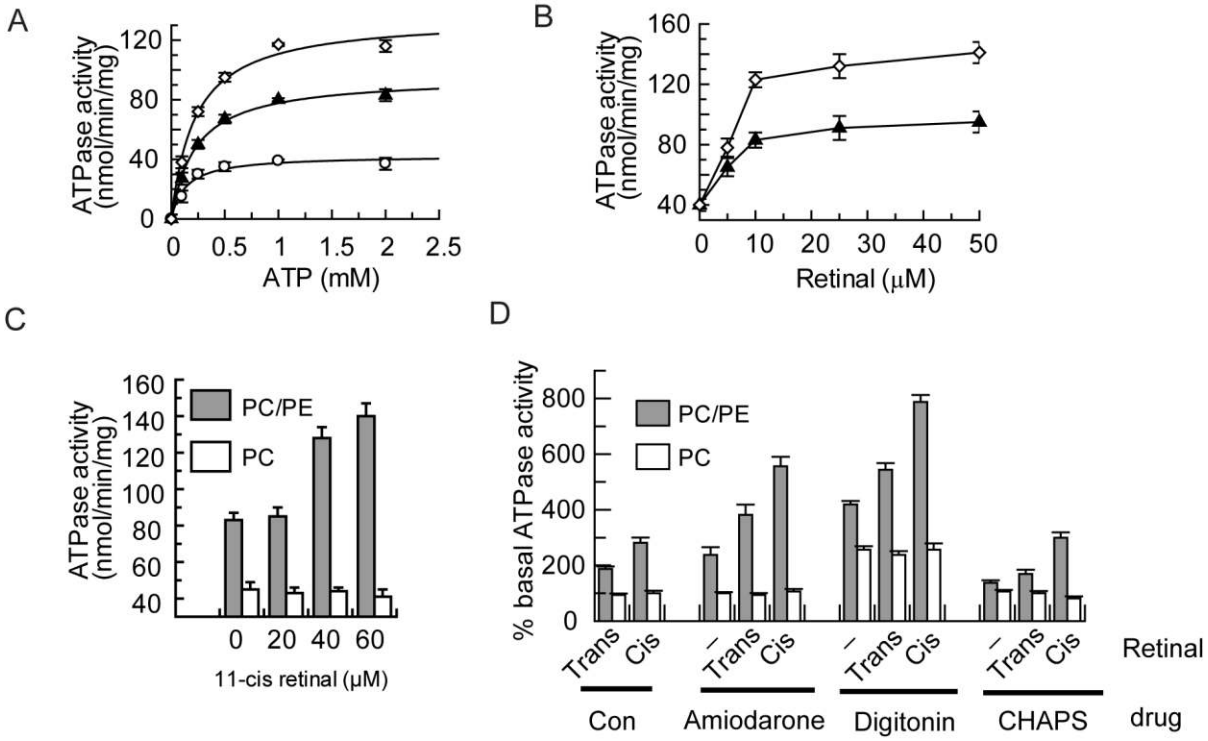

Figure 3.1 ABCA4 ATPase is Stimulated by 11-*Cis* retinal and is Activated by Drugs

A. ATPase activity of reconstituted ABCA4 Basal (○), 50 μM all-*trans* retinal (▲), 50 μM 11-*cis*-retinal (◊) stimulated ATPase activities as a function of ATP concentration performed at 37 ºC for 15 min. **B**. Effect of retinal on ATPase hydrolysis activity. Purified ABCA4 proteoliposomes was incubated with 50 μM 11-*cis* or all-*trans*-retinal at a fixed ATP concentration of 0.5 mM and fitted to the Michaelis-Menten equation. **C.** Competition of all-*trans* retinal with 11-*cis* retinal shows additive effect of retinal ATPase stimulation. Using 40 μM all-trans retinal, 11-*cis* retinal is doped in increasing concentrations in ABCA4 DOPC/DOPE (shaded) proteoliposomes and DOPC (white) proteoliposomes. **D.** Synergistic ATPase stimulation of purified and reconstituted ABCA4 by all-*trans* retinal and 11-*cis* retinal with a subset of low molecular drugs. ABCA4 DOPC/DOPE (shaded) proteoliposomes and DOPC (white) proteoliposomes. The bar graph shows the relative ATPase activity in the presence of 50 μM retinal, 40 μM amiodarone, and 30 μM digitonin. For digitonin comparison, 30 μM CHAPS was used in the buffer. For each experiment, the ATPase activity of wild-type ABCA4 in the absence of retinal (basal ATPase) is set to 100%. Results are the mean ± SD for three independent experiments.

3.3.2 ABCA4 Transfers 11-*Cis* Retinal with Similar Kinetics

We examined retinal transfer responses directly using ABCA4 donor proteoliposomes that enables functional characterization in response to the two isomers. Donor proteoliposomes and acceptor liposomes were loaded with radiolabelled retinal and ATP-dependent retinal transfer was monitored *in vitro*. ABCA4 transferred 11-*cis* retinal from the

lumen to the cytosolic side of donor proteoliposomes and was eventually transferred to acceptor liposomes in the import direction. As shown in Fig 3.2A, a 1 h specific activity assay of ABCA4 displayed significant 11-*cis* retinal transfer activity revealing a sigmoidal nature with a $K_{0.5}$ of 6.1 ± 0.4 μM and a Hill coefficient of 1.6 ± 0.3 consistent with transport characteristics of all-*trans* retinal ($K_{0.5}$ of 6.9 ± 0.4 μM; n = 1.7 ± 0.3). In addition, the maximal velocities of transfer were similar and did not parallel with the observed values in ATPase stimulation. The time course measurements whereby the donor and acceptor liposomes were preincubated with retinoid isomers followed by transfer assay initiation with ATP at 30 min also showed ABCA4 transfer of 11-*cis* retinal in a significant and similar manner to all-*trans* retinal (Fig 3.2B & 3.2C). The results suggest that potency of transfer may be regulated by the vesicle environment and we thus investigated the effect of retinoids by organic solvent extraction and HPLC analyses.

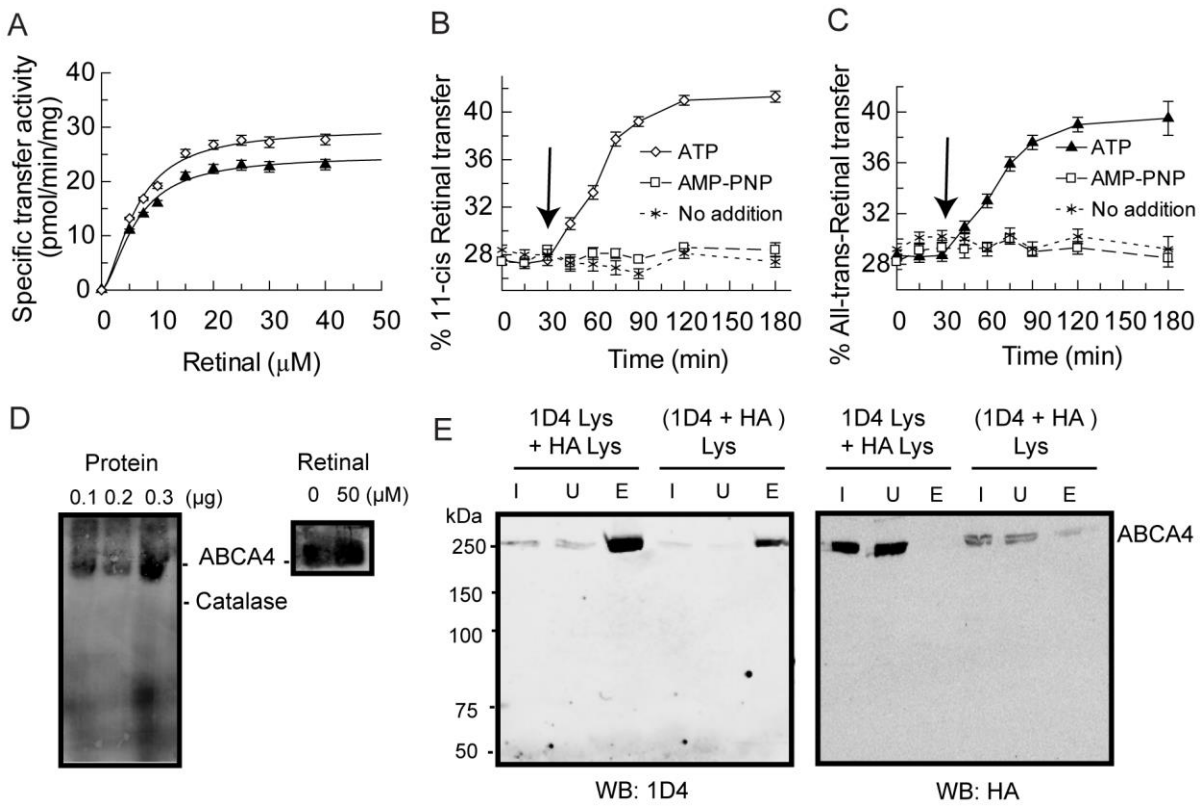

Figure 3.2 Active Transfer Kinetics, Time Courses of 11-*Cis* Retinal & All-*Trans* Retinal

A. ATP-dependent rate of [^{3}H] ATR transfer (retinal transfer activity) from ABCA4 proteoliposomes to acceptor liposomes as a function of 11- *cis* retinal (○) and all-*trans* retinal (▲) concentration. Data was fit to a sigmoidal allosteric curve for 11 *cis*-retinal with a $K_{0.5}$ of 6.1 ± 0.4 μM and a Hill coefficient of 1.6 ± 0.3; and for all-*trans* retinal with a $K_{0.5}$ of 6.9 ± 0.4 μM and a Hill coefficient of 1.7 ± 0.3. Data plotted as a mean ± s.d. for $n = 2$. Time course for the transfer of [^{3}H] 11 *cis*-retinal (**B**) and all-trans retinal (**C**) from ABCA4 proteoliposomes to acceptor vesicles. At 30 min, 5 mM ATP (arrow) or 5 mM AMP-PNP were added to start and monitor the transfer reaction. **D.** ABCA4 oligomerization (without reducing agent) was analysed by native page electrophoresis from CHAPS-solubilized and purified from rod outer segment membranes and labeled with 3F4. **E.** Immunoprecipitation of ABCA4 complex. Expression plasmids encoding HA-tag and 1D4-tag ABCA4 were transfected separately or co-transfected into HEK293T cells. On a sepharose coupled 1D4 column, detergent solubilized cell lysates from different transfections were mixed (*1D4 Lys + HA Lys*) along with solubilized co-transfected samples (*1D4 + HA lys*). Western blots of extracts from HEK293T cells transfected with ABCA4-1D4 and ABCA4-HA plasmid were labeled with antibodies to HA (right) and Rho 1D4 (left). The input (I), unbound fraction (U) and purified eluted protein (E) were probed. The ABCA4-HA did not co-immunoprecipitate (E) with ABCA4-1D4 from CHAPS-solubilized ABCA4-1D4 (I) with the 1D4 antibody.

Because the nature of transport allostery is observed in both retinal isomers, we assessed the protein oligomerization state of ABCA4. Native polyacrylamide gel

electrophoresis (PAGE) analysis of solubilized rod outer segments or purified ABCA4 in the absence of Dtt revealed that ABCA4 migrates mainly at or near the catalase standard protein (~230 kDa; Fig 3.2D), which suggests that ABCA4 exists as a monomer, and to a lesser extent as an oligomer complex, in disc membranes. In addition, using HEK293T expression studies ABCA4-1D4, ABCA4-HA tag constructs were transfected and expressed either singly or in combination. When cell lysates from ABCA4-1D4 and ABCA4-HA were solubilized and mixed together, ABCA4-1D4 pulls down nearly ~10% of ABCA4-HA protein in coimmunoprecipitation analysis (Fig 3.2E *left-half of 1D4 & HA blot*). In addition, when both ABCA4-1D4 and ABCA4-HA tag constructs were transfected together, nearly 15% of ABCA4-HA tag pulls down with the ABCA4-1D4 elution (Fig 3.2E *right-half of 1D4 & HA blot*). Solubilized cell lysates of ABCA4-HA failed to bind to the 1D4 tag column ensuring the specificity of the purification column. Collectively, these findings support a role in which ABCA4 in monomeric or oligomeric form may promote energy-dependent transfer of retinal.

3.3.3 11-*Cis* Retinal Displays Dark Isomerization Mediated by Phospholipid PE

11-*cis* retinal is an unstable and sensitive isomer capable of isomerizing in select organic solvents and light. To investigate how 11-*cis* retinal is transported over time, we determined the retinoid composition during the active transport process. To determine whether retinal is affected by liposomal vesicles, we first tested retinoid composition in purified and reconstituted rod outer segment lipids. A simple hydroxylamine derivatization was used to analyze and efficiently extract retinal from the sample at different times. At 0 h, 11-*cis* retinal shows a predominant peak with syn- and anti-configurations of the oxime derivative, whereas at 30 min, 11-*cis* retinal displayed a drastic ~50% isomerization to all-

trans retinal oximes (Fig 3.2B,C). In a next set of experiments, synthetic lipids were studied to analyze retinal isomerization in two vesicle populations: PC:PE (6:4) and PC only (Fig 3.3D). As expected, 11-*cis* retinal isomerized to all-*trans* retinal in PC:PE fraction, yielding a half-life of 2h (Fig 3.3E). In addition, the effect of isomerization is specific for phospholipid PE as PC vesicles displayed minimal isomerization (7% in 12h). In either ROS lipid vesicles or ROS discs fraction, isomerization is 50% complete in around 30 minutes, approximately 4-fold quicker than in synthetic PC/PE vesicles (Fig 3.3E). This suggests that the Schiff base formation between the aldehyde group of 11-*cis* retinal and the primary amino group of phospholipid PE may influence *cis*-to-*trans* isomerization. Thus, prolonged incubation of the *cis* isomer in the transport assay may result in a concomitant reduction in 11-*cis* retinal and an increase in all-*trans* retinal concentration, thus precluding its actual transfer activity.

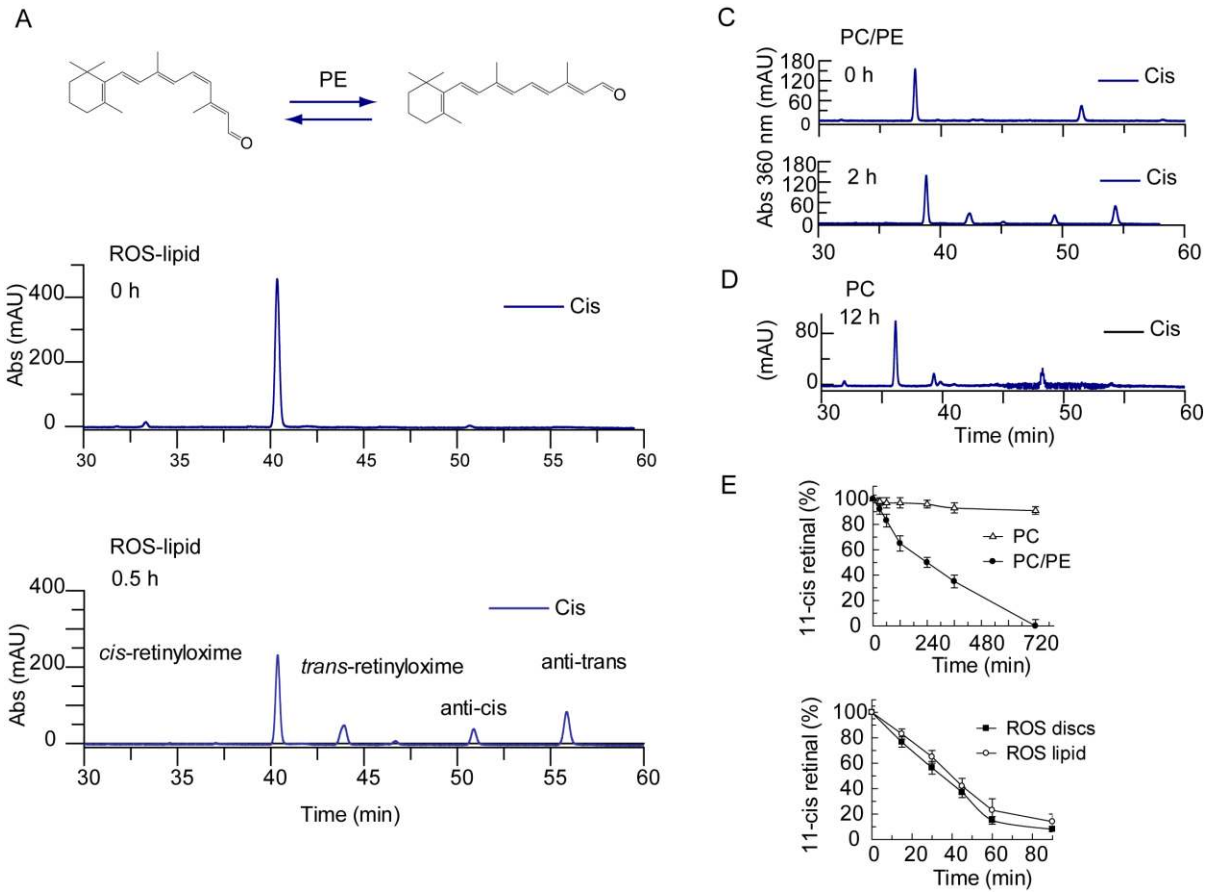

Figure 3.3 Dark Isomerization of 11-*Cis* Retinal and All-*Trans* Retinal in Lipid Vesicles

A. 11 *cis*-retinal isomerizes to other retinal isomers including all-*trans* retinal. **B.** Under dark conditions, retinal (0.1 mM) is incubated with 1 ml of ROS lipid vesicles (1.5 mM phospholipid) in 60 mM phosphate buffer (pH 7.2) at 37°C. Representative chromatographic separation of retinoid oximes of 11-*cis* retinal (blue) and all-*trans* retinal (dotted) by normal phase HPLC taken at two different time points. Incubation of retinal with ROS lipid resulted in a progressive increase in isomerization to all-*trans* retinal. Chromatogram B shows *syn*- and *anti*-11-*cis* retinal oximes and *syn*- and *anti*-all-*trans* retinal oximes. Retinal was also incubated with DOPC/DOPE (60:40) (**C**) and DOPC (**D**) vesicles for different incubation periods and analyzed by chromatography after derivatization. **E**. Time course of dark isomerization of 11-*cis* retinal in ROS lipid and ROS disc together with DOPC/DOPE (60:40), and DOPC vesicles.

3.3.4 Accumulation of A2E in Liposomal Vesicles

A2E, the major hydrophobic and possible cytotoxic component of lipofuscin, is formed from two molecules of all-*trans* retinal and one molecule of phosphatidylethanolamine. Ineffective clearance and eventual reduction results in enhanced

levels of all-*trans* retinal, predicting increased levels of A2E that is toxic to the retina. Several lines of evidence also demonstrated that A2PE forms within photoreceptor outer segments (Ben-Shabat et al., 2002; Liu et al., 2000). Thus, we used HPLC to detect whether A2PE forms during incubation in ROS lipid vesicles at different times. *In vitro* incubation of exogenously added all-*trans* retinal for 4h and monitoring the reaction mixture by reverse phase HPLC using a gradient of acetonitrile and water (with 0.1% TFA) revealed a broad unresolved peak that had a retention time of ~10.5 min and exhibited a UV-Vis absorbance spectra characterized by λ_{max} 450 and 340 nm (Fig 3.4A). This may suggest a heterogeneous mixture of A2PE exists based on the variable fatty acid composition of PE containing lipids. Addition of phospholipase D yields peaks in the chromatogram that can be identified as distinct A2E and iso-A2E at ~ 5 min characterized by λ_{max} 490 and 330 nm (Fig 3.4B).

To test for bisretinoid formation in rod outer segments, we next carried out A2E quantification with ROS disc vesicles under NADPH and non-NADPH conditions. Addition of exogenous NADPH should reduce retinal to retinol and the reaction should be stopped with addition of phospholipase D. Again, the starting compounds were all-*trans* retinal and separate reaction mixtures were incubated in parallel at 1, 4, and 8 h and 1, 3, and 7 days. Under NADPH conditions, only retinol peaks were observed by normal-phase HPLC . However, under non-NADPH conditions, peaks attributable to A2PE were apparent after 4h incubation and substantially increased at 1, 3, and 7 days incubation. Phospholipase D treatment resulted in hydrolysis of A2PE fraction and generation of A2E. Using integrative analysis of peaks, levels of A2E/isoA2E increased from 4h to 3 days reaching ~20% retinal being converted to bisretinoids. Retinal does remain in significant proportion with the vesicles over prolonged incubation. Thus, retinal isomerization precedes bisretinoid

formation in photoreceptors, because A2E formation takes a relatively long time to form and ABCA4 may aid in importing retinylidene PE of either retinal isomer into the disc cytosol.

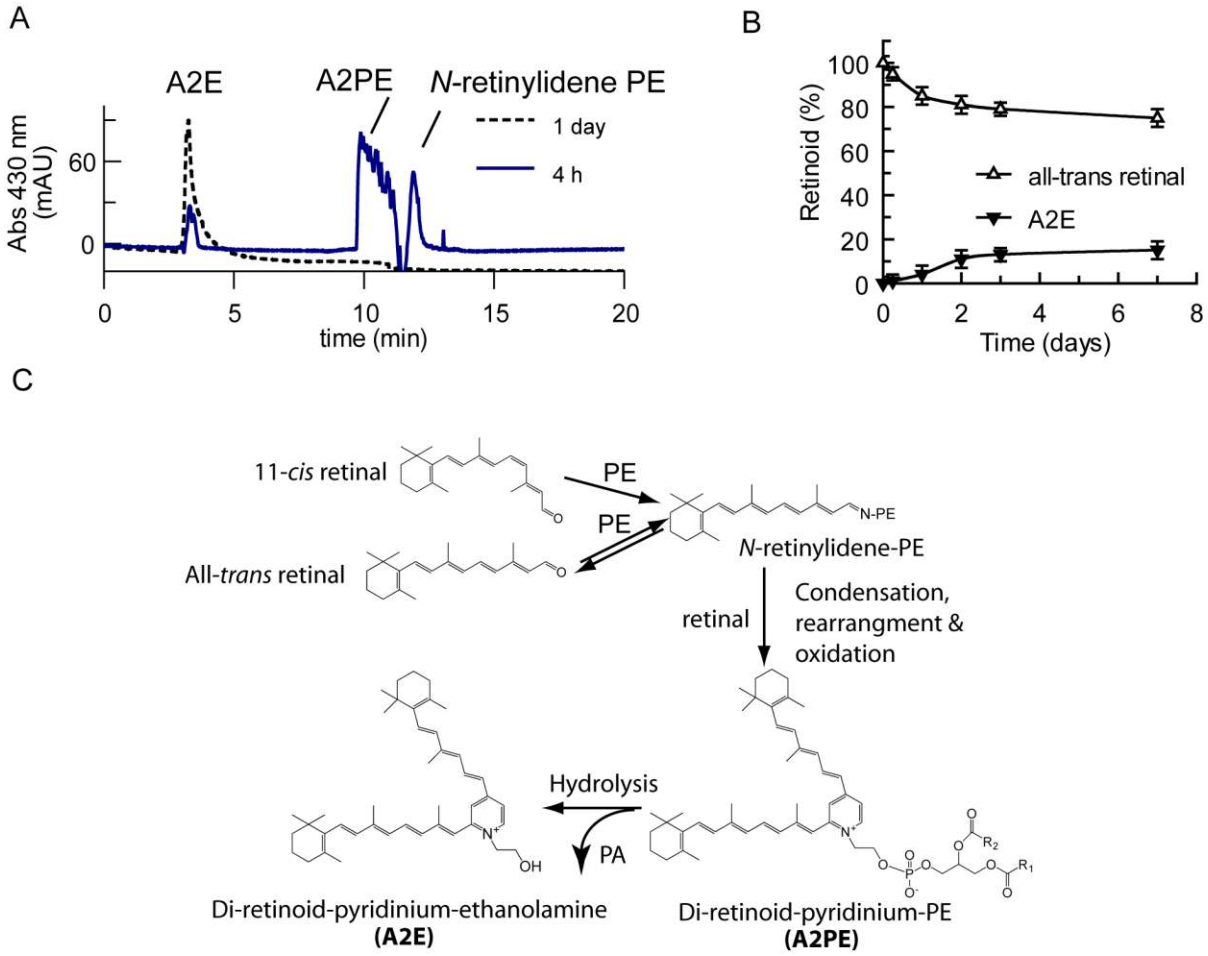

Figure 3.4 Dark Formation of A2E and A2PE by HPLC Analysis

A. Under dark conditions, retinal (0.1 mM) is incubated with 1 ml of ROS lipid vesicles (1.5 mM phospholipid) in 60 mM phosphate buffer (pH 7.2) at 37°C. The reaction mixture was incubated at room temperature in the dark for 4h, and 1, 3 or 7 days. Next, it was treated in the presence or absence of phospholipase D and the constituents of the mixture were separated by reverse phase HPLC with monitoring at 430 nm. Incubation of retinal with ROS lipid resulted in a progressive increase in formation of A2E and A2PE. **B**. Time course of A2E formation in ROS. **C.** Reaction scheme of A2PE and A2E formation from both 11-*cis* retinal and all-*trans* retinal.

3.4 Discussion

In this study, we show how 11-*cis* retinal provided by the visual cycle produces robust stimulation in ABCA4 ATPase and that ABCA4 prefers the 11-*cis* retinal isomer, more than all-*trans* retinal, required for retinal transport. The similarity between 11-*cis* retinal and all-*trans* retinal in the mode of phospholipid PE dependence, synergistic-drug activation and the effect on the Michaelis-Menten ATPase parameters are notable. The data also suggests that the two isomers contribute to drug synergistic activation, and suggests that each isomer may effect different drug-inducible conformational changes. It has been shown that differences in affinity, hydrophobic nature, and size contributed to the 13-fold and 3-fold stimulation with verapamil and cyclosporine substrates of Pgp-mediated ATPase activity (Senior et al., 1998; Sharom et al., 1995). In addition, ABCA4 showed that either isomer can stimulate ATPase to different levels, co-stimulation with both isomers did not produce synergistic activation. This illustrated differences in the mechanism of ABCA4 transporter, which has different drug- and substrate-binding sites.

Clearance of retinal in the first step of the visual cycle of photoreceptors involves two steps: (1) diffusion of all-*trans* retinal and ABCA4 mediated active transport of *N*-retinylidene PE from the lumen to the cytosolic side of disc membranes and; (2) reduction of all-*trans* retinal to all-*trans* retinol by RDHs. The transfer assay experiments suggested that ABCA4 also flips 11-*cis* retinylidene PE from the lumen to the cytosolic side of proteoliposomes. In disc membranes, this implies that *N*-retinylidene PE moves up the concentration gradient, given that 11-*cis* retinal diffuses passively and moves down the concentration gradient from the photoreceptor plasma membrane (Frederiksen et al., 2012). Biochemically, the sigmoidal concentration dependence indicates allosteric regulation by

multiple substrate binding sites or by itself. The allosteric behaviour is not due to protein oligomerization because there was no significant binding of ABCA4 to itself in co-immunoprecipitation experiments and native PAGE experiments indicated the presence of monomeric ABCA4 species. Recently, single particle electron microscopy analysis predominantly showed monomeric form of ABCA4 (Tsybovsky et al., 2012). Thus, functional ABCA4 is largely monomeric and substrate binding through the transmembrane domains where translocation occurs and retinal binding to soluble protein domains, in either ECD or NBD domains, mediates the allosteric transport process of ABCA4.

Isomerization of retinal under dark and non-protein mediated conditions can be a differential nature of photoreceptor disc membranes. Groenendijk *et al.* showed that when phospholipid PE in ROS lipid membranes forms a Schiff base with retinal isomers, selective and substantial retinal isomerization takes place (Groenendijk et al., 1980). In this study, using similar vesicle preparations and time scale analyses, we show the two retinal isomers show specificity in PE-induced retinal isomerization: 11-*cis* → all-*trans* + 13-*cis* and all-*trans* → all-*trans* + 13-*cis*. ROS lipid and BPL lipid vesicles were extremely proficient at isomerizing 11-*cis* retinal to all-*trans* retinal along with a fraction of 13-*cis* retinal, whereas the rate of isomerization is slower in synthetic DOPC/DOPE vesicles and largely unaffected by DOPC vesicles. The heterogeneous and aggregated mixture of the fatty acyl chains may influence the isomerization rate of *N*-retinylidene PE. At 37 ºC, in both former compositions of vesicles, 11-*cis* retinal was completely isomerized in 1h. ABCA4 specific transfer activities and transport time courses may, in part, underestimate the transport parameters of 11-*cis* retinal. In addition, similar 11-*cis* retinal levels observed following bleaching studies of *Abca4*$^{-/-}$ mice may have been precluded by rapid isomerization with phospholipid PE

(Boyer et al., 2012; Mata et al., 2001; Mata et al., 2000). 11-*cis* retinal is not reduced in photoreceptor outer segments and recently, it was shown that 11-*cis* retinal flux is also maintained in bleached conditions (Boyer et al., 2012). Rdh8 largely accounts for the broad specificity and retinal reduction would proceed after retinal isomerization to all-*trans* retinal and 13-*cis* retinal (Maeda et al., 2009a; Palczewski, 1994).

Our studies showed that incubation of retinal with ROS vesicles resulted in A2E formation after phospholipase D treatment. In the absence of NADPH, *in vitro* retinal incubation increased the presence of A2PE over 7 days but with substantial unreacted retinal. This is relevant with the *Abca4*$^{-/-}$ mice studies that exhibited large increases in RPE lipofuscin and A2E accumulation (Kim et al., 2007; Mata et al., 2001; Mata et al., 2000; Weng et al., 1999). The amount of A2E increase varies with the mouse background ranging from 6.5 fold increase (129/sv) to at least 10- fold (C57Bl/6) compared with wild type controls (Boyer et al., 2012; Charbel Issa et al., 2012). It is now evident that generation of A2E in *Abca4*$^{-/-}$ mice is largely light-independent and primarily forms from 11-*cis* retinal (Boyer et al., 2012). Furthermore, 11-*cis* retinal flux may occur in the dark during formation of new photoreceptor discs (Boyer et al., 2012; LaVail, 1980). The implication of this work is that A2E precursors such as A2PE form relatively slower compared to retinal isomerization. This does not account for other condensation products as at least 20 distinct lipofuscin species have been characterized to date (Wu et al., 2009). *N*- or *cis*-retinylidene PE in the disc lumen renders it favorable for the slow reaction with a second retinal. Phagocytosis of photoreceptor discs with A2PE and related intermediates results in hydrolyzes to A2E-like compounds. Regardless of the mechanism, 11-*cis* retinal fluxes originating from the RPE and its isomerization in the visual cycle raise two possibilities for

ABCA4. First, in a dark-state photoreceptor following regeneration of opsin, excess 11-*cis* retinylidene PE is transported by ABCA4 from the disc lumen to the cytosol. Its dissociation and isomerization feeds back into the reduction activity of Rdh8. Second, in a bleached-state, ABCA4 translocates *N*-retinylidene PE produced after photobleaching and release of all-*trans* retinal.

Chapter 4: Phospholipid Transport by ATP Binding Cassette Proteins ABCA1, ABCA7, and ABCA4 and Disease-Causing Mutants*

4.1 Introduction

Cholesterol is a structural component of the cell and is vital for cellular and lipid homeostasis, although its excess often leads to inflammatory responses, atherosclerosis, and/or cell death (Singaraja et al., 2006; van Dam et al., 2002). To prevent overload, ABCA1, which is ubiquitously expressed in the plasma membrane of tissues, mediates the efflux of cholesterol and phospholipids to lipid poor ApoA-I to generate HDL. ABCA1 shares ~50% sequence homology with a subset of the ABCA subfamily members that includes ABCA2, ABCA4, and ABCA7.

Nearly a ~100 mutations in ABCA1 cause Tangier disease and familial high-density lipoprotein deficiency characterized by reduced amounts or near absence of circulating HDL (Bodzioch et al., 1999; Oram, 2002; Rust et al., 1998; Singaraja et al., 2006; van Dam et al., 2002). Crosslinking and mutagenesis studies indicate that ApoA-I directly binds to ABCA1 through electrostatic interactions involving lysine residues within the ECDs of ABCA1 (Chroni et al., 2004; Fitzgerald et al., 2004; Nagao et al., 2011). MDCKII and HeLa cells expressing ABCA1-GFP show enhanced redistribution of endogenous PS and fluorescent labeled-PS from the cytosolic side to the extracellular side of the plasma membrane (Woehlecke et al., 2003). Several disease-associated ABCA1 mutants exhibit a decrease in phospholipid and cholesterol efflux compared to wild-type ABCA1 in heterologous cell expression studies (Fitzgerald et al., 2002; Singaraja et al., 2006; Tanaka et al., 2003).

* This chapter has been submitted and is in press.
Quazi. F, Molday, RS. (2013). Differential Phospholipid Substrates and Directional Transport by ATP Binding Cassette Proteins ABCA1, ABCA7, and ABCA4 and Disease-causing Mutants J. Biol. Chem.

Moreover, ABCA7, which is expressed in select tissues, only promotes efflux of PC and SM to ApoA-I in cell-based studies (Wang et al., 2003). In the ABCA subfamily, direct biochemical evidence of lipid flipping was only shown for ABCA4 flipping PE from the lumen to the cytosolic side of membranes (Quazi et al., 2012). However, the direction and the identity of lipid substrates flipped by the homologous ABCA proteins mediating efflux are not clear.

In order to understand the biochemical function, we have purified and reconstituted ABCA1, ABCA7 and ABCA4 into liposomes for ATPase and fluorescent-lipid transport studies. PC, PS, and SM are broadly transported substrates by ABCA1 from the cytosolic side to the lumen side of reconstituted proteoliposomes. ABCA7 primarily transports PS in the same direction, whereas ABCA4 flipped only PE in the opposite direction. ABCA1 Tangier mutants and corresponding ABCA4 Stargardt mutants showed significantly reduced phospholipid transport activity and subcellular mislocalization. These studies provide the first direct evidence for ABCA1 and ABCA7 functioning as phospholipid transporters and suggest that this activity is an essential step in the loading of ApoA-I with phospholipids for HDL formation.

4.2 Methods

4.2.1 Materials

Cholesteryl hemisuccinate, 1,2 dioleoyl-*sn*-glycero-3-phosphatidylglycerol (DOPG), and fluorescent-labeled [7-nitro-2-1,3-benzoxadiazol-4-yl)] or *NBD*-labeled phospholipids, C6-*NBD*-labeled PG (Fl-PG), C6-*NBD*-labeled-SM (Fl-SM) were purchased from Avanti Polar Lipids (Alabaster, AL). Anti-calnexin was from Abcam and secondary anti-mouse and anti-rabbit antibodies conjugated to Alexa-488 and Alexa-594 was from Molecular Probes. Additional materials are described in Chapter 2.2.1.

4.2.2 DNA Constructs

ABCA7 was a generous gift of Dr. Kazumitsu Ueda and subcloned with a C-terminal 1D4 tag (T-E-T-S-Q-V-A-P-A) into a pCEP4 vector at *Not*1/*Hind*III Sites (Invitrogen) (Abe-Dohmae et al., 2004). Human ABCA4 and human ABCA1 with a C-terminal 1D4 tag subcloned in pCEP4 vectors at its *Not*I/*NheI* and *Not*I/*Not*I sites, respectively, were used for site-directed mutagenesis as described previously (Ahn et al., 2000; Tsybovsky et al., 2011). Mutations introduced by overlap-extension PCR using Pfu AD DNA polymerase in ABCA1 included: S100C, W590S, F593L, N935S, T929I, C1477R, T1512M, R2081W, and P2150L. Corresponding ABCA4 mutations determined by amino acid alignment with ABCA1 included: S100P, W605S, F608L, T959I, N965S, C1502R, T1537M, R2107P, and P2180L. ABCA1-MM was constructed to harbor the Walker A-motif lysine-to-methionine mutations K939M/K1952M by the nested PCR method; ABCA4-MM had the corresponding K969M/K1969M Walker A mutations (Ahn et al., 2000); and ABCA7-MM had the K847M/K1833M Walker A mutations. The presence of these mutations was confirmed by DNA sequencing.

4.2.3 Expression of ABCA Proteins in HEK293T and COS-7 Cells

HEK293T cells were cultured according to Chapter 2.2.3. COS-7 cells were transfected in six-well plates containing polylysine-treated coverslips with 5.0 µg of each plasmid.

4.2.4 Purification of ABCA Proteins

After 24h post-transfection, a cell suspension from nine 10-cm dishes was added slowly to 1.5 ml Buffer A (50 mM HEPES, pH 7.4, 0.2 mg/ml BPL, 0.002% cholesteryl hemisuccinate, 150 mM NaCl, 1 mM $MgCl_2$, 10% glycerol, 1 mM DTT) containing 18 mM CHAPS and protease inhibitor and stirred for 45 min at 4 °C. The supernatant after a 10 min centrifugation at 100,000xg (TLA110.4 rotor in a Beckman Optima TL centrifuge) was mixed with 50 µl of Rho1D4-Sepharose 2B for 1 h at 4 °C. The matrix was washed six times in Buffer A containing 10 mM CHAPS, 0.002% cholesteryl hemisuccinate. The protein was eluted thrice (3 X 150 µl) at 12 °C over 60 min in the same buffer with 0.2 mg/ml 1D4 peptide. A small fraction was analyzed by SDS-PAGE and western blotting using Rho1D4 antibody. The concentrated eluted protein (20-70 ng of ABCA/µl) was promptly used for proteoliposome reconstitution.

4.2.5 Preparation of Liposomes

For the preparation of unilamellar vesicles, the designated lipid compositions were prepared in chloroform and dried under N_2. For fluorescent phospholipid (Fl-PL) transport assays, DOPG or DOPC was mixed at a weight ratio of 99.4:0.6 with Fl-PL lipid. The lipids were resuspended in buffer containing 20 mM HEPES pH 7.4, 150 mM NaCl, 2 mM $MgCl_2$, 10% glycerol, 3.5 mM CHAPS at a concentration of 2.5 mg/ml by bath sonication and incubated at room temperature for 3 h. In a typical reconstitution experiment, 250 µg of

lipids were incubated with the ABCA protein (2-6 µg in detergent with DTT) at 4 °C for 1 h containing 4 mM CHAPS. Detergent was removed by dialysis for at least 24 h at 4 °C with a minimum of three 1 liter changes of buffer C (10 mM HEPES, pH 7.4, 150 mM NaCl, 2 mM $MgCl_2$, 10% sucrose and 1 mM DTT).

4.2.6 Collisional Quenching Experiments.

To assess the steady-state distribution of the Fl-PL across the membranes of proteoliposomes, collisional quenching of fluorescent lipid probes was performed with potassium iodide (KI) (Rajasekharan et al., 2013). ABCA protein was reconstituted using buffer C but with 250 mM NaCl and devoid of sucrose. Excitation and emission wavelengths were set at 470 and 530 nm, respectively. Fluorescence intensity of Fl-PL-containing proteoliposomes was measured for samples consisting of 50 µl of vesicles diluted into 100 µl of buffer containing 10 mM HEPES pH 7.4, 10 mM $Na_2S_2O_3$, and the quencher KI (0 to 250 mM). NaCl was used to adjust the ionic strength to 250 mM and maintain the osmolarity of the solution while $Na_2S_2O_3$ prevented production of I_2. Parallel samples were measured using NaCl instead of KI. Data were analyzed according to the modified Stern-Volmer equation:

$$\frac{F_0}{\Delta F} = \left(\frac{1}{fa.K[Q]}\right) + \frac{1}{fa}$$

where F_o is the fluorescence intensity in the absence of the quencher, ΔF is the fluorescence intensity in the presence of the quencher at concentration $[Q]$, f_a is the fraction of fluorescence which is accessible to the quencher, and K is the Stern-Volmer quenching constant.

4.2.7 Immunofluorescence Microscopy

COS-7 cells transfected with 1D4-tagged ABCA proteins were fixed in 4% paraformaldehyde, 100 mM phosphate buffer (PB) (pH 7.4), for 1 h and subsequently

blocked and permeabilized with 10% normal goat serum and 0.2% Triton X-100 in PB for 30 min. The cells were then labeled for 2h at room temperature with Rho-1D4 hybridoma culture fluid diluted 1:50 in PB containing 2.5% normal goat serum and 0.1% Triton X-100 and an anti-calnexin polyclonal antibody (Abcam) diluted 1:200 in the same buffer. The cells were labeled with secondary 1:1000 diluted anti-mouse and anti-rabbit antibodies conjugated to Alexa-488 and Alexa-594 (Molecular Probes), respectively. Samples were visualized under a Zeiss LSM 700 confocal microscope. Relative quantification of co-labeling of ABCA1 and calnexin as an ER marker was determined using ImageJ software (http://rsb.info.nih.gov/nih-image/) as follows: In the micrographs, mean pixel background ± 3xSD intensity in a selected area without cells for both green and red channels was subtracted from the respective micrograph. Each cell was delimited with the ROI tool and a binary mask was formed to multiply both channels. Co-localization was analyzed using the JaCop plugin (Just Another Co-localization Plugin) for ImageJ, and Pearson's coefficient (r) was calculated with a JaCop plugin (Bolte and Cordelieres, 2006).

4.2.8 Flippase Assays, Membrane Preparation, and SDS-PAGE

Flippase and ATPase assays were performed according to Chapter 2.2.8 and 2.2.10. Membranes from transfected HEK293T cells were also prepared as described previously (Ahn et al., 2003) except that the procedure was scaled down, and the cell suspension originated from two 10-cm dishes of HEK293T cells. SDS-PAGE and Western blots were performed according to Chapter 2.2.11.

4.3 Results

4.3.1 Purification and Reconstitution of ABCA1 and ABCA4 into Proteoliposomes

Wild-type ABCA1, ABCA4, and ABCA7 and corresponding mutant proteins in which lysine residues in the Walker A motifs (GxxGxKS/T) of NBD1 and NBD2 were replaced with methionine (ABCA-MM), all containing a 9 amino acid C-terminal 1D4 tag, were transiently expressed in HEK293 cells and purified from CHAPS-solubilized cell lysates on a Rho1D4 immunoaffinity matrix. A typical Coomassie blue stained SDS gel and Rho 1D4 antibody-labeled western blot of the cell lysates and immunoaffinity-purified ABCA1 and ABCA7 is shown in Fig 4.1A. The level of expression and extent of purification were similar for the WT and mutant proteins. Similar results were obtained for ABCA4 as previously reported (Quazi et al., 2012; Zhong et al., 2009).

The immunoaffinity-purified ABCA proteins were subsequently reconstituted into brain polar lipid (BPL) at a lipid:protein weight ratio of ~ 20:1 for analysis of their ATPase activities. BPL was used in these initial studies since it contains a variety of known phospholipids (12.6% PC, 33.1% PE, 4.1% PI, 18.5% PS, and 0.8% PA) along with 30.9% unknown components (Avanti Polar Lipids). As shown in Fig 4.1B, all WT ABCA proteins exhibited significant ATPase activity whereas the ABCA-MM mutant proteins were devoid of activity.

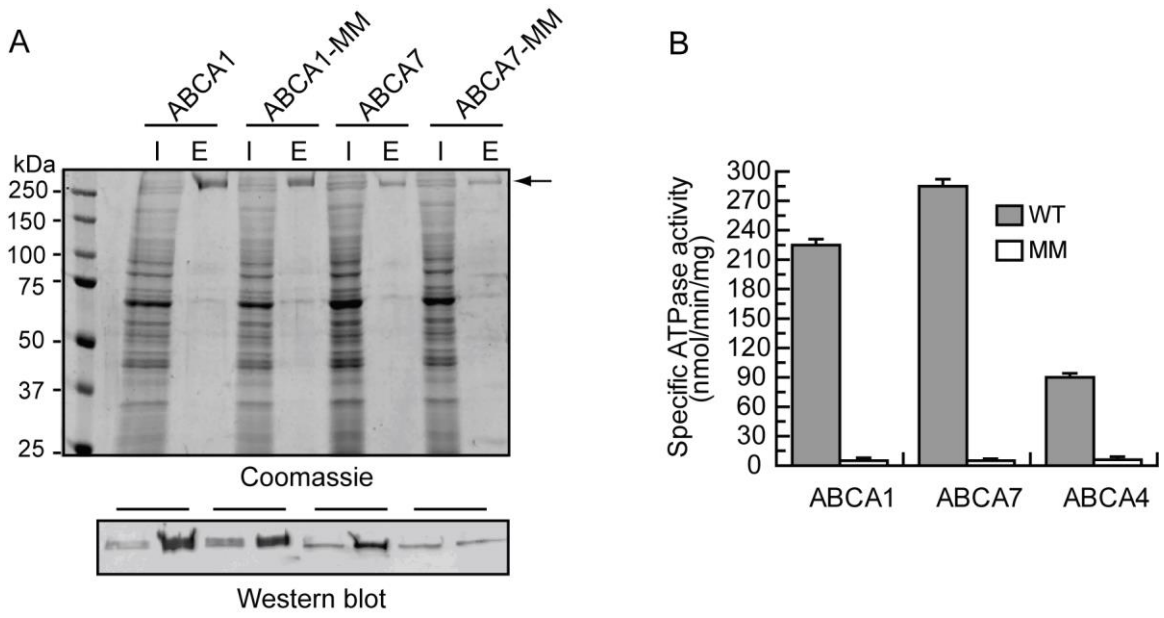

Figure 4.1 Purification and ATPase Activity of ABCA1, ABCA7, and ABCA4

Purification and ATPase activity of ABCA1, ABCA7, and ABCA4. Wild-type (WT) and mutant ABCA1, ABCA4, and ABCA7 in which lysine residues in the Walker A motifs of NBD1 and NBD2 were replaced with methionine (ABCA-MM) all containing a 9 amino acid C-terminal epitope were expressed in HEK293T cells and purified on a Rho-1D4 immunoaffinity matrix. **A**. Commassie blue stained gel and Rho1D4 labeled western blot of the ABCA1 and ABCA7 detergent-solubilized cell lysate (lane labeled I) and purified protein eluted from the immunoaffinity column with the 1D4 peptide (lane labeled E). The arrow identifies the position of the ABCA1 and ABCA7 transporters. **B**. ATPase activity of WT and mutant ABCA proteins. Immunoaffinity purified WT ABCA1, ABCA7 and ABCA4 and their MM mutants were reconstituted into brain polar lipid for analysis of their ATPase activity. Results are the mean ± SD for three independent experiments.

4.3.2 Stimulation of ABCA1, ABCA4 & ABCA7 ATPase by Membrane Lipids

The phospholipid specificity of the ABCA transporters was studied by reconstituting the proteins in liposomes consisting of 1,2 dioleoyl phosphatidylglycerol (DOPG abbreviated here as PG) as the base phospholipid for ABCA1 and ABCA7, and 1,2 dioleoylphosphatidylcholine (DOPC abbreviated as PC) for ABCA4. This lipid composition was modified by replacing a portion of the base phospholipid with a defined amount of 1,2 dioleoylphospholipids, PC, PS, PE, PI, PG, sphingomyelin (SM) or cholesterol. The average diameter of the proteoliposomes was typically 70 ± 25 nm. The orientation of the

reconstituted ABCA transporters in the liposomes was determined from the increase in ATPase activity following detergent permeabilization. In the case of the ABCA proteins reconstituted into PC vesicles, approximately 60% of the protein was oriented in an inside-out configuration i.e. nucleotide-binding domains (NBD) exposed on the outside of the vesicles. ABCA proteins reconstituted in liposomes composed of PC/PS (7:3), PC/PE (7:3) or PG were oriented with 70-80% of the protein having their NBDs on the outer side of the proteoliposomes.

The effect of various phospholipids, sphingolipids, and cholesterol on the ATPase activity of reconstituted ABCA1, ABCA7, and ABCA4 is shown in Fig 4.2A-C. The ATPase activity of ABCA1 was stimulated 2-fold and 1.6-fold by the addition of 30 mol % PC and PS, respectively, with a smaller 1.4-fold increase for 30 mol % SM. In contrast, a decrease in activity was found when ABCA1 proteoliposomes were doped with 30 mol% PE, PI, cholesterol, or ceramide. These data indicate that PC, PS and SM specifically stimulate the ATPase activity of ABCA1 over the ATPase activity in pure PG liposomes. The ATPase activity of ABCA7 was also stimulated by PC, PS and SM, but PS was more effective than PC for this transporter. For comparison, the effect of these lipids on the ATPase activity of ABCA4 was also measured in PC liposomes containing 30 mol% added lipid. In agreement with earlier studies (Quazi et al., 2012), maximal stimulation was observed for PE. In contrast, a decrease in ATPase activity was observed for PI, cholesterol and ceramide.

The effect of varying the PC, PS and PE content of the liposomes on the ATPase activity of these ABCA transporters was also determined (Fig. 4.2D-E). A maximum relative increase in ATPase activity of 75-85% was observed at 30% PC for ABCA1, 30% PS for ABCA7, and 20% PE for ABCA4.

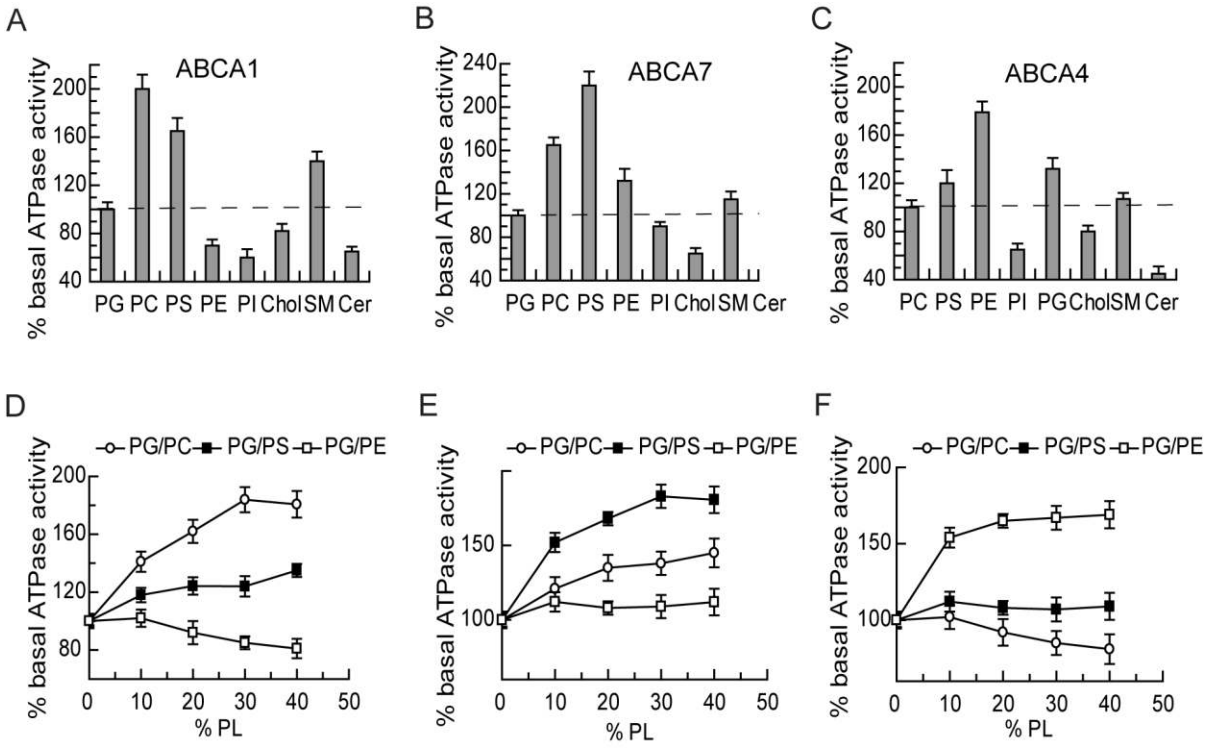

Figure 4.2 Effect of Membrane Lipids on the ATPase of ABCA1, ABCA7, and ABCA4

Immunoaffinity purified ABCA1 and ABCA7 were reconstituted into PG liposomes and ABCA4 was reconstituted into PC liposomes as the base lipids. The activity of the ABCA transporters in these liposomes was set at 100%. **A-C.** The effect of various lipids was determined by replacing 30 mol% of the base lipid with the 1,2 dioleoylphospholipids, PC, PS, PE, or PI, cholesterol (Chol), sphingomyelin (SM), or ceramide (Cer). **D-F**. The effect of increasing phospholipid (PL) concentration on the ATPase activity of ABCA1, ABCA7 and ABCA4. ATP hydrolysis was measured at 37^{o}C for 40 min. Results are the mean ± SD for three independent experiments.

4.3.3 Transport of Phospholipids by ABCA Transporters

Stimulation of the ATPase activity of ABCA1, ABCA7, and ABCA4 by selected phospholipids suggests that these lipids may serve as substrates that are actively transported or flipped across the lipid bilayer by these transporters. To test this possibility and determine the direction of transport, we utilized a well-established dithionite phospholipid fluorescence bleaching technique (Coleman et al., 2009; Romsicki and Sharom, 2001). Proteoliposomes reconstituted with purified ABCA proteins were prepared with a low concentration (0.6%) of fluorescent-labeled phospholipid (Fl-PL). ATP was added to the proteoliposomes to initiate

active transport with the nonhydrolyzable derivative AMP-PNP added to the control sample. After 1 hour, sodium dithionite, an impermeable reducing agent, was added to bleach the Fl-PL exposed on the outer leaflet of the proteoliposome. The amount of Fl-lipid transported was determined from the difference in fluorescence between the ATP and AMP-PNP treated samples after dithionite addition. Fig 4.3A shows typical fluorescence traces for the transport of Fl-PC across the lipid bilayer of PG proteoliposomes reconstituted with ABCA1. ATP addition resulted in a decrease in the degree of dithionite bleaching (higher fluorescent signal) compared to the control AMP-PNP indicating that ABCA1 promoted an energy dependent transport of Fl-PC from the outer to the inner leaflet of the proteoliposome, a direction which is consistent with PC transport from the cytoplasmic to the extracellular/lumenal side of biological membranes. Similar results were obtained for the transport of Fl-PC by ABCA7.

For comparison this assay was used to measure the transport of Fl-PE across the membrane of proteoliposomes reconstituted with ABCA4 (Fig 4.3B). In this case the addition of ATP resulted in an increase in dithionite-mediated fluorescence bleaching relative to the AMP-PNP indicating that ABCA4 transports Fl-PE in the opposite direction i.e. from the extracellular/lumenal leaflet to the cytoplasmic leaflet of cells.

The time course for the flipping of phospholipids across the lipid bilayer was determined for ABCA1 and ABCA4 reconstituted into liposomes (Fig. 4.3C-E). A linear increase in Fl-PC and Fl-PS flipped from the outer (cytoplasmic) to the inner (lumen) leaflet was observed over 60 min for ABCA1 reconstituted into PG liposomes. A linear decrease in the amount of Fl-PE in the inner leaflet was observed for ABCA4 reconstituted into PC liposomes.

ABCA1 and ABCA4 catalyzed phospholipid transport was also measured using collisional fluorescence quenching method (Fig 4.3F-H) (Rajasekharan et al., 2013). In this technique, membrane-impermeable iodide ion was used to quench the fluorescence contribution of Fl-labeled lipid on the outer leaflet of the proteoliposomes after the addition of ATP or AMP-PNP. The results shown in a modified Stern-Volmer plot (Lakowicz, 1980) confirms the results obtained using the dithionite fluorescence bleaching assay indicating that ABCA1 transports Fl-PC and Fl-PS from the inner to the outer leaflet of the proteasomes (Fig 4.3F,G), whereas ABCA4 transports Fl-PE in the opposite direction (Fig 4.3H).

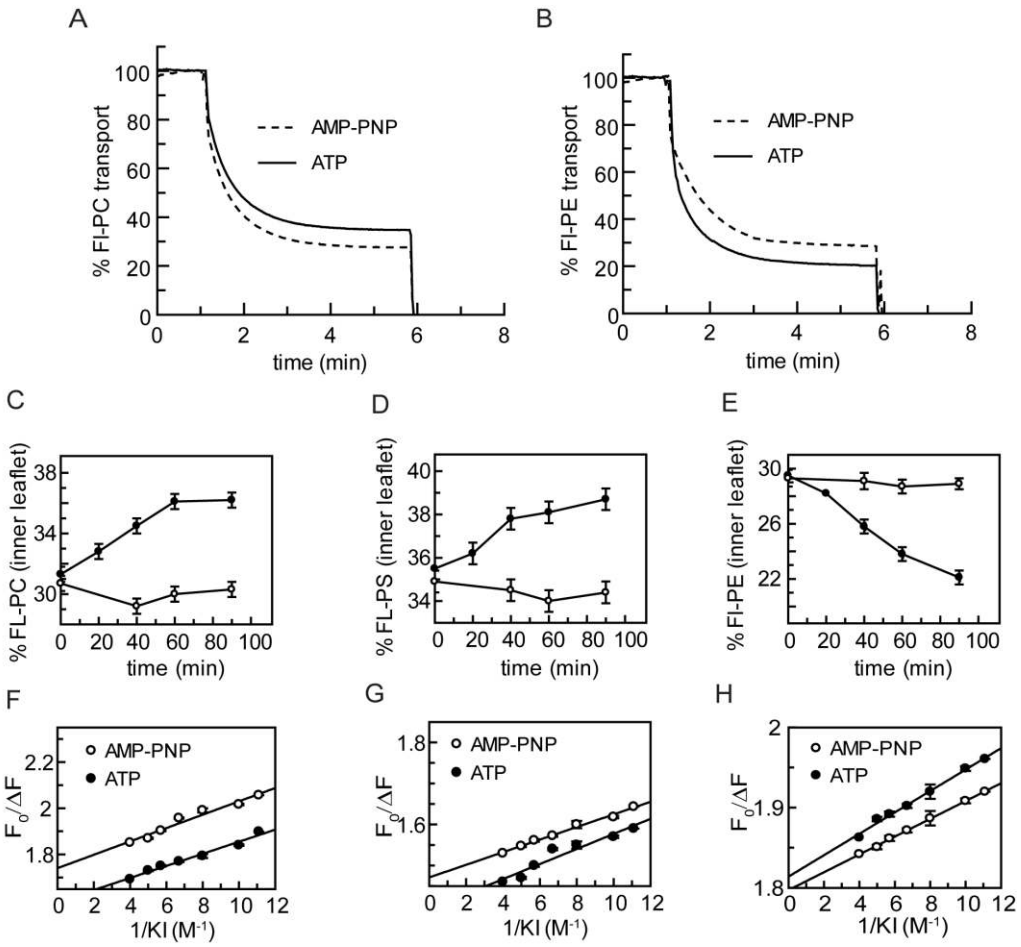

Figure 4.3 Transport of Fluorescent-Labeled Phospholipid by ABCA1 and ABCA4

A. ABCA1 reconstituted into PG liposomes containing 0.6% (w/w) fluorescently-labeled PC (Fl-PC) and **B.** ABCA4 reconstituted into PG liposomes containing 0.6% (w/w) fluorescently-labeled PE (Fl-PE) were incubated at 37 ºC with 1 mM ATP or 1 mM AMP-PNP as a control. After 1h, the fluorescence (λ_{ex} =465 nm, λ_{em} =540 nm) was monitored at 22 ºC. Dithionite (4 mM) was added to bleach fluorescent lipids on the outer leaflet of the liposomes. After the fluorescence stabilized, 1% (w/v) TX-100 (~ 6 min) was added to bleach the remaining fluorescent lipids on the inner leaflet. ABCA1 showed reduced bleaching after ATP treatment relative to AMP-PNP treatment, whereas ABCA4 showed the reverse indicative of differential vectoral transport (flipping) of the fluorescent phospholipids by these transporters. **C-E.** Rate of transport of Fl-PL across the lipid bilayer in the presence of 1 mM ATP (-●-) and AMP-PNP (-○-). **C.** Fl-PC transport by ABCA1 reconstituted into PG liposomes; **D.** Fl-PS transport by ABCA1 reconstituted into PG liposomes; **E.** Fl-PE transport by ABCA4 reconstituted into PC liposomes. **F-G.** Determination of the fraction of Fl-PL accessible on the outer leaflet of proteoliposomes *via* collisional quenching of Fl-PL with iodide ions. PG liposomes reconstituted with ABCA1 and containing 0.6% (w/w) Fl-PC (**F**) and Fl-PS (**G**) and PG liposomes reconstituted with ABCA4 and containing 0.6% Fl-PE (**H**) were treated with 1 mM AMP-PNP or 1 mM ATP prior to iodide quenching. The data is presented as modified Stern-Volmer plots. F_o is the fluorescence intensity of the sample in the absence of quencher; ΔF is the fluorescence intensity at a given iodide ion concentration; KI is the concentration of potassium iodide. The connecting lines were obtained by linear regression. The inverse of the *y*-intercept represents the fraction of Fl-PL that is accessible to the quencher. Errors bars represent S.D.

4.3.4 Transport of Specific Lipids by ABCA1, ABCA7, and ABCA4

A number of fluorescent phospholipids including Fl-PC, Fl-PS, Fl-PE, Fl-PG and Fl-SM were used to define the lipid specificity of the ABCA transporters. We first compared the specificity of ABCA1 and ABCA7 for Fl-PC and Fl-PS. As shown in Fig 4.4A, ABCA1 showed a preference for PC over PS, whereas ABCA7 preferred PS over PC. In control experiments, the ATPase-deficient mutants (ABCA-MM) showed no significant transport activity. The differential specificity of ABCA1 and ABCA7 for PC and PS transport is in agreement with the differential stimulatory effect of these phospholipids on the ATPase activity of these transporters (Fig 4.2).

The lipid transport activity of ABCA1 and ABCA4 reconstituted into PC and PG vesicles was examined for various Fl-PLs. The transport activity of ABCA1 and ABCA4 was significantly enhanced in PG vesicles (Fig 4.4B,C). ABCA1 transported Fl-PC, Fl-PS and Fl-SM, but not Fl-PE or Fl-PG, whereas ABCA4 was highly specific for Fl-PE.

The effect of Fl-PL concentration, various phosphate analogs, ATPase inhibitors and protein modifying reagents on phospholipid transport by ABCA1 was investigated. As shown in Fig 4.4D, the transport of Fl-PC and Fl-PS was dependent on the concentration of FL-lipid reaching a limiting value for Fl-PL concentrations above 1%. Addition of 200 μM beryllium fluoride (BeF_x) and aluminum fluoride (AlF_x) reduced the Fl-PC transport by 83% and 63%, respectively, whereas 1 mM vanadate had only a modest reduction in transport of 20% (Fig 4.4E). Treatment of ABCA1 with NEM prior to reconstitution resulted in the loss of phospholipid flippase activity, whereas ouabain and azide had no significant effect. Similar results were observed for the inhibition of Fl-PE transport by ABCA4 (Fig 4.4F).

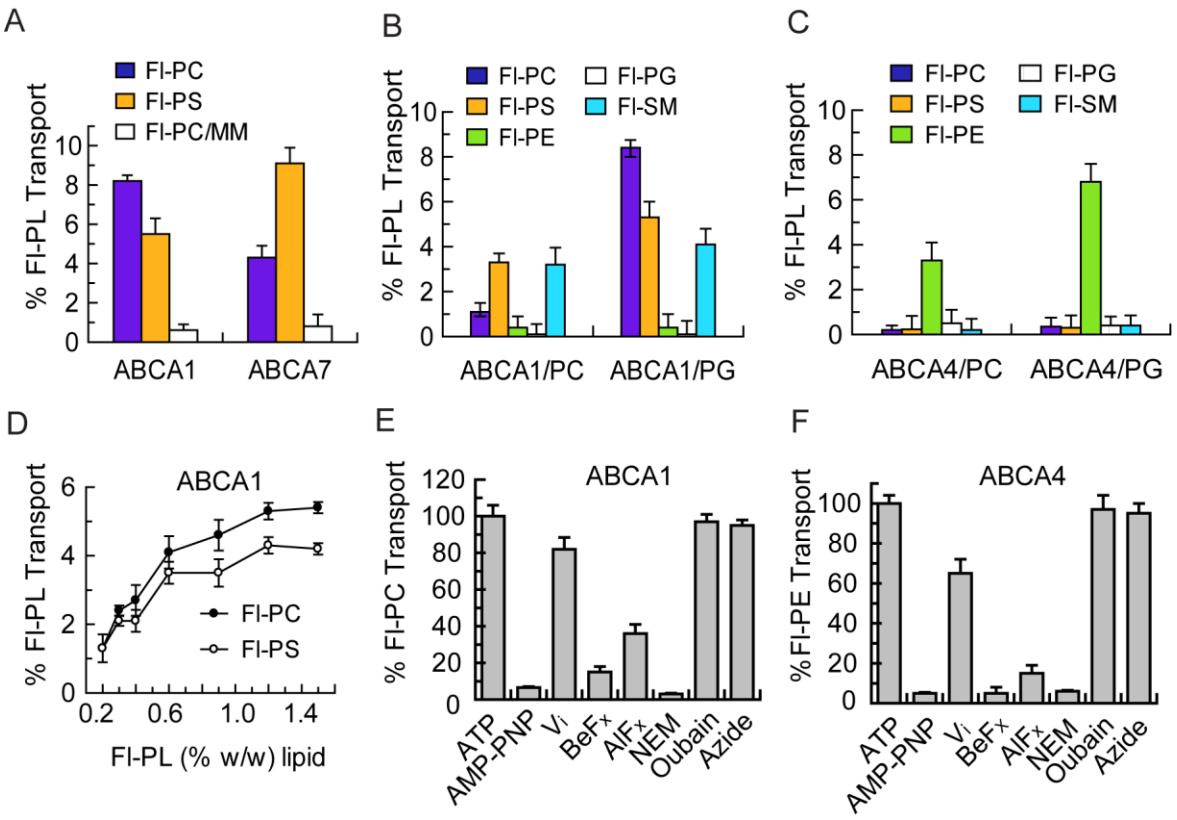

Figure 4.4 Transport of Fluorescent-Labeled Lipids by ABCA1, ABCA7, and ABCA4

The dithionite Fl-PL bleaching assay was used to determine the phospholipid specificity and effect of nucleotides and inhibitors on phospholipid transport by ABCA proteins. **A**. Phospholipid transport (flipping) by WT ABCA1 and ABCA7 and MM mutants reconstituted into PG liposomes containing 0.6% (w/w) Fl-PL. **B.** Phospholipid transport by ABCA1 reconstituted into PC or PG liposomes. Unlabeled PC effectively competes with Fl-PC in PC liposomes reducing the transport of Fl-PS and Fl-SM (sphingomyelin) compared to liposomes comprised of PG base lipid. **C**. Phospholipid transport by ABCA4 reconstituted into PC and PG liposomes. **D.** Effect of increasing Fl-PL concentration on transport by ABCA1 reconstituted into PG liposomes. **E-F.** Effect of nucleotides, phosphate analogs, and inhibitors on the Fl-PC transport or flipping by ABCA1 (**E**) and Fl-PE by ABCA4 (**F**). Proteoliposomes were incubated at 37 ºC for 60 min in the presence of AMP-PNP or ATP with or without the addition of 200 μM V_i, 200 μM AlF_x or 200 μM BeF_x, 1 mM ouabain, and 1 mM azide. In the case of NEM, the ABCA proteins were incubated with 10 mM NEM for 25 min prior to Fl-PL transport. Results are the mean of three independent experiments. Error bars show SEM.

4.3.5 Effect of Cholesterol on Phospholipid Transport

Earlier cell-based assays have implicated ABCA1 in the efflux of cholesterol as well as phospholipids from cells. To determine if cholesterol affects phospholipid transport activity, ATP-dependent flipping of Fl-PC across the lipid bilayer was measured for proteoliposomes

containing ABCA1 and increasing concentrations of cholesterol. As shown in Fig 4.5A, a 30-35% decrease in Fl-PC flippase activity of ABCA1 was observed at 20-30% cholesterol. Cholesterol had a similar effect on the Fl-PE flippase activity of ABCA4 reconstituted into PC vesicles. Cholesterol mediated decrease in phospholipid transport activity is in agreement with the decrease in ATPase activity of ABCA transporters by cholesterol (Fig 4.2).

To further assess the effect of lipid environment on the phospholipid flippase activity of these transporters, ABCA1 and ABCA4 was reconstituted into PG and PC based liposomes containing various phospholipids. The addition of 10% PE or 10% or 50% PI had little effect of the transport activity of ABCA1 relative to its activity in pure PG vesicles (Fig 4.5 B). However, addition of 10% unlabeled PC or brain polar lipid (BPL) which contains ~ 10% PC suppressed Fl-PC transport. Similarly, Fl-PE transport by ABCA4 was unaffected by the addition of PI, but suppressed by the addition of unlabeled 10% PE and BPL (Fig 4.5C). These results indicate that cholesterol modestly reduces the phospholipid flippase activity of ABCA1 and ABCA4 presumably by altering the lipid environment of the protein. Unlabeled PC decreases the Fl-PC flippase activity of ABCA1 and unlabeled PE decreases the Fl-PE flippase activity of ABCA4 through the competing effect of these unlabeled PL for transport of the Fl-PL.

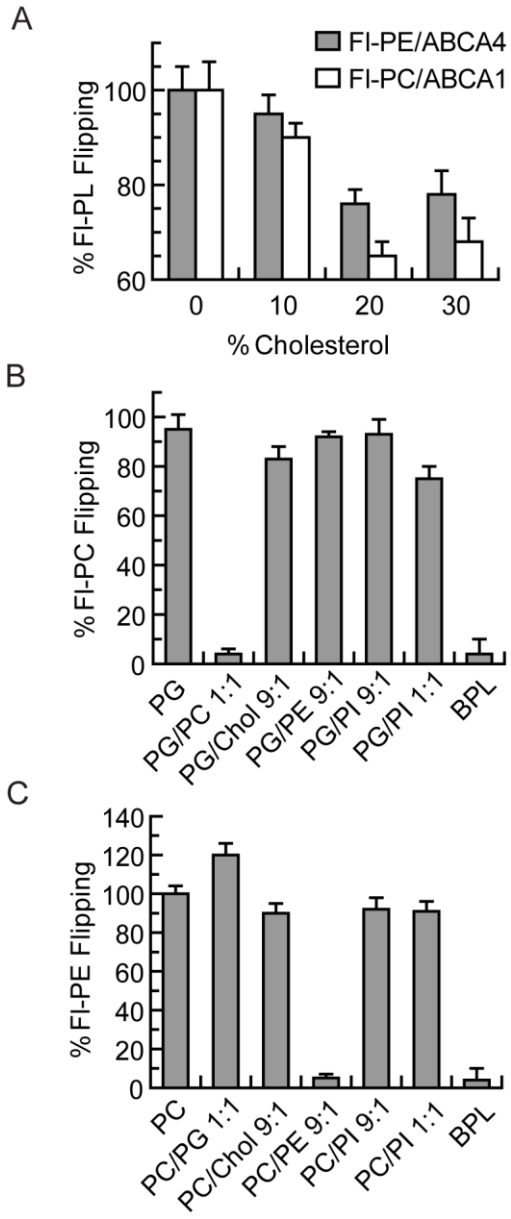

Figure 4.5 Effect of Cholesterol and Phospholipids on ABCA1 and ABCA4 Flippase

A. Fl-PC transport activity of ABCA1 and Fl-PE transport activity of ABCA4 reconstituted in PG liposomes containing 0-30% (w/w) cholesterol. **B.** Effect of PC, PE, and PI on the transport of Fl-PC by ABCA1 reconstituted into PG liposomes. Unlabeled PC and brain polar lipid (BPL) effectively competes with Fl-PC for transport by ABCA1 whereas PI has little effect. **C**. Effect of PC, PE, and PI on the transport of Fl-PE by ABCA4 reconstituted into PC liposomes. Unlabeled PE and BPL effectively competes with Fl-PE for transport by ABCA4 whereas PC and PI have little effect. Results are the mean ± SD for three independent experiments.

4.3.6 Expression and Purification of Disease ABCA1 & ABCA4 Mutants

As part of this study, we have generated a number of disease-causing mutations in ABCA1 and ABCA4 in order to determine their effect on the expression and functional properties of these transporters. We focused our studies on nine missense mutations in ABCA1 known to cause Tangiers disease including three (S100C, W590S, and F593L) in ECD1, two (T929I and N935S) in NBD1, two (C1477R and T1512M) in ECD2, and two (R2081W and P2150L) in the C-terminal segment as shown in Fig 4.6A (*blue*). Alignment of the ABCA1 and ABCA4 sequences indicated that six mutations in corresponding positions in ABCA4 are associated with Stargardt disease (S100P, F608L, N965S, T959I, T1537M, and R2107P) (Fig 4.6A – *red*). Mutations in residues W605 and P2180 of ABCA4 have yet to be linked to Stargardt disorder. These two residues were replaced with serine and leucine, respectively, (W605S and P2180L) corresponding to the disease-causing substitutions in ABCA1. Finally, the null mutant C1502X associated with Stargardt disease was modified to C1502R to reflect the primary sequence change of corresponding C1477R mutant in ABCA1 linked to Tangier disease.

These mutants were expressed in HEK293T cells and purified by immunoaffinity chromatography. Fig 4.6B shows the expression profile of the ABCA1 and ABCA4 mutants. The level of expression of the ABCA1 and ABCA4 mutants were generally lower than the corresponding wild-type (WT) proteins with the ABCA1 mutants S100C and R2081W and the corresponding ABCA4 mutants S100P and R2107P expressing at levels less than 25% of WT and the remaining mutants expressing in the range of 35% - 90% WT proteins. Despite the differences in expression levels, all mutants could be purified by immunoaffinity

chromatography on Rho 1D4-Sepharose matrix in sufficient quantities for functional studies (Fig 4.6C).

Figure 4.6 Expression and Purification of ABCA1 and ABCA4 Disease Mutants

A.Topological diagram of human ABCA1 and ABCA4 showing the position of the nine ABCA1 mutants associated with Tangier disease mutants (*blue*) and related ABCA4 mutants many of which are associated with Stargardt disease (red) in relation to the various domains (exocytoplasmic domains ECD1 & ECD2; nucleotide binding domains NBD1 & NBD1, and C-terminal domain CT). Some disease alleles such as W590S, C1477R & P2150L (ABCA1) have conserved residues in ABCA4 but mutations in these positions in ABCA4 have yet to be linked to Stargardt disease. **B**. Expression profile of ABCA1 and ABCA4 disease-associated mutant relative to the WT protein. Proteins containing a 1D4 epitope were expressed in HEK293T cells and extracts were resolved by SDS-gel electrophoresis. An example of a Western blot labeled with the Rho1D4 antibody is shown along with quantitation from 3 independent experiments. **C.** Purification of mutants on a Rho1D4 immunoaffinity matrix. Upper panel is a Commassie blue stained gel of the WT extract (I) and 1D4 peptide-eluted protein (E). Lower panel is a Western blot labeled with the Rho1D4 antibody.

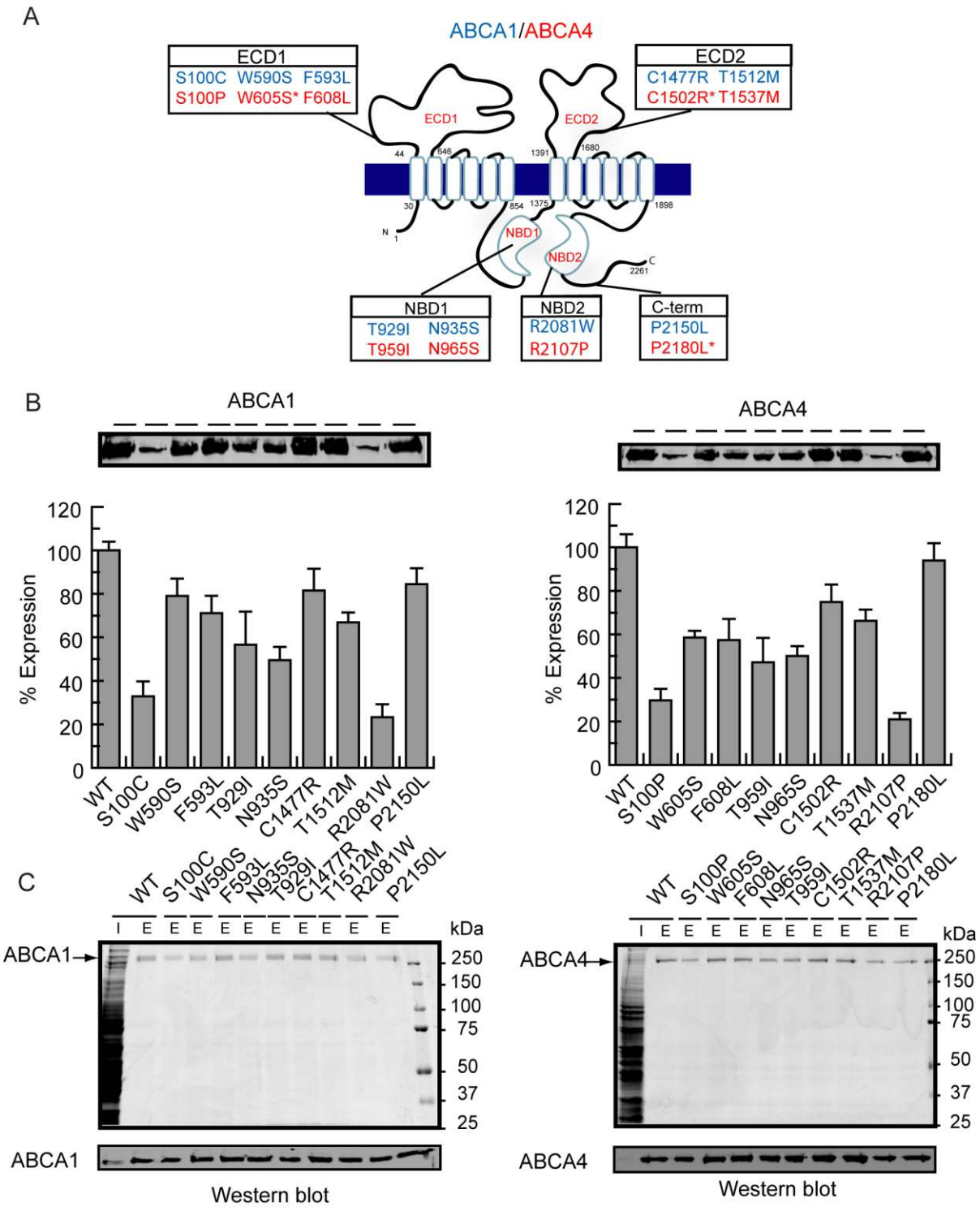
A
ABCA1/ABCA4
ECD1
S100C W590S F593L
S100P W605S* F608L
ECD2
C1477R T1512M
C1502R* T1537M
NBD1
T929I N935S
T959I N965S
NBD2
R2081W
R2107P
C-term
P2150L
P2180L*
B
ABCA1
ABCA4
% Expression
WT S100C W590S F593L T929I N935S C1477R T1512M R2081W P2150L
WT S100P W605S F608L T959I N965S C1502R T1537M R2107P P2180L
C
kDa
250 150 100 75 50 37 25
ABCA1
ABCA4
Western blot

4.3.7 ATPase Activities of Disease Variants

The purified ABCA1 and ABCA4 mutants were reconstituted into liposomes containing BPL in order to determine the effect of the mutations on the ATPase activity of these proteins. Variants in the ECD1 (S100C, W590S, and F593L), NBD1 (T929I and N935S), and NBD2 (R2081W) of ABCA1 showed significantly reduced ATPase activities in the range of 20-35% of WT activity (Fig 4.7A). By contrast, the T1512M mutation in ECD2 and P2150L in the C-terminal segment exhibited ATPase activity similar to the WT protein. The C1477R mutant in ECD2 showed an intermediate reduction in activity. ABCA4 variants showed a similar ATPase activity profile as the ABCA1 mutants with the exception of the T1537M mutation of ABCA4 which was significant lower than the corresponding T1512M mutant in ABCA1.

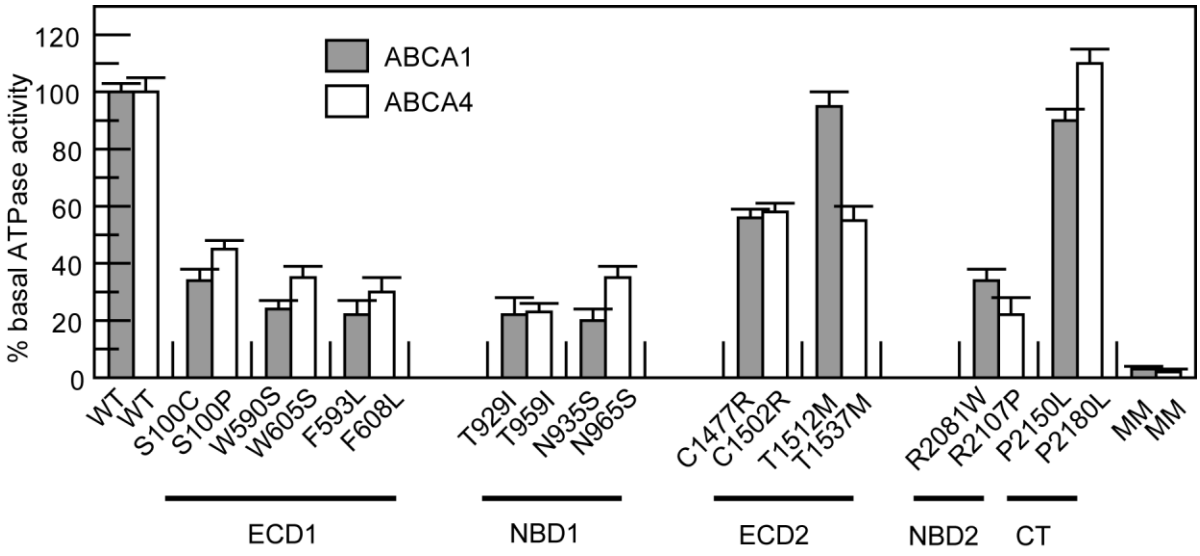

Figure 4.7 Relative ATPase Activity of ABCA1 and ABCA4 Disease Mutants

WT and mutant ABCA1 and ABCA4 containing the 1D4 epitope were expressed and purified from HEK293T cells by immunoaffinity chromatography and reconstituted into liposomes composed of brain polar lipid for analysis of ATPase activity. The ATPase activity of the disease-associated mutants was lower than that of the WT protein, but significantly higher than the ATPase deficient MM mutant. Results are the mean ± SD for three independent experiments.

4.3.8 Phospholipid Flippase Activities of Disease Variants

The ATP-dependent phospholipid transport properties of the ABCA1 and ABCA4 mutants were also investigated by the fluorescence dithionite bleaching protocol. As shown in Figure 4.8A and 4.8B, the Fl-PC flippase activity of the ABCA1 mutants and the Fl-PE flippase activity of ABCA4 mutants have a similar profile with the ABCA1 variants C1477R, T1512M and P2150L and corresponding ABCA4 variants C1502R, T1537M, and P2180L showing transport activities ranging from 60-80% of the WT protein and the other mutants showing reduced activity in the range of 20-40% of the WT protein. Interestingly, the PS transport activity of most mutants showed a larger decrease in activity than the PC transport activity relative to the respective transport activity of the WT proteins.

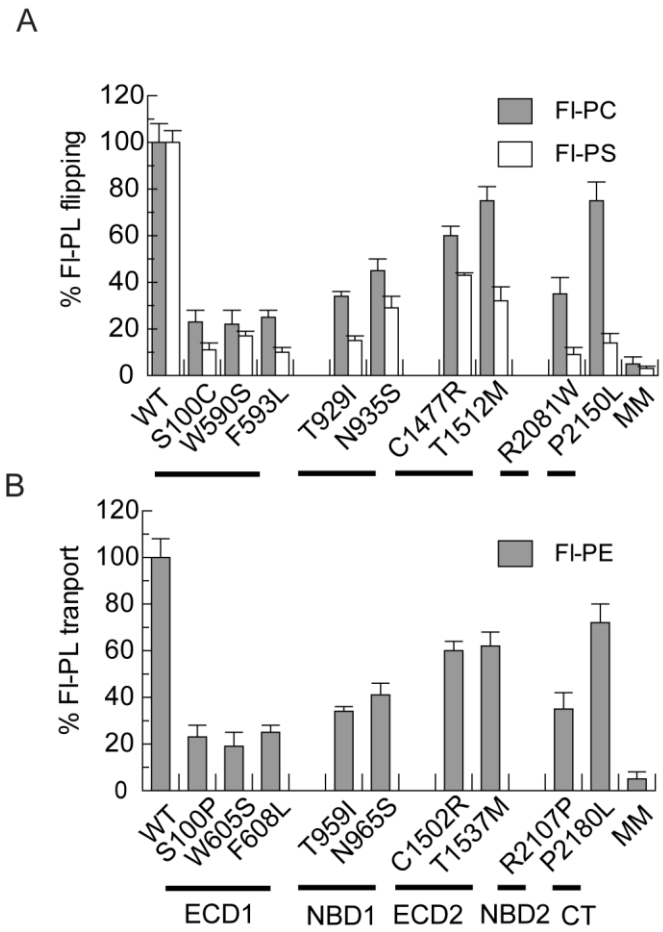

Figure 4.8 Relative Fluorescent-Lipid Flipping of ABCA1 & ABCA4 Disease Mutants

A. Purified ABCA1 WT and disease-assoicated mutants were reconstituted into PG liposomes containing 0.6% Fl-PC or Fl-PS for analysis of transport activity by the dithionite fluorescence bleaching assay. **B.** Purified ABCA4 WT and mutants were reconstituted into PC liposomes containing 0.6% Fl-PE for transport activity measurements. Results are the mean ± SD for three independent experiments.

4.3.9 Cellular Localization of WT and Mutant ABCA Proteins in COS-7

The effect of disease-causing mutations on the localization of ABCA1 and ABCA4 in transfected COS7 cells was investigated by immunofluorescence microscopy. In agreement with earlier studies, WT ABCA1 localized primarily to the plasma membrane and intracellular endosomes, whereas WT ABCA4 was present in large intracellular vesicles (Fig 4.9A,B). The ABCA1-MM and ABCA4-MM showed a similar distribution as their WT

counterparts indicating that these functionally inactive mutants fold into a native-like conformation allowing their exit from the ER. In contrast some of the mutants including ABCA1 mutants T929I and R2081W and ABCA4 mutants T959I and R2107P showed partial or complete co-localization with calnexin in a reticular pattern characteristic of the ER. This indicates that some of the mutants are highly misfolded and retained in the ER by the cellular quality control system. The extent of co-localization of ABCA1 mutants with calnexin is quantified from double labeling experiments in Fig 4.9C.

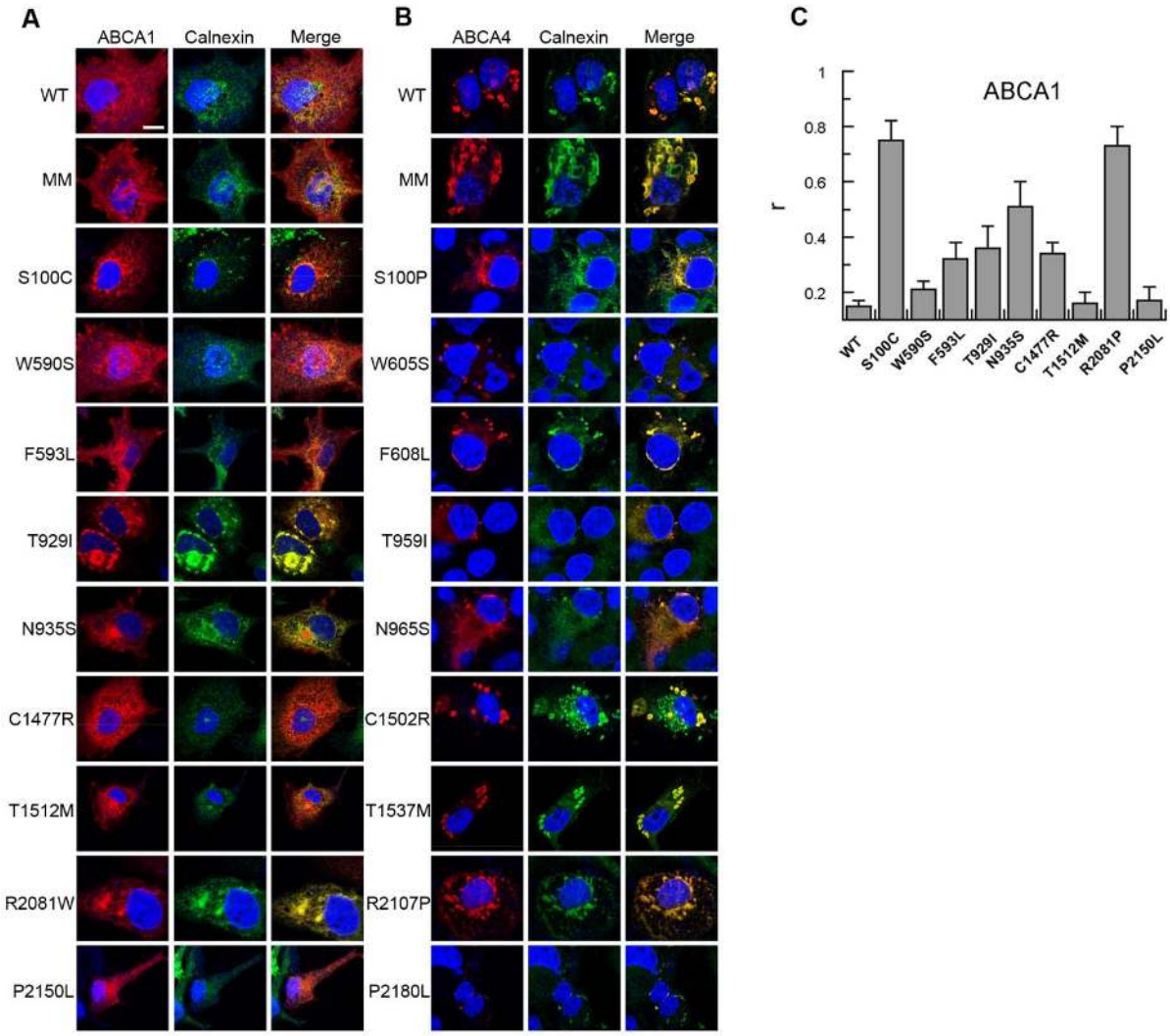

Figure 4.9 Localization of ABCA1 and ABCA4 Disease Mutants

COS7 cells expressing WT or disease-associated mutants of ABCA1 (**A**) or ABCA4 **(B**) were double labeled with the Rho1D4 monoclonal antibody (red) to localize ABCA1 or ABCA4 and a calnexin polyclonal antibody (green) as an ER marker for analysis by confocal scanning microscopy. WT and MM mutant ABCA1 localize to plasma membrane and endosomes whereas most Tangier causing mutants showed variable co-localization with the calnexin in a characteristic ER reticular pattern. WT and MM mutant ABCA4 are localized to large intracellular vesicles which also contain calnexin. Many ABCA4 mutants showed a reticular pattern of labeling within the cells characteristic of ER localization. Scale bar represents 10 μm. **C.** Extent of colocalization of ABCA1 mutants and calnexin in transfected COS7 cells quantified using ImageJ analysis software. Pearson's coefficient (r) provided a relative indicator of co-localization with r = 0 indicating no colocalization and r = 1 indicating complete co-localization.

4.4 Discussion

Although previous cell-based studies have implicated ABCA1 and ABCA7 in the efflux of phospholipids and cholesterol from cells as a critical step in the reverse cholesterol transport (RCT) pathway, it has been unclear if these proteins directly transport the lipids across the membrane or simply mediate lipid transfer to ApoA-1 through an indirect 'regulatory' mechanism (Szakacs et al., 2001). In this study we provide the first direct biochemical evidence that ABCA1 and ABCA7 transport or flip specific phospholipids from the cytoplasmic leaflet to the exocytoplasmic leaflet of the lipid bilayer and determine the phospholipid specificity for these ABCA transporters. This was achieved through analysis of ATP-dependent transport of Fl-PL by these transporters and supported by the stimulation of their ATPase activity by the same phospholipids.

Immunoaffinity purified ABCA1, ABCA7, and ABCA4 exhibited significant ATPase activity upon reconstitution in liposomes consisting of BPL, in contrast to the ABCA-MM Walker A mutants which were devoid of activity. The ATPase activity of ABCA1 and ABCA7 (~ 220-280 nmol/min/mg) was within the range of values observed in previous studies (Ahn et al., 2000; Takahashi et al., 2006), but significantly lower than values observed for other ABC proteins (1.7-1.9 μmol/min/mg) such as P-glycoprotein and the TAP complex (Herget et al., 2009; Urbatsch et al., 2001). The ATPase activity of ABCA1 in PG liposomes was activated ~2-fold by PC and to a lesser degree by PS and SM, whereas the activity of ABCA7 showed a preference for PS over PC. Little, if any activation was observed for PE in contrast to ABCA4 which was specific for PE. In agreement with an earlier report (Takahashi et al., 2006), cholesterol did not activate the ATPase activity of ABCA1, but instead decreased the activity of ABCA1, ABCA7 and ABCA4 by 20-30%.

This general inhibitory effect most likely occurs through the effect of cholesterol on overall lipid environment of the reconstituted transporters.

Analysis of the phospholipid transport properties of ABCA1, ABCA7 and ABCA4 was a central focus of this study. Previously, we had shown that ABCA4 functions as an importer flipping *N*-retinylidene-PE from the lumen to the cytosolic leaflet of photoreceptor disc membranes and proteoliposomes. In the present study we have used both the Fl-PL dithionite bleaching assay and the Fl-PL collisional quenching method to further examine phospholipid transport by reconstituted ABCA1, ABCA7 and ABCA4. Although these ABCA transporters share a high degree of sequence identity (~50%), ABCA1 and ABCA7 functioned as exporters flipping phospholipids from the cytoplasmic to the exocytoplasmic leaflet of membranes, whereas ABCA4 transported PE in the opposite direction. ABCA1 actively transported PC, PS, and SM with a preference for PC, whereas ABCA7 preferentially transported PS in general agreement with the phospholipid ATPase activation studies. Cholesterol inhibited the phospholipid transport activity of ABCA1, ABCA7 and ABCA4 to the same degree as it inhibited their ATPase activity suggesting that cholesterol is not co-transported with phospholipids. Our results are consistent with a previous study reporting the inability of photoactivatable cholesterol derivative to bind ABCA1(Wang et al., 2001).

Several models have been proposed to explain ABCA1-mediated cholesterol and phospholipid efflux from cells to ApoA-I. In the concurrent model, PC and cholesterol are effluxed together to ApoA-I by ABCA1 (Smith et al., 2004). In the two-step model, ABCA1 first mediates PC efflux to ApoA-I, and this ApoA-I PC complex subsequently accepts cholesterol from the outer leaflet of the plasma membrane independent of ABCA1 (Fielding

et al., 2000; Wang et al., 2001). In a third model, ABCA1 mediates the translocation of phospholipids to the outer leaflet to generate a phospholipid imbalance between the inner and outer leaflets resulting in membrane bending. The resulting protrusions promote transient binding of ApoA-I to the membrane and a solubilization of the exovesiculated lipid domain leading to the loading of ApoA-I with phospholipids and cholesterol for the generation of nascent HDL particles (Iatan et al., 2011; Krimbou et al., 2005; Vedhachalam et al., 2007). Other models stress the importance of the interconversion of ABCA1 monomers to dimers and membrane meso-domain organization in ApoA-I binding and HDL formation (Nagao et al., 2011; Nagata et al., 2013).

Our studies support the active export of the phospholipids by ABCA1 as an important initial step in RCT and argue against the direct transport of cholesterol by ABCA1 as postulated in the concurrent model. ABCA1 may simply flip PC, PS and SM from the cytoplasmic to the extracellular leaflet of cells thereby altering the surface area of the opposing leaflets resulting in cell protrusions which facilitate the loading of ApoA-1 with cholesterol and phospholipids. Alternatively, ABCA1 may directly efflux phospholipids to ApoA-1 directly bound to ABCA1 as a preloading step prior to the loading of cholesterol as suggested in the two step model. Since we were unable to reconstitute the ABCA1-ApoA-1 complex into liposomes we could not determine if ABCA1 can directly translocate phospholipids onto ApoA-1 or if ABCA1 primarily functions as a phospholipid flippase. Further studies are needed to delineate between these mechanisms.

As part of this study, we determined the effect of disease-causing missense mutations in ECD1, NBD1, ECD2, NBD2 and C-terminus of ABCA1 and corresponding mutations in ABCA4 on protein expression, phospholipid specific ATPase activity, ATP-dependent

phospholipid flippase activity, and subcellular localization. The mutants expressed at levels ranging from 20% to 100% WT and were readily purified by immunoaffinity chromatography after solubilization in CHAPS buffer. The ATPase and phospholipid transport activities of the various mutants were in general lower than WT ranging from 20% to 80% that of WT activity. Interestingly, the overall profiles of the ABCA1 and ABCA4 mutants were strikingly similar. The ABCA1/ABCA4 mutants in the ECD1 (S100C/S100P, W590S/W605S, F593L/F608L) displayed the lowest activities (20-30% WT) while those in the ECD2 (C1477R/C1502R, T1512M/T1537M) and the P2150L/P2180L mutants in the C-terminus showed the highest activities (60-100% WT). This suggests that the structure-function relationships of ABCA1 and ABCA4 are broadly similar despite the fact that they transport different phospholipids in different directions. A low resolution structure of ABCA4 has recently been determined by single particle EM (Tsybovsky et al., 2013). One may surmise that ABCA1 will have a similar overall structure and undergo similar conformational changes as ABCA4 during the transport cycle although the high affinity access phospholipid binding site most likely resides on different sides of the proteins with the initial PL binding site for ABCA1 on the cytoplasmic side and the PE binding for ABCA4 on the exocytoplasmic (lumen/extracellular) side.

Several reports have described the effect of some of the Tangier associated mutations on ApoA-1 binding, phospholipid and cholesterol efflux, and subcellular localization of ABCA1 (Fitzgerald et al., 2002; Singaraja et al., 2006; Tanaka et al., 2003). In these studies the disease-associated mutants all showed reduced activity particularly with regard to phospholipid and cholesterol efflux. Our data on the effect of disease-associated mutations on phospholipid transport broadly agrees with their effect on phospholipid efflux as reported

in the literature. For example the P2150L showed only mild loss in phospholipid transport and efflux whereas R2081W showed a more pronounced effect. However, the extent of reduction in these activities differs for some mutants. For example the C1477R mutant shows intermediate (~60% WT) phospholipid transport activity, whereas it shows minimum (<20% WT) phospholipid efflux activity. It is possible that this mutant is relatively active in flipping PC/PS across the bilayer but due to its more limited ability to bind ApoA-1, it shows a more marked decrease in phospholipid efflux activity. The C1477 residue has been implicated in intramolecular disulfide bonding between the ECDs of ABCA1 (Hozoji et al., 2009) which may be required for efficient binding of ApoA-1. Finally, our results showing that some mutants with limited functional activity are able to exit the ER is in agreement with previous studies showing that some, but not all, ABCA1 and ABCA4 mutants show subcellular localization similar to the WT proteins.

To date relatively few eukaryotic ABC transporters have been purified for identification of their substrates and analysis of their transport mechanism. The immunoaffinity purification and reconstitution methodology used here to characterize ABCA1, ABCA4, and ABCA7 have broad application for analysis of other ABC transporters as well as other membrane proteins (Reboul et al., 2013; Wong et al., 2009). It will be of particular interest to identify the putative lipid substrates and direction of transport for ABCA3 associated with neonatal surfactant deficiency and pediatric interstitial lung disease and ABCA12 linked to harlequin ichthyosis as well as other members of the ABCA subfamily including ABCA2.

Chapter 5: Functional and Protein Misfolding Rescue of ABCA4

5.1 Introduction

Amiodarone is the most effective antiarrhythmic drug for treating cardiac arrhythmias. It inhibits Na^+, K^+ , Ca^{2+} channels and beta-adrenergic receptors and prolongs the cardiac action potential (Singh et al., 1989; Varbiro et al., 2003). Extra side-effects including thyroid, hepatic, and pulmonary toxicity have been a limiting factor in clinical pharmacology (Kathofer et al., 2005; Singh et al., 1989). Structurally related to amiodarone, dronedarone is a relatively new anti-arrhythmic drug possessing multi-channel blocking properties but lacks most adverse side-effects of amiodarone (Gautier et al., 2003; Lalevee et al., 2003). Both amiodarone and dronedarone are potent inhibitors of the ABC drug transporter, Pgp. Dose-dependent inhibition by amiodarone has been specifically demonstrated for Pgp-mediated digoxin transport (Kakumoto et al., 2002; Katoh et al., 2001; Vallakati et al., 2011). Paradoxically, it has been reported that amiodarone and the detergent, digitonin, act as allosteric activators of ABCA4 ATPase activity displaying atleast a 4-to 10-fold increase in retinal-stimulated ATPase activity (Sun et al., 1999). It remains unknown whether the inherent capacity of allosteric activation of ABCA4 with antiarrhythmic drugs may rescue transport activity of disease ABCA4 mutant proteins.

Previous studies on disease missense mutations of ABCA4 demonstrated impaired expression disrupted by impaired folding and assembly (Cideciyan et al., 2009; Zhong et al., 2009). Hypotheses for poor expression include chaperone systems reducing unfavorable interactions of disease mutant folding polypeptides. A chemical chaperone, 4-phenylbutyrate (PBA), has attracted substantial attention in cystic fibrosis pathology due to its capacity to traffic ΔF508-CFTR ABC transporter to the cell membrane and restore chloride conductance

in lung cells (Riordan, 2008; Singh et al., 2008). In photoreceptors, the P23H mutant causes retention of rhodopsin in the ER and aggregation in the form of intracellular inclusions. PBA treatment demonstrated restoration of P23H rhodopsin mutant and translocation to the outer segment of rod photoreceptors (Mendes and Cheetham, 2008). Native ligands and substrate analogs have been identified as pharmacologic chaperones that interact specifically with target proteins. 11-*cis* retinal serves as a pharmacological chaperone and stabilizes the P23H rhodopsin protein from misfolding (Moritz and Tam, 2010). β-ionone, structurally similar to retinal, showed a 2.5-fold rescue to P23H rhodopsin (Noorwez et al., 2008). Wiszniewsk *et al.* demonstrated that several ABCA4-disease mutants mislocalize in the inner segment of photoreceptors (Wiszniewski et al., 2005). Exactly how folding ABCA4 mutant polypeptides contributes to the pathophysiology of SD is poorly understood.

The precise roles of antiarrhythmic drugs during the transport process of ABCA4 are unknown. It is also not clear whether improper ABCA4 protein folding, associated with newly synthesized disease polypeptides, can be rescued by small molecules intervening protein quality control pathways. Here we show that reconstituted ABCA4 proteoliposomes treated with dronedarone stimulate the transport of *N*-retinylidene PE in wild-type and select disease mutants. Of the three chemical chaperones tested (glycerol, β-ionone, & PBA), a few mutants substantially retained in the ER – G818E, G863A, and N965S – were only rescued by PBA. The differential effects of rescue among Stargardt disease ABCA4 mutant proteins with small molecules can serve to aid therapeutic development.

5.2 Methods

5.2.1 Materials

Digitonin was from Fluka; amiodarone, dronedarone, and CHAPS were from Sigma. 4-phenylbutyric acid was from Toric Biosciences. The drugs were dissolved in MeOH and added to <0.1% in the reaction. Additional materials are described in Chapter 2.2.1 and Chapter 3.2.1.

5.2.2 DNA Constructs

The generation of G863A and N965S ABCA4 expression vectors has been described previously in Chapter 2.2.3. Additional mutations introduced by overlap-extension PCR using Pfu AD DNA polymerase in ABCA4 included: G818E, R1898H, and G1961E.

5.2.3 Expression of ABCA4 in HEK293T and COS-7 Cells

HEK293T cells and COS-7 cells were cultured according to Chapter 2.2.4 and Chapter 4.2.7.

5.2.4 Purification and Functional Analysis of ABCA4

Purification, Western blotting, retinal transfer activity with reconstituted proteoliposomes, and retinoid binding to ABCA4 were performed as described in Chapter 2

5.2.5 Immunofluorescence Microscopy

Mammalian cell cultures were labeled according to Chapter 4.2.7.

5.3 Results

5.3.1 Dronedarone Synergistically Activates ABCA4 Retinal ATPase

First, we studied the effects of dronedarone, amiodarone, and digitonin on ABCA4 ATPase activity. In proteoliposomes containing purified and reconstituted ABCA4, dronedarone increased the retinal-stimulated activity with a half maximal activation at 20 μM and a maximum at 100 μM. At concentrations above 100 μM, no further stimulatory effect

was observed (Fig 5.1A). In contrast, digitonin, showed maximal activation at 30 μM, and inhibition at elevated concentrations. As revealed by ATP hydrolysis kinetics, the 4-fold dronedarone stimulatory effect was due to an increased in V_{max} without a significant effect on K_m (Fig 5.1B). Little contribution to synergistic activation was found when dronedarone was examined individually or in combination with amiodarone. In addition, both anti-arrhythmic drugs had little effect on *N*-retinylidene PE binding and release with ATP suggesting that these drugs do not occupy the preferred substrate binding site (Fig 5.1C). However, stimulation was dependent on membrane lipids as the presence of PE in DOPC/DOPE proteoliposomes or as present in brain polar lipids showed that both dronedarone and amiodarone produced a 1.8- and 2-fold increase, respectively, in specific ATPase activity compared to ABCA4-PC proteoliposomes (Fig 5.1D). While, digitonin was capable of enhanced activation (~5-fold) in brain polar lipid or PC/PE proteoliposomes, a 3-fold activation was also observed in PC liposomes suggesting that digitonin has a different mode of interaction with ABCA4. Thus, these results suggest that PE-based activity is also stimulated by dronedarone. Together, these data suggest that the independent and uncompetitive mode of dronedarone and amiodarone may induce positive allosteric effects in the functional activity of Stargard disease associated mutations (Fig 5.1E).

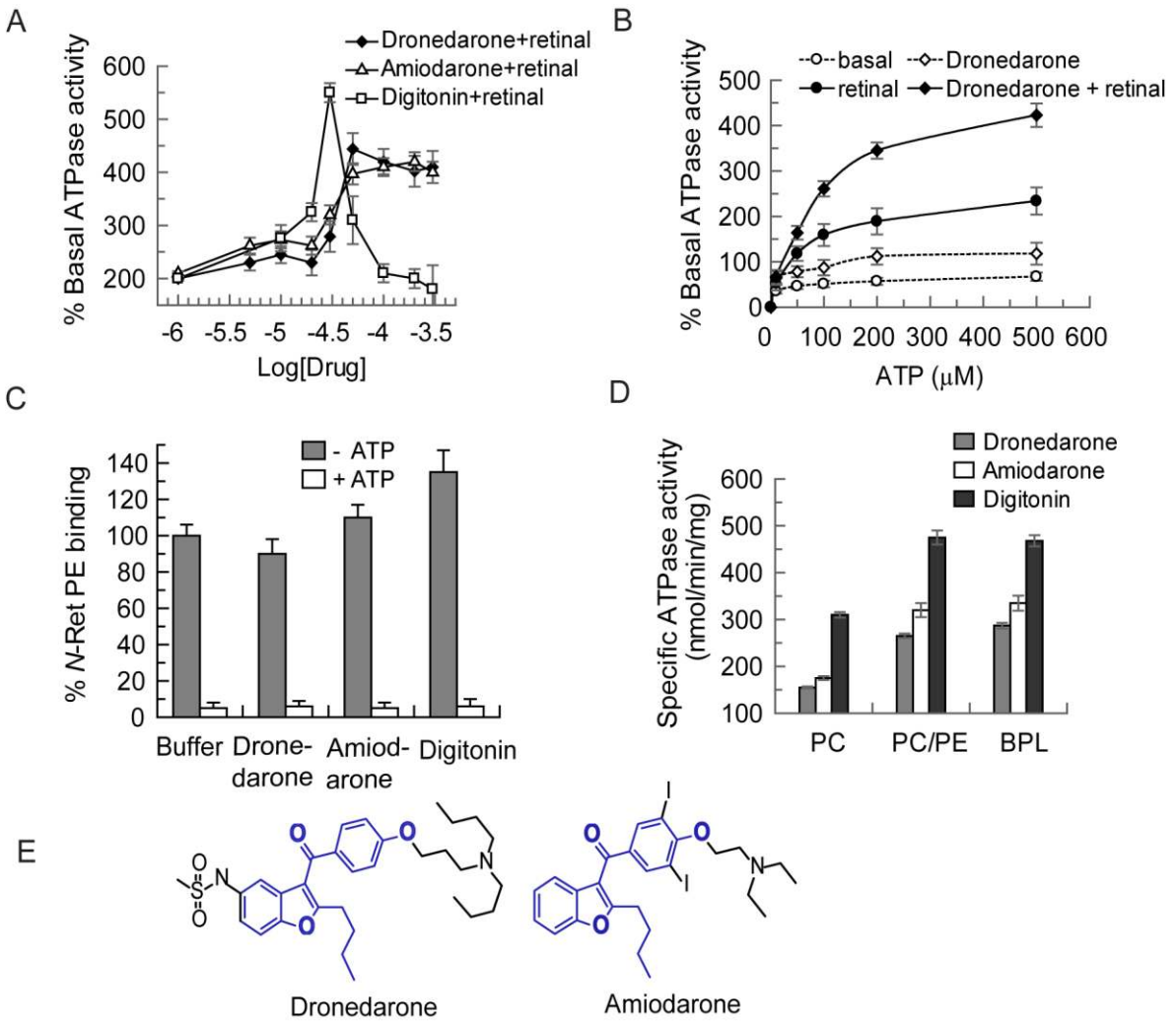

Figure 5.1 Anti-Arrhythmic Drugs Synergistically Activate ABCA4 ATPase

A. Concentration curves of dronedarone, amiodarone, and digitonin on retinal (40 μM) stimulated ATPase activity in ABCA4 proteoliposomes. ATPase activities were expressed as % with respect to basal ATPase activity. Basal ATP hydrolysis was 57.4 ± 0.6 nmol/mg/min. (SD; n=3). **B.** ATP Hydrolysis at different concentrations in the presence or absence of 40 μM dronedarone with all-trans retinal (50 μM). **C**. Binding of *N*-retinylidene-PE to ABCA4 in the presence of 40 μM amiodarone, dronedarone, or 20 μM digitonin. The matrix was washed to remove unbound substrate and incubated in the absence or presence of 0.5 mM ATP. The bound *N*-ret-PE was eluted with ethanol and quantified by scintillation counting. Data represent the average of three or more experiments ± S.D. **D.** Effect of lipid environment on synergistic stimulation of ABCA4 ATPase. Purified ABCA4 was reconstituted in brain polar lipid extract (BPL), DOPC/DOPE (7:3) or DOPC and assayed for ATPase activity in the presence of all-*trans* retinal (50 μM), dronedarone (40 μM), amiodarone (40 μM), and digitonin (20 μM). ATPase is expressed as a percent over the basal hydrolysis. **E.** Dronedarone and Amiodarone ion channel ligands have a benzofuran backbone (blue) at their core. Amiodarone has two iodine atoms as part of the covalent structure.

5.3.2 Membrane Protein Expression and Cellular Localization

In a previous analysis of 37 ABCA4 Stargardt disease mutants, most expressing variants had biochemical defects associated with impaired ATPase activities or protein misfolding or a combination of both (Sun and Nathans, 1997). In particular, sites associated with NBDs mostly displayed compromised ATPase activities with some effect on protein expression, while TMD mutants had reduced protein expression levels with variable ATPase activities. In Chapter 2, we have seen how G863A and N965S displayed reduced transport and ATPase activities. In this study, additional NBD mutants, G818E, R1898H, and G1961E, were also studied to better understand the impact of drug molecular mechanisms on alleviating biochemical dysfunction (Fig 5.2A). First, ABCA4 protein levels were compared in expressed membranes prepared from transfected HEK293T cells. As shown in Fig 5.2B, mutants G818E, G863A, N965S, and G1961E were present at reduced levels (</~ 50%). In contrast, R1898H displayed near to wild-type protein expression levels.

Next, we investigated the localization of the mutant ABCA4 proteins by immunoconfocal microscopy. As shown in Fig 5.2C, signals corresponding to R1898H and to certain extent N965S and G1961E were present substantially in intracellular vesicles. The other four mutants were observed primarily as a reticular pattern and colocalized with calnexin, indicating that a significant fraction of the membrane protein mutants was retained in the ER. This was particularly evident for G818E and G863A where co-localization with calnexin was the most pronounced and is consistent with the reduced membrane protein expression levels. Together, these observations indicate that disease substitutions, in particular G818E and G1961E, cause differential levels of protein misfolding.

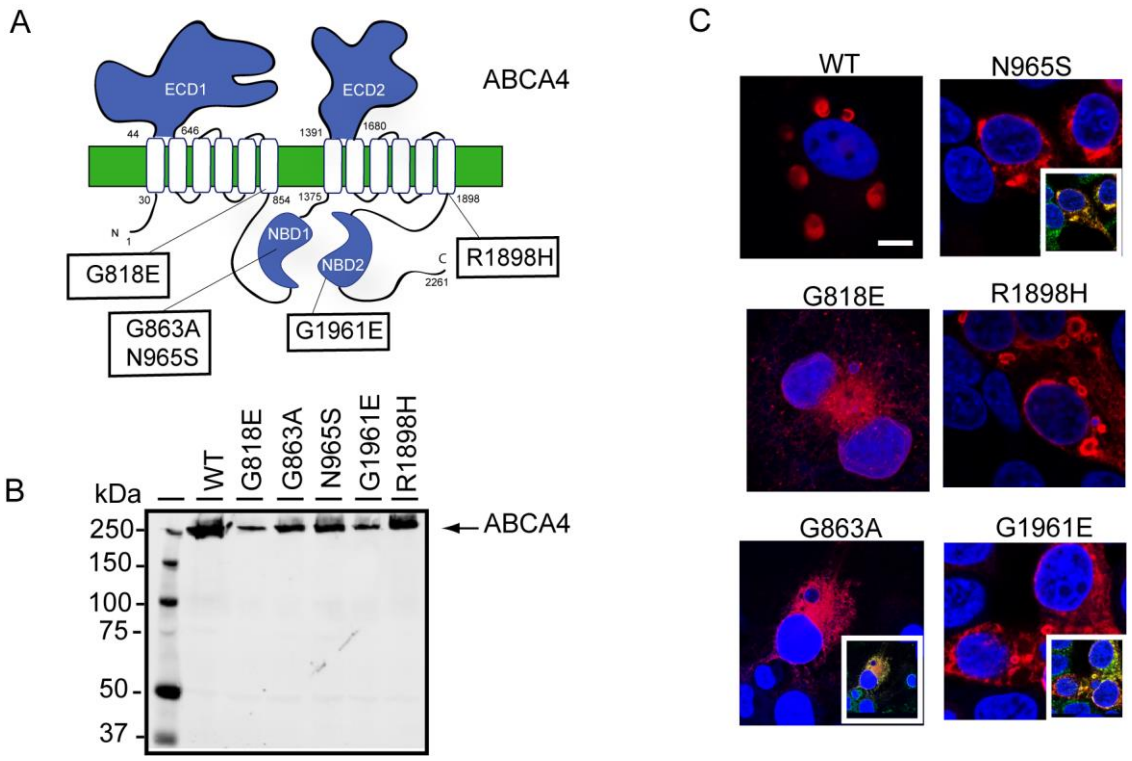

Figure 5.2 Protein Expression Levels and Localization of Mutant ABCA4 Proteins

A. Topology model of ABCA4 showing the five amino acids whose mutated residues in the nucleotide binding domains cause Stargardt disease are examined in this study. **B.** Relative expression levels of HEK293T membranes derived from transiently transfected ABCA4 wild-type and mutants and labeled with 1D4 antibody on a Western blot. **C.** Confocal microscopy of HEK293T cells 48 h after transfection. Cells were analyzed by immunofluorescence with ABCA4 tag mouse Rho 1D4 (*red*), and rabbit anti-calnexin mAb (*green*) binding was detected with Alexa Fluor 546 and Alexa Fluor 488-conjugated secondary antibodies, respectively. Nuclei were stained with DAPI (*blue*). Scale bar 10 µm.

5.3.3 Dronedarone Rescues Activity of ABCA4 SD Mutants

To investigate potential differences in allosteric activation, we first examined the basal and retinal-stimulated ATP hydrolysis of ABCA4 mutants purified and reconstituted in BPL proteoliposomes. Consistent with previous studies, the two mutants, G863A and N965S, show a decrease in both basal and retinal-stimulated ATPase, with G863A showing the greater decrease (Fig 5.3A) (Quazi et al., 2012; Sun et al., 2000). G818E is similar to G863A with respect to basal and retinal-stimulated ATP hydrolysis. Among the NBD2 mutants,

G1961E is abrogated in that it exhibited a reduced basal ATPase activity and was inhibited, rather than stimulated, by retinal. Mutant R1898H had reduced basal ATPase but showed 2-fold stimulation by retinal addition (Fig 5.3A).

To determine whether dronedarone is responsive at allosterically activating the ATPase activity, we analysed dose-dependence activity curves of the mutant proteins. The two NBD1 mutants along with G818E exhibit activation together with retinal in ATPase activities, albeit with different allosteric activation (Fig 5.3B & 5.3C). For NBD1 mutants, dronedarone together with all-*trans* retinal increased the basal ATPase 4-, 3.6-, and 3.3-fold of G818E, G863A, and N965S, respectively, within an apparent half maximal concentration of ~10 µM. However, NBD2 mutant, G19161E was inhibited or unresponsive to both retinal and dronedarone addition. By contrast, R1898H displayed a strong 3.7-fold activation of ATPase activity by dronedarone and retinal. This suggests that allosteric coupling of NBDs are required for synergistic dronedarone activation.

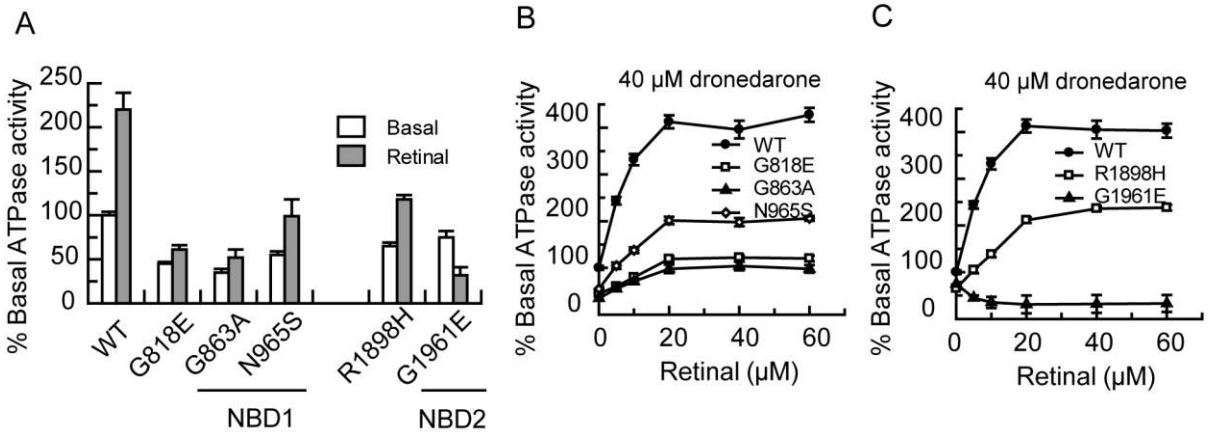

Figure 5.3 Effect of Retinal and Dronedarone on ATPase of Stargardt Mutants

A. ABCA4 ATPase of variants preceding or residing in NBD1 & NBD2 and its response to retinal-stimulation. Retinal specific stimulation of variants together with dronedarone (40 µM) and its effects on ABCA4 mutations snear or in NBD1 (**B**) and adjacent to or in NBD2 (**C**). For each panel, the wild-type and mutant ABCA4 proteins were transfected, purified, reconstituted and assayed in parallel to minimize experimental variation and the ATPase activity of wild-type ABCA4 in the absence of retinal is normalized as basal activity (100%). Slight variations in WT stimulated activity are a property of experimental variation and reproducibility.

Next, we determined the effect of ABCA4 retinal transport with dronedarone treatment. The rate of retinal transport is linear over the course of 1hr but was too quick to quantify with dronedarone during the same incubation period. Therefore, time courses were performed at a reduced time point (30 min); wild-type ABCA4 shows 5.5% of transport of 10 μM all-*trans* retinal incubated in the assay during 30 min (Fig 5.4A). Inclusion of dronedarone increases the rate to 7.3%, which is 1.4-fold higher than in standard assay measurements (Fig 5.4B). Addition of 20 μM dronedarone does not significantly alter the partition of labeled retinal among the donor and acceptor vesicles of the reaction assay (Fig 5.4B). Under similar proteoliposome preparations of G818E, G863A, and N965S, dronedarone increased the retinal transport between ~2-3.2%. With R1898H, addition of dronedarone increased retinal transfer to ~5.1%, which was near to wild-type levels without any drug addition (Fig 5.4C). But, G1961E was not rescued and did not transfer retinal upon dronedarone addition. Nonetheless, for the remaining mutants measurable levels of enhanced retinal transport.were observed. In particular, N965S and R1898H retinal transport with dronedarone addition showed a restoration of retinal transfer to near wild-type levels (Fig 5.4C). Thus, dronedarone was effective at enhancing *N*-retinylidene PE transport for several NBD mutants.

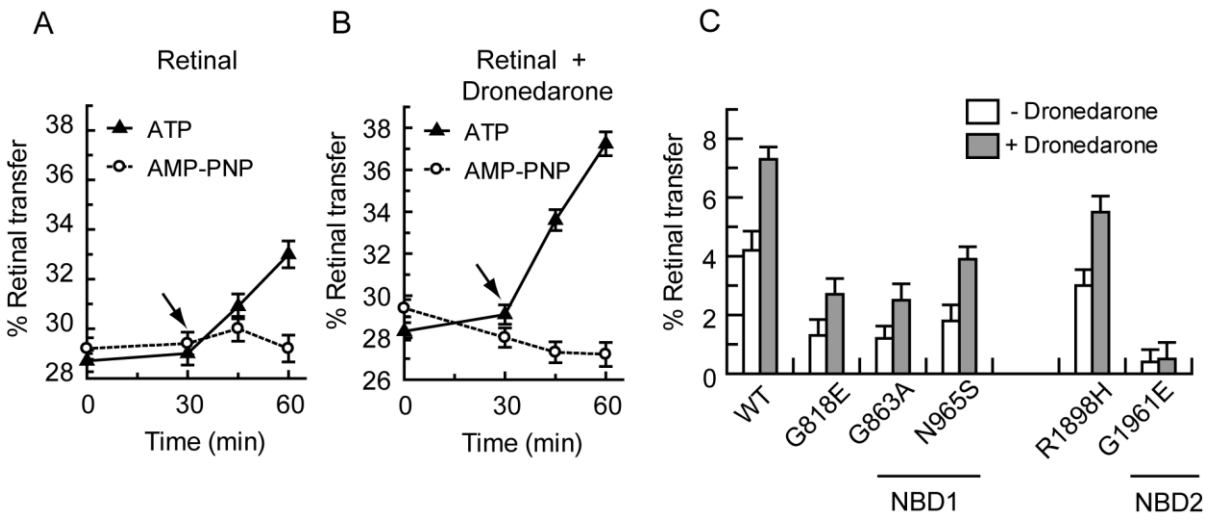

Figure 5.4 Effect of Dronedarone on the Retinal Transport of Stargardt Mutants

Vesicular retinal transfer assay of WT-ABCA4 using donor and acceptor liposomes doped with retinal(**A**) or with retinal and dronedarone (20 μM) (**B**) Partition of radiolabel retinal is not significantly altered with dronedarone addition as seen by the AMP-PNP level curves **C.** Retinal transport activity of the mutant proteoliposome vesicles as ATP-dependent transfer of [^{3}H] all-*trans* retinal in the absence and presence of dronedarone (20 μM). The values shown have been adjusted to take into account differences in ABCA4 protein levels as shown in panel **A**. The results shown are the means (±S.D.) of triplicate experiments.

5.3.4 Chemical Chaperones Differentially Enhance ABCA4 SD Protein Levels

We next investigated the effect of chemical and pharmacological chaperones on the protein levels of G818E, G863A, N965S, G1961E, and R1898H. Transfected HEK293T cells were treated with 3% glycerol, 50 μM β-ionone, or 5 mM 4-PBA for 36h and the levels of ABCA4 proteins were compared by immunoblot analysis of detergent-solubilized cell lysates. As shown in Fig 5.5A, exposure of cells to the glycerol had no significant effect on wild-type and mutant ABCA4 levels. Fifty μM β-ionone was toxic to HEK293T cells resulting in the death of most growing viable cells. As a result, protein levels of wild-type and mutants were severely reduced. However, treatment with PBA resulted in substantial but differentially increased levels of the mutants. Expression levels of G818E, G863A, and N965S were increased to a level comparable with wild-type ABCA4. In contrast, the level

for R1898H was not affected by PBA treatment and the level of G1961E was only modestly affected. Because mutant ABCA4 levels were most affected by PBA treatment, subsequent studies focused on characterizing the ABCA4 mutants with this chemical chaperone.

5.3.5 PBA Dose-Dependence and Incubation Duration on ABCA4 Mutant Levels

The dose-dependent and time-dependent effect of PBA on the expression levels of the five mutants was investigated. First, HEK293T cells expressing wild-type and mutant ABCA4 were treated with different concentrations of PBA (1, 2, or 5 mM) for 36h. Detergent solubilized lysates were prepared and the levels of ABCA4 were compared by western blot analysis. As shown in Fig 5.5B, an enhanced level of mutant protein G863A was observed at 5 mM PBA. This behavior was also observed with N965S (Fig 5.5C). To determine the time dependence of the PBA effect, cells were exposed to PBA (5mM) for 12, 24, or 36h and levels of ABCA4 were assessed in the solubilized lysates. A 12 h treatment showed only minimal effect on mutant protein levels but 36 h exposure of cells to PBA showed a moderate increase in the range of 30 -70% for all the four mutants (Fig 5.5D). Hence, subsequent experiments were carried out using cells exposed to 5 mM PBA for 36h based on these observations.

5.3.6 Effect of PBA on Cellular Localization of ABCA4

To investigate whether trafficking of mutant ABCA4 could be rescued, PBA was applied to COS-7 cells expressing missense variants G818E, G863A, N965S, G1961E, and R1898H and visualized by confocal microscopy. Addition of 5 mM PBA to COS-7 cells transfected with G818E and G863A markedly altered ABCA4 localization from the ER to large intracellular vesicles, without altering the intracellular localization of ABCA4-WT (Fig 5.5E). Vesicles with N965S and R1898H stained positively with intracellular vesicles. In

marked contrast, G1961E did not display much change, which showed both intracellular vesicles and partial colocalization with the ER marker calnexin, while R1898H was primarily found in intracellular vesicles (Fig 5.5E).

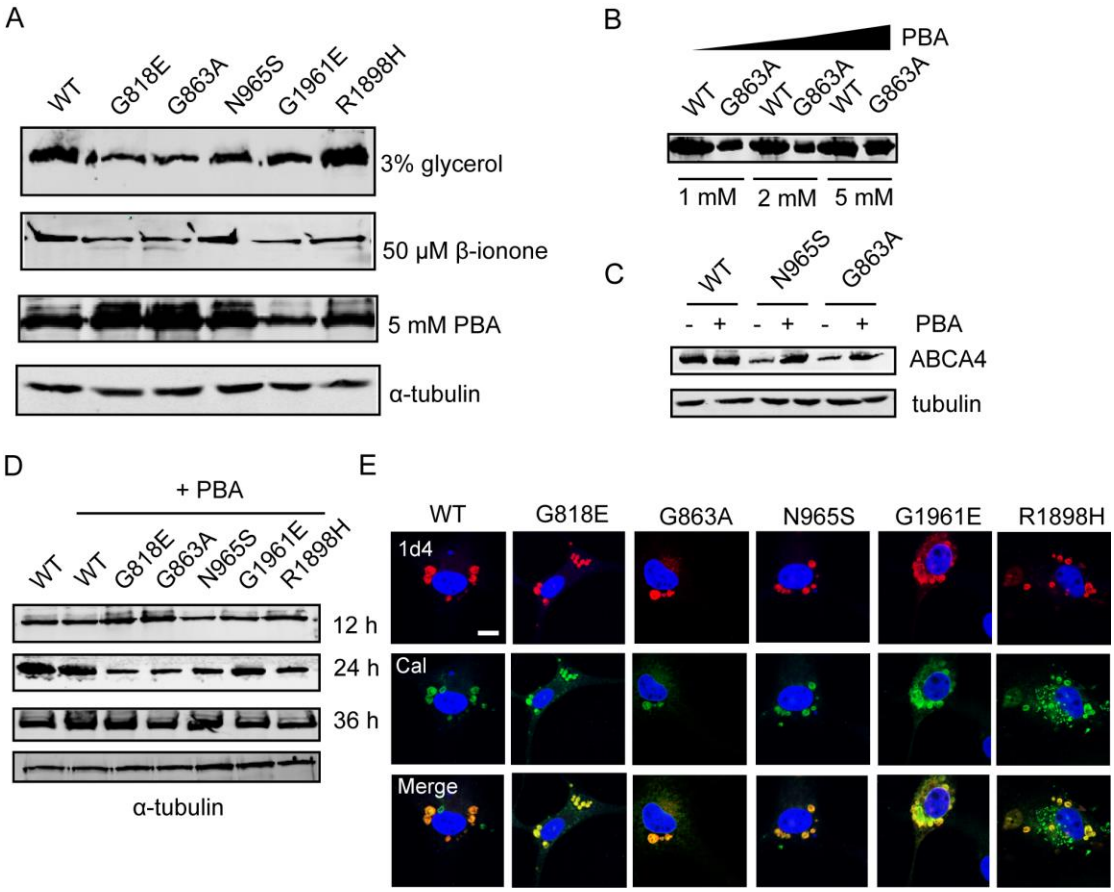

Figure 5.5 Effect of Chemical Chaperones on ABCA4 Mutant Expression & Localization

A. Representative western blots of CHAPS-solubilized cell lysates (10 μg of protein per lane) prepared from HEK293T membranes that were incubated for 36 h after transfection in the presence of the indicated chemical supplements [glycerol, β-ionone, and 4-phenylbutyrate (PBA)]. Equal loading from PBA treatment was confirmed with α-tubulin shown at the bottom. Similar results were obtained with cell lysates prepared from at least three independent transfections. **B**, **C**, and **D**. Similar to (**A**), in **B**, cells transfected with WT and G863A were incubated for 36 h after transfection in the presence of increasing concentrations of PBA, and **C.** cells were transfected with WT, G863A, and N965S in the presence of 5 mM PBA, and **D.** cells were transfected with WT, G818E, G863A, N965S, G1961E, and R1898H and incubated for 36 h in the presence of 5 mM PBA for the indicated times. Untreated WT shown as a control and equal loading confirmed with α-tubulin. Similar results were obtained from two independent transfections. **E.** shown is confocal microscopy of transfected COS-7 cells after incubation for 36 h in the presence of 5mM 4-PBA. Cells were analyzed by indirect immunofluorescence with mAb 1D4 (*red*) and an anti-calnexin mAb (*green*) binding. Nuclei were stained with DAPI (*blue*). COS-7 transfections and imaging were performed in three independent experiments.

5.3.7 Functional Characterization of ABCA4 Mutants Rescued by PBA

As shown earlier, synergistic drug activation in conjunction with retinal substrate offers an avenue to complement protein function in the photoreceptor disc membrane environment. To determine if PBA-rescued G818E, G863A, N965S, R1898H, and G1961E mutants were functionally affected, their retinal transfer activities were measured. Proteoliposomes of ABCA4 proteins were prepared and purified from transfected HEK293 cells. The Western blot and Coommassie SDS-PAGE gel showed that levels of mutant ABCA4 G818E, G863A, and N965S were comparable with wild type ABCA4 levels whereas levels of the R1898H and G1961E mutants were unchanged (Fig 5.6A & 5.6B).

When ^{3}H-retinal transfer was assayed for wild-type ABCA4 prepared from cells with or without 4-PBA treatment, no significant difference in activity was observed (Fig 5.6C). Retinal transfer by R1898H proteoliposomes was ~70% of wild-type. By contrast, G818E, G863A, and N965S showed a 25-40% reduction in retinal transfer compared to wild-type and remained unchanged compared to the purified protein obtained from untreated cells (after accounting for differences in protein levels). In contrast, G1961E still did not exhibit any observable retinal transfer activity. These results indicate that although PBA shows significant rescue of cellular localization, no change in retinal transfer activity was observed for the purified and reconstituted G818E, G863A, N965S, and G1961E mutants.

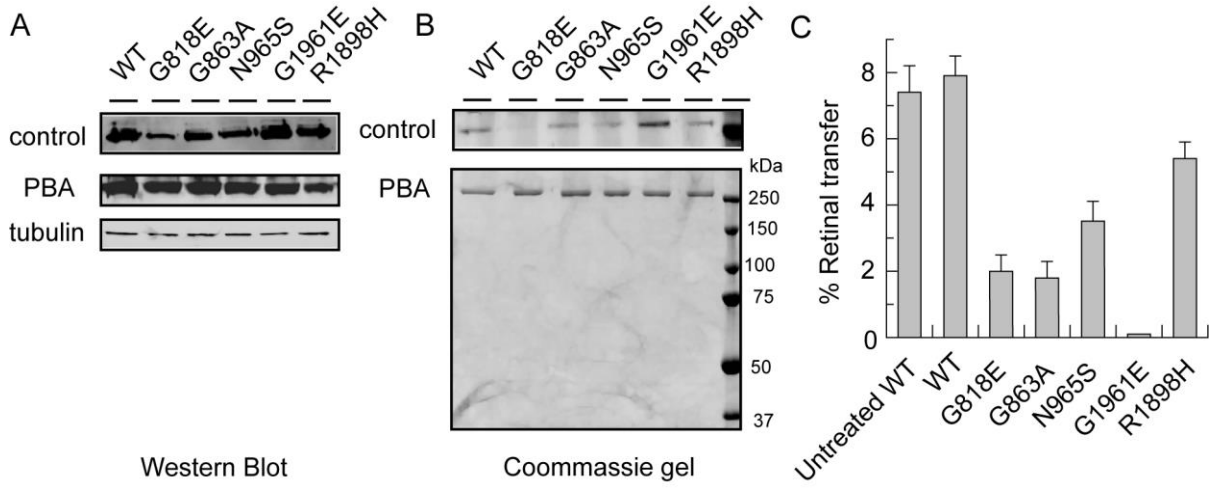

Figure 5.6 Effect of PBA on ABCA4 Mutant Expression and Retinal Transport

A. Shown is a representative western blot of solubilized cell lysates prepared from HEK293T cells incubated for 36 h after transfection in the absence or presence of 5 mM PBA after transfection with WT and mutant ABCA4 expression vectors. **B.** Similar to **A.** except ABCA4 proteins were purified on a 1D4-immunoaffinity column and resolved on SDS-PAGE gel. Unmarked lane is protein molecular marker **C.** Retinal transport activity was measured at 1 h as ATP-dependent ^{3}H-retinal transfer between donor proteoliposomes and acceptor liposomes. The results are the means of two independent experiments.

5.4 Discussion

We have developed a strategy that combines drug testing evaluation with conventional ABCA4 protein purification to identify biologically-responsive disease variants using transport and ATPase assays. This strategy may be generally applicable to testing mutant proteins prior to using cell- or mice-based model studies. We showed that class III antiarrhythmic drugs, dronedarone and amiodarone, are direct ABCA4 activators. The iodine atoms of amiodarone do not appear to be critical for activation, and a methyl-sulfonamide group present in dronedarone reduces neurotoxic and other adverse effects (Patel et al., 2009). In particular, dronedarone was found to activate ATP hydrolysis and retinal transport with ABCA4 proteoliposomes in a dose-dependent manner. As a proof of principle, we used

this strategy to identify which ABCA4 disease mutant proteins may be functionally rescued with dronedarone.

Structurally related benzofuran derivatives, dronedarone and amiodarone, enhanced ABCA4 ATPase in a near identical manner. In contrast, digitonin displays biphasic behavior, with stimulation observed at low concentrations, and inhibition at higher concentrations. We found that dronedarone enhanced retinal stimulated ATPase and *N*-retinylidene PE transport activity of NBD1 mutants (G818E, G863A, and N965S) and one NBD2 mutant, R1898H. Interestingly, the increase in retinal transfer of N965S mediated by the compound was sufficient to rescue to levels of WT retinal-stimulated activity. The other two mutants, G818E and G863A, were also responsive to dronedarone approaching ~70% levels of WT retinal transfer activity. R1898H, which is mildly impaired in ATPase displays near WT retinal transfer activity when treated with dronedarone. The NBD2 mutant, G1961E, which showed a loss or insensitivity to retinal ATPase stimulation was unaffected by the addition of dronedarone. G1961 lies within the Walker A motif of the NBD2 domain. The conversion to a charged residue may induce secondary consequences in ATPase hydrolysis coupled to substrate transport. Altogether, these findings show that small molecules exert selective activation of the mutant protein. Clearly, dronedarone provides a therapeutic opportunity to understand the novel mechanism underlying synergistic activation of ABCA4 and requires further study with dysfunctional protein-drug interaction.

It can be speculated that dronedarone binds to an allosteric site, which is distinct from the substrate binding site. This hypothesis is supported by the previous observation that amiodarone does not alter the K_m of ATPase in biochemical studies (Sun et al., 1999). Interestingly, amiodarone inhibits the transport activity of ABC drug transporters, including

Pgp (Knorre et al., 2009; Tiberghien and Loor, 1996). Allosteric binding of dronedarone rather than at the substrate binding site offers a selectivity advantage. Given the conservation of ABCA subfamily members, a compound that targets these sites may exhibit cross reactivity among multiple family members. We anticipate that dronedarone interacts with a region unique to ABCA4 or to the ABCA family. Amiodarone is currently the most-used class III antiarrhythmic drug and is prescribed for patients with atrial fibrillation. Both amiodarone and dronedarone bind uncompetitively to β-adrenergic receptors and also block Na^+ channels, L-type Ca^{2+} channels, K^+ channels, and the Na^+/Ca^{2+} exchanger (Chatelain et al., 1995; Patel et al., 2009). The synergistic activation of dronedarone on ABCA4 could provide a rationale for Stargardt disease therapy. Because both therapeutic and adverse drug effects have been associated with dronedarone, identifying features of biased ABCA4 activation by rational drug design may facilitate the development of effective therapeutics for Stargardt disease.

Our results not only demonstrate that small molecules can functionally rescue impaired ABCA4 activity, but also reveal low molecular-weight chemical chaperones as another approach to rescuing membrane protein expression and trafficking. Mutations in rhodopsin, including P23H, that result in misfolding and mislocalization to the inner segments of photoreceptors can be rescued by application of a retinal analog, β-ionone (Noorwez et al., 2008). In ABC transporter diseases, such as cystic fibrosis, the most common disease mutant, ΔF508-CFTR, can be rescued by application of PBA (Brown et al., 1996; Papp and Csermely, 2006). In this study, ABCA4 mutants varied in their response to the different compounds. β-ionone inhibited protein expression of wild-type and mutant ABCA4 in HEK293T cells whereas PBA enhanced expression of NBD1 mutants – G818E,

G863A, and N965S – to near wild-type levels. This indicates that the conformation of the NBD1 mutants was substantial and PBA shifted the folding equilibrium towards a more native-protein folded state. On the other hand, G1961E was mildly responsive to PBA while R1898H which displayed near wild-type expression levels before treatment was unaffected by PBA application. Together, these findings suggest how residues located near and residing in both NBDs have distinct roles in folding and assembly of ABCA4, with the folding defects caused by substitution of G818, G863 being the most severe and those caused by R1898 and R2030 being the least affected. It is interesting to note that within the ABCA subfamily, G818, G863, and N965 are highly conserved, whereas R1898 is much less so. Expectedly, the mutants showed no significant changes in retinal transport or ATPase activity. Thus, in a photoreceptor cell, the rescue in transport activity of the mutants could largely, if not wholly, be attributed to increase in trafficking of the properly folded membrane protein.

The PBA-rescued mutants from the NBD1 domain correctly trafficked to the intracellular vesicles. It has been suggested that the chaperone-like activity of PBA can be explained by its ability to promote cytosolic-solubility of surface-exposed hydrophobic regions of the translating polypeptide. This prevents aggregation and promotes folding of membrane proteins (Papp and Csermely, 2006). In addition, PBA and related derivatives are also known to be histone deacetylase inhibitors, and modulate the expression of heat shock proteins that act as cellular chaperones to facilitate the folding process. For ΔF508-CFTR, disease mutants of ABCA1 and ABCB4, PBA promotes expression of cellular chaperones and allows the mutant to traffic and exit from the ER as a folded polypeptide (Brown et al., 1996; Gautherot et al., 2012; Riordan, 2008; Sorrenson et al., 2013). But, several mutants of ABCC1 have been shown to be rescued by the chemical-like activity of PBA (Iram and Cole,

2012). Similarly, PBA has been reported to rescue expression of other membrane proteins, low density lipoprotein receptor and CNG channels in cone photoreceptors, independent of its histone deacetylase activity (Duricka et al., 2012; Tveten et al., 2007).

The effectiveness of rescue with allosteric modulators and chemical chaperones used in the six mutants was mutant-specific. This biochemical- and cell-based approach showed that NBD1 mutants were both amenable to synergistic activation with dronedarone and was able to overcome folding defects with PBA. For the NBD2 mutants, it had little or no effect with G1961E, while R1898H had sufficient transport rescue with dronedarone activation to near wild-type synergistic-activated levels. We propose that the large spectrum of Stargardt disease mutations may have residual functional activity and/or mislocalized protein retained in the inner segment of photoreceptor cells. The partial activity of ABCA4 mutants could result in constitutive and retinal-activated protein with dronedarone application and the efficacy of chemical chaperones like PBA may ensure proper folding and assembly of ABCA4.

Chapter 6: Conclusions

6.1 Chapter Summary

The contribution of ABCA4 in the visual cycle was initially studied in chapter 2. Proving that ABCA4 functioned as a retinoid transporter and defining the direction of transport motivated the development of an *in vitro* ABCA4 transfer assay. Purified ABCA4 reconstituted into liposomes or disc membrane vesicles containing ABCA4 showed ATPase-dependent transfer of radiolabeled all-*trans* retinal to acceptor liposomes. The reaction followed sigmoidal kinetics with a Hill coefficient of ~2 and was inhibited by *N*-retinyl PE, a substrate analog. Positive cooperativity in the transport process may suggest binding of retinal to an allosteric site that may govern conformational changes associated during *N*-retinylidene PE transport. Retinal transport was absent in proteoliposomes containing ABCA4 with mutations in the Walker-A motifs and disc membranes from *Abca4*$^{-/-}$ knockout mice. ABCA4 was also purified and reconstituted into liposomes containing fluorescent-labeled phospholipids. ABCA4 demonstrated fluorescent-labeled PE specific flipping across from the inner leaflet of liposomes (= disc lumen of cell membranes) to the outer leaflet of liposomes (= cytosolic leaflet). These studies provide the first direct biochemical evidence of an ABC mammalian importer. By doing so, ABCA4 facilitates the import of *N*-retinylidene PE that dissociates into PE and all-*trans* retinal, the latter of which is subsequently reduced to all-*trans* retinol in photoreceptor cells.

Fluorescence imaging of dark adapted *Abca4*$^{-/-}$ mice directly identified enhanced levels of lipofuscin present in the RPE owing to 11-*cis* retinal fluxes. The regeneration of opsin predicts the need for the high flux of 11-*cis* retinal. However it is unclear if ABCA4 can transport the 11-*cis* derivative of *N*-retinylidene PE and prevent the buildup of excess

free 11-*cis* retinal in disc membranes. In chapter 3, the transport and HPLC characterization of both retinal isomers demonstrated similar translocation of 11-*cis* retinylidene PE from the inner leaflet to the outer leaflet of liposomes reconstituted with ABCA4 purified from photoreceptor OS. ABCA4 ATPase measurements showed robust stimulation with 11-*cis* retinal that was elevated with amiodarone to a higher degree than all-*trans* retinal. In addition, under non-protein and dark-incubated conditions with phospholipid liposomes, substantial isomerization of retinal isomers takes place. In PE containing vesicles, but not PC, 11-*cis* retinal irreversibly isomerizes to all-*trans* retinal and 13-*cis* retinal, while all-*trans* retinal shows partial isomerization to 13-*cis* retinal. ROS lipid and BPL lipid vesicles were extremely proficient at isomerizing 11-*cis* retinal whereas the rate of isomerization was slower in synthetic DOPC/DOPE vesicles. Moreover, the isomerization activity precedes the formation of A2PE species originating from all-*trans* retinal and 11-*cis* retinal upon prolonged incubation of these retinoids with ROS disc vesicles. The similarities of ABCA4 *N*-retinylidene PE transport of both *cis* and *trans* isomers is indicative of reducing the levels of the Schiff base conjugate in the disc lumen while photoreceptors maintain rapid retinal fluxes across photoreceptor organelles. 11-*cis* retinal is continuously supplied to rod photoreceptors whose levels may be regulated by phospholipid isomerization in bleached and unbleached conditions. Generation of lipofuscin precursors in ROS disc vesicles due to accumulated retinal highlights the crucial need for ABCA4 activity and further implicates ABCA4 in the transport of Schiff base conjugates of 13-*cis* retinal and other retinal isomers in disc membranes.

In chapter 4, the biochemical basis and identification of lipid substrates flipped by homologous ABCA transporters were examined. Extracellular lipid transport and cellular

lipid homeostasis are largely implicated from disease-associated phenotypes, analysis of knockout mice and cell-based studies, but the substrates and direction of transport have not been firmly established by ABCA transporters. This study demonstrates that ABCA1 reconstituted into liposomes with fluorescent-labeled lipids showed robust translocation of PC, PS, and SM analogs from the cytosolic side to the lumen side of vesicles. Similarly, ABCA7 preferentially translocated PS and to a certain extent, PC whereas ABCA4 only translocated PE in the opposite direction. By contrast, flippase activity for ABCA1 and ABCA4 was reduced by the presence of cholesterol. The broad specificity of ABCA1 may suggest translocation of various lipid substrates to the extracellular side is coupled to altering the surface area of cellular membranes. This results in cell protrusions which facilitates cholesterol and phospholipids loading onto ApoA-I. As suggested in the two step model, ABCA1 may first directly efflux phospholipids to ApoA-I directly bound to ABCA1 followed by loading of cholesterol. Nine different ABCA1 Tangier mutants and the corresponding SD ABCA4 mutants from different domains showed varying and decreased levels of phospholipid flipping activity. This suggests that the the disease mutations broadly affect the function and proper folding of ABCA1 and ABCA4 when transporting phospholipids in different directions. These studies also offer the first direct evidence for ABCA1 and ABCA7 functioning as phospholipid transporters and suggest that this activity is essential in ApoA-I loading for HDL formation.

Lastly, in chapter 5 the molecular mechanisms of small molecules that regulate ABCA4 activity and proper folding were examined. Considerable progress used to “correct” biosynthetic defects has been made for human mutations related to ABC transporters. Small molecules function as a ‘corrector’ enhancing function, or serve as a ‘chaperone’ effecting

protein folding and trafficking, or are conducive to both enhancing function and correct trafficking. Since, the understanding of small molecule intervention on mutations of ABCA4 remains limited, a systematic protein-rescue characterization of dronedarone and 4-phenylbutyrate was elucidated with SD mutant proteins preceding or residing in NBD1 (G818E, G863A, N965S) and NBD2 (R1898H, G1961E and R2030Q). In these results G818E, G863A, and N965S mutants had reduced *N*-retinylidene PE transport activities. Dronedarone treatment partially rescued the the transport activities of these mutants, but failed to rescue the G1961E mutant. Low protein expression indicates improper folding of G818E, G863A, N965S, and G1961E. However, protein degradation was not examined directly assuming protein synthesis is unchanged. Treatment with 4-phenylbutyrate was effective at restoring expression and cellular native-like cellular localization of G818E, G863A, and N965S. These findings illustrate the first basis of small molecule intervention that enhances functional activity and protein folding of ABCA4 in photoreceptor cells.

6.2 Implications

6.2.1 The Toolbox of Visual Cycle, OS proteins, and ABCA4

How does the function of ABCA4 fit in with the visual cycle, retinal levels, and mouse studies? First, we consider the dark adapted case in photoreceptors whereby opsin regenerates with 11-*cis* retinal flux within 15-20 min and there is no all-*trans* retinal flux out of disc rhodopsin (Lamb and Pugh, 2004). In the dark, free 11-*cis*-retinal flows into photoreceptors for OS renewal and opsin regeneration (Young, 1971). 11-*cis* retinal partitions in the disc membrane bilayer in its free form or equilibrates with PE as a Schiff base conjugate. In rod disc vesicles, 11-*cis* retinal isomerization is 50% complete in ~30 minutes. As such, levels of free 11-*cis* retinal in photoreceptors convert to all-*trans* retinal,

which feeds back into the visual cycle *via* Rdh8 reduction. *In situ*, the rate of retinol formation is slower (0.06 min^{-1}) than the rate of *N*-retinylidene PE transfer in disc membranes (24.5 min^{-1}) (Chen et al., 2009; Quazi et al., 2012). Translocation of 11-*cis*-retinylidene PE by ABCA4 to the cytoplasmic side prevents buildup of 11-*cis* retinal in the disc lumen. Since Rdh8 cannot reduce it, 11-*cis* retinal remains on the cytosolic side of photoreceptor disc organelles. Strikingly, the studies from Chapter 2 and Chapter 3 implicate retinal isomerization as a consequence of elevated levels of all-*trans* retinal in retinas of *Abca4*$^{-/-}$ mice.

Second, when photoreceptors are bleached in light, the rate of release of all-*trans* retinal from disc membranes is fast (0.3 min^{-1}) (Heck et al., 2003). Retinol formation by Rdh8 in photoreceptors is biphasic and defined by rapid and slow phases (Blakeley et al., 2011; Chen et al., 2009). The first phase of retinol formation suggests a rapid reduction of free all-*trans* retinal while the secondary slow component in retinol formation may be due to progressive reduction of retinal dissociating from the *N*-retinylidene PE equilibrium. As in the dark, 11-*cis* retinal entering the photoreceptors is subjected to phospholipid disc isomerization and may be regulated and influenced by protein binding in both bleached and dark-adapted conditions. ABCA4 translocates *N*-retinylidene PE of either retinal isomer to the cytosolic side of rod discs. Specifically, the rate of A2E and lipofuscin in RPE formation increased and was light-independent in *Abca4*$^{-/-}$ mice (Boyer et al., 2012).

In terms of phospholipid asymmetry in disc membranes, the opsin scramblase activity is 4 orders and 2 orders of magnitude higher compared to ABCA4 and ATP8a2. This would overwhelm the functional activity of both ATP8a2 and ABCA4 (Appendix A.10). In this case, PS asymmetry would primarily arise from negative electrostatic charges on the

cytosolic side of rhodopsin.

6.2.2 Basis of Substrate Binding

Another molecular flux phenomenon associated with transport occurs with abscisic acid movement in plants. This ubiquitous hormone passively diffuses among cells but the hormone is rapidly needed during pH stress conditions in vascular cells to elicit a timely response. Between two related plant ABC transporters, ABCG25 mediates abscisic acid export from the inside to the outside of cells and ABCG40 mediates abscisic acid import from the outside to the inside of cells (Kang et al., 2010; Kuromori et al., 2010). Computational data reveal conserved motifs in NBDs responsible for conformational changes coupled to the TMDs. In ABC importers, it is possible the binding site of *N*-retinylidene PE and abscisic acid may reside close to the extracytosolic leaflet.

What is the basis for retinal binding in membrane and cytosolic proteins? In the cellular retinol binding protein, a plasma serum protein, a large binding cavity allows flexibility and the retinal polyene chain is stabilized by hydrophobic interactions from threonine, tryptophan, and tyrosine residues (Wang et al., 2013). Intriguingly, the ionone ring end doesn't require stacking interaction from an aromatic side chain residue. In addition, conserved arginine residues play a role in 11-*cis* retinal binding in CRALBP residing in the RPE and Muller cells (He et al., 2009). ABCA4 mediated binding of a non-protonated Schiff base *N*-retinylidene PE may due to the absence of a counteranion as seen in opsin. Two combinations of substrate binding can be envisioned: 1) Retinal binds to the charged extracytosolic/lumenal loop between the 5^{th} and 6^{th} TMD of either half of the protein and forms a Schiff base with PE from within the TMD lipid binding site; 2) and alternatively, a small hydrophobic cleft in the TMD would serve as the retinal binding site conjugated to PE

in an adjacent site within the TMD substrate binding pocket.

6.2.3 Models of Lipid and Cholesterol Efflux

Based on the two-step model of lipid efflux, identification of lipid substrates translocated to the extracellular side by ABCA1 during lipid efflux seems logical. At present, it is still unclear to what extent cholesterol participates in ABCA1 efflux. Recent progress in cellular studies illustrated lipid microdomain formation contributing to the lipid efflux process. In one model, ABCA1-dependent activity creates a PC-rich membrane binding site for ApoA-I on the plasma membrane that has ~ 10-fold higher capacity to bind ApoA-I compared to ABCA1 (Iatan et al., 2011). After lipidation of ApoA-I by ABCA1, ApoA-I further desorbs PC from the PC-rich regions and lipid microdomains, thereby becoming an efficient acceptor of cholesterol. In addition, single-particle analysis using ABCA1-GFP suggests that transporter dimerization forms the functional unit in ApoA-I binding and lipid efflux (Nagata et al., 2012). In line with these models, the studies suggest that: (1) cholesterol affects membrane fluidity, interacts directly with ABCA1 and regulates lipid loading of ApoA-I; (2) SM and PC flipping by ABCA1 creates spontaneous SM and cholesterol microdomains; and, (3) cholesterol may stimulate ABCA1 activity only upon ApoA-I binding. The latter is similar to ABC importers whereby interacting proteins with bound substrate, transfers substrate directly to the transporter and initiates transport (Higgins and Linton, 2004).

6.2.4 Disease Mechanisms

Neurodegenerative diseases like Alzheimer's disease, ABC transporter diseases like cystic fibrosis, and some forms of autosomal dominant RP are associated with misfolding and aggregation of membrane and secreted proteins. Various human mutations have different

effects on disease progression, and this may also differ from the empty-background in *Abca4*$^{-/-}$ mice. The 800 mutations identified so far are typically distributed over the long primary sequence and lack a defined 'disease-hotspot'. ABCA4 residual activity cannot alone account for SD phenotypes as shown in previous studies (Sun et al., 2000; Zhong et al., 2009) and in Chapters 4 & 5. Recent statistical analysis of SD patients showed individuals with two missense or splicing mutations developed severe phenotypes than those with two truncating mutations (Cideciyan et al., 2009). *In vitro*, ABCA4 is unusually sensitive to photo-oxidative damage mediated by all-*trans*-retinal (Sun and Nathans, 2001). We also have evidence that transfection of some SD mutants – T901A and E2096K – decrease viability of HEK293T cells and cause cell death. Prolonged accumulation of misfolded proteins can induce ER stress responses, overwhelm quality control pathways, and cause cell death. ER stress sensors (BiP, caspase-12, CHOP, and others) are up-regulated in a time-dependent manner with unfolded and aggregated photoreceptor proteins including rhodopsin, PDI, and ELOVL4 (Karan et al., 2005; Yang et al., 2008). It is unknown if several low expressing ABCA4 mutants (Chapter 4 & 5) are associated with enhanced protein degradation and ER stress but can raise a link of ABCA4 misfolding and ER aggregation to SD and photoreceptor cell viability.

6.2.5 Re-evaluation of Risk Factors in Stargardt Disease

Retinal isomerization and dissociation drives the Schiff base equilibrium towards free all-*trans* retinal form. As seen in Chapter 3, this is necessary as *N*-retinylidene PE slowly reacts with free retinal and formation of A2PE in ROS vesicles begins to accumulate with either retinal isomer. Based on previous studies, enhanced accumulation of A2E and retinal degeneration in the SD macula seemed logical. A recent integration of MALDI-imaging and

lipofuscin fluorescence data of *Abca4*$^{-/-}$ mice models suggested that A2E spatially localized with lipofuscin in the posterior segment of the eye (Grey et al., 2011; Tang et al., 2013). In addition, A2E accumulated with age and correlated with lipofuscin fluorescence. In contrast to the mice models, A2E distribution in the human eyes did not correlate with lipofuscin. A2E accumulation was independent of age and was at least 50-fold abundant in the far periphery of the retina (Ablonczy et al., 2013). In the posterior pole of the eye, strong fluorescence without significant A2E presence poorly predicts RPE death and consequently loss of central vision in SD. Features of A2E toxic effects including impairment of lysosomal degradation of lipids, destabilization of cellular membranes and photo-oxidative damage *in vitro* may not strongly correlate with the disease progression of SD. Moreover, a detoxifying role for A2E has been proposed from studies of all-*trans* retinal removal by amines resulting in protection from light-induced retinal degeneration (Maeda et al., 2011). These new findings underline the difficulty to attribute lipofuscin fluorescence and accumulating toxicity to any individual component, including A2E.

Nevertheless for A2E, bisretinoids and other fluorescent molecules constituting lipofuscin, it is important to determine the toxic molecules associated with enhanced retinal fluorescence. Analytical methods such as MALDI imaging combined with biochemical studies can identify specific candidate molecules and show whether the toxic molecule contains a well-defined target (*i.e.* a defect in phagosome inhibition) and if the toxic molecule is able to accumulate at sufficient concentrations. One or several molecules may help clarify disease mechanisms of SD with ABCA4 in humans.

6.3 Future Outlook

6.3.1 Design of Dronedarone-Analog Activators

This is where interdiscliplinary studies can help to collect essential biochemical information of ABCA4. Both dronedarone and amiodarone are potent inhibitors of Pgp but fail to improve standard chemotherapy in preclinical culture studies (Fisher et al., 1996)(www.fda.gov/drugs). In addition, dronedarone blocks Na^+, K^+, and Ca^{2+} channels although which effect provides clinical relief in cardiac patients is uncertain (Patel et al., 2009). For these two classical antiarrhythmic drugs, we also do not how they activate ABCA4 and inhibit Pgp and whether this activation can occur in photoreceptor cells. Recently, a generation of fluorescent compounds using dronedarone as the core backbone was synthesized in our laboratory (Fig 6.1A). The premise centres on the ability of fluorescent analogs to bind and activate ABCA4 and thus be used for: (1) identification of the drug binding site by competition with parent drug molecules on ABCA4; and (2) subjecting ABCA4 to a drug wide-screen to determine novel drug binding molecules. In contrast to our finding with dronedarone and amiodarone, these compounds do not develop synergistic activation of ABCA4. The benzofuran derivative is common to all analogs but the bulky and steric fluorescent groups may affect allosteric-site residue interactions. One solution is to synthesize and screen a library of derivatives with less steric side-groups. Next, successive iterations of the analog design can be used to develop a drug synergistic-activity profile of ABCA4 focusing on median EC_{50} values ranging between 5 - 200 μM.

6.3.2 Bisretinoid Analysis *In Vivo*

The reduced functionality of ABCA4 by a specific mutation in the ABCA4 gene illustrates how a mutant protein can be functionally enhanced by a dronedarone analog, but

the example provided does not show whether bisretinoid formation can be impeded. A functional assay by which a drug can alter A2E/bisretinoids *in vivo* would be useful. One example is the measurement of cell-based bisretinoid accumulation in a suitable mammalian cell system supported by a constant supply of serum and retinal. A stable co-expression system using Rdh8 and ABCA4 genes permits cytosolic expression of Rdh8 while ABCA4 is synthesized and localizes to intracellular vesicles. Incoming retinal is reduced while *N*-retinylidene PE is transported from the lumen of the ABCA4 containing vesicles. An increase in hyperfluorescence in the vesicles containing mutant ABCA4 proteins should reflect the formation and accumulation of bisretinoid products. This approach may be helpful as a quick functional readout to determine whether a mutant protein functionally delays bisretinoid formation by using test doses of dronedarone analogs.

6.3.3 Membrane-Signature Mediated Photoreceptor ABCA4 Trafficking

To study protein trafficking to photoreceptor outer segments, proteomic and lipidomic studies can be used. The generation of proteomics data of photoreceptors lead to the identification of secretory-pathway proteins and of novel proteins, such as ATP8A2 (Kwok et al., 2008). However, specific types of lipids such as phosphatidylinositol phosphates (PIP) mark specific membrane-vesicle compartments. In this case, lipidomic studies play an essential role in defining protein-vesicle sorting pathways. Chuang et al. showed that PIP species play a key role in rhodopsin trafficking and depends on PIP interacting proteins and receptors (Chuang et al., 2007). PIP signalling facilitates formation of a protein complex that includes Rab11, a small GTPase, and mediates trafficking of rhodopsin to OS (Satoh et al., 2005). Another example is the recent study by Scholz *et al.* in which the TAP1/2 ABC transporter associated strongly with a PIP species together with PC

and PE annular phospholipids (Scholz et al., 2011).

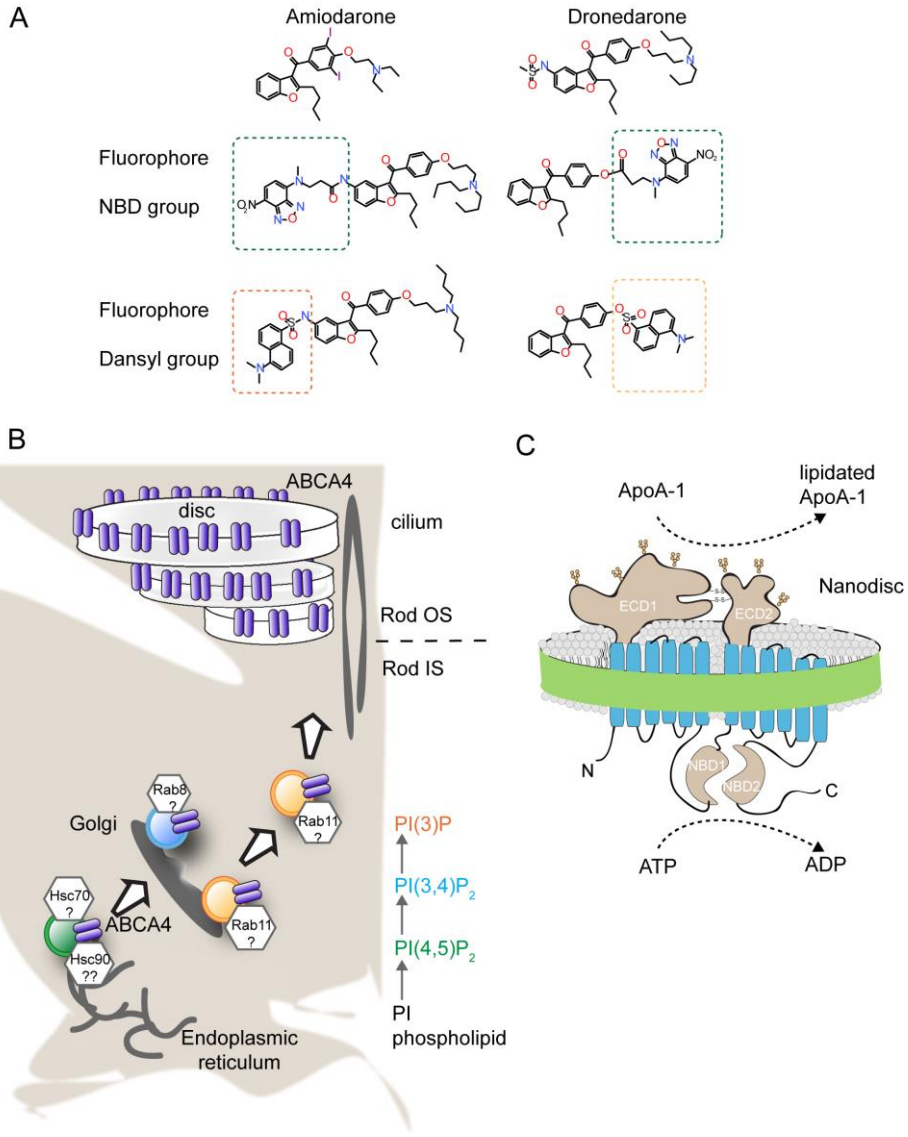

Figure 6.1 Future Directions

A. Synthesis and analysis of dronedarone analogs. Nitrobenzoxadiazole and dansyl-group fluorescent dervatives lack synergistic activation of retinal-stimulated ABCA4 ATPase. Additional analogs are required for testing. **B.** Trafficking pathway proteins and PIP lipids associated with ABCA4 OS trafficking in rods. **C.** Technological application of nanodiscs to analyze biochemical function of ApoA-I lipidation with purified ABCA proteins

The identity of ABCA4 intracellular vesicles in mammalian cell systems is unknown as is the trafficking pathway in photoreceptors. Do PIP species distinguish ABCA4 vesicles from others? If so, a potential mechanism may consist of a membrane signature of a particular PIP binding to ABCA4 vesicles. Next, trafficking proteins such as Hsc70, a heat shock protein, are recruited (Fig 6.1B). This pathway would remain intact in inner segment vesicles, not HEK293T intracellular vesicles where ABCA4 co-localizes with the ER marker calnexin. Identifying the PIPs enriched in these ABCA4 vesicles is helpful in assessing candidate proteins recruited for vesicle trafficking. In addition, the proteomics data reveals abundant peptides of Hsc90 and Hsc70 along with several Rab protein variants. It is worth visiting the cellular chaperones and lipids using sensitive mass-spectrometry analyses.

6.3.4 ABCA Transporters: General Considerations

Sequence analyses suggests human ABCA proteins may function as putative lipid transporters for those expressed in the oligodendrocytes of the brain (ABCA2), in the skeletal muscles (ABCA5/10), in the liver (ABCA6), and in the heart (ABCA9). The functional properties and substrate specificity of transporters associated with hereditary disorders such as interstitial lung disease (ABCA3) and harlequin ichthyosis (ABCA12) are still unknown. The immunoaffinity techniques of ABCA1/4/7 used in this study for analysis of phospholipid transport function should be useful for determining the substrate specificity and transport properties of other members of the ABCA subfamily. As a tool to characterize the remaining mechanisms of lipid efflux, the study of nanodisc protein reconstitution of purified ABCA1 may be informative given that nucleotide hydrolysis and ApoA-I binding occur on different sides of the membrane bilayer (Fig 6.1C). In addition, information related to ABCA4 phospholipid substrate specificity, protein-protein interactions, and regulatory properties

require further investigation. Studies of the recent low-resolution structure of ABCA4 delineate similarities with the ABC exporter family. Ideally, though, a high-resolution structure of ABCA4 should define *N*-retinylidene PE binding, enhance our understanding of the transport mechanism, and the molecular mechanism of ABCA4-drug activation. This is not only of functional biological interest but holds great potential for preserving vision.

There is clear strength in combining biochemistry with analytical methods, imaging, genetics, and pharmacology to study the complex disease mechanisms manifested by photoreceptors proteins. Future studies will undoubtedly add to the biochemical properties of ABCA4 and the search for therapeutics on Stargardt disease and macular degeneration.

References

Abe-Dohmae, S., Ikeda, Y., Matsuo, M., Hayashi, M., Okuhira, K., Ueda, K., and Yokoyama, S. (2004). Human ABCA7 supports apolipoprotein-mediated release of cellular cholesterol and phospholipid to generate high density lipoprotein. J Biol Chem *279*, 604-611.

Ablonczy, Z., Higbee, D., Grey, A. C., Koutalos, Y., Schey, K. L., and Crouch, R. K. (2013). Similar molecules spatially correlate with lipofuscin and N-retinylidene-N-retinylethanolamine in the mouse but not in the human retinal pigment epithelium. Arch Biochem Biophys.

Ahn, J., Beharry, S., Molday, L. L., and Molday, R. S. (2003). Functional interaction between the two halves of the photoreceptor-specific ATP binding cassette protein ABCR (ABCA4). Evidence for a non-exchangeable ADP in the first nucleotide binding domain. J Biol Chem *278*, 39600-39608.

Ahn, J., Wong, J. T., and Molday, R. S. (2000). The effect of lipid environment and retinoids on the ATPase activity of ABCR, the photoreceptor ABC transporter responsible for Stargardt macular dystrophy. J Biol Chem *275*, 20399-20405.

Akiyama, M., Sugiyama-Nakagiri, Y., Sakai, K., McMillan, J. R., Goto, M., Arita, K., Tsuji-Abe, Y., Tabata, N., Matsuoka, K., Sasaki, R.*, et al.* (2005). Mutations in lipid transporter ABCA12 in harlequin ichthyosis and functional recovery by corrective gene transfer. J Clin Invest *115*, 1777-1784.

Aller, S. G., Yu, J., Ward, A., Weng, Y., Chittaboina, S., Zhuo, R., Harrell, P. M., Trinh, Y. T., Zhang, Q., Urbatsch, I. L., and Chang, G. (2009). Structure of P-glycoprotein reveals a molecular basis for poly-specific drug binding. Science *323*, 1718-1722.

Allikmets, R. (2000). Simple and complex ABCR: genetic predisposition to retinal disease. Am J Hum Genet *67*, 793-799.

Allikmets, R., Singh, N., Sun, H., Shroyer, N. F., Hutchinson, A., Chidambaram, A., Gerrard, B., Baird, L., Stauffer, D., Peiffer, A.*, et al.* (1997). A photoreceptor cell-specific ATP-binding transporter gene (ABCR) is mutated in recessive Stargardt macular dystrophy. Nat Genet *15*, 236-246.

Ambudkar, S. V., Kim, I. W., Xia, D., and Sauna, Z. E. (2006). The A-loop, a novel conserved aromatic acid subdomain upstream of the Walker A motif in ABC transporters, is critical for ATP binding. FEBS Lett *580*, 1049-1055.

Atshaves, B. P., McIntosh, A. L., Payne, H. R., Gallegos, A. M., Landrock, K., Maeda, N., Kier, A. B., and Schroeder, F. (2007). SCP-2/SCP-x gene ablation alters lipid raft domains in primary cultured mouse hepatocytes. J Lipid Res *48*, 2193-2211.

Attie, A. D. (2007). ABCA1: at the nexus of cholesterol, HDL and atherosclerosis. Trends Biochem Sci *32*, 172-179.

Attie, A. D., Hamon, Y., Brooks-Wilson, A. R., Gray-Keller, M. P., MacDonald, M. L., Rigot, V., Tebon, A., Zhang, L. H., Mulligan, J. D., Singaraja, R. R.*, et al.* (2002). Identification and functional analysis of a naturally occurring E89K mutation in the ABCA1 gene of the WHAM chicken. J Lipid Res *43*, 1610-1617.

Baehr, W., Wu, S. M., Bird, A. C., and Palczewski, K. (2003). The retinoid cycle and retina disease. Vision Res *43*, 2957-2958.

Ban, N., Matsumura, Y., Sakai, H., Takanezawa, Y., Sasaki, M., Arai, H., and Inagaki, N. (2007). ABCA3 as a lipid transporter in pulmonary surfactant biogenesis. J Biol Chem *282*, 9628-9634.

Beharry, S., Zhong, M., and Molday, R. S. (2004). N-retinylidene-phosphatidylethanolamine is the preferred retinoid substrate for the photoreceptor-specific ABC transporter ABCA4 (ABCR). J Biol Chem *279*, 53972-53979.

Ben-Shabat, S., Parish, C. A., Vollmer, H. R., Itagaki, Y., Fishkin, N., Nakanishi, K., and Sparrow, J. R. (2002). Biosynthetic studies of A2E, a major fluorophore of retinal pigment epithelial lipofuscin. J Biol Chem *277*, 7183-7190.

Berdeaux, G. H., Nordmann, J. P., Colin, E., and Arnould, B. (2005). Vision-related quality of life in patients suffering from age-related macular degeneration. Am J Ophthalmol *139*, 271-279.

Bindewald, A., Bird, A. C., Dandekar, S. S., Dolar-Szczasny, J., Dreyhaupt, J., Fitzke, F. W., Einbock, W., Holz, F. G., Jorzik, J. J., Keilhauer, C.*, et al.* (2005). Classification of fundus autofluorescence patterns in early age-related macular disease. Invest Ophthalmol Vis Sci *46*, 3309-3314.

Biswas-Fiss, E. E., Affet, S., Ha, M., and Biswas, S. B. (2012). Retinoid binding properties of nucleotide binding domain 1 of the Stargardt disease-associated ATP binding cassette (ABC) transporter, ABCA4. J Biol Chem *287*, 44097-44107.

Biswas-Fiss, E. E., Kurpad, D. S., Joshi, K., and Biswas, S. B. (2010). Interaction of extracellular domain 2 of the human retina-specific ATP-binding cassette transporter (ABCA4) with all-trans-retinal. J Biol Chem *285*, 19372-19383.

Blakeley, L. R., Chen, C., Chen, C. K., Chen, J., Crouch, R. K., Travis, G. H., and Koutalos, Y. (2011). Rod outer segment retinol formation is independent of Abca4, arrestin, rhodopsin kinase, and rhodopsin palmitylation. Invest Ophthalmol Vis Sci *52*, 3483-3491.

Bodzioch, M., Orso, E., Klucken, J., Langmann, T., Bottcher, A., Diederich, W., Drobnik, W., Barlage, S., Buchler, C., Porsch-Ozcurumez, M.*, et al.* (1999). The gene encoding ATP-binding cassette transporter 1 is mutated in Tangier disease. Nat Genet *22*, 347-351.

Boesze-Battaglia, K., and Albert, A. D. (1989). Fatty acid composition of bovine rod outer segment plasma membrane. Exp Eye Res *49*, 699-701.

Bolte, S., and Cordelieres, F. P. (2006). A guided tour into subcellular colocalization analysis in light microscopy. J Microsc *224*, 213-232.

Borbat, P. P., Surendhran, K., Bortolus, M., Zou, P., Freed, J. H., and McHaourab, H. S. (2007). Conformational motion of the ABC transporter MsbA induced by ATP hydrolysis. PLoS Biol *5*, e271.

Borst, P., Zelcer, N., and van Helvoort, A. (2000). ABC transporters in lipid transport. Biochim Biophys Acta *1486*, 128-144.

Boyer, N. P., Higbee, D., Currin, M. B., Blakeley, L. R., Chen, C., Ablonczy, Z., Crouch, R. K., and Koutalos, Y. (2012). Lipofuscin and N-retinylidene-N-retinylethanolamine (A2E) accumulate in retinal pigment epithelium in absence of light exposure: their origin is 11-cis-retinal. J Biol Chem *287*, 22276-22286.

Brown, C. R., Hong-Brown, L. Q., Biwersi, J., Verkman, A. S., and Welch, W. J. (1996). Chemical chaperones correct the mutant phenotype of the delta F508 cystic fibrosis transmembrane conductance regulator protein. Cell Stress Chaperones *1*, 117-125.

Brunham, L. R., Singaraja, R. R., and Hayden, M. R. (2006). Variations on a gene: rare and common variants in ABCA1 and their impact on HDL cholesterol levels and atherosclerosis. Annu Rev Nutr *26*, 105-129.

Bui, T. V., Han, Y., Radu, R. A., Travis, G. H., and Mata, N. L. (2006). Characterization of native retinal fluorophores involved in biosynthesis of A2E and lipofuscin-associated retinopathies. J Biol Chem *281*, 18112-18119.

Bungert, S., Molday, L. L., and Molday, R. S. (2001). Membrane topology of the ATP binding cassette transporter ABCR and its relationship to ABC1 and related ABCA transporters: identification of N-linked glycosylation sites. J Biol Chem *276*, 23539-23546.

Chan, S. L., Kim, W. S., Kwok, J. B., Hill, A. F., Cappai, R., Rye, K. A., and Garner, B. (2008). ATP-binding cassette transporter A7 regulates processing of amyloid precursor protein in vitro. J Neurochem *106*, 793-804.

Charbel Issa, P., Barnard, A. R., Singh, M. S., Carter, E., Jiang, Z., Radu, R. A., Schraermeyer, U., and Maclaren, R. E. (2012). Fundus Autofluorescence in the Abca4-/- Mouse Model of Stargardt Disease - Correlation with Accumulation of A2E, Retinal Function and Histology. Invest Ophthalmol Vis Sci.

Chatelain, P., Meysmans, L., Matteazzi, J. R., Beaufort, P., and Clinet, M. (1995). Interaction of the antiarrhythmic agents SR 33589 and amiodarone with the beta-adrenoceptor and adenylate cyclase in rat heart. Br J Pharmacol *116*, 1949-1956.

Chen, C., Blakeley, L. R., and Koutalos, Y. (2009). Formation of all-trans retinol after visual pigment bleaching in mouse photoreceptors. Invest Ophthalmol Vis Sci *50*, 3589-3595.

Chen, J., Lu, G., Lin, J., Davidson, A. L., and Quiocho, F. A. (2003). A tweezers-like motion of the ATP-binding cassette dimer in an ABC transport cycle. Mol Cell *12*, 651-661.

Chrispell, J. D., Feathers, K. L., Kane, M. A., Kim, C. Y., Brooks, M., Khanna, R., Kurth, I., Hubner, C. A., Gal, A., Mears, A. J.*, et al.* (2009). Rdh12 activity and effects on retinoid processing in the murine retina. J Biol Chem *284*, 21468-21477.

Chroni, A., Liu, T., Fitzgerald, M. L., Freeman, M. W., and Zannis, V. I. (2004). Cross-linking and lipid efflux properties of apoA-I mutants suggest direct association between apoA-I helices and ABCA1. Biochemistry *43*, 2126-2139.

Chuang, J. Z., Zhao, Y., and Sung, C. H. (2007). SARA-regulated vesicular targeting underlies formation of the light-sensing organelle in mammalian rods. Cell *130*, 535-547.

Cideciyan, A. V., Aleman, T. S., Swider, M., Schwartz, S. B., Steinberg, J. D., Brucker, A. J., Maguire, A. M., Bennett, J., Stone, E. M., and Jacobson, S. G. (2004). Mutations in ABCA4 result in accumulation of lipofuscin before slowing of the retinoid cycle: a reappraisal of the human disease sequence. Hum Mol Genet *13*, 525-534.

Cideciyan, A. V., Swider, M., Aleman, T. S., Tsybovsky, Y., Schwartz, S. B., Windsor, E. A., Roman, A. J., Sumaroka, A., Steinberg, J. D., Jacobson, S. G.*, et al.* (2009). ABCA4 disease progression and a proposed strategy for gene therapy. Hum Mol Genet *18*, 931-941.

Clark, S. P., and Molday, R. S. (1979). Orientation of membrane glycoproteins in sealed rod outer segment disks. Biochemistry *18*, 5868-5873.

Coleman, J. A., Kwok, M. C., and Molday, R. S. (2009). Localization, purification, and functional reconstitution of the P4-ATPase Atp8a2, a phosphatidylserine flippase in photoreceptor disc membranes. J Biol Chem *284*, 32670-32679.

Coleman, J. A., and Molday, R. S. (2011). Critical role of the beta-subunit CDC50A in the stable expression, assembly, subcellular localization, and lipid transport activity of the P4-ATPase ATP8A2. J Biol Chem *286*, 17205-17216.

Coleman, J. A., Quazi, F., and Molday, R. S. (2013). Mammalian P4-ATPases and ABC transporters and their role in phospholipid transport. Biochim Biophys Acta *1831*, 555-574.

Cremers, F. P., van de Pol, D. J., van Driel, M., den Hollander, A. I., van Haren, F. J., Knoers, N. V., Tijmes, N., Bergen, A. A., Rohrschneider, K., Blankenagel, A.*, et al.* (1998). Autosomal recessive retinitis pigmentosa and cone-rod dystrophy caused by splice site mutations in the Stargardt's disease gene ABCR. Hum Mol Genet *7*, 355-362.

Davis, W., Jr. (2011). The ATP-binding cassette transporter-2 (ABCA2) regulates cholesterol homeostasis and low-density lipoprotein receptor metabolism in N2a neuroblastoma cells. Biochim Biophys Acta *1811*, 1152-1164.

Dawson, R. J., and Locher, K. P. (2006). Structure of a bacterial multidrug ABC transporter. Nature *443*, 180-185.

Dawson, R. J., and Locher, K. P. (2007). Structure of the multidrug ABC transporter Sav1866 from Staphylococcus aureus in complex with AMP-PNP. FEBS Lett *581*, 935-938.

de Vree, J. M., Jacquemin, E., Sturm, E., Cresteil, D., Bosma, P. J., Aten, J., Deleuze, J. F., Desrochers, M., Burdelski, M., Bernard, O.*, et al.* (1998). Mutations in the MDR3 gene cause progressive familial intrahepatic cholestasis. Proc Natl Acad Sci U S A *95*, 282-287.

Dean, M., and Allikmets, R. (1995). Evolution of ATP-binding cassette transporter genes. Curr Opin Genet Dev *5*, 779-785.

Deane, R., Wu, Z., Sagare, A., Davis, J., Du Yan, S., Hamm, K., Xu, F., Parisi, M., LaRue, B., Hu, H. W.*, et al.* (2004). LRP/amyloid beta-peptide interaction mediates differential brain efflux of Abeta isoforms. Neuron *43*, 333-344.

Delori, F. C., Staurenghi, G., Arend, O., Dorey, C. K., Goger, D. G., and Weiter, J. J. (1995). In vivo measurement of lipofuscin in Stargardt's disease--Fundus flavimaculatus. Invest Ophthalmol Vis Sci *36*, 2327-2331.

Denis, M., Haidar, B., Marcil, M., Bouvier, M., Krimbou, L., and Genest, J., Jr. (2004). Molecular and cellular physiology of apolipoprotein A-I lipidation by the ATP-binding cassette transporter A1 (ABCA1). J Biol Chem *279*, 7384-7394.

Duricka, D. L., Brown, R. L., and Varnum, M. D. (2012). Defective trafficking of cone photoreceptor CNG channels induces the unfolded protein response and ER-stress-associated cell death. Biochem J *441*, 685-696.

Einbock, W., Moessner, A., Schnurrbusch, U. E., Holz, F. G., and Wolf, S. (2005). Changes in fundus autofluorescence in patients with age-related maculopathy. Correlation to visual function: a prospective study. Graefes Arch Clin Exp Ophthalmol *243*, 300-305.

Fetsch, E. E., and Davidson, A. L. (2002). Vanadate-catalyzed photocleavage of the signature motif of an ATP-binding cassette (ABC) transporter. Proc Natl Acad Sci U S A *99*, 9685-9690.

Fielding, P. E., Nagao, K., Hakamata, H., Chimini, G., and Fielding, C. J. (2000). A two-step mechanism for free cholesterol and phospholipid efflux from human vascular cells to apolipoprotein A-1. Biochemistry *39*, 14113-14120.

Fisher, G. A., Lum, B. L., Hausdorff, J., and Sikic, B. I. (1996). Pharmacological considerations in the modulation of multidrug resistance. Eur J Cancer *32A*, 1082-1088.

Fishkin, N. E., Sparrow, J. R., Allikmets, R., and Nakanishi, K. (2005). Isolation and characterization of a retinal pigment epithelial cell fluorophore: an all-trans-retinal dimer conjugate. Proc Natl Acad Sci U S A *102*, 7091-7096.

Fishman, G. A., Farbman, J. S., and Alexander, K. R. (1991). Delayed rod dark adaptation in patients with Stargardt's disease. Ophthalmology *98*, 957-962.

Fishman, G. A., Stone, E. M., Grover, S., Derlacki, D. J., Haines, H. L., and Hockey, R. R. (1999). Variation of clinical expression in patients with Stargardt dystrophy and sequence variations in the ABCR gene. Arch Ophthalmol *117*, 504-510.

Fitzgerald, M. L., Morris, A. L., Chroni, A., Mendez, A. J., Zannis, V. I., and Freeman, M. W. (2004). ABCA1 and amphipathic apolipoproteins form high-affinity molecular complexes required for cholesterol efflux. J Lipid Res *45*, 287-294.

Fitzgerald, M. L., Morris, A. L., Rhee, J. S., Andersson, L. P., Mendez, A. J., and Freeman, M. W. (2002). Naturally occurring mutations in the largest extracellular loops of ABCA1 can disrupt its direct interaction with apolipoprotein A-I. J Biol Chem *277*, 33178-33187.

Folch, J., Lees, M., and Sloane Stanley, G. H. (1957). A simple method for the isolation and purification of total lipides from animal tissues. J Biol Chem *226*, 497-509.

Forrester, J. V., Dick, A.D., McMenamin, P.G. Lee, W.R. (2002). The Eye: Basic Sciences in Practice: WB Saunders).

Frederiksen, R., Boyer, N. P., Nickle, B., Chakrabarti, K. S., Koutalos, Y., Crouch, R. K., Oprian, D., and Cornwall, M. C. (2012). Low aqueous solubility of 11-cis-retinal limits the rate of pigment formation and dark adaptation in salamander rods. J Gen Physiol *139*, 493-505.

Friedman, D. S., O'Colmain, B. J., Munoz, B., Tomany, S. C., McCarty, C., de Jong, P. T., Nemesure, B., Mitchell, P., and Kempen, J. (2004). Prevalence of age-related macular degeneration in the United States. Arch Ophthalmol *122*, 564-572.

Garwin, G. G., and Saari, J. C. (2000). High-performance liquid chromatography analysis of visual cycle retinoids. Methods Enzymol *316*, 313-324.

Gautherot, J., Durand-Schneider, A. M., Delautier, D., Delaunay, J. L., Rada, A., Gabillet, J., Housset, C., Maurice, M., and Ait-Slimane, T. (2012). Effects of cellular, chemical, and pharmacological chaperones on the rescue of a trafficking-defective mutant of the ATP-binding cassette transporter proteins ABCB1/ABCB4. J Biol Chem *287*, 5070-5078.

Gautier, P., Guillemare, E., Marion, A., Bertrand, J. P., Tourneur, Y., and Nisato, D. (2003). Electrophysiologic characterization of dronedarone in guinea pig ventricular cells. J Cardiovasc Pharmacol *41*, 191-202.

Gelisken, O., and De Laey, J. J. (1985). A clinical review of Stargardt's disease and/or fundus flavimaculatus with follow-up. Int Ophthalmol *8*, 225-235.

Genead, M. A., Fishman, G. A., Stone, E. M., and Allikmets, R. (2009). The natural history of stargardt disease with specific sequence mutation in the ABCA4 gene. Invest Ophthalmol Vis Sci *50*, 5867-5871.

Gold, B., Merriam, J. E., Zernant, J., Hancox, L. S., Taiber, A. J., Gehrs, K., Cramer, K., Neel, J., Bergeron, J., Barile, G. R.*, et al.* (2006). Variation in factor B (BF) and complement component 2 (C2) genes is associated with age-related macular degeneration. Nat Genet *38*, 458-462.

Gorczyca, W. A., Polans, A. S., Surgucheva, I. G., Subbaraya, I., Baehr, W., and Palczewski, K. (1995). Guanylyl cyclase activating protein. A calcium-sensitive regulator of phototransduction. J Biol Chem *270*, 22029-22036.

Grey, A. C., Crouch, R. K., Koutalos, Y., Schey, K. L., and Ablonczy, Z. (2011). Spatial localization of A2E in the retinal pigment epithelium. Invest Ophthalmol Vis Sci *52*, 3926-3933.

Groenendijk, G. W., Jacobs, C. W., Bonting, S. L., and Daemen, F. J. (1980). Dark isomerization of retinals in the presence of phosphatidylethanolamine. Eur J Biochem *106*, 119-128.

Hageman, G. S., Anderson, D. H., Johnson, L. V., Hancox, L. S., Taiber, A. J., Hardisty, L. I., Hageman, J. L., Stockman, H. A., Borchardt, J. D., Gehrs, K. M.*, et al.* (2005). A common haplotype in the complement regulatory gene factor H (HF1/CFH) predisposes individuals to age-related macular degeneration. Proc Natl Acad Sci U S A *102*, 7227-7232.

Haim, M. (2002). Epidemiology of retinitis pigmentosa in Denmark. Acta Ophthalmol Scand Suppl, 1-34.

Hamel, C. P. (2007). Cone rod dystrophies. Orphanet J Rare Dis *2*, 7.

Hamon, Y., Broccardo, C., Chambenoit, O., Luciani, M. F., Toti, F., Chaslin, S., Freyssinet, J. M., Devaux, P. F., McNeish, J., Marguet, D., and Chimini, G. (2000). ABC1 promotes engulfment of apoptotic cells and transbilayer redistribution of phosphatidylserine. Nat Cell Biol *2*, 399-406.

He, X., Lobsiger, J., and Stocker, A. (2009). Bothnia dystrophy is caused by domino-like rearrangements in cellular retinaldehyde-binding protein mutant R234W. Proc Natl Acad Sci U S A *106*, 18545-18550.

Heck, M., Schadel, S. A., Maretzki, D., Bartl, F. J., Ritter, E., Palczewski, K., and Hofmann, K. P. (2003). Signaling states of rhodopsin. Formation of the storage form, metarhodopsin III, from active metarhodopsin II. J Biol Chem *278*, 3162-3169.

Herget, M., Kreissig, N., Kolbe, C., Scholz, C., Tampe, R., and Abele, R. (2009). Purification and reconstitution of the antigen transport complex TAP: a prerequisite for determination of peptide stoichiometry and ATP hydrolysis. J Biol Chem *284*, 33740-33749.

Hessel, E., Muller, P., Herrmann, A., and Hofmann, K. P. (2001). Light-induced reorganization of phospholipids in rod disc membranes. J Biol Chem *276*, 2538-2543.

Higgins, C. F. (1992). ABC transporters: from microorganisms to man. Annu Rev Cell Biol *8*, 67-113.

Higgins, C. F., and Linton, K. J. (2004). The ATP switch model for ABC transporters. Nat Struct Mol Biol *11*, 918-926.

Hohl, M., Briand, C., Grutter, M. G., and Seeger, M. A. (2012). Crystal structure of a heterodimeric ABC transporter in its inward-facing conformation. Nat Struct Mol Biol *19*, 395-402.

Hollenstein, K., Frei, D. C., and Locher, K. P. (2007). Structure of an ABC transporter in complex with its binding protein. Nature *446*, 213-216.

Hollingsworth, T. J., and Gross, A. K. (2012). Defective trafficking of rhodopsin and its role in retinal degenerations. Int Rev Cell Mol Biol *293*, 1-44.

Hollyfield, J. G. (1999). Hyaluronan and the functional organization of the interphotoreceptor matrix. Invest Ophthalmol Vis Sci *40*, 2767-2769.

Hozoji, M., Kimura, Y., Kioka, N., and Ueda, K. (2009). Formation of two intramolecular disulfide bonds is necessary for ApoA-I-dependent cholesterol efflux mediated by ABCA1. J Biol Chem *284*, 11293-11300.

Humphries, M. M., Rancourt, D., Farrar, G. J., Kenna, P., Hazel, M., Bush, R. A., Sieving, P. A., Sheils, D. M., McNally, N., Creighton, P.*, et al.* (1997). Retinopathy induced in mice by targeted disruption of the rhodopsin gene. Nat Genet *15*, 216-219.

Iatan, I., Bailey, D., Ruel, I., Hafiane, A., Campbell, S., Krimbou, L., and Genest, J. (2011). Membrane microdomains modulate oligomeric ABCA1 function: impact on apoAI-mediated lipid removal and phosphatidylcholine biosynthesis. J Lipid Res *52*, 2043-2055.

Illing, M., Molday, L. L., and Molday, R. S. (1997). The 220-kDa rim protein of retinal rod outer segments is a member of the ABC transporter superfamily. J Biol Chem *272*, 10303-10310.

Iram, S. H., and Cole, S. P. (2012). Mutation of Glu521 or Glu535 in cytoplasmic loop 5 causes differential misfolding in multiple domains of multidrug and organic anion transporter MRP1 (ABCC1). J Biol Chem *287*, 7543-7555.

Ishiguro, S., Suzuki, Y., Tamai, M., and Mizuno, K. (1991). Purification of retinol dehydrogenase from bovine retinal rod outer segments. J Biol Chem *266*, 15520-15524.

Iwamoto, N., Abe-Dohmae, S., Sato, R., and Yokoyama, S. (2006). ABCA7 expression is regulated by cellular cholesterol through the SREBP2 pathway and associated with phagocytosis. J Lipid Res *47*, 1915-1927.

Janecke, A. R., Thompson, D. A., Utermann, G., Becker, C., Hubner, C. A., Schmid, E., McHenry, C. L., Nair, A. R., Ruschendorf, F., Heckenlively, J.*, et al.* (2004). Mutations in RDH12 encoding a photoreceptor cell retinol dehydrogenase cause childhood-onset severe retinal dystrophy. Nat Genet *36*, 850-854.

Jang, G. F., Van Hooser, J. P., Kuksa, V., McBee, J. K., He, Y. G., Janssen, J. J., Driessen, C. A., and Palczewski, K. (2001). Characterization of a dehydrogenase activity responsible for oxidation of 11-cis-retinol in the retinal pigment epithelium of mice with a disrupted RDH5 gene. A model for the human hereditary disease fundus albipunctatus. J Biol Chem *276*, 32456-32465.

Jardetzky, O. (1966). Simple allosteric model for membrane pumps. Nature *211*, 969-970.

Jehle, A. W., Gardai, S. J., Li, S., Linsel-Nitschke, P., Morimoto, K., Janssen, W. J., Vandivier, R. W., Wang, N., Greenberg, S., Dale, B. M.*, et al.* (2006). ATP-binding cassette transporter A7 enhances phagocytosis of apoptotic cells and associated ERK signaling in macrophages. J Cell Biol *174*, 547-556.

Jin, M., Li, S., Moghrabi, W. N., Sun, H., and Travis, G. H. (2005). Rpe65 is the retinoid isomerase in bovine retinal pigment epithelium. Cell *122*, 449-459.

Jin, M., Li, S., Nusinowitz, S., Lloyd, M., Hu, J., Radu, R. A., Bok, D., and Travis, G. H. (2009). The role of interphotoreceptor retinoid-binding protein on the translocation of visual retinoids and function of cone photoreceptors. J Neurosci *29*, 1486-1495.

Jones, P. M., and George, A. M. (2004). The ABC transporter structure and mechanism: perspectives on recent research. Cell Mol Life Sci *61*, 682-699.

Jones, P. M., O'Mara, M. L., and George, A. M. (2009). ABC transporters: a riddle wrapped in a mystery inside an enigma. Trends Biochem Sci *34*, 520-531.

Kajiwara, K., Berson, E. L., and Dryja, T. P. (1994). Digenic retinitis pigmentosa due to mutations at the unlinked peripherin/RDS and ROM1 loci. Science *264*, 1604-1608.

Kakumoto, M., Takara, K., Sakaeda, T., Tanigawara, Y., Kita, T., and Okumura, K. (2002). MDR1-mediated interaction of digoxin with antiarrhythmic or antianginal drugs. Biol Pharm Bull *25*, 1604-1607.

Kaminski, W. E., Orso, E., Diederich, W., Klucken, J., Drobnik, W., and Schmitz, G. (2000). Identification of a novel human sterol-sensitive ATP-binding cassette transporter (ABCA7). Biochem Biophys Res Commun *273*, 532-538.

Kang, J., Hwang, J. U., Lee, M., Kim, Y. Y., Assmann, S. M., Martinoia, E., and Lee, Y. (2010). PDR-type ABC transporter mediates cellular uptake of the phytohormone abscisic acid. Proc Natl Acad Sci U S A *107*, 2355-2360.

Kang, M. J., and Ryoo, H. D. (2009). Suppression of retinal degeneration in Drosophila by stimulation of ER-associated degradation. Proc Natl Acad Sci U S A *106*, 17043-17048.

Karan, G., Yang, Z., Howes, K., Zhao, Y., Chen, Y., Cameron, D. J., Lin, Y., Pearson, E., and Zhang, K. (2005). Loss of ER retention and sequestration of the wild-type ELOVL4 by Stargardt disease dominant negative mutants. Mol Vis *11*, 657-664.

Kathofer, S., Thomas, D., and Karle, C. A. (2005). The novel antiarrhythmic drug dronedarone: comparison with amiodarone. Cardiovasc Drug Rev *23*, 217-230.

Katoh, M., Nakajima, M., Yamazaki, H., and Yokoi, T. (2001). Inhibitory effects of CYP3A4 substrates and their metabolites on P-glycoprotein-mediated transport. Eur J Pharm Sci *12*, 505-513.

Kim, S. R., Fishkin, N., Kong, J., Nakanishi, K., Allikmets, R., and Sparrow, J. R. (2004). Rpe65 Leu450Met variant is associated with reduced levels of the retinal pigment epithelium lipofuscin fluorophores A2E and iso-A2E. Proc Natl Acad Sci U S A *101*, 11668-11672.

Kim, S. R., Jang, Y. P., Jockusch, S., Fishkin, N. E., Turro, N. J., and Sparrow, J. R. (2007). The all-trans-retinal dimer series of lipofuscin pigments in retinal pigment epithelial cells in a recessive Stargardt disease model. Proc Natl Acad Sci U S A *104*, 19273-19278.

Kim, T. S., Reid, D. M., and Molday, R. S. (1998). Structure-function relationships and localization of the Na/Ca-K exchanger in rod photoreceptors. J Biol Chem *273*, 16561-16567.

Kim, W. S., Guillemin, G. J., Glaros, E. N., Lim, C. K., and Garner, B. (2006). Quantitation of ATP-binding cassette subfamily-A transporter gene expression in primary human brain cells. Neuroreport *17*, 891-896.

Knorre, D. A., Krivonosova, T. N., Markova, O. V., and Severin, F. F. (2009). Amiodarone inhibits multiple drug resistance in yeast Saccharomyces cerevisiae. Arch Microbiol *191*, 675-679.

Kobayashi, A., Takanezawa, Y., Hirata, T., Shimizu, Y., Misasa, K., Kioka, N., Arai, H., Ueda, K., and Matsuo, M. (2006). Efflux of sphingomyelin, cholesterol, and phosphatidylcholine by ABCG1. J Lipid Res *47*, 1791-1802.

Krimbou, L., Hajj Hassan, H., Blain, S., Rashid, S., Denis, M., Marcil, M., and Genest, J. (2005). Biogenesis and speciation of nascent apoA-I-containing particles in various cell lines. J Lipid Res *46*, 1668-1677.

Kuromori, T., Miyaji, T., Yabuuchi, H., Shimizu, H., Sugimoto, E., Kamiya, A., Moriyama, Y., and Shinozaki, K. (2010). ABC transporter AtABCG25 is involved in abscisic acid transport and responses. Proc Natl Acad Sci U S A *107*, 2361-2366.

Kwok, M. C., Holopainen, J. M., Molday, L. L., Foster, L. J., and Molday, R. S. (2008). Proteomics of photoreceptor outer segments identifies a subset of SNARE and Rab proteins implicated in membrane vesicle trafficking and fusion. Mol Cell Proteomics *7*, 1053-1066.

Lakowicz, J. R. (1980). Fluorescence spectroscopic investigations of the dynamic properties of proteins, membranes and nucleic acids. J Biochem Biophys Methods *2*, 91-119.

Lalevee, N., Nargeot, J., Barrere-Lemaire, S., Gautier, P., and Richard, S. (2003). Effects of amiodarone and dronedarone on voltage-dependent sodium current in human cardiomyocytes. J Cardiovasc Electrophysiol *14*, 885-890.

Lamb, T. D., and Pugh, E. N., Jr. (2004). Dark adaptation and the retinoid cycle of vision. Prog Retin Eye Res *23*, 307-380.

LaVail, M. M. (1980). Circadian nature of rod outer segment disc shedding in the rat. Invest Ophthalmol Vis Sci *19*, 407-411.

Lefevre, C., Audebert, S., Jobard, F., Bouadjar, B., Lakhdar, H., Boughdene-Stambouli, O., Blanchet-Bardon, C., Heilig, R., Foglio, M., Weissenbach, J.*, et al.* (2003). Mutations in the transporter ABCA12 are associated with lamellar ichthyosis type 2. Hum Mol Genet *12*, 2369-2378.

Lewis, R. A., Shroyer, N. F., Singh, N., Allikmets, R., Hutchinson, A., Li, Y., Lupski, J. R., Leppert, M., and Dean, M. (1999). Genotype/Phenotype analysis of a photoreceptor-specific ATP-binding cassette transporter gene, ABCR, in Stargardt disease. Am J Hum Genet *64*, 422-434.

Linsel-Nitschke, P., Jehle, A. W., Shan, J., Cao, G., Bacic, D., Lan, D., Wang, N., and Tall, A. R. (2005). Potential role of ABCA7 in cellular lipid efflux to apoA-I. J Lipid Res *46*, 86-92.

Liu, J., Itagaki, Y., Ben-Shabat, S., Nakanishi, K., and Sparrow, J. R. (2000). The biosynthesis of A2E, a fluorophore of aging retina, involves the formation of the precursor, A2-PE, in the photoreceptor outer segment membrane. J Biol Chem *275*, 29354-29360.

Liu, T., Jenwitheesuk, E., Teller, D. C., and Samudrala, R. (2005). Structural insights into the cellular retinaldehyde-binding protein (CRALBP). Proteins *61*, 412-422.

Loewen, C. J., Molday, R. S., and Molday, L. L. (2004). Role of subunit assembly in autosomal dominant retinitis pigmentosa linked to mutations in peripherin 2. Novartis Found Symp *255*, 95-112; discussion 113-116, 177-118.

Loo, T. W., Bartlett, M. C., and Clarke, D. M. (2003). Simultaneous binding of two different drugs in the binding pocket of the human multidrug resistance P-glycoprotein. J Biol Chem *278*, 39706-39710.

Lorenz, B., Wabbels, B., Wegscheider, E., Hamel, C. P., Drexler, W., and Preising, M. N. (2004). Lack of fundus autofluorescence to 488 nanometers from childhood on in patients with early-onset severe retinal dystrophy associated with mutations in RPE65. Ophthalmology *111*, 1585-1594.

MacKenzie, D., Arendt, A., Hargrave, P., McDowell, J. H., and Molday, R. S. (1984). Localization of binding sites for carboxyl terminal specific anti-rhodopsin monoclonal antibodies using synthetic peptides. Biochemistry *23*, 6544-6549.

Maeda, A., Golczak, M., Chen, Y., Okano, K., Kohno, H., Shiose, S., Ishikawa, K., Harte, W., Palczewska, G., Maeda, T., and Palczewski, K. (2011). Primary amines protect against retinal degeneration in mouse models of retinopathies. Nat Chem Biol *8*, 170-178.

Maeda, A., Golczak, M., Maeda, T., and Palczewski, K. (2009a). Limited roles of Rdh8, Rdh12, and Abca4 in all-trans-retinal clearance in mouse retina. Invest Ophthalmol Vis Sci *50*, 5435-5443.

Maeda, A., Maeda, T., Golczak, M., Chou, S., Desai, A., Hoppel, C. L., Matsuyama, S., and Palczewski, K. (2009b). Involvement of all-trans-retinal in acute light-induced retinopathy of mice. J Biol Chem *284*, 15173-15183.

Maeda, A., Maeda, T., Golczak, M., and Palczewski, K. (2008). Retinopathy in mice induced by disrupted all-trans-retinal clearance. J Biol Chem *283*, 26684-26693.

Maeda, A., Maeda, T., Imanishi, Y., Sun, W., Jastrzebska, B., Hatala, D. A., Winkens, H. J., Hofmann, K. P., Janssen, J. J., Baehr, W.*, et al.* (2006). Retinol dehydrogenase (RDH12) protects photoreceptors from light-induced degeneration in mice. J Biol Chem *281*, 37697-37704.

Maeda, A., Maeda, T., Sun, W., Zhang, H., Baehr, W., and Palczewski, K. (2007). Redundant and unique roles of retinol dehydrogenases in the mouse retina. Proc Natl Acad Sci U S A *104*, 19565-19570.

Martinez-Mir, A., Paloma, E., Allikmets, R., Ayuso, C., del Rio, T., Dean, M., Vilageliu, L., Gonzalez-Duarte, R., and Balcells, S. (1998). Retinitis pigmentosa caused by a homozygous mutation in the Stargardt disease gene ABCR. Nat Genet *18*, 11-12.

Mata, N. L., Tzekov, R. T., Liu, X., Weng, J., Birch, D. G., and Travis, G. H. (2001). Delayed dark-adaptation and lipofuscin accumulation in abcr+/- mice: implications for involvement of ABCR in age-related macular degeneration. Invest Ophthalmol Vis Sci *42*, 1685-1690.

Mata, N. L., Weng, J., and Travis, G. H. (2000). Biosynthesis of a major lipofuscin fluorophore in mice and humans with ABCR-mediated retinal and macular degeneration. Proc Natl Acad Sci U S A *97*, 7154-7159.

Maugeri, A., Klevering, B. J., Rohrschneider, K., Blankenagel, A., Brunner, H. G., Deutman, A. F., Hoyng, C. B., and Cremers, F. P. (2000). Mutations in the ABCA4 (ABCR) gene are the major cause of autosomal recessive cone-rod dystrophy. Am J Hum Genet *67*, 960-966.

Maugeri, A., van Driel, M. A., van de Pol, D. J., Klevering, B. J., van Haren, F. J., Tijmes, N., Bergen, A. A., Rohrschneider, K., Blankenagel, A., Pinckers, A. J.*, et al.* (1999). The 2588G-->C mutation in the ABCR gene is a mild frequent founder mutation in the Western European population and allows the classification of ABCR mutations in patients with Stargardt disease. Am J Hum Genet *64*, 1024-1035.

McBee, J. K., Palczewski, K., Baehr, W., and Pepperberg, D. R. (2001). Confronting complexity: the interlink of phototransduction and retinoid metabolism in the vertebrate retina. Prog Retin Eye Res *20*, 469-529.

McIlwain, J. T. (1996). Introduction to the Biology of Vision (Cambridge, UK: Cambridge University Press).

McIntyre, J. C., and Sleight, R. G. (1991). Fluorescence assay for phospholipid membrane asymmetry. Biochemistry *30*, 11819-11827.

Mcllwain, J. T. (1996). Introduction to the Biology of Vision (Cambridge: Cambridge University Press).

Mendes, H. F., and Cheetham, M. E. (2008). Pharmacological manipulation of gain-of-function and dominant-negative mechanisms in rhodopsin retinitis pigmentosa. Hum Mol Genet *17*, 3043-3054.

Mendes, H. F., van der Spuy, J., Chapple, J. P., and Cheetham, M. E. (2005). Mechanisms of cell death in rhodopsin retinitis pigmentosa: implications for therapy. Trends Mol Med *11*, 177-185.

Mendez, A., Burns, M. E., Roca, A., Lem, J., Wu, L. W., Simon, M. I., Baylor, D. A., and Chen, J. (2000). Rapid and reproducible deactivation of rhodopsin requires multiple phosphorylation sites. Neuron *28*, 153-164.

Menon, I., Huber, T., Sanyal, S., Banerjee, S., Barre, P., Canis, S., Warren, J. D., Hwa, J., Sakmar, T. P., and Menon, A. K. (2011). Opsin is a phospholipid flippase. Curr Biol *21*, 149-153.

Merbs, S. L., and Nathans, J. (1992). Absorption spectra of the hybrid pigments responsible for anomalous color vision. Science *258*, 464-466.

Michaelides, M., Hunt, D. M., and Moore, A. T. (2003). The genetics of inherited macular dystrophies. J Med Genet *40*, 641-650.

Miljanich, G. P., Sklar, L. A., White, D. L., and Dratz, E. A. (1979). Disaturated and dipolyunsaturated phospholipids in the bovine retinal rod outer segment disk membrane. Biochim Biophys Acta *552*, 294-306.

Mizutani, T., Masuda, M., Nakai, E., Furumiya, K., Togawa, H., Nakamura, Y., Kawai, Y., Nakahira, K., Shinkai, S., and Takahashi, K. (2008). Genuine functions of P-glycoprotein (ABCB1). Curr Drug Metab *9*, 167-174.

Moiseyev, G., Takahashi, Y., Chen, Y., Gentleman, S., Redmond, T. M., Crouch, R. K., and Ma, J. X. (2006). RPE65 is an iron(II)-dependent isomerohydrolase in the retinoid visual cycle. J Biol Chem *281*, 2835-2840.

Molday, R. S. (1998). Photoreceptor membrane proteins, phototransduction, and retinal degenerative diseases. The Friedenwald Lecture. Invest Ophthalmol Vis Sci *39*, 2491-2513.

Molday, R. S., and Molday, L. L. (1987). Differences in the protein composition of bovine retinal rod outer segment disk and plasma membranes isolated by a ricin-gold-dextran density perturbation method. J Cell Biol *105*, 2589-2601.

Moritz, O. L., and Tam, B. M. (2010). Recent insights into the mechanisms underlying light-dependent retinal degeneration from X. laevis models of retinitis pigmentosa. Adv Exp Med Biol *664*, 509-515.

Mulligan, J. D., Flowers, M. T., Tebon, A., Bitgood, J. J., Wellington, C., Hayden, M. R., and Attie, A. D. (2003). ABCA1 is essential for efficient basolateral cholesterol efflux during the absorption of dietary cholesterol in chickens. J Biol Chem *278*, 13356-13366.

Nagao, K., Kimura, Y., and Ueda, K. (2011). Lysine residues of ABCA1 are required for the interaction with apoA-I. Biochim Biophys Acta *1821*, 530-535.

Nagao, K., Zhao, Y., Takahashi, K., Kimura, Y., and Ueda, K. (2009). Sodium taurocholate-dependent lipid efflux by ABCA1: effects of W590S mutation on lipid translocation and apolipoprotein A-I dissociation. J Lipid Res *50*, 1165-1172.

Nagata, K. O., Nakada, C., Kasai, R. S., Kusumi, A., and Ueda, K. (2012). ABCA1 dimer-monomer interconversion during HDL generation revealed by single-molecule imaging. Proc Natl Acad Sci U S A *110*, 5034-5039.

Nagata, K. O., Nakada, C., Kasai, R. S., Kusumi, A., and Ueda, K. (2013). ABCA1 dimer-monomer interconversion during HDL generation revealed by single-molecule imaging. Proc Natl Acad Sci U S A *110*, 5034-5039.

Nakatani, K., and Yau, K. W. (1988). Calcium and magnesium fluxes across the plasma membrane of the toad rod outer segment. J Physiol *395*, 695-729.

Nathans, J., Thomas, D., and Hogness, D. S. (1986). Molecular genetics of human color vision: the genes encoding blue, green, and red pigments. Science *232*, 193-202.

Noorwez, S. M., Ostrov, D. A., McDowell, J. H., Krebs, M. P., and Kaushal, S. (2008). A high-throughput screening method for small-molecule pharmacologic chaperones of misfolded rhodopsin. Invest Ophthalmol Vis Sci *49*, 3224-3230.

Noy, N., and Xu, Z. J. (1990). Kinetic parameters of the interactions of retinol with lipid bilayers. Biochemistry *29*, 3883-3888.

Oancea, G., O'Mara, M. L., Bennett, W. F., Tieleman, D. P., Abele, R., and Tampe, R. (2009). Structural arrangement of the transmission interface in the antigen ABC transport complex TAP. Proc Natl Acad Sci U S A *106*, 5551-5556.

Oram, J. F. (2002). ATP-binding cassette transporter A1 and cholesterol trafficking. Curr Opin Lipidol *13*, 373-381.

Osterberg, G. (1935). Topography of the layer of rods and cones in the human retina. Acta Ophthalmol *6*.

Palczewski, K. (1994). Is vertebrate phototransduction solved? New insights into the molecular mechanism of phototransduction. Invest Ophthalmol Vis Sci *35*, 3577-3581.

Palczewski, K. (2006). G protein-coupled receptor rhodopsin. Annu Rev Biochem *75*, 743-767.

Palczewski, K., Jager, S., Buczylko, J., Crouch, R. K., Bredberg, D. L., Hofmann, K. P., Asson-Batres, M. A., and Saari, J. C. (1994). Rod outer segment retinol dehydrogenase: substrate specificity and role in phototransduction. Biochemistry *33*, 13741-13750.

Papermaster, D. S., and Dreyer, W. J. (1974). Rhodopsin content in the outer segment membranes of bovine and frog retinal rods. Biochemistry *13*, 2438-2444.

Papp, E., and Csermely, P. (2006). Chemical chaperones: mechanisms of action and potential use. Handb Exp Pharmacol, 405-416.

Patel, C., Yan, G. X., and Kowey, P. R. (2009). Dronedarone. Circulation *120*, 636-644.

Pedemonte, N., Lukacs, G. L., Du, K., Caci, E., Zegarra-Moran, O., Galietta, L. J., and Verkman, A. S. (2005). Small-molecule correctors of defective DeltaF508-CFTR cellular processing identified by high-throughput screening. J Clin Invest *115*, 2564-2571.

Pepperberg, D. R., Okajima, T. L., Wiggert, B., Ripps, H., Crouch, R. K., and Chader, G. J. (1993). Interphotoreceptor retinoid-binding protein (IRBP). Molecular biology and physiological role in the visual cycle of rhodopsin. Mol Neurobiol *7*, 61-85.

Plack, P. A., and Pritchard, D. J. (1969). Schiff bases formed from retinal and phosphatidylethanolamine, phosphatidylserine, ethanolamine or serine. Biochem J *115*, 927-934.

Pugh, E. N., Jr., and Lamb, T. D. (1993). Amplification and kinetics of the activation steps in phototransduction. Biochim Biophys Acta *1141*, 111-149.

Quazi, F., Lenevich, S., and Molday, R. S. (2012). ABCA4 is an N-retinylidene-phosphatidylethanolamine and phosphatidylethanolamine importer. Nat Commun *3*, 925.

Radu, R. A., Yuan, Q., Hu, J., Peng, J. H., Lloyd, M., Nusinowitz, S., Bok, D., and Travis, G. H. (2008). Accelerated accumulation of lipofuscin pigments in the RPE of a mouse model for ABCA4-mediated retinal dystrophies following Vitamin A supplementation. Invest Ophthalmol Vis Sci *49*, 3821-3829.

Raggers, R. J., van Helvoort, A., Evers, R., and van Meer, G. (1999). The human multidrug resistance protein MRP1 translocates sphingolipid analogs across the plasma membrane. J Cell Sci *112 (Pt 3)*, 415-422.

Rajasekharan, A., Francis, V. G., and Gummadi, S. (2013). Biochemical evidence for energy-independent flippase activity in bovine epididymal sperm membranes: an insight into membrane biogenesis. Reproduction.

Rando, R. R., and Bangerter, F. W. (1982). The rapid intermembraneous transfer of retinoids. Biochem Biophys Res Commun *104*, 430-436.

Rattner, A., Smallwood, P. M., and Nathans, J. (2000). Identification and characterization of all-trans-retinol dehydrogenase from photoreceptor outer segments, the visual cycle enzyme that reduces all-trans-retinal to all-trans-retinol. J Biol Chem *275*, 11034-11043.

Reboul, E., Dyka, F. M., Quazi, F., and Molday, R. S. (2013). Cholesterol transport via ABCA1: new insights from solid-phase binding assay. Biochimie *95*, 957-961.

Riordan, J. R. (2008). CFTR function and prospects for therapy. Annu Rev Biochem *77*, 701-726.

Rivera, A., White, K., Stohr, H., Steiner, K., Hemmrich, N., Grimm, T., Jurklies, B., Lorenz, B., Scholl, H. P., Apfelstedt-Sylla, E., and Weber, B. H. (2000). A comprehensive survey of sequence variation in the ABCA4 (ABCR) gene in Stargardt disease and age-related macular degeneration. Am J Hum Genet *67*, 800-813.

Rodieck, R. W. (1998). The First Steps in Seeing (Sunderland, Massachusetts, USA.: Sinauer Associates, Inc).

Rohrer, B., Lohr, H. R., Humphries, P., Redmond, T. M., Seeliger, M. W., and Crouch, R. K. (2005). Cone opsin mislocalization in Rpe65-/- mice: a defect that can be corrected by 11-cis retinal. Invest Ophthalmol Vis Sci *46*, 3876-3882.

Romsicki, Y., and Sharom, F. J. (2001). Phospholipid flippase activity of the reconstituted P-glycoprotein multidrug transporter. Biochemistry *40*, 6937-6947.

Roof, D. J., Adamian, M., and Hayes, A. (1994). Rhodopsin accumulation at abnormal sites in retinas of mice with a human P23H rhodopsin transgene. Invest Ophthalmol Vis Sci *35*, 4049-4062.

Rosenberg, T., Klie, F., Garred, P., and Schwartz, M. (2007). N965S is a common ABCA4 variant in Stargardt-related retinopathies in the Danish population. Mol Vis *13*, 1962-1969.

Rossmiller, B., Mao, H., and Lewin, A. S. (2012). Gene therapy in animal models of autosomal dominant retinitis pigmentosa. Mol Vis *18*, 2479-2496.

Rozet, J. M., Gerber, S., Souied, E., Ducroq, D., Perrault, I., Ghazi, I., Soubrane, G., Coscas, G., Dufier, J. L., Munnich, A., and Kaplan, J. (1999). The ABCR gene: a major disease gene in macular and peripheral retinal degenerations with onset from early childhood to the elderly. Mol Genet Metab *68*, 310-315.

Rust, S., Walter, M., Funke, H., von Eckardstein, A., Cullen, P., Kroes, H. Y., Hordijk, R., Geisel, J., Kastelein, J., Molhuizen, H. O., *et al.* (1998). Assignment of Tangier disease to chromosome 9q31 by a graphical linkage exclusion strategy. Nat Genet *20*, 96-98.

Saari, J. C. (2000). Biochemistry of visual pigment regeneration: the Friedenwald lecture. Invest Ophthalmol Vis Sci *41*, 337-348.

Saari, J. C., and Crabb, J. W. (2005). Focus on molecules: cellular retinaldehyde-binding protein (CRALBP). Exp Eye Res *81*, 245-246.

Saari, J. C., Nawrot, M., Kennedy, B. N., Garwin, G. G., Hurley, J. B., Huang, J., Possin, D. E., and Crabb, J. W. (2001). Visual cycle impairment in cellular retinaldehyde binding protein (CRALBP) knockout mice results in delayed dark adaptation. Neuron *29*, 739-748.

Saari, J. C., Nawrot, M., Stenkamp, R. E., Teller, D. C., and Garwin, G. G. (2009). Release of 11-cis-retinal from cellular retinaldehyde-binding protein by acidic lipids. Mol Vis *15*, 844-854.

Sakai, H., Tanaka, Y., Tanaka, M., Ban, N., Yamada, K., Matsumura, Y., Watanabe, D., Sasaki, M., Kita, T., and Inagaki, N. (2007). ABCA2 deficiency results in abnormal sphingolipid metabolism in mouse brain. J Biol Chem *282*, 19692-19699.

Satoh, A. K., O'Tousa, J. E., Ozaki, K., and Ready, D. F. (2005). Rab11 mediates post-Golgi trafficking of rhodopsin to the photosensitive apical membrane of Drosophila photoreceptors. Development *132*, 1487-1497.

Schmidt, S., Postel, E. A., Agarwal, A., Allen, I. C., Jr., Walters, S. N., De la Paz, M. A., Scott, W. K., Haines, J. L., Pericak-Vance, M. A., and Gilbert, J. R. (2003). Detailed analysis of allelic variation in the ABCA4 gene in age-related maculopathy. Invest Ophthalmol Vis Sci *44*, 2868-2875.

Scholz, C., Parcej, D., Ejsing, C. S., Robenek, H., Urbatsch, I. L., and Tampe, R. (2011). Specific lipids modulate the transporter associated with antigen processing (TAP). J Biol Chem *286*, 13346-13356.

Senior, A. E., al-Shawi, M. K., and Urbatsch, I. L. (1995). The catalytic cycle of P-glycoprotein. FEBS Lett *377*, 285-289.

Senior, A. E., al-Shawi, M. K., and Urbatsch, I. L. (1998). ATPase activity of Chinese hamster P-glycoprotein. Methods Enzymol *292*, 514-523.

Senior, A. E., and Bhagat, S. (1998). P-glycoprotein shows strong catalytic cooperativity between the two nucleotide sites. Biochemistry *37*, 831-836.

Seres, L., Cserepes, J., Elkind, N. B., Torocsik, D., Nagy, L., Sarkadi, B., and Homolya, L. (2008). Functional ABCG1 expression induces apoptosis in macrophages and other cell types. Biochim Biophys Acta *1778*, 2378-2387.

Shapiro, A. B., and Ling, V. (1994). ATPase activity of purified and reconstituted P-glycoprotein from Chinese hamster ovary cells. J Biol Chem *269*, 3745-3754.

Sharom, F. J., DiDiodato, G., Yu, X., and Ashbourne, K. J. (1995). Interaction of the P-glycoprotein multidrug transporter with peptides and ionophores. J Biol Chem *270*, 10334-10341.

Shitan, N., Bazin, I., Dan, K., Obata, K., Kigawa, K., Ueda, K., Sato, F., Forestier, C., and Yazaki, K. (2003). Involvement of CjMDR1, a plant multidrug-resistance-type ATP-binding cassette protein, in alkaloid transport in Coptis japonica. Proc Natl Acad Sci U S A *100*, 751-756.

Shulenin, S., Nogee, L. M., Annilo, T., Wert, S. E., Whitsett, J. A., and Dean, M. (2004). ABCA3 gene mutations in newborns with fatal surfactant deficiency. N Engl J Med *350*, 1296-1303.

Simonelli, F., Testa, F., de Crecchio, G., Rinaldi, E., Hutchinson, A., Atkinson, A., Dean, M., D'Urso, M., and Allikmets, R. (2000). New ABCR mutations and clinical phenotype in Italian patients with Stargardt disease. Invest Ophthalmol Vis Sci *41*, 892-897.

Singaraja, R. R., Visscher, H., James, E. R., Chroni, A., Coutinho, J. M., Brunham, L. R., Kang, M. H., Zannis, V. I., Chimini, G., and Hayden, M. R. (2006). Specific mutations in ABCA1 have discrete effects on ABCA1 function and lipid phenotypes both in vivo and in vitro. Circ Res *99*, 389-397.

Singh, B. N., Venkatesh, N., Nademanee, K., Josephson, M. A., and Kannan, R. (1989). The historical development, cellular electrophysiology and pharmacology of amiodarone. Prog Cardiovasc Dis *31*, 249-280.

Singh, O. V., Pollard, H. B., and Zeitlin, P. L. (2008). Chemical rescue of deltaF508-CFTR mimics genetic repair in cystic fibrosis bronchial epithelial cells. Mol Cell Proteomics *7*, 1099-1110.

Smith, H. G., Jr., Stubbs, G. W., and Litman, B. J. (1975). The isolation and purification of osmotically intact discs from retinal rod outer segments. Exp Eye Res *20*, 211-217.

Smith, J. D., Le Goff, W., Settle, M., Brubaker, G., Waelde, C., Horwitz, A., and Oda, M. N. (2004). ABCA1 mediates concurrent cholesterol and phospholipid efflux to apolipoprotein A-I. J Lipid Res *45*, 635-644.

Smriti, Krishnamurthy, S., Dixit, B. L., Gupta, C. M., Milewski, S., and Prasad, R. (2002). ABC transporters Cdr1p, Cdr2p and Cdr3p of a human pathogen Candida albicans are general phospholipid translocators. Yeast *19*, 303-318.

Sorrenson, B., Suetani, R. J., Williams, M. J., Bickley, V. M., George, P. M., Jones, G. T., and McCormick, S. P. (2013). Functional rescue of mutant ABCA1 proteins by sodium 4-phenylbutyrate. J Lipid Res *54*, 55-62.

Sparrow, J. R., Cai, B., Jang, Y. P., Zhou, J., and Nakanishi, K. (2006). A2E, a fluorophore of RPE lipofuscin, can destabilize membrane. Adv Exp Med Biol *572*, 63-68.

Sparrow, J. R., Parish, C. A., Hashimoto, M., and Nakanishi, K. (1999). A2E, a lipofuscin fluorophore, in human retinal pigmented epithelial cells in culture. Invest Ophthalmol Vis Sci *40*, 2988-2995.

Sparrow, J. R., Vollmer-Snarr, H. R., Zhou, J., Jang, Y. P., Jockusch, S., Itagaki, Y., and Nakanishi, K. (2003). A2E-epoxides damage DNA in retinal pigment epithelial cells. Vitamin E and other antioxidants inhibit A2E-epoxide formation. J Biol Chem *278*, 18207-18213.

Sparrow, J. R., Wu, Y., Kim, C. Y., and Zhou, J. (2010). Phospholipid meets all-trans-retinal: the making of RPE bisretinoids. J Lipid Res *51*, 247-261.

Stone, J., Maslim, J., Valter-Kocsi, K., Mervin, K., Bowers, F., Chu, Y., Barnett, N., Provis, J., Lewis, G., Fisher, S. K.*, et al.* (1999). Mechanisms of photoreceptor death and survival in mammalian retina. Prog Retin Eye Res *18*, 689-735.

Sun, H., Molday, R. S., and Nathans, J. (1999). Retinal stimulates ATP hydrolysis by purified and reconstituted ABCR, the photoreceptor-specific ATP-binding cassette transporter responsible for Stargardt disease. J Biol Chem *274*, 8269-8281.

Sun, H., and Nathans, J. (1997). Stargardt's ABCR is localized to the disc membrane of retinal rod outer segments. Nat Genet *17*, 15-16.

Sun, H., and Nathans, J. (2001). ABCR, the ATP-binding cassette transporter responsible for Stargardt macular dystrophy, is an efficient target of all-trans-retinal-mediated photooxidative damage in vitro. Implications for retinal disease. J Biol Chem *276*, 11766-11774.

Sun, H., Smallwood, P. M., and Nathans, J. (2000). Biochemical defects in ABCR protein variants associated with human retinopathies. Nat Genet *26*, 242-246.

Sung, C. H., and Chuang, J. Z. (2010). The cell biology of vision. J Cell Biol *190*, 953-963.

Sung, C. H., and Tai, A. W. (2000). Rhodopsin trafficking and its role in retinal dystrophies. Int Rev Cytol *195*, 215-267.

Szakacs, G., Langmann, T., Ozvegy, C., Orso, E., Schmitz, G., Varadi, A., and Sarkadi, B. (2001). Characterization of the ATPase cycle of human ABCA1: implications for its function as a regulator rather than an active transporter. Biochem Biophys Res Commun *288*, 1258-1264.

Takahashi, K., Kimura, Y., Kioka, N., Matsuo, M., and Ueda, K. (2006). Purification and ATPase activity of human ABCA1. J Biol Chem *281*, 10760-10768.

Tanaka, A. R., Abe-Dohmae, S., Ohnishi, T., Aoki, R., Morinaga, G., Okuhira, K., Ikeda, Y., Kano, F., Matsuo, M., Kioka, N., *et al.* (2003). Effects of mutations of ABCA1 in the first extracellular domain on subcellular trafficking and ATP binding/hydrolysis. J Biol Chem *278*, 8815-8819.

Tanaka, N., Abe-Dohmae, S., Iwamoto, N., Fitzgerald, M. L., and Yokoyama, S. (2010). Helical apolipoproteins of high-density lipoprotein enhance phagocytosis by stabilizing ATP-binding cassette transporter A7. J Lipid Res *51*, 2591-2599.

Tang, P. H., Kono, M., Koutalos, Y., Ablonczy, Z., and Crouch, R. K. (2013). New insights into retinoid metabolism and cycling within the retina. Prog Retin Eye Res *32*, 48-63.

Tiberghien, F., and Loor, F. (1996). Ranking of P-glycoprotein substrates and inhibitors by a calcein-AM fluorometry screening assay. Anticancer Drugs *7*, 568-578.

Timmins, J. M., Lee, J. Y., Boudyguina, E., Kluckman, K. D., Brunham, L. R., Mulya, A., Gebre, A. K., Coutinho, J. M., Colvin, P. L., Smith, T. L., *et al.* (2005). Targeted inactivation of hepatic Abca1 causes profound hypoalphalipoproteinemia and kidney hypercatabolism of apoA-I. J Clin Invest *115*, 1333-1342.

Travis, G. H., Golczak, M., Moise, A. R., and Palczewski, K. (2007). Diseases caused by defects in the visual cycle: retinoids as potential therapeutic agents. Annu Rev Pharmacol Toxicol *47*, 469-512.

Tsybovsky, Y., Orban, T., Molday, R. S., Taylor, D., and Palczewski, K. (2012). Molecular organization and ATP-induced conformational changes of ABCA4, the photoreceptor-specific ABC transporter. Structure *21*, 854-860.

Tsybovsky, Y., Orban, T., Molday, R. S., Taylor, D., and Palczewski, K. (2013). Molecular Organization and ATP-Induced Conformational Changes of ABCA4, the Photoreceptor-Specific ABC Transporter. Structure *21*, 854-860.

Tsybovsky, Y., Wang, B., Quazi, F., Molday, R. S., and Palczewski, K. (2011). Posttranslational modifications of the photoreceptor-specific ABC transporter ABCA4. Biochemistry *50*, 6855-6866.

Tveten, K., Holla, O. L., Ranheim, T., Berge, K. E., Leren, T. P., and Kulseth, M. A. (2007). 4-Phenylbutyrate restores the functionality of a misfolded mutant low-density lipoprotein receptor. Febs J *274*, 1881-1893.

Urbatsch, I. L., al-Shawi, M. K., and Senior, A. E. (1994). Characterization of the ATPase activity of purified Chinese hamster P-glycoprotein. Biochemistry *33*, 7069-7076.

Urbatsch, I. L., Wilke-Mounts, S., Gimi, K., and Senior, A. E. (2001). Purification and characterization of N-glycosylation mutant mouse and human P-glycoproteins expressed in Pichia pastoris cells. Arch Biochem Biophys *388*, 171-177.

Vallakati, A., Chandra, P. A., Pednekar, M., Frankel, R., and Shani, J. (2011). Dronedarone-Induced Digoxin Toxicity: New Drug, New Interactions. Am J Ther.

van Dam, M. J., de Groot, E., Clee, S. M., Hovingh, G. K., Roelants, R., Brooks-Wilson, A., Zwinderman, A. H., Smit, A. J., Smelt, A. H., Groen, A. K., *et al.* (2002). Association between increased arterial-wall thickness and impairment in ABCA1-driven cholesterol efflux: an observational study. Lancet *359*, 37-42.

Van Goor, F., Straley, K. S., Cao, D., Gonzalez, J., Hadida, S., Hazlewood, A., Joubran, J., Knapp, T., Makings, L. R., Miller, M., *et al.* (2006). Rescue of DeltaF508-CFTR trafficking and gating in human cystic fibrosis airway primary cultures by small molecules. Am J Physiol Lung Cell Mol Physiol *290*, L1117-1130.

van Helvoort, A., Smith, A. J., Sprong, H., Fritzsche, I., Schinkel, A. H., Borst, P., and van Meer, G. (1996). MDR1 P-glycoprotein is a lipid translocase of broad specificity, while MDR3 P-glycoprotein specifically translocates phosphatidylcholine. Cell *87*, 507-517.

van Meer, G., Halter, D., Sprong, H., Somerharju, P., and Egmond, M. R. (2006). ABC lipid transporters: extruders, flippases, or flopless activators? FEBS Lett *580*, 1171-1177.

van Meer, G., Voelker, D. R., and Feigenson, G. W. (2008). Membrane lipids: where they are and how they behave. Nat Rev Mol Cell Biol *9*, 112-124.

Varbiro, G., Toth, A., Tapodi, A., Veres, B., Sumegi, B., and Gallyas, F., Jr. (2003). Concentration dependent mitochondrial effect of amiodarone. Biochem Pharmacol *65*, 1115-1128.

Vaughan, A. M., and Oram, J. F. (2006). ABCA1 and ABCG1 or ABCG4 act sequentially to remove cellular cholesterol and generate cholesterol-rich HDL. J Lipid Res *47*, 2433-2443.

Vedhachalam, C., Duong, P. T., Nickel, M., Nguyen, D., Dhanasekaran, P., Saito, H., Rothblat, G. H., Lund-Katz, S., and Phillips, M. C. (2007). Mechanism of ATP-binding cassette transporter A1-mediated cellular lipid efflux to apolipoprotein A-I and formation of high density lipoprotein particles. J Biol Chem *282*, 25123-25130.

Velamakanni, S., Janvilisri, T., Shahi, S., and van Veen, H. W. (2008). A functional steroid-binding element in an ATP-binding cassette multidrug transporter. Mol Pharmacol *73*, 12-17.

Wang, N., Lan, D., Gerbod-Giannone, M., Linsel-Nitschke, P., Jehle, A. W., Chen, W., Martinez, L. O., and Tall, A. R. (2003). ATP-binding cassette transporter A7 (ABCA7) binds apolipoprotein A-I and mediates cellular phospholipid but not cholesterol efflux. J Biol Chem *278*, 42906-42912.

Wang, N., Silver, D. L., Thiele, C., and Tall, A. R. (2001). ATP-binding cassette transporter A1 (ABCA1) functions as a cholesterol efflux regulatory protein. J Biol Chem *276*, 23742-23747.

Wang, W., Nossoni, Z., Berbasova, T., Watson, C. T., Yapici, I., Lee, K. S., Vasileiou, C., Geiger, J. H., and Borhan, B. (2013). Tuning the electronic absorption of protein-embedded all-trans-retinal. Science *338*, 1340-1343.

Ward, A., Reyes, C. L., Yu, J., Roth, C. B., and Chang, G. (2007). Flexibility in the ABC transporter MsbA: Alternating access with a twist. Proc Natl Acad Sci U S A *104*, 19005-19010.

Webster, A. R., Heon, E., Lotery, A. J., Vandenburgh, K., Casavant, T. L., Oh, K. T., Beck, G., Fishman, G. A., Lam, B. L., Levin, A*., et al.* (2001). An analysis of allelic variation in the ABCA4 gene. Invest Ophthalmol Vis Sci *42*, 1179-1189.

Weleber, R. G. (1994). Stargardt's macular dystrophy. Arch Ophthalmol *112*, 752-754.

Weng, J., Mata, N. L., Azarian, S. M., Tzekov, R. T., Birch, D. G., and Travis, G. H. (1999). Insights into the function of Rim protein in photoreceptors and etiology of Stargardt's disease from the phenotype in abcr knockout mice. Cell *98*, 13-23.

Wiszniewski, W., Zaremba, C. M., Yatsenko, A. N., Jamrich, M., Wensel, T. G., Lewis, R. A., and Lupski, J. R. (2005). ABCA4 mutations causing mislocalization are found frequently in patients with severe retinal dystrophies. Hum Mol Genet *14*, 2769-2778.

Woehlecke, H., Pohl, A., Alder-Baerens, N., Lage, H., and Herrmann, A. (2003). Enhanced exposure of phosphatidylserine in human gastric carcinoma cells overexpressing the half-size ABC transporter BCRP (ABCG2). Biochem J *376*, 489-495.

Wong, J. P., Reboul, E., Molday, R. S., and Kast, J. (2009). A carboxy-terminal affinity tag for the purification and mass spectrometric characterization of integral membrane proteins. J Proteome Res *8*, 2388-2396.

Wu, G., and Hubbell, W. L. (1993). Phospholipid asymmetry and transmembrane diffusion in photoreceptor disc membranes. Biochemistry *32*, 879-888.

Wu, Y., Fishkin, N. E., Pande, A., Pande, J., and Sparrow, J. R. (2009). Novel lipofuscin bisretinoids prominent in human retina and in a model of recessive Stargardt disease. J Biol Chem *284*, 20155-20166.

Yang, Z., Chen, Y., Lillo, C., Chien, J., Yu, Z., Michaelides, M., Klein, M., Howes, K. A., Li, Y., Kaminoh, Y., *et al.* (2008). Mutant prominin 1 found in patients with macular degeneration disrupts photoreceptor disk morphogenesis in mice. J Clin Invest *118*, 2908-2916.

Yokoyama, S. (2000). Release of cellular cholesterol: molecular mechanism for cholesterol homeostasis in cells and in the body. Biochim Biophys Acta *1529*, 231-244.

Young, R. W. (1971). The renewal of rod and cone outer segments in the rhesus monkey. J Cell Biol *49*, 303-318.

Zaitseva, J., Jenewein, S., Jumpertz, T., Holland, I. B., and Schmitt, L. (2005). H662 is the linchpin of ATP hydrolysis in the nucleotide-binding domain of the ABC transporter HlyB. Embo J *24*, 1901-1910.

Zhong, M., Molday, L. L., and Molday, R. S. (2009). Role of the C terminus of the photoreceptor ABCA4 transporter in protein folding, function, and retinal degenerative diseases. J Biol Chem *284*, 3640-3649.

Zolnerciks, J. K., Wooding, C., and Linton, K. J. (2007). Evidence for a Sav1866-like architecture for the human multidrug transporter P-glycoprotein. Faseb J *21*, 3937-3948.

Zou, P., and McHaourab, H. S. (2009). Alternating access of the putative substrate-binding chamber in the ABC transporter MsbA. J Mol Biol *393*, 574-585.

Zuo, Y., Zhuang, D. Z., Han, R., Isaac, G., Tobin, J. J., McKee, M., Welti, R., Brissette, J. L., Fitzgerald, M. L., and Freeman, M. W. (2008). ABCA12 maintains the epidermal lipid permeability barrier by facilitating formation of ceramide linoleic esters. J Biol Chem *283*, 36624-36635.

Appendices

Appendix A

A.1 Effect of ABCA4 Protein Levels and Retinoids on Retinal Transfer

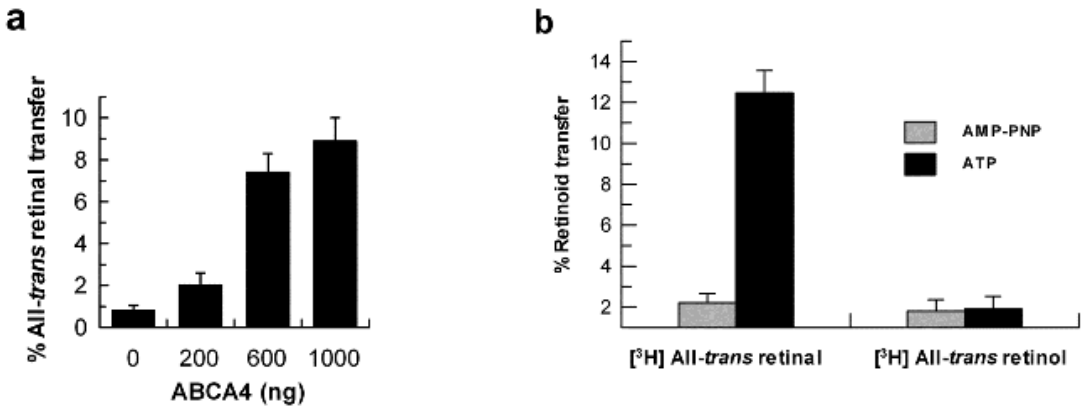

ABCA4 was purified from bovine rod outer segments by immunoaffinity chromatography and reconstituted into donor proteoliposomes. (a). Effect of increasing amounts of ABCA4 on ATP-dependent [^{3}H] all-*trans* retinal transfer activity. Concentrations of ABCA4 were adjusted prior to dialysis such that the same volume of proteoliposomes was used in the assay. (b) ABCA4-mediated all-*trans* retinal and all-*trans* retinol transfer activity of from donor proteoliposomes to acceptor liposomes. Vesicles were incubated with either 10 μM [^{3}H] all-*trans* retinal or [^{3}H] all-*trans* retinol (1.68 kBq, 3.36 GBq/mmol). Retinoid transfer from donor to acceptor vesicles was measured after the addition of 2 mM ATP or AMP-PNP at 37 °C for 1 h. Data are plotted as mean S.D. for n =3.

A.2 Effect of EDTA on ATP-Dependent Retinal Transfer in Acceptor Liposomes

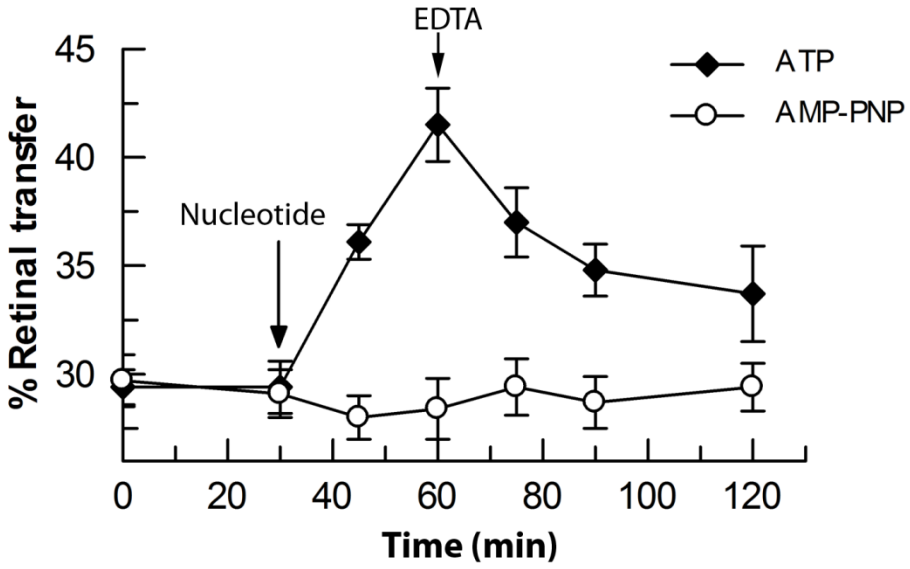

Nucleotide (2 mM ATP or AMP-PNP and 3 mM $MgCl_2$) was added after 30 min. At 60 min. 10 mM EDTA was added to chelate Mg^{2+} required for ATP binding and hydrolysis. A decrease in accumulated nucleotide in the liposomes was observed representing the back flow of accumulated retinal to the proteoliposomes in the absence of ATP. AMP-PNP had no significant effect on accumulation or reversal. Data are plotted as mean S.D. for n =3.

A.3 ABCA4 Retinal Transfer with Divalent Ions Mg^{2+}, Ca^{2+}, Zn^{2+}, and Mn^{2+}

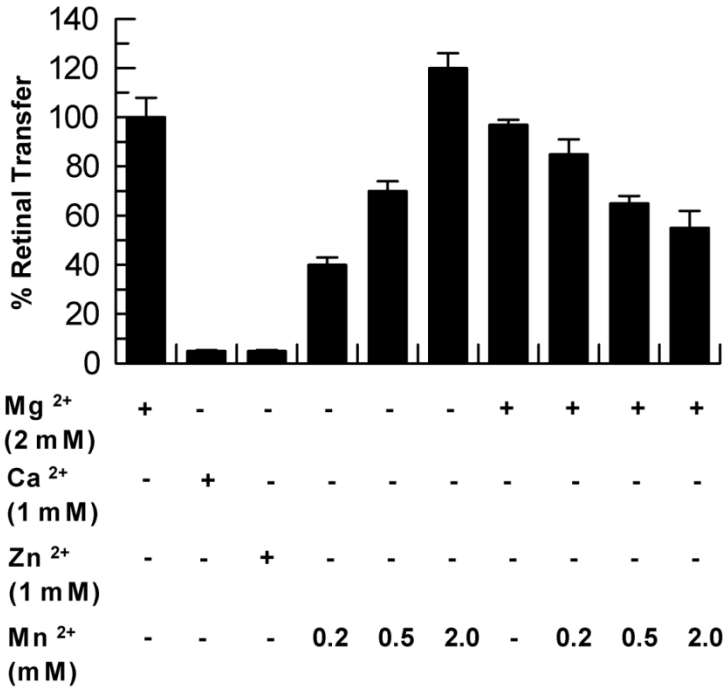

No activity was detected when cations were omitted from the reaction. Both Mg^{2+} and Mn^{2+} support transfer activity but were inhibitory when mixed together. Data are plotted as mean S.D. for n =3.

A.4 Determination of pK_a of *N*-retinylidene-PE in a Liposome System

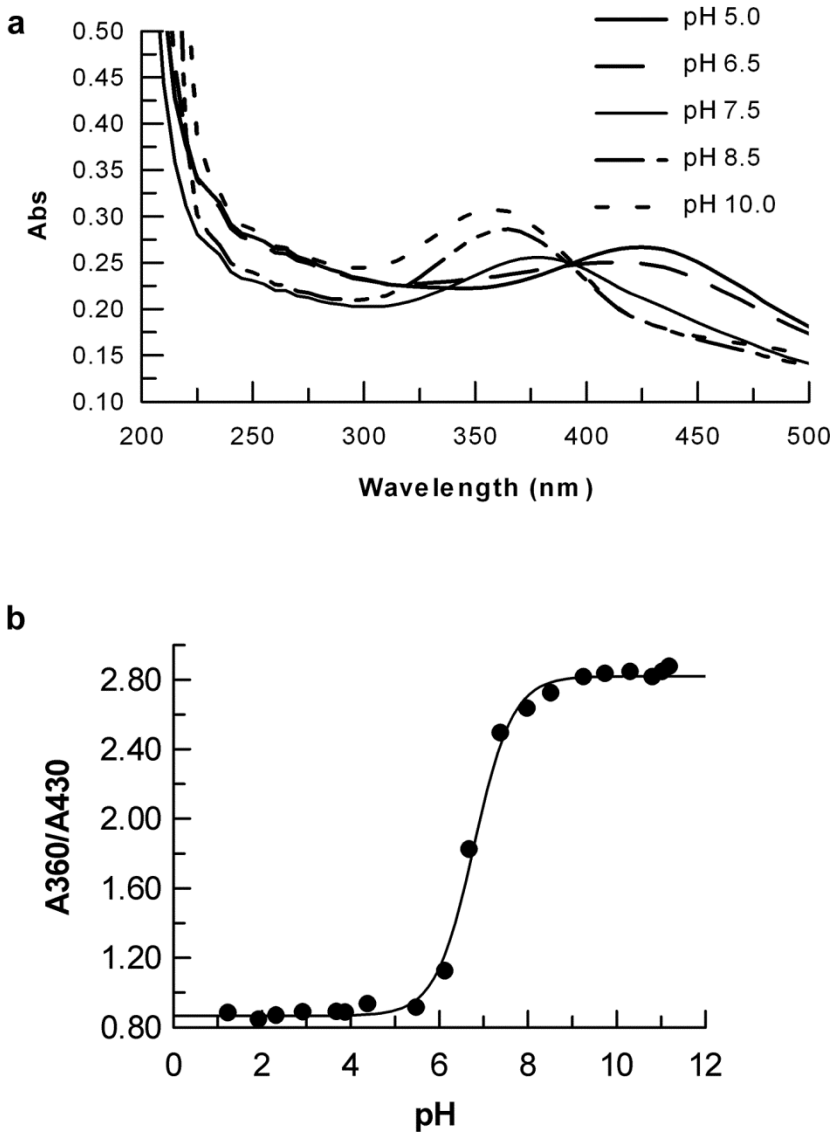

DOPC/DOPE vesicles (150 μm) were mixed with 1 μm all-*trans* retinal in 3 ml buffer consisting of 0.5 mM HEPES, pH 8.0, and 1 mM NaCl. The pH was changed by the addition of HCl or NaOH (a) Examples of the absorption spectra of N-retinylidene-PE at various pH values. (b) Titration curve for *N*-retinylidene-PE is shown in which the ratio $A_{360\ nm}/ A_{430\ nm}$ of *N*-retinylidene PE is plotted as a function of pH; the curve (solid line) was fitted with the Henderson-Hasselbalch equation yielding a pKa of 6.9.

A.5 Dependence of Retinal Transfer on pH

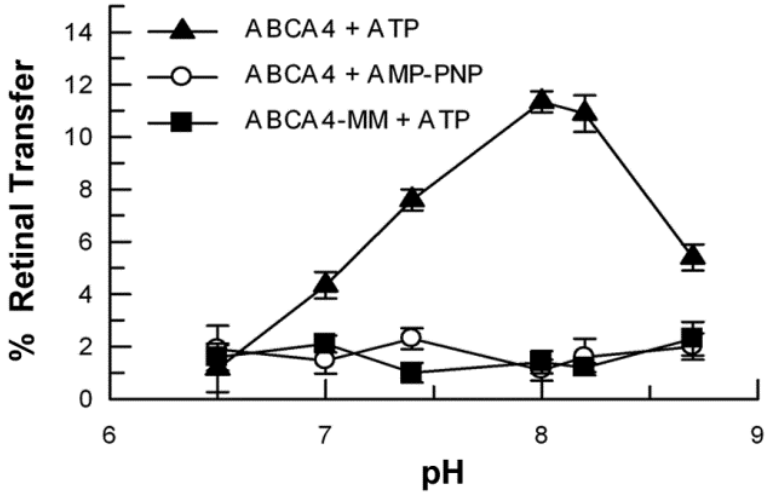

Donor proteoliposomes reconstituted with either wild-type ABCA4 or the ATPase-deficient mutant (ABCA4-MM) were mixed with DOPC/DOPE acceptor vesicles at the designated pH in the presence of 10 µM [^{3}H]-ATR. ATP or AMP-PNP (2 mM) was added to initiate ATR (Retinal) transfer. % Retinal transfer was measured after 1 h at 37^{o}C. Data are plotted as mean S.D. for *n* =3.

A.6 Fluorescence Traces Used to Evaluate the PE Flippase Activity of ABCA4

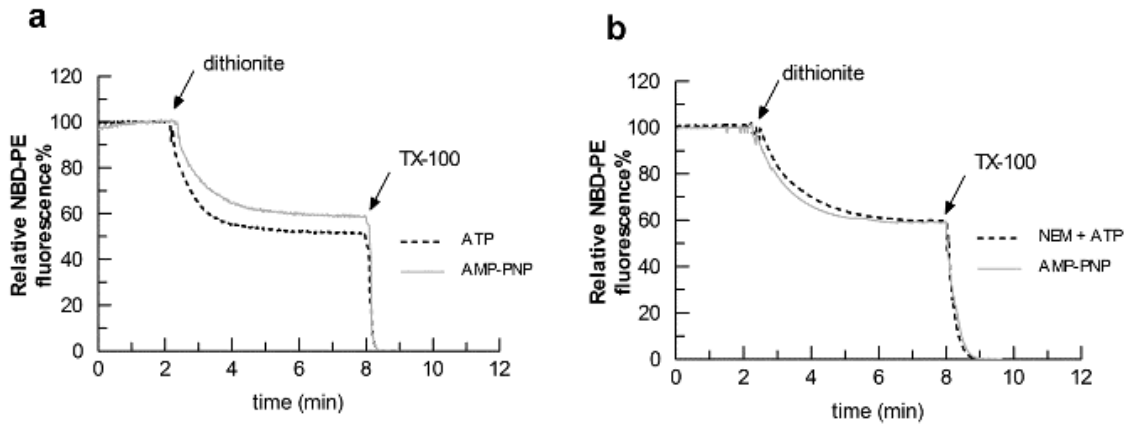

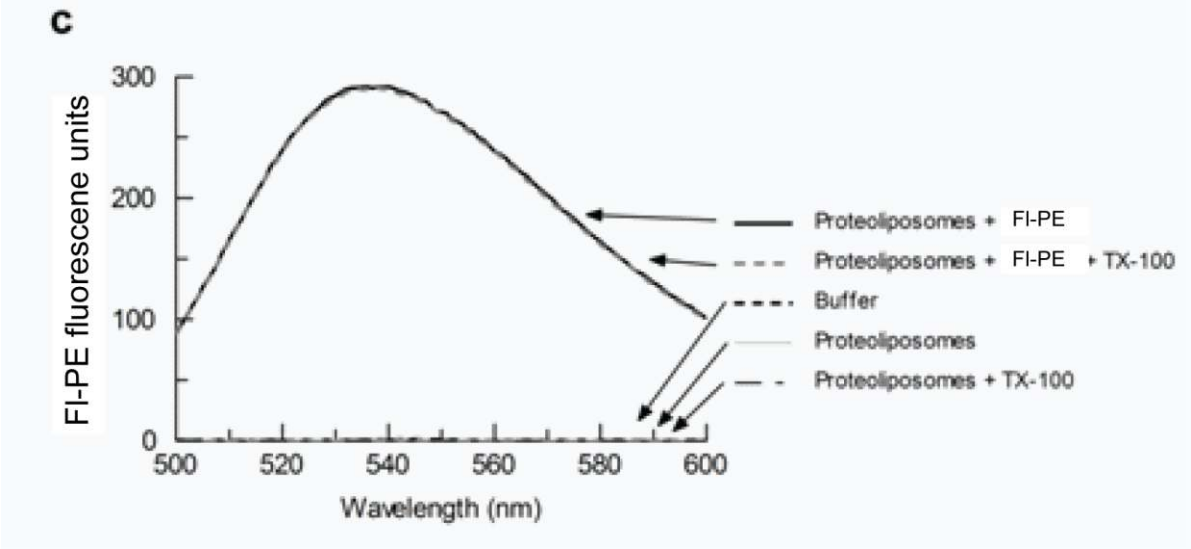

ABCA4 was reconstituted into PC liposomes containing 0.6% Fl-labeled-PE. The proteoliposomes were incubated with nucleotides (1 mM ATP or AMP-PNP) for 1 hour at 37^0C to initiate Fl-labeled-PE flipping and subsequently treated with the impermeable reducing agent dithionite (4mM) to bleach Fl-labeled-PE on the outer leaflet of the vesicles. After a stable baseline was obtained 1% Trition X-100 was added to permeabilize the membrane and bleach the remaining Fl-labeled-PE derivatives. (a) Extent of flipping was determined from the difference in fluorescence for the ATP and AMP-PNP treated samples as described in the experimental methods. (b) Control samples in which ABCA4 activity was inhibited by the addition of 10 mM NEM showed no difference between ATP and AMP-PNP. (c) Examples of emission scans at 540 nm for Fl-labeled-PE and proteoliposomes in the presence and absence of Triton-X-100 (TX-100).

A.7 Determination of Proteoliposome Orientation by ATPase Activities

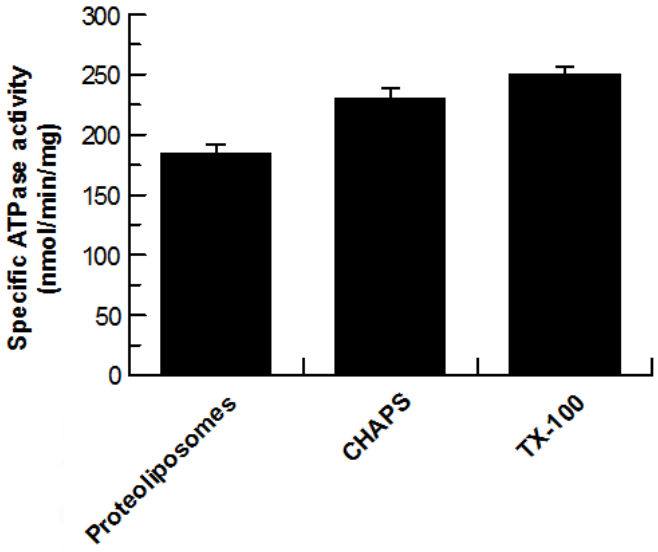

The retinal-stimulated ATPase activity of ABCA4 reconstituted in proteoliposomes was determined in the absence (proteoliposomes) and presence of either 15 mM CHAPS or 0.1% Triton X-100 to solubilize or permeabilize the proteoliposomes. The increase in ATPase activity in the detergent-treated samples was used to estimate the total accessibility of ABCA4 to ATP. A 1.25 and 1.34 fold increase in ATPase activity was observed for CHAPS and TX-100 treated samples indicating that as much as 70-80% of ABCA4 is oriented with its NBDs exposed to the outside of the proteoliposomes. Data are plotted as mean S.D. for *n* =3.

A.8 Vesicle Separation Efficiency Probed by Fluorescence Intensity of Fl-PE

Acceptor Vesicle	Donor vesicle	Treatment	Fluorescence Intensity %
DOPC/DOPE/N-Fl-PE	*DOPC/DOPE*	-	100 ± 1.4
DOPC/DOPE/N-Fl-PE	*DOPC/DOPE*	1 mM ATP	101 ± 0.8
DOPC/DOPE	*DOPC/DOPE/N-Fl-PE*	1 mM ATP	0.7 ± 0.5
DOPC/DOPE	*DOPC/DOPE/N-Fl-PE*	10 μM All-*trans* retinal + 1 mM ATP	0.4 ± 1.1
DOPC/DOPE	*ABCA4/DOPC/DOPE/N-Fl-PE*	1 mM ATP	0.5 ± 1.2
DOPC/DOPE	*ABCA4/DOPC/DOPE/N-Fl-PE*	10 μM All-*trans* retinal + 1 mM ATP	1.2 ± 1.1

[a] For the preparation of labeled vesicles, *N*-Fl-labeled-PE is included at 1 mol % each. Vesicles are composed of DOPC/DOPE (~70/30 mol%). Lipids are solubilized at 18 mM CHAPS in an aqueous buffer containing 10 mM HEPES, pH 7.6, 150 mM NaCl and reconstituted by overnight dialysis. DOPC/DOPE/Fl-labeled-PE vesicles with 10% sucrose and unlabeled DOPC/DOPE vesicles were added to a final concentration of 500 μM each into 2 ml 10 mm HEPES, pH 7.6 ,150 mM NaCl for 1 h at 37 ºC. After ultracentrifugation separation, in 10 mM HEPES, pH 7.6, 75 mm NaCl, 150 mM sucrose, acceptor vesicles were resuspended and fluorescence intensity monitored for Fl-labeled-PE using excitation and emission wavelengths of 467 and 540 nm, respectively with an emission filter of 530 nm. In the last four set of trials, the Fl-labeled-PE fluorophore was reconstituted into lighter donor vesicles and incubated with unlabeled acceptor vesicles. Retinal does not have intrinsic fluorescence and the N-Fl fluorescent label is covalently bound to the amino moiety present in the head group PE.

A.9 Vesicle Fusion Analysis by N-Fl-PE and N-Rh PE Quenching

	Fluorescence quenching %			
vesicles	none	Ca^{2+}	ATP	Triton X-100
N-Rh PE + N-Fl PE	0.3 ± 0.1	2 ± 1.2	4.2 ± 2.1	96 ± 3
ABCA4/N-Rh PE + N-Fl-PE	4.2 ± 1.5	4 ± 2.4	4 ± 1.7	100 ± 4

b Vesicle-vesicle fusion analysis. Vesicles contained 3 mol% of the indicated fluorescent phospholipid derivative. Fluorescence donor *N*-Fl-PE and acceptor *N*-Rh-PE were incorporated in separate vesicle populations. DOPC/DOPE/N-Rh-PE (67:30:3) vesicles were prepared in CHAPS/PC/10% sucrose buffer and dialyzed while N-Fl-PE and/or ABCA4 vesicles were reconstituted into DOPC/BPL/DOPE/N-Fl-PE (57:20:20:3). Vesicle fusion was monitored with resonance energy transfer. ABCA4 was incorporated in *N*-Rh-PE populations and subjected to 1 mM ATP treatment. Fusion/quenching was initiated by addition of 5 mM Ca^{2+} or 1 % Triton X-100. Ca^{2+} or Mg^{2+} did not produce fluorescence quenching suggesting that fusion events did not occur in these vesicle compositions. Fluorescence quenching of the samples were recorded by excitation at 475 nm and monitored at 530 nm with 2.5 nm band-widths. Any fusion of the vesicles will result in intermixing of the membrane lipids so that the fluorescence donor and acceptor come into close proximity and effect fluorescent quenching.

A.10 Flippase activities of Opsin, ATP8a2, and ABCA4

We consider the phospholipid asymmetry contribution activities. In artificial vesicles, a single opsin membrane protein flips phospholipids is described by a single exponential function (Menon et al., 2011).

$\tau = 10$ s

⇨ $t1/2 = \ln(2) \times \tau = 4.8$ s $= 0.08$ min

Opsin flips 0.5 mol % fluorescent labeled phospholipid from a steady state distribution of ~ 50% fluorescent lipid distributed symmetrically in protein free liposomes to ~85% in proteoliposomes reconstituted with 1 opsin per proteoliposome. This means a change of ~35% in lipid flipping is specifically achieved by opsin. One mg Opsin is reconstituted into 1 mmol of phospholipid vesicle.

1 mg opsin = 27 x 10^-6 mmol opsin

Therefore the rate of phospholipid flipping is

= 0.5/100 x 35/100 x 1 mmol phospholipid/ (0.08 min x 27 x 10^-6 min)

$= 810$ min^{-1}

This suggests that opsin molecule flips 810 phospholipid molecules per minute.

Similarly, ATP8a2 has a specific PS transport rate of 50,400 nmol/min/mg (Coleman et al., 2009).

= 50,400 nmol PS/7.69 nmol

= 6550 min^{-1}

And, ABCA4 has turnovers of 24.5 min^{-1} and 3.8 min^{-1} for *N*-retinylidene PE and PE, respectively.

However, disc membranes have a rhodopsin to phospholipid ratio of 1:400. So, one can assume the visual pigment flipping 400 phospholipid molecules in a minute. The relative abundance of major membrane proteins of discs is rhodopsin (85%), ABCA4 (3-5%), ATP8a2 (0.1%), with other proteins being less abundant. As an example, if there are

1200 (opsin molecules): 10 (ABCA4 molecules): 1 (ATP8a2 molecule)

Then the lipid molecules flipped by the contributing proteins are:

480,000 (PC/PS/PE): 40 (PE): 6550 (PS)

The experimental conditions in the opsin flippase study used 1 opsin protein per reconstituted phospholipid vesicle. Increasing the protein content in liposomes to reflect physiological conditions may give an appropriate estimate to lipid flipping.

The average cholesterol content (10%) of disc membranes has no detectable effect on opsin phospholipid flipping (Menon et al., 2011). However, at least 40% mol cholesterol exists in the plasma membrane of outer segments (Boesze-Battaglia and Albert, 1989). This may restrict the flippase activity of opsin and enable ATP8a2 to flip PS towards the cytoplasmic side of outer segments. However, for generating phospholipid asymmetry with PC and SM on the extracytosolic side, an ABC transporter may be needed. This would have to occur at <0.1% and be able to achieve transport rate 100-fold higher than ABCA4.